RNAi-based anti-cancer strategies - targeting the proto-oncogene PIM1 and oncogenic miRNAs

Dissertation

zur Erlangung des Doktorgrades
der Naturwissenschaften (Dr. rer. nat.)

dem Fachbereich Pharmazie
der Philipps-Universität Marburg
vorgelegt von

Maren Thomas
aus Freudenberg (Südwestfalen)

Marburg (Lahn) 2013

Dem Fachbereich Pharmazie
der Philipps-Universität Marburg (Hochschulkennziffer 1180)
vorgelegt am 12.03.2013 und
als Dissertation am 23.04.2013 angenommen.

Erstgutachter: Prof. Dr. Roland K. Hartmann
Zweitgutachter: Prof. Dr. Jens Kurreck

Tag der mündlichen Prüfung am 23.04.2013

Zusammenfassung

Krebs ist eine chronische Erkrankung, bei der Körperzellen durch Mutationen entarten, unkontrolliert wachsen und unter bestimmten Voraussetzungen gesundes Gewebe infiltrieren. Heutzutage zählt Krebs als zweithäufigste Todesursache der westlichen Welt zu den wichtigsten epidemiologischen Krankheitsbildern unserer Gesellschaft. Neben klassischen Behandlungsmethoden wie Resektion des Tumorgewebes, Chemo- oder auch Immuntherapie ist die Entwicklung neuer Therapieoptionen von großer Bedeutung. Eine mögliche neue therapeutische Alternative ist der Einsatz kleiner, nicht kodierender, regulatorischer RNAs wie z.B. miRNAs. MiRNAs sind an der Regulation wesentlicher biologischer Prozesse wie Entwicklung, Differenzierung oder Proliferation beteiligt, indem sie die Genexpression über den Mechanismus der RNA-Interferenz beeinflussen. Seit ihrer Entdeckung bestätigte sich die Annahme, dass miRNAs sowohl tumorsuppressive als auch onkogene Funktionen ausüben, weshalb sie sich nicht nur als diagnostische oder prognostische Biomarker des Krebsgewebes eignen, sondern auch als Therapeutika selbst eingesetzt werden könnten. In einer miRNA-Substitutionstherapie wird der Verlust oder die Herunterregulierung einer miRNA mit tumorsuppressiver Wirkung durch externe Zugabe ausgeglichen. Eine *Antisense*-Therapie vermittelt hingegen eine Inhibition onkogener miRNAs durch komplementäre Oligonukleotide. Eine sichere und effiziente Aufnahme der RNA-Moleküle zum Wirkort muss in beiden Ansätzen sichergestellt werden. Zurzeit ist die Entwicklung effizienter *Delivery*-Systeme der limitierende Faktor für miRNA-basierte Therapieansätze.

In dieser Arbeit wurde zunächst das Proto-Onkogen PIM1 bezüglich einer möglichen RNAi-basierten Antikrebstherapie untersucht. Eine Überexpression der PIM1 Kinase wird in zahlreichen soliden Tumoren oder malignen Entartungen des hämatopoetischen Systems beobachtet und ist in der Regel mit einem schwerwiegenden Krankheitsverlauf assoziiert. *In vitro*-Studien an humanen Leukämie- und Kolonkarzinom-Zelllinien konnten erstmalig zeigen, dass die zelluläre PIM1 Proteinexpression durch eine miRNA mit tumorsuppressiver Wirkung, nämlich miR-33a, spezifisch herunterreguliert wird, woraus zusätzlich ein proliferationsinhibierender Effekt resultiert. Ein erfolgreiches *Delivery* von nanopartikulären Vesikeln aus miR-33a Oligonukleotiden und einem nicht toxischen, verzweigtkettigen Polyethylenimin (PEI F25 LMW) führte in Maus-Tumor-Modellen zu einem antitumorigenen Effekt, der durch eine Reduktion des Tumorvolumens gezeigt werden konnte. Diese *in vitro*- und *in vivo*-Studien weisen das Proto-Onkogen PIM1 erstmalig als erfolgversprechendes Zielobjekt für eine miRNA-vermittelte Substitutionstherapie aus.

Der Fokus des zweiten Projektes lag auf der Entwicklung neuartiger LNA-basierter miRNA Inhibitoren, im Weiteren LNA-*Antiseeds* genannt, bestehend aus einzelsträngigen Oligonukleotiden mit sog. *Locked Nucleic Acid* (LNA)-Modifikationen und einem natürlich vorkommenden Phosphodiester-Nukleotidrückgrat. Im Allgemeinen erhöht ein LNA-*Design* sowohl die Resistenz der Oligonukleotide gegenüber einem Abbau durch zelluläre Nukleasen als auch ihre Affinität zur Ziel-miRNA, wobei durch komplementäre Bindung an onkogene miRNAs deren zelluläre Funktionen ausgeschaltet werden. Bereits die Verwendung geringer Konzentrationen an LNA-*Antiseeds* zeigte in humanen Krebs-Zelllinien eine nahezu vollständige Inhibition onkogener miRNAs der miR-106b Familie, die durch eine Steigerung der endogenen Derepression des Tumorsuppressors P21 gezeigt wurde. Eine erfolgreiche Verpackung der neuartigen LNA-basierten miRNA Inhibitoren mit dem verzweigtkettigen Polyethylenimin PEI F25 LMW sowie die funktionelle Aufnahme der gebildeten Nanopartikel in humane Krebszelllinien konnte in weiteren *in vitro*-Experimenten gezeigt werden. Der Einsatz von PEI F25 LMW komplexierten LNA-*Antiseed* miRNA-Inhibitoren könnte nun auch in Xenograft-Tumor-Modellen der Maus als ein erfolgversprechender Ansatz einer *Antisense*-Therapie getestet werden.

Im dritten Themenkomplex dieser Arbeit wurde die transkriptionelle Regulation des onkogenen miRNA Clusters miR-17-92 untersucht. Eine Überexpression dieses Clusters ist mit gesteigerter Proliferation, Angiogenese und verminderter Apoptose assoziiert und wird in zahlreichen hämatopoetischen und soliden Tumoren beobachtet. Die Transkription von miR-17-92 wird dabei maßgeblich durch das Onkogen MYC reguliert. *In vitro*-Experimente in humanen Krebs-Zelllinien zeigten, dass auch der miR-17-92 Cluster zu jenen 20 % aller MYC regulierten Gene gehört, dessen Transkription durch einen Synergismus zwischen MYC und PIM1 gesteuert wird. Weitere Untersuchungen hinsichtlich der transkriptionellen Regulation von miRNA Promotoren könnten zukünftig dazu beitragen, die Zusammenhänge zwischen miRNA-Expression und der Entstehung von Krebs näher zu charakterisieren.

Abstract

Cancer is a chronic disease caused by a degeneration of somatic cells due to mutations. In general cells grow erratic and under certain conditions this leads to an infiltration of even healthy tissues. To date cancer is the second most common cause of death in the Western world and belongs to one of the most important epidemiological diseases of our society. Besides traditional methods in cancer treatment such as resection of tumor tissue, chemo- or immunotherapy, the development of novel therapeutic strategies is of the highest importance. One therapeutic option would include the use of small non-coding regulatory RNAs such as miRNAs. MiRNAs are involved in the regulation of crucial biological processes such as development, differentiation or proliferation due to the control of the cell's gene expression via RNA interference. Since the discovery of miRNAs, evidence has emerged that they can exert either tumor-suppressive or oncogenic functions. Thus miRNAs are not only applied as diagnostic or prognostic biomarkers of cancerous tissues, but can also function as therapeutics. In miRNA replacement therapy a loss or downregulation of a tumor-suppressive miRNA is adjusted with addition of this single miRNA. On the contrary an antisense therapy approach mediates the inhibition of oncogenic miRNAs by antisense oligonucleotides. Safe and efficient delivery of the oligonucleotides has to be guaranteed for both approaches. Currently the development of such efficient delivery systems is the critical and limiting factor upon miRNA-based therapy designs.

In this thesis the proto-oncogene PIM1 was considered regarding a putative RNA-based anti-cancer strategy. Overexpression of PIM1 kinase usually is associated with severe forms of cancers with bad prognosis in several solid tumors or malign degenerations of the hematopoietic system. *In vitro* studies revealed a specific reduction of PIM1 protein levels in human leukemia and colon carcinoma cell lines due to a miRNA with tumor-suppressive potential, namely miR-33a. Additionally this decrease in PIM1 resulted in an inhibition of proliferation. Successful delivery with nanoparticle complexes composed of miR-33a oligonucleotides and a non-toxic branched polyethylenimine (PEI F25 LMW) showed an anti-tumor effect in mouse colon carcinoma models that was obtained through a reduction in tumor size. These *in vitro* and *in vivo* studies provide evidence for the first time that the proto-oncogene PIM1 is a promising target for miRNA replacement therapy.

The second project dealt with the development of novel LNA-based miRNA inhibitors, termed LNA antiseeds, composed of single-stranded RNA oligonucleotides with *locked nucleic acid* (LNA) modifications and a natural phosphodiester backbone. In general an LNA design enhances the resistance of oligonucleotides against cellular degradation by nucleases.

Furthermore affinity of the molecule to the miRNA of interest is increased. Cellular functions of the targeted oncogenic miRNAs are silenced due to complementary binding to the inhibitor. A use of minor amounts of LNA antiseeds already revealed an almost complete inhibition of miRNAs of the miR-106b family in human cancer cell lines which was connected to an endogenous derepression of the tumor suppressor P21. Successful complex formation of the novel LNA antiseeds with the branched polyethylenimine PEI F25 LMW has been proven. Furthermore *in vitro* experiments confirmed a functional delivery of the resulting nanoparticles into human cancer cell lines. Application of PEI F25 LMW complexed LNA antiseed miRNA inhibitors could now be tested as a promising antisense therapy approach in xenograft tumor mouse models.

The third topic addressed the transcriptional regulation of the oncogenic miRNA cluster miR-17-92. Overexpression of this miRNA cluster is associated with enhanced proliferation, sustained angiogenesis and reduced apoptosis in several hematopoietic malignancies and solid tumors. Transcription of human miR-17-92 is significantly regulated by the oncogene MYC. *In vitro* experiments in human cancer cell lines confirmed that miR-17-92 belongs to one of those 20 % of MYC regulated genes which transcription is controlled by a synergism of MYC and PIM1. Further investigations regarding transcriptional control of miRNA promoters could provide profound evidences for a better understanding of a connection between miRNA expression levels and the development of cancer.

Publications

This thesis is based on the following publications which in the text will be referred to by their Roman numerals:

I Thomas M, Lange-Grünweller K, Weirauch U, Gutsch D, Aigner A, Grünweller A and Hartmann RK: **The proto-oncogene Pim-1 is a target of miR-33a.** *Oncogene (2012)*, *31*, 918-928

II Ibrahim AF, Weirauch U, Thomas M, Grünweller A, Hartmann RK and Aigner A: **MicroRNA Replacement Therapy for miR-145 and miR-33a Is Efficacious in a Model of Colon Carcinoma.** *Cancer Res (2011)*, *71*, 5214-5224

III Thomas M, Lange-Grünweller K, Dayyoub E, Bakowsky U, Weirauch U, Aigner A, Hartmann RK and Grünweller A: **PEI-complexed LNA antiseeds as miRNA inhibitors.** *RNA Biology (2012)*, *9(8)*, 1088-1098

IV Thomas M, Lange-Grünweller K, Hartmann D, Golde L, Schlereth J, Aigner A, Grünweller A and Hartmann RK: **Pim-1 Dependent Transcriptional Regulation of the Human miR-17-92 Cluster.** *Manuscript in preparation*

Contents

1 Introduction

1.1 Cancer

Cancer is defined as a chronic disease (1) and includes more than 100 distinct types and subtypes of malignancies found within different organs (2). In general cancer is known as a malignant neoplasm which develops as a clone from one single cell of origin (3) after one or more oncogenic events have occurred (Figure 1).

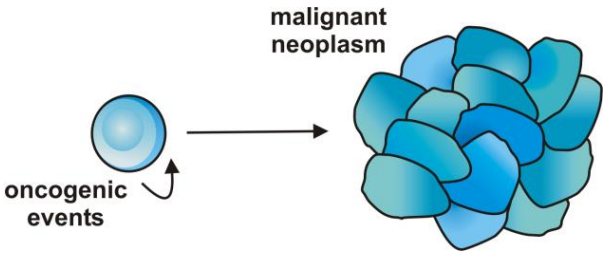

Figure 1: Formation of a malignant neoplasm. A malignant neoplasm generates after several oncogenic events have occurred (following Visvader, 2011 (4)).

Since the ancient Egyptian time period, malignant diseases have awoken the interests of scientists; in particular to clarify their origins and to understand more about molecular mechanisms, prevention, etiology, pathogenesis and treatment of cancer (5). The treatment of tumors was described in ancient Egyptian and Greek literature and the histological diagnosis of cancer in an Egyptian mummy (6) provided evidence that this disease is not only a current problem. Thus to treat cancer it is important to understand the underlying molecular mechanisms in order to predict how a neoplasm will evolve. Then we maybe will have the ability to interfere with and disrupt the clonal evolution of a neoplasm to prevent cancer formation. Even if initiation of a neoplasm cannot be prevented, early detection and correct diagnosis of malignant cancer will probably lead to increased cure rates (7). Therefore it is necessary to classify tumors and differentiate between benign and malignant instances. Whereas benign tumors are not cancerous and do not spread out in the body, malignant neoplasms are characterized by their ability to invade nearby tissues and organs, also known as metastasis (8), (9). In general tumors are classified in various categories depending on the cell type or tissue they evolve from. For instance a carcinoma is defined as a tumor beginning in any internal organ, leukemia is a cancer that arises from hematopoietic cells and a lymphoma or myeloma derives from cells of the immune system (9). In Germany approximately 470,000 new cases of cancer were estimated in 2008 by the Robert Koch Institute (10). The causes of cancer are multiple and can be assigned to environmental

factors like diet or smoking, reproductive and sexual behavior, geophysical factors, occupational exposures, medicine and/or infections (11), (12).

1.1.1 Carcinogenesis

In literature carcinogenesis is described as the formation and development of cancer. It is characterized by a progression of changes on genetic and cellular levels. Reprogramming of a cell leads to uncontrolled cell division, thus forming a malignant neoplasm. The cause of cancer development is diverse and only in a few cases is it caused by one single factor (2). In general, 3-12 (or even more) physiological relevant mutations are required to form a malignant neoplasm (13) (Figure 1). The accumulation of mutations during a cell's lifetime is called somatic evolution (3), (7). At the cellular level, a selection benefit exists for increased cell proliferation and survival for those cells harboring a competitive advantage in at least one of six essential alterations: (i) self-sufficiency in proliferative signals, (ii) insensitivity to growth suppressors, (iii) tissue invasion and metastasis, (iv) limitless replicative potential, (v) sustained angiogenesis and (vi) the evasion of programmed cell death (2) (Figure 2).

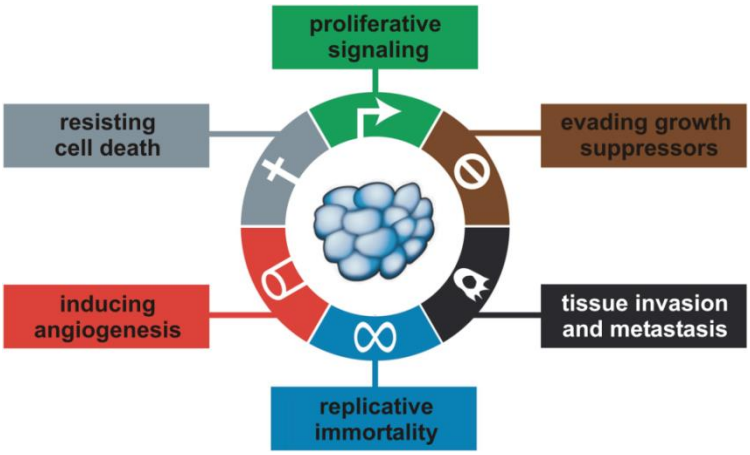

Figure 2: Selection benefit of cancer cells. Most cancers have acquired a selection benefit during their development mediated through one of those six mechanistic strategies (following Hanahan & Weinberg, 2011 (1)).

All of the aforementioned biological properties are additionally accelerated by genomic instability (2). Capabilities such as proliferation and immortality that allow cancer cells to survive are complemented by the inflammatory state of the cell, autophagy, necrosis or the reprogramming of the cell's energy metabolism (1). Furthermore the growth advantage and increased survival of the tumor is a consequence of chromosomal rearrangements, mutations and gene amplifications caused by the inactivation of tumor suppressor genes (14) or the activation of oncogenes (15). A tumor suppressor gene, a so-called anti-oncogene, is a gene that encodes for a protein which blocks the development of cancer in the cell e.g. by

the regulation and/or control of cell division or by initiation of apoptosis (16). In contrast an oncogene is a gene that has the potential to cause cancer and evolves by e.g. the mutation or overexpression of a proto-oncogene, and thus becomes activated (17). In general oncogenes can be subdivided into six major groups: (i) chromatin remodelers, (ii) transcription factors, (iii) growth factors, (iv) growth factor receptors, (v) signal transducers and (vi) apoptosis regulators (15). Likewise, small non-coding RNAs (ncRNAs), in particular the class of microRNAs (miRNAs), are associated with tumor development (18). It has been reported that even half of all annotated miRNAs map within fragile chromosomal regions that can be linked to human cancer (19).

1.1.2 Treatment of cancer

Due to the fact that cancer is the second most common cause of death (5) in the Western world, treatment of malignant neoplasms is of the highest importance. Although crude cancer surgery took place in the ancient Egypt (5), the establishment of radiation by Emil Grubbe in 1957 (20), followed by subsequent research, means that nowadays treatments are much more focused on individual patients (21). New healing procedures, earlier diagnosis of cancer and 'personalized' therapy are the first steps of translating cancer research into targeted therapeutics (22). Such molecular techniques (23) include the development of small molecules, peptide mimetics, monoclonal antibodies (mABs) and antisense oligonucleotides (24). Several mABs and small molecule compounds have now been approved for cancer therapy (24). In general mABs show significant promise due to their low toxicity profiles in clinical studies (25). Moreover they are well-tolerated compared with conventional chemotherapeutic agents (25). Since miRNA expression profiles are used to classify tumors (26) based on the tissue type and/or stage of disease (27), (18) one promising therapeutic strategy is miRNA-based therapy (18) which has been successfully established using *in vivo* animal models thus far (28) and already has been tested in clinical trials (29).

1.2 RNA interference and miRNAs

1.2.1 Discovery of miRNAs

RNA interference (RNAi), a form of post-transcriptional gene silencing (30), was first described in 1998 by Fire and Mello (31) in the worm *C. elegans*. RNAi, which is thought to be the oldest and most ubiquitous cellular antiviral defense system, is a biological process in which small non-coding double-stranded RNA molecules interfere with messenger RNAs (mRNAs) to inhibit gene expression (32). Before the discovery of RNAi, the gene *lin-4* was

found in 1993 by Ambros and Lee in *C. elegans* (33). Cel-*lin-4* codes for two small transcripts of ~61 and 22 nt which show complementarity to a sequence located in the 3'-UTR of Cel-*lin-14* (33). Later on the Cel-*lethal-7* (Cel-*let-7*) gene was described. It encodes a 21 nt long RNA transcript that has been shown to regulate the expression of several genes which are involved in the timing of developmental transition in *C. elegans* (34). These findings preceded a new class of small non-coding regulatory RNAs being described - microRNAs (miRNAs) (35), (36), (37). To date more than 15,000 miRNA gene loci are annotated and expressed in over 140 different species and organisms (38). In mammals ~2000 miRNAs (38) represent about 1 % of the human genome (39). MiRNAs are able to target dozens or even hundreds of different mRNAs to regulate and fine-tune the cellular expression of about 50 % of all protein-coding genes (40). This regulation takes place in almost all biological processes and is important for genome functions such as chromosome segregation, transcription, RNA stability, RNA processing, and translation (41). Furthermore, miRNAs play crucial roles in cellular processes; they are involved in development, proliferation, differentiation, the stress response and apoptosis (39).

1.2.2 Genomics, biogenesis and mechanism of miRNAs

In general miRNAs are encoded in the genome and can be subdivided into intergenic, intronic or exonic genomic organized miRNAs (42) (Figure 3). Intergenic miRNAs are found in genomic regions which are not part of known functional transcription units (TUs). They are generally monocistronic or polycistronic and have their own promoter and/or other regulatory elements (43) and a primary miRNA (pri-miRNA) transcript length of several kb (44). About 50 % of all known miRNA genes are encoded within TUs (45) (either protein-coding or non-coding (35)), and are termed intronic miRNAs. Intronic miRNAs themselves can be transcribed either by the host gene promoter or an own promoter element as single or clustered pri-miRNA transcripts (46). In some special cases, a whole intron acts as a pri-miRNA transcript and therefore is called mirtron. This pri-miRNA is recognized and processed by the splicing machinery (47). Exonic located miRNAs are very rare and overlap with exons of ncRNAs (42). The transcription of miRNA genes is a complex process that until now has been only poorly understood (48).

The biogenesis and generation of mature miRNAs can be divided into several processing steps (Figure 3).

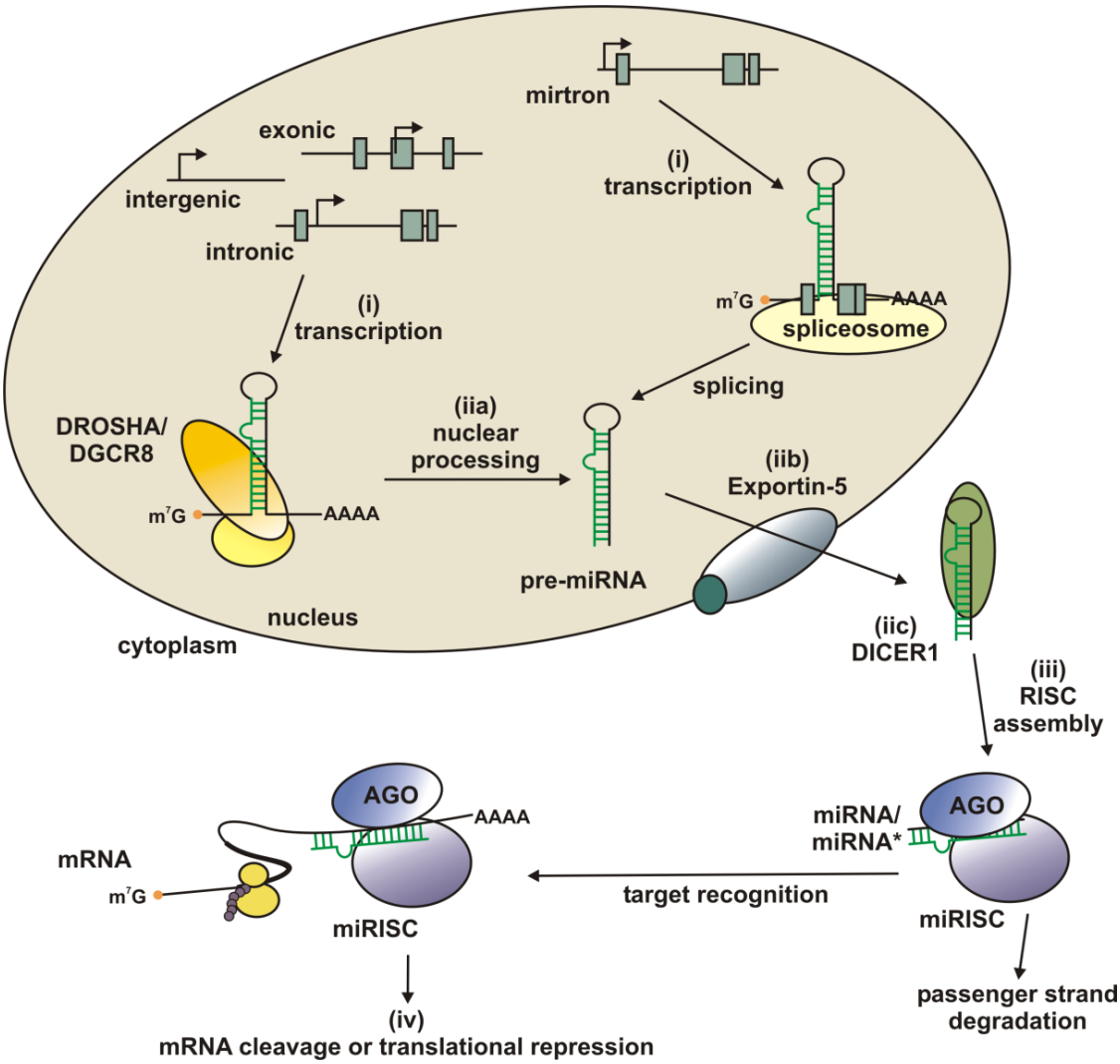

Figure 3: Biogenesis of miRNAs. (**i**) Transcription of exonic, intergenic or intronic miRNA genes is followed by (**iia**) nuclear processing of the pri-miRNA transcript by the microprocessor complex (DROSHA/DGCR8) generating the pre-miRNA. (**i**) Transcription of a mirtron is performed by the spliceosome generating a pre-miRNA transcript. (**iib**) The pre-miRNA is actively exported into the cytoplasm by Exportin-5 using RAN-GTP. (**iic**) In the cytoplasm the pre-miRNA is processed by the RNase III enzyme DICER1 into the double-stranded miRNA/miRNA*. (**iii**) Passenger strand degradation follows the incorporation of the miRNA/miRNA* duplex into the miRISC complex. (**iv**) After target recognition of the miRNA binding site in the 3'-UTR of an mRNA, translational repression and/or mRNA cleavage occurs mediated by proteins of the AGO family.

Firstly, (i) transcription of the miRNA gene has to occur followed by (ii) several maturation steps, then (iii) the RNA-induced silencing complex (RISC) assembly has to form (49) before finally (iv) mRNA cleavage or translational repression can take place. (i) Transcription of partially long pri-miRNA transcripts (49) is dependent on RNA polymerase II (POLR2) based on the findings that these primary transcripts contain cap-structures as well as poly(A) tails (48) which are classical signals for POLR2 transcription maturation. (ii) The first maturation step in human miRNA processing is initiated by the microprocessor complex (50) composed

of the nuclear RNase III enzyme DROSHA (51) associated with DiGeorge syndrome chromosomal region 8 (DGCR8) protein (52). In this step the longer primary transcript is cleaved into an approximately 70 nt long precursor miRNA (pre-miRNA) (43) which folds into a defined stem-loop structure (35) harboring a 5'-phosphate and a 2 nt overhang on the 3'-OH terminus (53). The pre-miRNA afterwards is exported from the nucleus into the cytoplasm. This active transport process is mediated by the export receptor XPO5 termed Exportin-5 using RAN-GTP (54), (55) and is triggered by the matured stem-loop structure (56). The second end of the precursor miRNA is processed in the cytoplasm by the RNase III endonuclease Dcr-1 homolog (Drosophila) (DICER1) (57), (58), (51) generating again a 5'-phosphate and a 2 nt overhang on the 3'-OH terminus on the opposite site (49) of the miRNA. Thus a short (approximately 22 nt long) duplex termed miRNA/miRNA* is formed (37). (iii) The RISC assembly follows DROSHA cleavage, nucleocytoplasmic export and cytoplasmic DICER1 cleavage. Several proteins of the argonaute family (argonaute RISC catalytic component 1-4, AGO 1-4) are part of this miRNA-induced silencing complex (miRISC) including its catalytic core (59), (60), (61). The strand of the miRNA duplex with its 5'-end less tightly paired (62) (and thus shows higher thermodynamic instability) enters the miRISC complex and generates the mature and functional miRNA (63), (64), (59). The miRNA* strand of the matured duplex is degraded (65). Subsequently the miRISC complex leads to post-transcriptional gene silencing via target recognition of mRNAs in the cytoplasm. Post-transcriptional gene silencing can happen by two different mechanisms depending on the identity of the target: (i) mRNA cleavage or (ii) translational repression (49). (i) Cleavage of an mRNA occurs if the miRNA has sufficient complementarity to the mRNA. The cleavage site appears between the nucleotides pairing to residues 10 and 11 of the miRNA (59). (ii) After the discovery of miRNAs it was proposed that miRNAs modulate post-transcriptional gene expression via translational repression (66). The most efficient translational inhibition is provided by a cooperative mechanism (67) and specific target selection of miRNAs (68). The ability to translationally repress a target mRNA mostly depends on perfect Watson-Crick base pairing of the miRNA's *seed* region (69), mainly the first 8 nt on the 5'-end of the mature miRNA. In some cases additional pairing of the 3'-end of the miRNA is needed (69). It was recently discovered that miRNAs can also target other genomic regions such as 5'-UTRs (70), coding regions (71) or promoter elements (72) after their import into the nucleus (73). All findings implicate the important regulatory mechanisms of this class of small non-coding RNAs and demonstrate the enormous ability of these post-transcriptional gene regulators to intervene in the pathogenesis of human cancers (74) by targeting either tumor suppressor genes or oncogenes.

1.2.3 MiRNAs associated with cancer

Since the discovery of miRNAs, evidence has emerged that miRNAs can function as tumor suppressors or as oncogenes, by blocking or activating the cell's malignant potential respectively, and are therefore referred to as oncomiRs (19), (74). Their role in cancer development is based on three important observations (75). Firstly, they are involved in cell proliferation and apoptosis (33) and can affect all other stated hallmarks of cancer such as tissue invasion or metastasis (74). Secondly, miRNAs are frequently located at fragile regions of chromosomes (76). Thirdly, miRNA expression is deregulated in several malignant tumors (77).

In 2002 it was reported for the first time that miRNAs are deregulated and as a result are involved in the development of human cancer (78). A deletion of a 30 kb region on chromosome 13q14, encoding the miRNA genes of miR-15a and miR-16-1, or a down regulation of these miRNAs is associated with B-cell chronic lymphocytic leukemia (B-CLL) (79). Additionally it has been found that those two miRNAs act as tumor suppressors and induce apoptosis by targeting the oncogene B-cell lymphoma 2 (BCL2) (80). Ongoing studies and miRNA profilings of human cancers have revealed cell type and tissue specific signatures of miRNAs (39). MiRNAs, which had overall higher expression levels, were identified as oncogenic miRNAs that generally repress tumor suppressor genes. As an example, miR-155 overexpressed in B-cell lymphomas (81) has been reported to target the suppressor of cytokine signaling (SOCS) proteins (82). Another miRNA, oncogenic miR-21, is overexpressed in breast cancer (83) and targets several tumor suppressor genes like phosphatase and tensin homolog (PTEN) (84), BCL2 (85) and tissue growth factor beta (TGFB) (86) mediating cell survival, proliferation and differentiation of cells. Further important oncogenic miRNAs are encoded in the miR-17-92 polycistron (87) and are described to be involved in several cellular processes such as proliferation or angiogenesis (88). Several miRNAs are transcriptionally induced by tumor suppressors or oncogenes (78). The tumor protein 53 (TP53) induces the transcription of the miR-34 family in response to DNA damage (89), (90) and v-myc myelocytomatosis viral oncogene homolog (avian) (MYC) protein, a classical oncogene, transcriptionally activates the expression of the oncogenic miRNAs miR-17-92 (91) or represses the transcription of tumor-suppressive miRNAs like let-7 (92). An increased risk of cancer formation is also associated with mutations and/or single nucleotide polymorphisms (SNPs) in miRNA binding sites of oncogenes such as the Kirsten rat sarcoma viral oncogene homolog (KRAS) protein (93) regulated by miRNA let-7. These multiple functions of miRNAs in carcinogenesis implicate that miRNAs are

considerably beneficial as diagnostic and prognostic biomarkers to differentiate between malignant and benign forms of tumors (77), (94), (95).

1.3 MiRNAs as cancer therapeutics

In the last decade two major findings have established the use of miRNAs as an anti-cancer therapy: (i) miRNA expression differs in cancerous and normal tissues (79), (96), (81), (97) and (ii) a change in the cancer's phenotype can be caused by targeting miRNA expression (98), (99), (100). As previously mentioned miRNAs are involved in the post-transcriptional gene regulation of several genes being part of a large cellular regulatory network (100). Thus an enormous advantage of miRNA-based therapeutic strategies in the cancer treatment is the ability of miRNAs to target multiple genes which are connected to distinct biological cellular processes in different molecular pathways such as normal or malignant homeostasis (89), (101). A modification of the miRNA expression levels in cancer tissues to restore normal homeostasis is possible because miRNAs show key functions in the coordination of the whole cancer network (100). To address the pharmacological modulation of cancer-associated miRNAs there are two possible strategies available: (i) use of drugs that allow the modulation of miRNA expression e.g. blocking their processing in the cellular system (102), or (ii) a direct regulation of miRNA expression levels by either the substitution of less expressed tumor suppressor miRNAs (called miRNA replacement) (103), (28) or the inhibition of oncogenic miRNAs by antisense oligonucleotides (104).

1.3.1 Strategies to restore tumor-suppressive miRNAs

Restoring a lost or downregulated tumor-suppressive miRNA, which targets an oncogene, can be modulated by miRNA replacement therapy. An enhanced expression of the miRNA can either be mediated by (i) virus-associated vector systems or (ii) the introduction of synthetic oligonucleotides, termed miRNA mimics. (i) In the case of using vector systems the miRNA gene of interest is packed in the virus and expressed after transduction into cells or tissues. Viral vector-based systems, including adenovirus-associated (AAV) or lentivirus-associated vectors (LAV), have a high transduction efficiency of target cells, but there might be a residual risk of viral infections for treated patients (105). In 2009 it was shown that an AAV-mediated delivery successfully increased the expression of tumor-suppressive miR-26a in a murine liver cancer model and suppressed tumorigenesis without measurable toxicity (106). (ii) MiRNA mimics are usually double-stranded molecules. The guide strand is identical to the selected miRNA of interest whereas the passenger strand is chemically modified at the 5'- and 3'-termini to avoid loading into the miRISC complex

(105). For delivery of miRNA mimics, they have to be formulated for their uptake into cellular systems. Recently restoring of several downregulated tumor-suppressive miRNAs has been successfully tested to reduce tumor growth in mouse cancer models (28), (107).

The advantage of miRNA replacement therapy is that a restored miRNA has the same sequence as the deleted or downregulated miRNA of interest, and thus is expected to target the identical set of mRNAs (108). As a consequence, miRNA replacement therapy offers the possibility of recovering those cellular programs which are active in normal cells. Cellular pathways that are necessary for the generation of a malignant tumor are switched by re-introduction of tumor-suppressive miRNA mimics (108), hopefully without any side effects. MiRNA replacement has emerged as a promising therapy in the treatment of cancer, particularly because of an overall lower expression of miRNAs in tumor versus normal tissues (77).

1.3.2 Strategies to inhibit oncogenic miRNAs

Effective inhibition of oncogenic miRNAs can be achieved using anti-miRNAs in the treatment of cancer. In general those anti-miRNAs are single-stranded antisense oligonucleotides, termed antimiRs, which are complementary to the miRNA of interest. AntimiRs are used to sequester oncogenic cellular miRNAs leading to their functional inhibition (109). However the ability of the miRNA to repress endogenous target mRNAs of e.g. tumor suppressors is prevented by several cellular mechanisms (105). To reach the best possible resistance against cellular nucleases and to increase the binding affinity to the miRNA, the antisense oligonucleotides have to be chemically modified including modifications in (i) the internucleotide linkages and/or (ii) the sugar (109). (i) In phosphorothioate modified oligonucleotides a sulfur atom replaces one of the non-bridging oxygen atoms in the phosphate group of the backbone linkage; this modification leads to improved nuclease stability as well as an increased binding to plasma proteins (110). (ii) The most commonly used modifications in antimiR design are several variations in the 2'-sugar position (Figure 4).

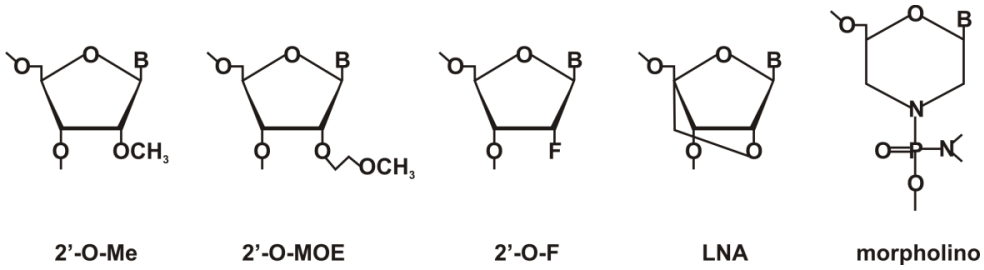

Figure 4: Modifications of antimiRs. Schematic overview of antisense oligonucleotide modifications including a 2'-O-methyl (2'-O-Me), a 2'-O-methoxyethyl (2'-O-MOE), a 2'-fluoro (2'-F), a locked nucleic acid (LNA) or a morpholino modification.

The first sequence-specific inhibition of let-7 miRNA function was demonstrated using a 2'-O-methyl (2'-O-Me) modified antisense oligonucleotide (111). To date several other modifications have been described such as 2'-O-methoxyethyl (2'-O-MOE), 2'-fluoro (2'-F) or locked nucleic acid (LNA), a class of bicyclic RNA analogues (112). In LNA the ribose is locked in a C3'-endo conformation by introduction of a methylene bridge between the 2'-oxygen and the 4'-carbon of the sugar. This modification results in an increased affinity towards the complementary miRNA of 2 to 8 °C per introduced LNA modification (113), (114), (115). Morpholino oligomers are another modification. In these uncharged molecules the ribose moiety is exchanged for a six-membered morpholino ring (116). This antimiR design has been successfully tested in zebrafish models to target pri-miRNAs and miRNAs. In this study, morpholino-modified antisense oligonucleotides acted sequence-specific and non-toxic (117). Beneath an increase of target affinity, all antimiRs with variations in the ribose moiety show nuclease resistance and delayed degradation in the cellular system (109). Presently, approaches to block and inhibit oncogenic miRNAs with antimiRs of different designs hold a lot of promise as anti-cancer drugs. Further establishment of anti-miRNA treatments may open new ways in combination therapies to modulate or even cure cancer.

1.3.3 Delivery and perspective of miRNA-based therapeutics

For the establishment of (i) miRNA replacement therapies or (ii) antimiR strategies to inhibit miRNAs, the delivery of the oligonucleotides into cells, tissues and/or organs is the major bottleneck. A safe and efficient delivery of these molecules is the critical factor upon development of miRNA-based therapeutics. (i) In case of miRNA replacement therapy either viral vector-based systems (107) or formulated, double-stranded miRNA mimics (28) shall gain the loss of the respective miRNA (Figure 5). To date several studies have implicated the promising possibility of miRNA replacement therapy in the treatment of cancer. Several

downregulated tumor-suppressive miRNAs have been successfully re-introduced into cells and/or tissues to decrease tumor growth in mouse models. MiRNA replacements of the let-7 miRNA (118) or miR-34 (119) have been described to act as cancer therapeutics in murine lung cancers; the systemic delivery of miR-16 inhibits the growth of metastatic prostate tumors (120) and miRNA replacement therapy of miR-145 and miR-33a mimics are efficacious in a model of colon carcinoma (28). An optimized formulation for efficient and safe *in vivo* delivery of miRNA mimics in mouse cancer models has been shown for intravenous (121), intratumoral (28), intraperitoneal (28) and intranasal (107) application so far (105). The delivery of miRNAs has been done by using liposome nanoparticles (122), atelocollagen (120) or polyethyleneimine (28) implicating a formulated antimiR delivery. (ii) To date several antimiR designs (Figure 5) have been established either *in vitro* or *in vivo* (123). In 2005 a novel class of antisense oligonucleotides, termed antagomiRs, was described (124). These antagomiRs are 3'-cholesterol-conjugated single-stranded 2'-O-Me oligonucleotides complementary to the miRNA of interest. Pharmacological inhibition was shown for e.g. miR-16 or miR-122. Furthermore the cholesterol conjugation was found to improve cellular uptake of these molecules *in vivo* (124). Another *in vivo* delivery approach has been described for unconjugated, phosphorothioate modified antisense oligonucleotides (125), (126) targeting oncogenic and liver-specific miR-122. Either longer oligonucleotides which are comprised of DNA and LNA modifications (125) or short 8-mer *tiny LNAs* (126) exhibit good tissue uptake and good pharmacokinetic properties *in vivo* (105). A recent *in vitro* study also described polyethyleneimine formulated 14-meric *LNA* antiseeds as promising miRNA inhibitors (104). This approach enables the possibility to target even whole miRNA families characterized by the same nucleotides in the *seed* region of the miRNA (104).

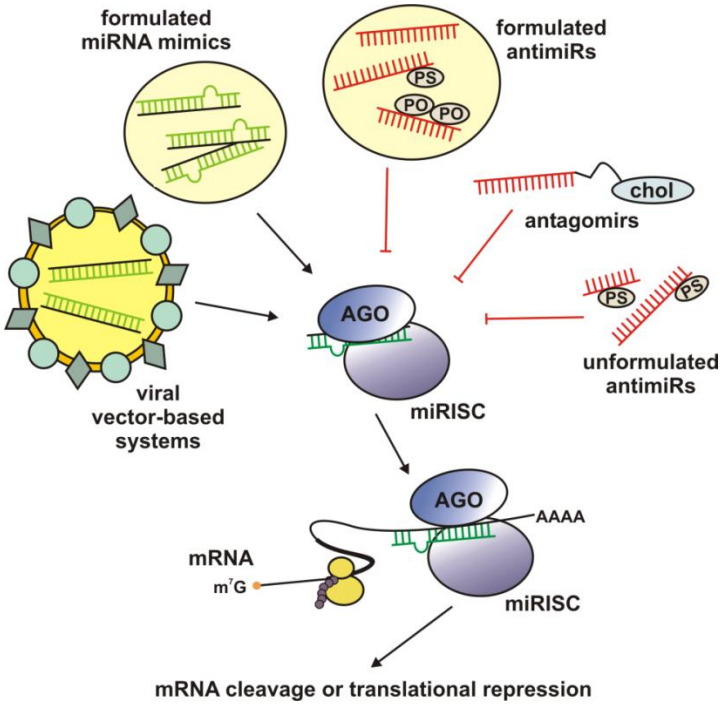

Figure 5: Design of miRNA-based therapeutics. MiRNA-based therapies can be divided into miRNA replacement therapy to restore a loss of a miRNA mediated by viral vector based systems or formulated miRNA mimics (black arrows) or an antimiR design such as antagomiRs, formulated or unformulated antimiRs (red line) to inhibit cellular functions of oncogenic miRNAs.

The development of novel anti-cancer therapeutics holds great promise and the first miRNA-based therapeutic has reached clinical trials (105). This therapeutic is an LNA-phosphorothioate-modified miRNA inhibitor against miR-122, termed *miravirsen* (29). MiR-122 is specifically expressed in the human liver and plays a role in the modulation of cholesterol homeostasis (127). Besides it facilitates RNA replication of the hepatitis C virus (HCV) following infection of humans (128). In 2012 *miravirsen* was tested in HCV-infected human patients for the first time. Its application is well-tolerated and shows long-lasting suppression of viremia (29). The design and development of miRNA-based therapeutics is opening up new possibilities for the treatment of cancer and may become a powerful therapeutic strategy in combination therapies if standard treatment approaches are unsuccessful due to chemo-resistance, metastasis and/or recurrence of the tumor (129).

1.4 Analyzed oncogenes

1.4.1 The human PIM1 kinase

The *PIM1* gene was identified in 1984 as a proto-oncogene in several mouse tumor models. In murine leukemia virus (MuLV)-induced lymphomas, transcriptional activation of the *PIM1* gene was associated with a proviral insertion into a quite small chromosomal region (130) within the *PIM1* domain. In general the PIM kinases (PIM1, PIM2 and PIM3 (131), (132)) belong to a family of constitutively active serine/threonine kinases with several cellular targets (133). They are naturally expressed in several tissues such as bone marrow, thymus, spleen, prostate or hippocampus (134) being involved in e.g. T-cell activation (135) or fetal hematopoiesis (136). They play crucial roles in the process of malignant transformation even in human cancer (137) because they are associated with proliferation, differentiation, apoptosis and tumorigenesis (138). Overexpression of PIM kinases is correlated with a very poor prognosis in a wide range of hematopoietic malignancies such as mantle cell lymphoma or non-Hodgkin's lymphoma and solid cancers such as prostate cancer (139), (140). To study the physiological effects of PIM kinases, *PIM* knockout mice have been generated. It was shown that *PIM1* deficient mice grow almost normally, but show a specific defect in interleukin (IL)-3 and -7-dependent growth of pre-B-cells and mast cells (141), (142). Triple knockout mice, with PIM1, PIM2 and PIM3 deficiencies, are viable and fertile, but have obviously manifested a phenotype showing reduction of body size and moderate defects in growth factor signaling and T-cell proliferation (132). In humans the *PIM1* gene is located on chromosome 6p21.1-p21.31, a region of approximately 5 kb harboring six exons and five introns. The mRNA transcript (NM_002648) has a length of 2684 bp (137) and produces two proteins of 34 and 44 kDa due to an alternative translation initiation at an upstream CUG codon (143) (Figure 6a). PIM1 expression is tightly controlled by (i) transcriptional, (ii) post-transcriptional, (iii) translational and (iv) post-translational regulation (138) (Figure 6b). Transcriptional activation of the *PIM1* gene is dependent on several growth factors, hormones or cytokines such as GM-CSF, prolactin and IL-3, -5, -7 or -12 that activate the signal transducer and activator of transcription 3 and 5 (STAT3/STAT5) (137), (138). (ii) Post-transcriptional regulation of PIM1 is associated with miRNA binding. It has been reported that miR-1 (144), miR-33a (103) and miR-328 (145) target the 3'-UTR of *PIM1* mRNA and modulate and/or decrease protein expression. (iii) Translation of the *PIM1* mRNA is shown to be cap-dependent (146) because of long GC-rich destabilizing regions in the 5'-UTR of *PIM1* mRNA. Furthermore it was reported that translation is regulated by the eukaryotic translation initiation factor 4E (EIF4E) binding to an EIF4E sensitivity element in the *PIM1* 3'-UTR which mediates nuclear export and enhances

translation (147). (iv) The first evidence that the PIM1 protein is post-translationally regulated arose from variable turnover rates of the different protein isoforms (34 and 44 kDa isoform) showing half-lives of approximately 1 h and 10 min, respectively (138). PIM1 is able to activate itself by autophosphorylation on serine 8 and 190 (S8, S190) residues (137). The kinase is stabilized by heat shock protein 90 (HSP 90) (148); a decrease of PIM1 protein levels is catalyzed by the protein phosphatase 2A (PP2A) (149), followed by ubiquitination and degradation of PIM1 in the proteasome. Many phosphorylation targets of PIM1 have biological functions associated with cell cycle progression and apoptosis (137) such as the cyclin-dependent kinase inhibitors CDKN1A (in the following termed P21) (150) and CDKN1B (P27) (151), the cell division cycle 25A (CDC25A) (152) and C (CDC25C) (153) proteins or the pro-apoptotic protein BCL-2 associated agonist of cell death (BAD) (154). Another phosphorylation target of PIM1 is the chromobox homolog 3 (CBX3) protein, also referred to as heterochromatin protein 1 gamma homolog (Drosophila) (HP1G) which is associated with transcriptional repression via chromatin silencing (155) or gene activation being localized with elongating POLR2 (156). Furthermore PIM1 phosphorylation mediates stabilization of the oncogene MYC and thereby enhances transcriptional activity (157). A strong synergism of MYC and PIM1 has been established in tumorigenesis of transgene mice (158). MYC was shown to recruit PIM1 to MYC/MYC-associated factor X (MAX) complexes which are associated with enhancer box elements (E-boxes) in enhancer segments of euchromatin regions, followed by PIM1 mediated phosphorylation on histone 3 serine 10 (H3S10) residues to induce gene expression (159).

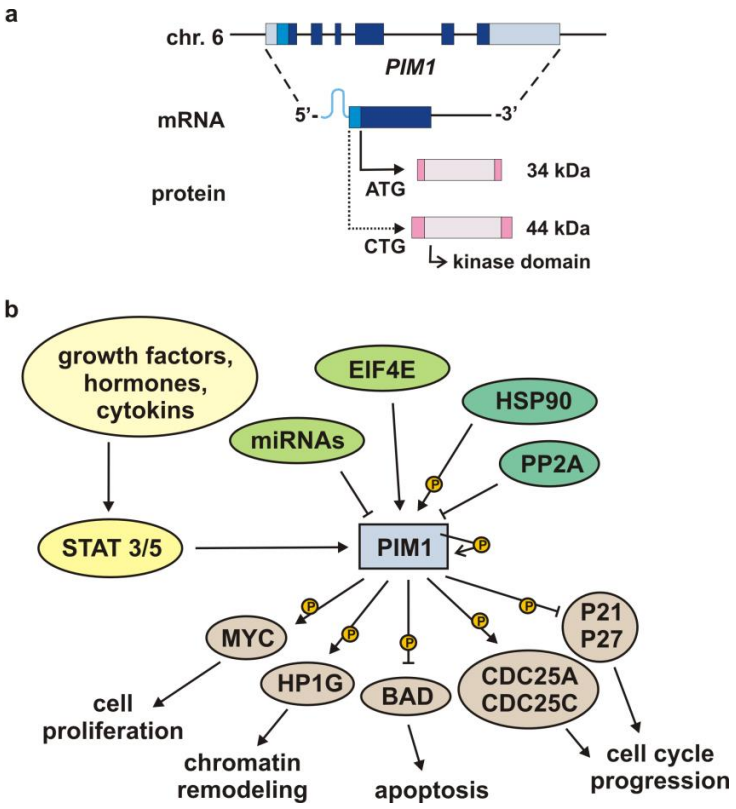

Figure 6: Regulatory network of PIM1. (**a**) *PIM1* gene, transcript and proteins. The human *PIM1* gene is located on chromosome 6 and encodes six exons (dark blue boxes) with large 5'- and 3'-UTRs containing GC-rich regions (light blue area). The two protein isoforms are synthesized using alternative translation initiation sites (solid and dashed arrows); additional codons are present at the 5'-end of the mRNA (light blue box). PIM proteins have different molecular masses and their kinase domain is indicated by a white box (following Nawijn, Alendar & Berns, 2011 (133)). (**b**) Involvement of PIM1 in signal transduction pathways. The expression of PIM1 is directly regulated by STAT3/5 induced by growth factors hormones or cytokines (light yellow ovals). Post-transcriptional regulation of *PIM1* mRNA is mediated by miRNAs or EIF4E (light green ovals). HSP90 and PP2A post-translationally modify PIM1 protein levels (green ovals). Several phosphorylation targets of PIM1 (yellow P) are indicated (violet ovals) which are involved in various cellular signaling pathways (following Bachmann & Möröy, 2005 (137)).

PIM kinases are promising targets for pharmacological inhibition (133) because they control several important signaling pathways in cellular processes. If these processes such as apoptosis, hypoxia or cell cycle control are deregulated, a malignant transformation is promoted (160). To date several small-molecule PIM kinase inhibitors (161), (162), (163) have been designed. All of them are ATP-competitive binders within the catalytic ATP-binding domain of the kinase and prevent PIM-dependent phosphorylation of the cellular targets (160). Another promising targeting strategy is RNAi to post-transcriptionally downregulate PIM1 protein levels. So far a PIM1-specific siRNA and one miRNA, namely

miR-33a, have been successfully used to target PIM1 in a colon carcinoma xenograft mouse model (28) to inhibit tumor growth.

1.4.2 The human miRNA cluster miR-17-92

The human miRNA cluster miR-17-92 is one of the best characterized polycistronic miRNA clusters. Known as oncomiR-1, the cluster encodes six miRNAs, namely miR-17, miR-18a, miR-19a, miR-20a, miR-19b-1 and miR-92-1 (164), deriving from a long primary transcript (87). In mammals two highly conserved paralogs have been identified: the miR-106a-363 and the miR-106b-25 clusters (164). The miRNAs of these three clusters can be categorized into four different miRNA families: (i) the miR-17 family which comprises miR-17, miR-20a/b, miR-93 and miR-106a/b, (ii) the miR-18 family with miR-18a/b, (iii) the miR-19 family which consists of miR-19a and miR-19b-1 and -2 and (iv) the miR-92 family consisting of miR-25, miR-92a-1 and -2 and miR-363 (88). The human miR-17-92 cluster can be found at chromosome 13q31.3 (NG_032702.1) and was identified in 2004 as a novel gene, named chromosome 13 open reading frame 25 (*C13orf25*) (Figure 7a) which was amplified in hematopoietic malignancies (96) and solid tumors (165). The genomic locus consists of four exons and three introns from which a 5058 bp long non-protein coding RNA transcript (AB176708.1) is generated (96). The coding sequence of miR-17-92 is located in intron 3 with a primary transcript of about 1 kb in length (164). The sequence upstream of the cluster's coding sequence can be subdivided into AT- and GC-rich parts. The host gene promoter is controlled by the E2F transcription factor 1-3 (E2F1-3) with E2F3 being the main E2F variant associated with the host gene promoter (166). The core promoter region is found in exon 1 in the GC-rich part about 3.4 kb apart from the miR-17-92 coding sequence, where a consensus initiator sequence is located downstream of a non-consensus TATA-box (167), (166). However, in line with the findings that almost a third of intronic miRNAs show transcriptional activity, which is independent of a host gene promoter (168), O'Donnell et al. found highly conserved enhancer box elements (E-boxes) close to the AT-rich sequence region (91). Additionally at this chromosomal region an intronic TSS was predicted to be localized approximately 200 bp downstream of E-box 3 (169). These E-box elements are consensus sequences recognized by the transcriptional activator MYC (91). The results suggest that transcriptional activity of the miR-17-92 cluster may be generated by two independent TSSs (91), (169).

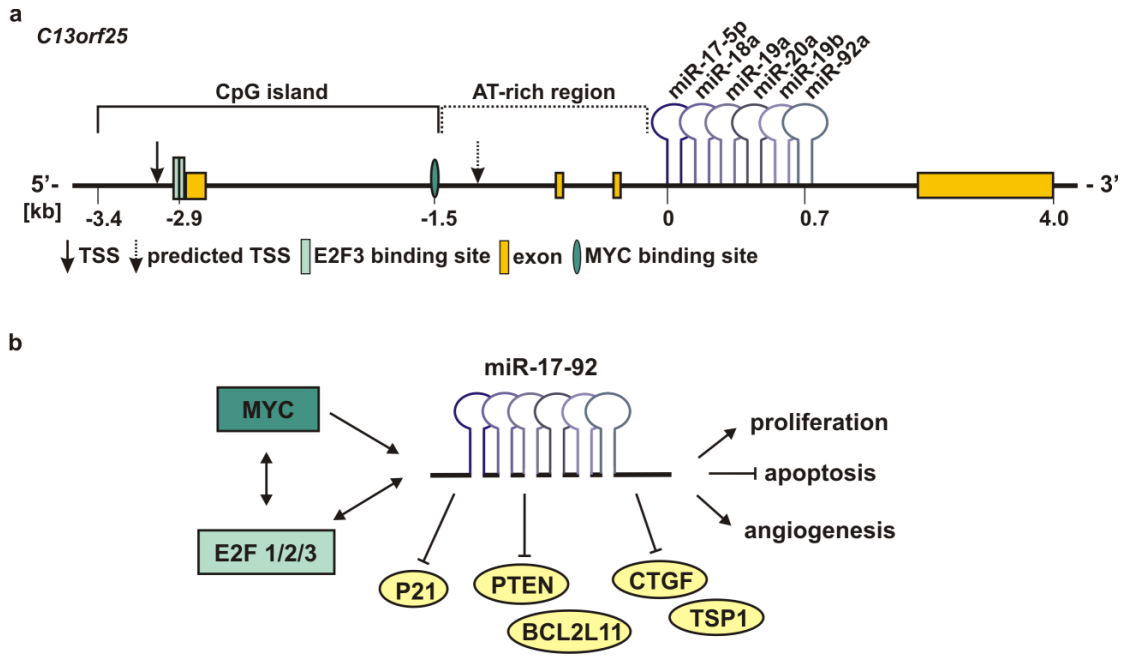

Figure 7: Regulatory network of the human miR-17-92 cluster. (**a**) Genomic organization of human miR-17-92 on *C13orf25*. The locus consists of four exons (orange boxes) and the sequence upstream of the cluster can be subdivided in an AT-rich and GC-rich part; the host gene promoter controlled by E2F3 (167) (light green box) is located at the beginning of the GC-rich part, while the functional MYC site E3 (91), (169) (green oval) is close to the intronic AT-rich region. Two transcription start sites (TSS) are indicated (black and dashed arrow) (**b**) Pleiotropic functions of miR-17-92 achieved by repressing specific targets (light yellow ovals). Transcription of miR-17-92 may be generated by MYC and/or E2F1/2/3 (green and light green boxes) which trans-activate each other. Depending on the physiological context and cell type, miR-17-92 can promote proliferation, increase angiogenesis and inhibit apoptosis (following Olive, Jiang & He, 2010 (88)).

The oncogenic activity of the miR-17-92 cluster was first seen in an *in vivo* mouse B-cell lymphoma model in which the cluster cooperated with the oncogene MYC (87) and accelerated tumorigenesis (Figure 7b). MiR-19 was identified as the key oncogenic miRNA of the cluster targeting the tumor suppressor protein PTEN (170), (171), thus mediating repression of apoptosis and promoting tumorigenesis of MYC induced lymphomas. To date overexpression of the miR-17-92 cluster has been intensely investigated in human cell culture and several animal models to elucidate its pleiotropic functions during normal development and/or malignant transformation (88). Thus the pleiotropic functions implicate that the role of miR-17-92 is manifold and arise from post-transcriptional regulation of several targets which are part of different physiological contexts, placing miR-17-92 in between a complex regulatory signaling network (Figure 7b). One important auto-regulatory feedback loop has been reported between E2F factors, MYC and miR-17-92 expression. In this network, the miRNAs miR-17 and miR-20a target the pro-apoptotic protein E2F1 and maintain a homeostasis towards proliferative signals (167). Other targets of miR-17-92 are

the pro-apoptotic protein BCL2-like 11 apoptosis facilitator (BCL2L11) and the tumor suppressor PTEN or the cyclin-dependent kinase inhibitor P21. Repression of these specific targets promotes proliferation and shows less activation-induced cell death in transgenic mice (172), (173), (174). The angiogenic activity of the miR-17-92 cluster is mediated by miR-18 and miR-19 which repress the thrombospondin 1 (TSP1) protein and the connective tissue growth factor (CTGF) (175). However, understanding the functions of miR-17-92 may help to explore the role of miRNAs in the network of cancer and offers the possibility to investigate clinical applications of anti-miRNA treatments.

1.5 Goal of the project

MiRNAs play crucial roles in important cellular processes such as development, proliferation, differentiation, the stress response and apoptosis (39). They can be used either as diagnostic and prognostic biomarkers (77) or as novel anti-cancer strategies to treat malignant forms of tumors (100).

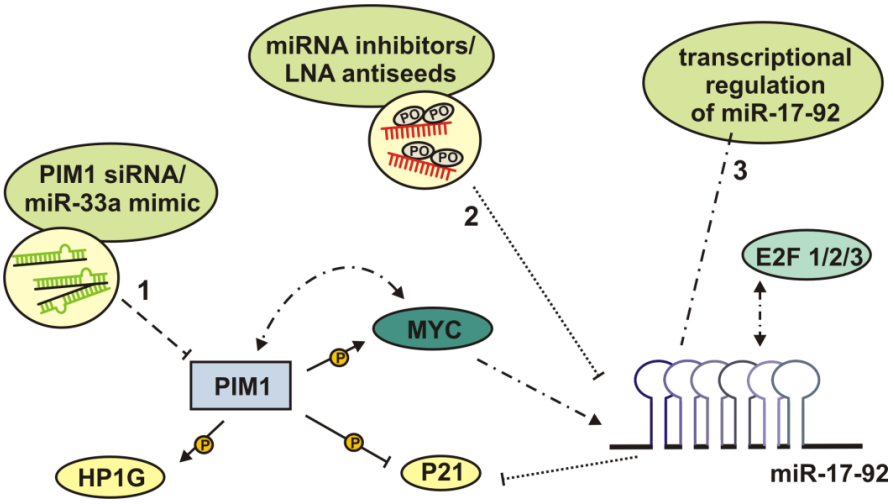

Figure 8: Goal of the project. (**1**) The proto-oncogene PIM1 as a target of miR-33a *in vitro* and *in vivo*. (**2**) Establishment of novel miRNA inhibitors, called LNA antiseeds, to scrutinize inhibition of oncogenic miRNAs of the miR-17-92 cluster on the tumor suppressor P21. (**3**) Investigation of the transcriptional regulation of the human miR-17-92 cluster by E2F3 and MYC considering a putative MYC/PIM1 synergism.

In the first project, the proto-oncogene PIM1 was established as target for miRNAs. PIM1 was chosen because the constitutively active serine/threonine kinase PIM1 is overexpressed in different cancer types and as a consequence leads to severe forms of cancer associated with poor prognosis (133). The proto-oncogene PIM1 has been described as an important cellular target for cancer therapies and to date there has been extensive research into designing novel and specific inhibitors against PIM kinases. To selectively reduce cellular levels of PIM1 protein *in vitro* and *in vivo*, one focus of the project was to use RNAi to target PIM1 (Figure 8, 1) which can be mediated either by small interfering RNA (siRNA) or miR-33a. On condition that PIM1 is a target of miR-33a *in vitro* in different cell lines, this tumor-suppressive acting miRNA should be established in miRNA replacement therapy in subcutaneous colon carcinoma mouse models. Delivery of miR-33a would be mediated by a branched cationic polyethylenimine (PEI F25 LMW) which in previous studies has been used as powerful delivery agent for siRNAs (176).

A second project was to develop novel miRNA inhibitors for the use in miRNA-based therapies (Figure 8, 2). Because overexpression of oncogenic miRNAs is associated with the

development of cancer due to a reprogramming of the cell's homeostasis, we designed small LNA-modified oligonucleotides harboring a natural phosphodiester backbone, termed LNA antiseeds, to block and inhibit oncogenic miRNAs. Delivery of these molecules should be performed with this polyethylenimine PEI F25 LMW and thus complex formation and delivery of the nanoparticles has to be established *in vitro*, initially.

The third project involved the investigation of the transcriptional regulation of the human miRNA cluster miR-17-92 (Figure 8, 3). MiR-17-92 is one of the best characterized polycistronic miRNA clusters in humans associated with oncogenic activity. Unfortunately little is known about its transcriptional regulation. The cluster is placed between a complex regulatory network of the oncogene MYC and E2F transcription factors (91), (167). Thus deletion analyses of the AT-rich promoter region should reveal MYC dependence on transcriptional activation. Furthermore colocalization of the proto-oncogene PIM1 and its phosphorylation target HP1G were investigated. Analysis of the pri-mir-17-92 expression levels after RNAi-mediated silencing of MYC, E2F3 and PIM1 proteins should provide presumption that transcriptional regulation of the miR-17-92 cluster partially is PIM1-dependent.

2 Materials and Methods

2.1 Buffers, Media and Solutions

Individual conditions for buffers, media and solutions which were used throughout the complete laboratory work are figured out in the single chapters to facilitate their correlation to the different disciplines. All buffers were generated with double-distilled water (ddH_2O) and sterile filtered if not indicated otherwise. In case of preparing large amounts of media or solutions they were formulated with demineralized water and autoclaved 121 °C for 20 min using 1 bar pressure.

2.2 Oligonucleotides

2.2.1 DNA oligonucleotides

All DNA primers used throughout this thesis were purchased from Metabion (Martinsried, Germany) and ordered as 100 µM stock solutions. For longer time storage the primers were kept at 4 °C in a refrigerator. All DNA primers were used for PCR reactions and designed using the software tool Oligo Analyzer 3.1 (Integrated DNA Technologies, Munich, Germany).

2.2.1.1 Primers for cloning

Primers that were needed for cloning experiments are listed in Appendix J. They were phosphorylated before usage (2.15.2) or were designed carrying the respective palindromic sequence for a restriction endonuclease (2.15.4). Primers that were used for mutagenesis PCR (2.15.8.2) have a much longer nucleotide sequence harboring point mutations in the middle of the primer sequence.

2.2.1.2 Primers for DNA sequencing

To verify DNA sequences of generated plasmid constructs Sanger sequencing was performed at eurofins mwgloperon (2.15.10) using primer sequences listed in Appendix K.

2.2.1.3 Primers for RNA analyses

Quantitative PCR reactions (2.15.8.3) of human mRNA or non-coding RNA levels were done using primer sequences listed in Table 1.

Table 1: Primers for RNA analyses.

RNA transcript	Name of DNA primer	Sequence 5' → 3'	Product length [bp]
hsa 5S rRNA	qPCR 5S rRNA fwd	5'- TCT CGT CTG ATC TCG GAA GC	88
	qPCR 5S rRNA rev	5'- AGC CTA CAG CAC CCG GTA TT	
hsa ß-Actin	qPCR Actin fwd	5'- CCA ACC GCG AGA AGA TGA	97
	qPCR Actin rev	5'- CCA GAG GCG TAC AGG GAT AG	
hsa MYC	qPCR MYC fwd	5'- CCT TGC AGC TGC TTA GAC	116
	qPCR MYC rev	5'- GAG TCG TAG TCG AGG TCA T	
hsa E2F3	qPCR E2F3 fwd	5'- GAG ACT GAA ACA CAC AGT CC	98
	qPCR E2F3 rev	5'- CCT GAG TTG GTT GAA GCC	
hsa PIM1	qPCR PIM1 fwd	5'- ATC AGG GGC CAG GTT TTC T	73
	qPCR PIM1 rev	5'- GGG CCA AGC ACC ATC TAA T	
hsa pri-mir-17-92	qPCR pri-17-92 fwd	5'- CAT CTA CTG CCC TAA GTG CTC CTT	68
	qPCR pri-17-92 rev	5'- GCT TGG CTT GAA TTA TTG GAT GA	

2.2.1.4 Primers for cDNA generation of miRNAs

To generate cDNA (2.15.7) of human miRNAs specific stem-loop miRNA primers were designed according to Chen et al. (178). A list of all used primers is depicted in Table 2. The 6/7 nt indicated by lower case letters are reverse complementary to the 3'-end of the miRNAs listed in Appendix L.

Table 2: Primers for cDNA generation of miRNAs.

MiRNA	Name of DNA primer	Sequence 5' → 3'
hsa-miR-15a	loop miR-15a RT	5'- GTC GTA TCC AGT GCA GGG TCC GAG GTA TTC GCA CTG GAT ACG ACc aca aac
hsa-miR-16-1	loop miR-16-1 RT	5'- GTC GTA TCC AGT GCA GGG TCC GAG GTA TTC GCA CTG GAT ACG ACc gcc aat
hsa-miR-17/20a	loop miR-17/20a RT	5'- GTC GTA TCC AGT GCA GGG TCC GAG GTA TTC GCA CTG GAT ACG ACc tac ctg
hsa-miR-24-1	loop miR-24-1 RT	5'- GTC GTA TCC AGT GCA GGG TCC GAG GTA TTC GCA CTG GAT ACG ACc tgt tc
hsa-miR-26a	loop miR-26a RT	5'- GTC GTA TCC AGT GCA GGG TCC GAG GTA TTC GCA CTG GAT ACG ACa gcc tat
hsa-miR-33a	loop miR-33a RT	5'- TGG ATA TCC ACA CCA GGG TCC GAG GTA TTC GGT GTG GAT ATC CAt gca atg
hsa-miR-33b	loop miR-33b RT	5'- GUC GUA UGG UCA CGA GGG UCC GAG GUA UUC CGU GAC CAU ACG ACg caa ug
hsa-miR-144	loop miR-144 RT	5'- GTC GTA TCC AGT GCA GGG TCC GAG GTA TTC GCA CTG GAT ACG ACa gta cat
hsa-miR-374a	loop miR-374a RT	5'- GTC GTA TCC AGT GCA GGG TCC GAG GTA TTC GCA CTG GAT ACG ACc act tat
has-miR-423	loop miR-423 RT	5'- GTC GTA TCC AGT GCA GGG TCC GAG GTA TTC GCA CTG GAT ACG ACa aag tct

2.2.1.5 Primers for qPCR of miRNAs

Quantitative PCR reactions (2.15.8.3) were conducted to determine human miRNA levels in several cell lines. The primers are based on the human miRNA sequences which are listed in Appendix L. To obtain roughly the same melting temperature of the individual primers in subsequent qPCR reactions, a 5'-overhang was designed that is indicated by lower case letters in Table 3.

Table 3: Primers for qPCR of miRNAs.

MiRNA	Name of DNA primer	Sequence 5' → 3'	Product length [bp]
hsa-miR-15a	miR-15a QT forward	5'- cgc gcT AGC AGC ACA TAA TG	61
hsa-miR-16-1	miR-16-1 QT forward	5'- cgc gcT AGC AGC ACG TAA AT	61
hsa-miR-17	miR-17 QT forward	5'- cgc gcC AAA GTG CTT ACA GTG	62
hsa-miR-20a	miR-20a QT forward	5'- gcc gcg cTA AAG TGC TTA TAG TG	64
hsa-miR-24-1	miR-24-1 QT forward	5'- cgc gcT GGCTCA GTT CAG CAG	62
hsa-miR-26a	miR-26a-1 QT forward	5'- cgc gcT TCA AGT AAT CCA GG	61
hsa-miR-33a	miR-33a QT forward	5'- cgc gcG TGC ATT GTA GTT G	60
hsa-miR-33b	miR-33b QT forward	5'- cgc gcG TGC ATT GCT GTT G	60
hsa-miR-144	miR-144 QT forward	5'- gcg cgc gcT ACA GTA TAG ATG	62
hsa-miR-374a	miR-374a QT forward	5'- gcc gcg cTT ATA ATA CAA CCT G	63
has-miR-423	miR-423 QT forward	5'- cTG AGG GGC AGA GAG CG	58
	reverse primer miR-33a	5'- CAC CAG GGT CCG AGG T	-
	reverse primer miR-33b	5'- CAC GAG GGT CCG AGG TA	-
	uni reverse primer QT	5'- GTG CAG GGT CCG AGG T	-

2.2.2 RNA oligonucleotides

RNA oligonucleotides used in this thesis were purchased from different companies as indicated in the following chapters. They were ordered lyophilized and diluted in double-distilled water if not indicated otherwise. For long time storage RNA oligonucleotides were kept at -20 to -80 °C.

2.2.2.1 SiRNAs

Used siRNAs were purchased from Metabion (Martinsried, Germany), Ambion® Life Technologies (Darmstadt, Germany) or Dharmacon Thermo Fisher Scienific (Lafayette, CO, USA) and listed in Table 4. All siRNA oligonucleotides were designed as double-stranded DICER1 processing products (sense and antisense orientation) with an overhang of two

deoxythymidines (dT) positioned on their 3'-end. The sense strand is specific and fully complementary (location either in the coding sequence or the 3'-UTR) to the human mRNA of interest.

Table 4: SiRNAs.

MRNA of interest	Name of siRNA	Sequence 5' → 3'	
VR1 mRNA	VR1 siRNA (179)	sense	5'- GCG CAU CUU CUA CUU CAA CdTdT
		antisense	5'- GUU GAA GUA GAA GAU GCG CdTdT
PIM1 mRNA	PIM1 siRNA (1130)	sense	5'- GAU AUG GUG UGU GGA GAU AdTdT
		antisense	5'- UAU CUC CAC ACA CCA UAU CdTdT
	PIM1 siRNA (1491)	sense	5'- GGA ACA ACA UUU ACA ACU CdTdT
		antisense	5'- GAG UUG UAA AUG UUG UUC CdTdT
	siRNA 33a	sense	5'- AAA AUG CAC AAA CAA UGC AdTdT
		antisense	5'- UGC AUU GUU UGU GCA UUU UdTdT
luc mRNA	siRNA luc	sense	5'- CUU ACG CUG AGU ACU UCG AdTdT
		antisense	5'- UCG AAG UAC UCA GCG UAA GdTdT
MYC mRNA	siRNA MYC	sense	5'- CAG GAA CUA UGA CCU CGA CUA dTdT
		antisense	5'- UAG UCG AGG UCA UAG UUC CUG dTdT
E2F3 mRNA	siRNA E2F3	sense	5'- ACA GCA AUC UUC CUU AAU AdTdT
		antisense	5'- UAU UAA GGA AGA UUG CUG UdTdT

SiRNAs were ordered lyophilized and were diluted in siRNA buffer (30 mM HEPES KOH pH 7.4, 100 mM KCl, 2 mM Mg_2Cl, 50 mM NH_4Ac) to reach concentrations up to 2 µg/µL. After determination of siRNA concentration (2.14.1) they were prepared for long time storage at -80 °C.

2.2.2.2 MiRNA Mimics

Modified miRNA mimics, called miRIDIAN miRNA mimics, were purchased from Dharmacon Thermo Fisher Scientific (Lafayette, CO, USA). MiRIDIAN miRNA mimics are intended to mimic native miRNAs and are generated as double-stranded RNA molecules which are chemically enhanced with a proprietary design. Their sequences are based on the human endogenous, mature miRNAs listed in the miRBase Sequence Database 16.0 (180). All miRNAs were dissolved in ddH_20 and prepared for storage at -80 °C. Used miRNAs are listed below (Table 5):

Table 5: MiRNA mimics.

MiRNA of interest	Order Number	Sequence 5' → 3'	
hsa-miR-33a	(C-300509-07)	5'- GUG CAU UGU AGU UGC AUU GCA	
hsa-miR-33b	(C-300958-03)	5'- GUG CAU UGC UGU UGC AUU GC	
hsa-miR-15a	(C-300482-03)	5'- UAG CAG CAC AUA AUG GUU UGU G	
hsa-miR-16-1	(C-300483-03)	5'- UAG CAG CAC GUA AAU AUU GGC G	
Negative control mimic #1	(CN-001000-01)	no sequence available	
hsa-miR-33a	-	leader	5'- GUG CAU UGU AGU UGC AUU GCA
		passenger	5'- TGC AAT GCA ACT ACA ATG CAC
hsa-miR-33b	-	leader	5'- GUG CAU UGC UGU UGC AUU GC
		passenger	5'- CAG UGC CUC GGC AGU GCA GCC C

In case of hsa-miR-33a and -33b the DICER1 processing product of pre-miR-33a and pre-miR-33b as published in the miRBase Sequence Database 14.0 (2.18.6) was additionally purchased by eurofins mwg|operon (Table 5), but lacking the 5'-terminal phosphate. The leader and passenger strand were dissolved in siRNA annealing buffer (30 mM HEPES KOH pH 7.4, 100 mM KCl, 2 mM Mg_2Cl, 50 mM NH_4Ac) respectively. After measuring RNA concentration (2.14.1) equimolar amounts of each strand were mixed and heated to 95 °C. Annealing of both strands was done for 1 h at 37 °C to receive the double-stranded DICER1 processed miRNA product.

2.2.2.3 MiRNA hairpin inhibitors

MiRNA hairpin inhibitors, called miRIDIAN hairpin inhibitors, were purchased from Dharmacon Thermo Scientific (Lafayette, CO, USA). MiRIDIAN hairpin inhibitors are chemically enhanced RNA molecules that are designed to inhibit endogenous miRNA functions. Thus their purpose is to discover and investigate natural functions of miRNAs (181). Their sequences are based on the human endogenous mature miRNAs listed in the miRBase Sequence Database 16.0 (180). All miRIDIAN hairpin inhibitors were dissolved in double-distilled water and prepared for long-term storage at -80 °C. Used miRIDIAN hairpin inhibitors are depicted in Table 6:

Table 6: MiRIDIAN hairpin inhibitors.

MiRNA of interest	Order number	Sequence 5' → 3'
hsa-let-7a	(IH-300473-07)	5'- UGA GGU AGU AGG UUG UAU AGU U
hsa-miR-17	(IH-300485-06)	5'- CAA AGU GCU UAC AGU GCA GGU AG
hsa-miR-20a	(IH-300491-05)	5'- UAA AGU GCU UAU AGU GCA GGU AG

2.2.3 LNA-based oligonucleotides

As a second class of miRNA inhibitors RNA oligonucleotides containing an LNA (Locked Nucleic Acid) modification were designed. This modification mimics an RNA structure because it contains an O2'-C4'-methylene-linked bicyclic ribose unit which locks its conformation in the C3'-endo conformation and thus increases the stability of this oligonucleotide (113), (114). The LNA based oligonucleotides were purchased from RiboTask (Odense, Denmark). They were ordered as lyophilized dry powder, dissolved in double-distilled water and stored at -20 °C.

2.2.3.1 LNA miRNA inhibitors

All LNA-modified oligonucleotides showed fully complementarity to the human miRNAs of interest to gain miRNA inhibition. The ordered LNA oligonucleotides (Table 7) harbor a natural phosphodiester (PO) backbone with one exception containing a modified phosphorothioate (PS) backbone. They have introduced the LNA modification at some or all positions of the oligonucleotide, except for isolated 2'-oxymethyl pyrimidine residues, marked as [mU] and [mC] (Table 7), that are introduced to lower self-pairing of the individual oligonucleotides.

Table 7: LNA miRNA inhibitors.

MiRNA of interest	Name of LNA oligonucleotide	Sequence 5' → 3'
hsa-miR-17-5p hsa-miR-20a	LNA (PS) miR-17/20a	5'- GCA CT[mU] TG
hsa-miR-17-5p	LNA miR-17	5'- CTG TAA GCA CT[mU] TG
hsa-miR-20a	LNA miR-20a	5'- CTA TAA GCA [mC]T[mU] TA
hsa-let-7a	LNA let-7a (8-mer)	5'- CTA CCT CA
hsa-let-7a	LNA let-7a (10-mer)	5'- TAC TAC CTC A
hsa-let-7a	LNA let-7a (12-mer)	5'- CCT ACT ACC TCA
hsa-let-7a	LNA let-7a (14-mer)	5'- AAC CTA CTA CCT CA
-	LNA anti-RNase P (182)	5'-CAA GCA GCC UAC CC

2.3 Antibodies

All primary and secondary antibodies were used for Western Blot experiments (2.9.2) or chromatin immunoprecipitation assays (2.15.11) and are listed below (Table 8, Table 9). They were purchased from Santa Cruz Biotechnology (Heidelberg, Germany) expect for the

ABCA1 antibody which was ordered from Abcam (Cambridge, UK) and the Phospho HP1G antibody that was purchased from Cell Signaling (Danvers, MA, USA).

Table 8: Primary antibodies.

Name of primary antibody	Order number	Isotype specificity	Dilution for WB	ChIP assay
AbcA1 (AB.H10)	ab-18180	mouse monoclonal IgG_1	1:1,000	-
ß-Actin (C4)	sc-47778	mouse monoclonal IgG_1	1:1,000; 1:5,000; 1:10,000	-
Cdk6 (C-21)	sc-177	rabbit polyclonal IgG	1:2,000	-
c-Myc (9E10)	sc-40	mouse monoclonal IgG_1	-	1 µg
p21 (F-5)	sc-6246	mouse monoclonal IgG_{2b}	1:200	-
p53 (DO-1)	sc-126	mouse monoclonal IgG_{2a}	1:1,000	-
Phospho HP1G (Ser83)	2600S	rabbit polyclonal IgG_1	-	1 µg
Pim-1 (12H8)	sc-13513	mouse monoclonal IgG_1	1:500	1 µg

Table 9: Secondary antibodies.

Name of secondary antibody	Order number	Isotype specificity	Dilution for WB	ChIP assay
Goat anti-mouse IgG-HRP	sc-2005	IgG_1, IgG_{2a}, IgG_{2b}, IgG_3, IgG_4	1:5,000	1 µg
Goat anti-rabbit IgG-HRP	sc-2004	IgG_1, IgG_{2a}, IgG_{2b}, IgG_3, IgG_4	1:5,000	-

2.4 Size markers

For size detection of proteins, DNA or RNA molecules several size markers were used which are listed in Table 10. All ladders were applied according to the manufacturer's protocols respectively.

Table 10: Size markers.

Name of ladder	Company	Type	Size range	Purpose
PageRuler Plus Prestained Protein Ladder	Thermo Fisher Scientific	protein	10-250 kDa	WB analyses
2-Log DNA Ladder	New England Biolabs®	DNA	0.1-10.0 kb	Cloning
10 bp DNA Ladder	Invitrogen®	DNA	10-330 bp	qPCR analyses

2.5 Bacterial cell culture

Microbial cell culture is a standard method in molecular biology. It was used for cloning experiments to multiply bacteria containing different plasmids of interest. All media, buffer, flasks or pipets needed for bacterial cell culture were autoclaved for 20 min at 121 °C and 1 bar pressure.

2.5.1 Bacterial strains

For all cloning experiments the bacterial strain *E. coli* DH5α (genotype: *supE44 hsdR17 recA1 endA1 gyrA96 thi-1 relA1*, (183)) was used. This strain has an ampicillin resistance gene to select clones after transformation of plasmids.

2.5.2 Bacterial growth on agar plates

To grow bacterial cells on agar plates, LB medium (Lysogeny Broth, (184); 5 g/L yeast extract, 10 g/L peptone, 10 g/L NaCl) was supplemented with agar (15 g/L). The agar plates were stored at 4 °C for up to one month. To amplify *E. coli* DH5α strains, ampicillin was added into the agar culture medium with a final concentration of 100 µg/mL and *E. coli* strains of interest were spread out on agar plates. After overnight incubation at 37 °C one single colony was used to inoculate liquid bacterial growth medium.

2.5.3 Bacterial cell culture in liquid medium

E. coli DH5α strains were cultivated in LB medium (5 g/L yeast extract, 10 g/L peptone, 10 g/L NaCl) supplemented with 100 µg/mL ampicillin at 37 °C from 8 h till overnight. For long time storage of designed constructs and strains, the cultures were diluted 1:1 with sterile 98 % glycerol, frozen with liquid nitrogen and stored at -80 °C. In general grown bacterial cell cultures were used for plasmid preparation (2.15.1).

2.5.4 Preparation of chemically competent *E. coli* DH5α cells

To prepare chemically competent *E. coli* DH5α cells, 150 mL of LB medium were pre-warmed and inoculated with 3 mL of an overnight culture. Cells were grown at 37 °C and shaken at 200 rpm in an incubator (GFL 3033) till an optical density OD_{576} of 0.6 was reached. After pelleting the cells at 5000 rpm and 4 °C for 7 min, cells were carefully resuspended in 15 mL of pre-cooled TFB-1 solution (10 mM MOPS pH 7.0, 10 mM RbCl) and were pelleted again. Afterwards cell pellet was resuspended in 6 mL of pre-cooled TFB-3 solution (100 mM MOPS pH 6.5, 50 mM $CaCl_2$, 10 mM KCl, 15 % glycerin) and 50 µL

aliquots were frozen in liquid nitrogen before chemically competent *E. coli* DH5α cells were stored at -80 °C.

2.5.5 Transformation of bacterial cells

Transformation of bacterial cells was discovered in 1928 by the bacteriologist Griffith (185) and is a standard laboratory procedure in molecular biology. Transformation allows uptake, incorporation and expression of genetic material e.g. plasmid DNA into bacterial cells. First of all chemically competent *E. coli* DH5α cells were thawed on ice. After addition of negatively charged plasmid DNA (up to 1 µg, 2.15.1) or ligation reaction (up to 20 µL, 0), cells were incubated on ice for 30 min. DNA uptake occurred after pre-cooled cells were heat-shocked at 42 °C for 45 sec. After incubation of the mixture on ice for 2 min, 300 µL of pre-warmed LB medium without antibiotic was added. Cells were shaken at 600 *g* and 37 °C for 30-60 min. Subsequently the transformation reaction was spread out onto agar plates and incubated as described above (2.5.2).

2.6 Eukaryotic cell culture

In mammalian cell culture immortalized cell lines of interest can be subcultured under sterile conditions in a laminar air flow (Thermo Scientific, Schwerte, Germany) and cultivated in a humidified atmosphere (NuAire, Plymouth, USA) at 37 °C and 5 % CO_2. Cell lines derive from isolated tumors of different organs or tissues. Cultivation of these cells depends on their method to grow. Suspension cell lines are easily passaged with a small amount of culture diluted with media, whereas adherent cell cultures have to be detached before only a small proportion can be seeded into new culture flasks. To allow optimal growth conditions, media for cultivation of eukaryotic cells have to be supplemented with several nutrients including Fetal Calf Serum (FCS).

2.6.1 Eukaryotic cell culture of suspension cell lines

2.6.1.1 K562

The chronic myelogenous leukemia cell line K562 was derived from the pleural effusion of a 53-year old female with terminal blast crises by Lozzio and Lozzio (186). This cell line grows in suspension and is cultured in RPMI 1640 (Roswell Park Memorial Institute) medium containing 10 % FCS. In general cells were subcultured every 2-3 days with a cell density of 0.25-1 * 10^6 cells/mL and were incubated in a humidified atmosphere (37 °C, 5 % CO_2).

2.6.2 Eukaryotic cell culture of adherent cell lines

2.6.2.1 HeLa

The adherent cell line HeLa was established in 1951 as the first immortal cell line and derived from cervical cancer cells of a 51-year-old female named Henrietta Lacks (187). Cells were cultivated in a humidified atmosphere (37 °C, 5 % CO_2) in IMDM medium (Iscove's Modified Dulbecco Medium) supplemented with 10 % FCS. HeLa cells were subcultured twice a week by rinsing the medium, washing cells with PBS and detaching adherent cells with 2 mL of trypsin/EDTA solution (0,25 % (w/v) trypsin, 0,53 mM EDTA). The cell suspension was filled up with 8 mL of IMDM medium and cells were seeded in a subculture ratio of 1:10 or 1:20 in fresh culture vessels.

2.6.2.2 LS174T

LS174T cells were received as a trypsinized variant of the colorectal adenocarcinoma cell line LS180 which derived from a 58-year-old female patient (188). Multiplication of the cells was done according to the procedure for HeLa cells, but LS174T cells were seeded into culture flasks in a ratio of 1:5.

2.6.2.3 Skov-3

The ovarian carcinoma cell line Skov-3 was isolated from a 64-year-old Caucasian female (189). Cells were cultured in the same manner as described aforementioned. A ratio of 1:3 to 1:5 was used for subcultures.

2.6.2.4 HCT 116

HCT 116 cells, generated from an adult male gender, derive from a colorectal carcinoma cell line growing as adherent cells. Cells were subcultured as described above and were seeded in a ratio of 1:5 to 1:8 twice a week.

2.7 Experimental working with animals

For this thesis subcutaneous colon carcinoma xenograft mouse experiments were performed to establish the first miRNA replacement therapy (28) based on the cationic polyethylenimine PEI F25 LMW. All studies including keeping, treatment and therapy establishment of mice were done in the working group of Prof. Dr. Achim Aigner.

2.7.1 Athymic nude mice

Athymic nude mice (Hsd:Athymic Nude-Foxn1^{nu}, 6-8 weeks old) were obtained from Harlan Winkelmann (Borchen, Germany) and were kept in tight stages at 23 °C in a humidified atmosphere with standard rodent chow, water available *ad libitum* and a 12 hour light/dark cycle. Animal studies were done according to the national regulations and were approved by the *Regierungspräsidum* Gießen (Germany).

2.7.2 Subcutaneous xenograft colon carcinoma tumor models

To generate subcutaneous xenograft mouse models, a total of 1.5 * 10^6 LS174T or HCT116 cells in a total volume of 150 µL PBS were *s.c.*-injected into both flanks of the mice. After establishment of solid tumors and randomizing animals in specific treatment groups, the treatment with PEI/miRNA or PEI/siRNA complexes was done according to the information given at Ibrahim et al. (28). Tumor volumes were monitored during the experiment that was finished by scarification of the mice. Afterwards tumor tissues were prepared for selected analyses.

2.7.3 MiRNA tissue uptake *in vivo*

Radioactive determination of miRNA tissue distribution was done with [^{32}P]-end labeled miRNAs. In mice, subcutaneous tumors were initiated until a size of approximately 8 mm in diameter was reached (2.7.2). PEI F25 LMW complex formation was performed using [^{32}P]-end labeled miRNAs of interest (2.8.2.2). Complexes were introduced into the mice via *i.p.*- or *i.v.*-injection and 4 h later they were sacrificed. To quantitate tissue distribution of the miRNAs, total RNA was isolated from different tissues (more information available at Ibrahim et al. (28)).

2.8 Transfection of mammalian cell lines

Transfection of mammalian cell lines is a process to introduce nucleic acids such as DNA or RNA molecules into cells. In general the term transfection is used for non-viral targeting of eukaryotic cells where transient pores in the cell membrane allow uptake of the material. This transient pores can be generated by using several techniques. For electroporation the cells are exposed to a short single electric impulse which transiently increases the permeability of the cell membrane. A very efficient transfection method is liposome delivery via cationic polymers such as polyethylenimine. The polycation interacts with the negatively charged nucleic acids and thus forms liposomes which are taken up via endocytosis.

2.8.1 Transfection procedure of suspension cell lines

For transfection of the suspension cell line K562 with plasmid DNA, siRNA, miRNA mimics or LNA-modified antisense oligonucleotides cells were harvested for 5 min at 390 *g*. Afterwards cells were washed twice with 10 mL of RPMI 1640 without FCS. $2 * 10^6$ cells, in a total volume of 100 µL medium, were electroporated in a 4 mm cuvette with a single pulse for 10 ms at 330 V using a Bio-Rad Gene Pulser Xcell (Bio-Rad, Munich, Germany). Per $1 * 10^6$ cells 5 µg of plasmid DNA or 1 µg of siRNA, miRNA mimic or LNA-modified antisense oligonucleotide was used. After electroporation cells were seeded into 12-well cell culture plates containing 1.5 mL RPMI 1640 supplemented with 10 % FCS. Cells were incubated for up to 120 h in a humidified atmosphere (37 °C, 5 % CO_2). Subsequently cells were prepared either for Western Blot analysis, WST-1 assay, luciferase assay or total RNA extraction (2.9.2, 2.10.2, 2.9.5, 2.16.2).

2.8.2 Transfection procedure of adherent cell lines

Transfection of adherent cell lines was done by liposome delivery using either Lipofectamine™ 2000 (Life Technologies Invitrogen, Darmstadt, Germany) or the cationic polymer PolyEthyleneImine F25 Low Molecular Weight (PEI F25 LMW; Sigma Aldrich, Taufkirchen, Germany) prepared and purified as described at Werth et al. (190).

2.8.2.1 Transfection with Lipofectamine™ 2000

The adherent cell lines HeLa, LS174T and Skov-3 were transfected with Lipofectamine™ 2000 (Life Technologies Invitrogen, Darmstadt, Germany) according to the manufacturer's protocol.

$8 * 10^4$ HeLa cells were seeded in a 24-well plate the day before transfection. Transfection procedure was proceeded in 400 µL IMDM medium without FCS. 0.5 µg of individual pGL3 reporter construct was diluted in 50 µL of Optimem I (Life Technologies Invitrogen, Darmstadt, Germany) and for co-transfection mixed with the respective amount of LNA antiseed, LNA control, siRNA, miRNA mimic or miRNA control. 1.5 µL of Lipofectamine™ 2000 were used per transfection and diluted in 50 µL of Optimem I. After incubation at room temperature for 5 min both components were mixed and incubated another 15 min. Afterwards complexes were added to the media. The medium was aspirated 4-6 h later and exchanged by IMDM supplemented with 10 % FCS. 24-96 h after transfection cells were prepared for luciferase reporter assays, total RNA extractions, WST-1 assays or Western Blotting experiments (2.9.5, 2.16.2, 2.10.2, 2.9.2).

To transfect LS174T cells, 0.5 * 10^6 cells were seeded in a 12-well plate one day prior treatment. 40 pmol PIM1-specific siRNA, miRNA mimics or controls were used and mixed with 2 µL of Lipofectamine™ 2000 according to the manufacturer's protocol. Cells were incubated 24-96 h in a humidified atmosphere.

For transfection of Skov-3 cells 1 * 10^5 cells were seeded into a 12-well plate. The day of co-transfection 2 µL of Lipofectamine™ 2000 were mixed with 25 ng of the *PIM1* cDNA clones (2.13.1) and 20 pmol PIM1-specific siRNA or miRNA mimic according to the manufacturer's protocol. After incubation for 48 h in a humidified atmosphere cells were prepared for Western Blotting experiments (2.9.2).

2.8.2.2 Transfection with PEI F25 LMW

For complexation of miRNA inhibitors with PEI F25 LMW HeLa cells were pre-transfected with pGL3 control reporter vector DNA using Lipofectamine™ 2000 as described above. After 6 h the medium was replaced by IMDM containing 10 % FCS and PEI complexes were added. For PEI F25 LMW complexation indicated amounts of siRNA, LNA antiseeds or miRIDIAN hairpin inhibitors were diluted in 50 µL complexation buffer (150 mM NaCl, 10 mM HEPES pH 7.4) and equilibrated for 5 min at room temperature (RT). In general a PEI/oligonucleotide mass ratio of 2.5:1 or 5:1 was obtained. A ratio of 5:1 resulted in a N/P ratio of 33 which had been determined as optimal for siRNA complexation (190), (176). The N/P ratio is based on a ratio of PEI Nitrogen per nucleic acid Phosphate. After equilibration of PEI F25 LMW in 50 µL complexation buffer the oligonucleotide and the PEI solution were mixed and briefly vortexed. An incubation step at room temperature for 30-60 min followed to allow the complexes to form. PEI F25 LMW complexes were added to the cells. 48 h later cells were lyzed and prepared for reporter assay measurements (2.9.5), determination of PEI F25 LMW complexation efficacy (2.10.2) or atomic force microscopy (2.17).

2.9 Protein techniques

2.9.1 SDS PAGE

SDS PAGE (SodiumDodecylSulfate PolyAcrylamide Gel Electrophoresis) is a method to separate denatured proteins according to their electrophoretic mobility. SDS functions as detergent and binds to amino acids of linearized proteins what results in a negative charge of the protein samples. The disc electrophoresis evolved by Ornstein and Davis (191) resulted in an improvement concerning the sharpness of separated proteins caused by a pH shift in

the stacking and separating buffer conditions. To prepare 15 % SDS gels the components depicted in Table 11 were mixed and polymerized between two glass plates.

Table 11: Composition of 15 % SDS PAGE gels.

Ingredient	Separating gel	Stacking gel
4x separating gel buffer (1.5 M Tris-HCl pH 8.8, 0.6 % SDS)	4 mL	-
4x stacking gel buffer (0.5 M Tris-HCl pH 6.8, 0.6 % SDS)	-	1,8 mL
acrylamide/bisacrylamide (30 % solution)	8 mL	1 mL
APS (10 % solution)	160 µL	75 µL
TEMED	16 µL	7,5 µL
ddH_20	ad 16 mL	ad 7,5 mL

SDS PAGE was performed subsequent to fixation of the gel matrix. Protein samples of interest were resuspended in 100-200 µL of lysis buffer (125 mM Tris-HCl pH 6.8, 4 % SDS, 1.4 M 2-mercaptoethanol, 0.05 % bromophenol blue) and heated to 95 °C for 5 min. Electrophoresis was performed in a Bio-Rad Mini-PROTEAN® 3 cell mini gel system (Bio-Rad, Munich, Germany) in 1x running buffer (192 mM glycine, 25 mM Tris-HCl, 0.01 % SDS) for 1 h at 180 V.

2.9.2 Western Blot

The Western Blot method was devised in 1979 (192) to transfer separated proteins onto a solid carrier like a PVDF (PolyVinyliDine Fluoride) membrane following polyacrylamide gel electrophoresis. Immobilized proteins can be probed with specific antibodies and visualized by chemo-luminescence or colorimetric techniques. After finishing SDS PAGE (2.9.1) the polyacrylamide gel was incubated in transfer buffer (25 mM Tris-HCl pH 8.3, 192 mM glycine, 10 % methanol) for 30 min to fix the proteins in the gel matrix. Proteins were transferred onto an Immobilon™-P PVDF membrane (Millipore, MA, USA). The membrane was activated in methanol for 2 min before incubating for 15 min in transfer buffer. Similarly, the blotting paper was soaked in transfer buffer. Protein transfer was done in a Trans-Blot® SD Semi-Dry Transfer Cell (Bio-Rad, Munich, Germany) for 30 min at 10 V. Afterwards the membrane was incubated for 2 h in 5 % milk powder in TBST (10 mM Tris-HCl pH 7.6, 150 mM NaCl, 0.1 % Tween 20) before overnight incubation with the primary antibody started. After three washing steps in TBST the incubation with an individual secondary antibody followed for 1 h. The primary and secondary antibodies which were used

for Western Blot experiments are depicted in Table 8 and Table 9. After a final washing step blots were incubated with Amersham ECL™ or ECLplus™ Western Blotting Detection Reagents according to the manufacturer's protocol. For detection of chemo-luminescence Kodak® BioMax™ light films, Kodak® GBX Developer and Replenisher and GBX Fixer and Replenisher were used. The exposure time differed between 1 to 15 min depending on the protein that was detected. To visualize the internal loading control, the blots were treated with stripping buffer (62.5 mM Tris-HCl pH 6.7, 100 mM 2-mercaptoethanol, 2 % SDS) for 30 min at 50 °C in a hybridization oven (Biometra, Goettingen, Germany), were blocked again for 1 h in milk powder (5 % solution in TBST) and afterwards were incubated with the ß-Actin antibody.

2.9.3 ELISA

Enzyme Linked Immunosorbent Assay (ELISA) is a powerful analytical biochemistry assay. This technique can be used for diagnostic differentiation of protein levels in treated versus untreated tumor tissues. For this thesis the group of Prof. Dr. Achim Aigner performed a PIM1-specific ELISA to analyze xenograft colon carcinoma tumor samples in mice which were treated with PIM1-specific siRNA or a miR-33a-mimic. Furthermore ELISA experiments were conducted to detect changes in TNFα and LPS levels monitoring unspecific effects of PEI/miRNA or PEI/siRNA treatment (for detailed information see (28)). After coating the antibody onto a 96-well plate overnight the supernatant of a tumor sample lysate was added to the plate the next morning. Several washing steps followed, before the specific detection antibody was applied to each single well. Detection was performed using a HRP-coated secondary antibody which was able to turn the offered substrate into a colored product. Subsequently the rising amounts of colored product were detected in a FLUOstar OPTIMA micro plate reader (BMG Labtech, NYC, USA).

2.9.4 Liver enzyme activity assays

To determine non-specific and/or toxic effects of PEI/miRNA complexes in mouse experiments, changes in the activity of the liver enzymes aspartate aminotransferase (AST, SGOT) and alanine aminotransferase (ALT, SGPT) were determined using an enzyme assay kit obtained from DiaSys Diagnostic Systems (Holzheim, Germany). Evaluation of the assay was done 60 min after four consecutive *i.p.*-injection-treatments. Enzyme activity assays were performed in Prof. Dr. Achim Aigner group; further information can be found at Ibrahim et al. (28).

2.9.5 Luciferase reporter assay

48 h after incubation of K562 or HeLa cells with the respective pGL3 luciferase reporter plasmids and/or siRNAs, miRNA mimics or LNA-modified antisense oligonucleotides, luciferase reporter assays were performed using the Promega Luciferase Assay System (Promega, Mannheim, Germany). K562 were centrifuged (5 min, 390 *g*, RT), washed with 500 µL of PBS and pelleted before lyzing with 200 µL of 1.2x reporter lysis buffer (Promega, Mannheim, Germany). The media of HeLa cells or other adherent growing cells was aspirated and cells were lyzed in 100 µL of 1.2x reporter lysis buffer after a previous washing step with PBS. Cells were incubated in reporter lysis buffer for 1 h at room temperature, while shaking at 1,800 rpm. Next assay measurement was performed in a white 96-well plate. 10 µL of cell lysate were mixed with 10 µL of luciferase substrate. Luminescence was measured immediately in a Safire^{2TM} micro plate reader (Tecan, Crailsheim, Germany). Custom settings for measurement were defined as 'Luminescence' for measurement mode, '10 msec' were set as integration time with a shake duration of '3 sec' and as plate definition 'GRE96fw.pdf' was chosen.

2.10 Cell cycle analyses

The cell cycle, also termed cell-division cycle, leads to division and replication of a mother cell into two daughter cells. In mammalian cells this can be departed into four phases including two periods, interphase and cell division. Thus the interphase is consisting of G- and S-phase, in which cells first increase in size, then DNA synthesis starts, replication occurs and afterwards cell division into two daughter cells can take place in mitosis phase. Mitosis itself is divided in prophase, prometaphase, metaphase, anaphase and telophase. The regulation of the cell cycle is strongly controlled in mammalian cellular systems and is used as a checkpoint for proliferation of cells in tumor studies. Anti-cancer treatments can store the cell cycle at one distinct point or can delay the proliferation of cells. This has to be considered using several different experimental methods.

2.10.1 Cell cycle analyses using nocodazole

For cell cycle analyses the chemical nocodazole was used. This anti-neoplastic agent affects the cytoskeleton and synchronizes cells by blocking a formation of metaphase spindles after entry into mitosis. Nocodazole was used for cell cycle analyses in K562 and LS174T cells. In case of K562 cells nocodazole was added 24 h after transfection of siRNAs or miRNAs (2.8.1, 2.8.2). LS174T cells were treated 48 h after transfection. Nocodazole was applied to

the medium at a final concentration of 100 ng/mL. A 16 h (LS174T) to 24 h (K562) incubation step followed in a humidified atmosphere at 37 °C, before cells were washed with PBS and fresh medium was added to release cells from the mitotic block. Cells were cultivated for another 48 h before harvesting. Then fixation of the cells was performed to do FACS analysis (2.12).

2.10.2 WST-1 assay

Before usage of modified RNA oligonucleotides as therapeutic agents it is important to question whether these molecules cause a growth delay, have cytotoxic effects or influence cell viability. Thus cell viability of different mammalian cells can be determined with the water soluble tetrazolium salt WST-1 (Roche Applied Science, Mannheim, Germany). During the assay the tetrazolium salt is cleaved to a dark red formazan dye by cellular mitochondrial dehydrogenases that are present in viable cells. Absorbance directly correlates with the amount of viable and metabolically active cells in the culture. The assay was performed in a micro titer plate as indicated in the protocol of the manufacturer. Cells of interest (e.g. $0.5 * 10^4$ HeLa cells) were seeded one day prior to transfection. The day of transfection cells were treated with RNA oligonucleotide complexes of interest (2.8.2). 48 h after transfection a WST-1 proliferation assay was done using 10 µL of water soluble tetrazolium salt which was directly given to the cultured cells. Measurement of resulting formazan dye was performed after a 2 h incubation step at 37 °C in a humidified atmosphere in a Safire^{2TM} micro plate reader (Tecan, Crailsheim, Germany). Absorbance was determined at 450 nm choosing a reference wavelength of 650 nm. Cell viability was calculated using a background control as reference.

2.10.3 Cell counting method

To determine the increase of the total number of viable cells in suspension cell lines, it is more likely to use cell counting. The enzymatic catalytic reaction of the formazan dye used in the WST-1 assay is possible, but uniform colorization of the product is limited. Thus cell counting was performed to consider antiproliferative effects on growth of the suspension cell line K562 after siRNA, miRNA mimic or LNA antiseed treatment. Cells were cultivated two days prior to transfection or treatment in the indicated medium (2.8.1) containing only 2 % FCS to slow down the cell cycle due to serum starvation. The day the experiment was started, cells were counted and $1 * 10^6$ cells were seeded into a 12-well plate containing 1.5 mL of RPMI 1640 supplemented with 2 % FCS. Every 24 h cells were counted with a hemocytometer (Marienfeld, Lauda-Königshofen, Germany) and the medium was exchanged

by pelleting the cells at 2050 rpm for 5 min if necessary. By analyzing the total number of cells, cell proliferation of untreated versus treated cells was compared.

2.11 Apoptosis assays

Apoptosis is the process of programmed cell death which occurs in multicellular organisms. Characteristic changes in e.g. the morphology of cells include cell shrinking, nuclear or chromosomal DNA fragmentation as well as chromatin condensation. These biochemical events afterwards lead to cell death. The principle of apoptosis was first described in 1842 by the German scientist Carl Vogt and later studied and further described by a number of scientists (193). The process of apoptosis can be controlled by either extracellular (e.g. toxins, cytokines) or intracellular (e.g. glucocorticoids, hypoxia) signals and to date can be detected via multiple assay systems.

2.11.1 Cell death detection assay

Induction of apoptosis after PIM1-specific siRNA or miR-33a treatment (2.8.1) was determined in a cell death detection assay. For K562 cells the Cell Death Detection ELISA (Roche Applied Biosciences, Mannheim, Germany) was used according to the manufacturer's protocol. Microtiter plates were pre-coated with an anti-histone antibody (clone H 11-4) and were incubated with lyzed cells. Addition of an anti-DNA antibody (clone MCA-33) was followed by an incubation step for 90 min. For detection of mono- and oligo-nucleosomes 2,2'-Azinobis-3-ethylBenzThiazolin-6-Sulfonic acid (ABTS) substrate solution was applied. This substrate is cleaved by peroxidases which are bound to the immune-complexes. The resulting ABTS-radical can be photometrically determined. Absorbance was measured with a Safire^{2}™ micro plate reader at 405 nm (Tecan, Crailsheim, Germany).

2.11.2 Caspase assay

To determine the apoptosis rate in LS174T cells, the Caspase-Glo® 3/7 Assay (Promega, Mannheim, Germany) was used according to the manufacturer's protocol. The assay provides a proluminescent caspase-3/-7 substrate which is cleaved to release aminoluciferin. Thereafter this cleaved product is used by luciferase for the production of light that in the following can be detected. Briefly 1 * 10^3 cells per well were seeded in 96-well plates and transfected with PIM1-specific siRNA or miRNA (2.8.2). After 120 h the caspase Glo® 3/7 substrate was prepared in serum-free medium and 100 µL were added to

the cells prior to incubation for 1 h at room temperature. For the detection of caspase activity luminescence was measured using a FLUOstar OPTIMA micro plate reader (BMG Labtech, NYC, USA).

2.12 FACS

A powerful biophysical technique to allow cell counting, sorting or protein engineering is flow cytometry. A specialized type is Fluorescence-Activated Cell Sorting (FACS) which sorts a heterogeneous mixture of biological cells. Cells are illuminated with a single light impulse and a number of detectors evaluate combination of scattered and fluorescent light. By this one single cell at a time is sorted based upon its specific fluorescence or light pattern.

2.12.1 Cell sorting via propidium iodide staining

One defined viability assay is performed by measuring cell membranes integrity. This can be done via a staining with the fluorescent dye propidium iodide which is an intercalating agent. Propidium iodide is impermeable for cell membranes of viable cells and thus colours only DNA fragments of dead cells. For FACS analysis K562 and LS174T cells were harvested after synchronizing their cell cycle with nocodazole (2.10.1), were fixed in 70 % ethanol in PBS and incubated for 1 h on ice. After incubation with 50 µg/mL RNase A (Thermo Fisher Scientific, Schwerte, Germany) at 37 °C for 30 min, cells were stained with 50 µg/mL propidium iodide solution. Afterwards FACS analyses were done using a BD FACSCalibur™ system (Becton-Dickinson, Heidelberg, Germany). These analyses were performed with the help of the working group of Prof. Dr. Achim Aigner.

2.13 Plasmid construction

In general plasmids are DNA molecules that are independent of genomic DNA. Plasmid DNA mainly is circular and differs in size. In case of genetic engineering plasmids are called vectors and are a powerful tool in molecular biology to amplify DNA or proteins of interest. All vectors used in this thesis are designed to allow amplification in eukaryotic cells.

2.13.1 Full-length *PIM1* cDNA clone

To obtain ectopic PIM1 expression in PIM1 negative mammalian cell lines, a full-length *PIM1* cDNA clone (Cat. No.: SC110975, Accession No.: NM_002648.2 hsa PIM1 oncogene, vector pCMV6-XL4; vector sequence imprinted in Appendix P) was purchased from OriGene (Rockville, MD, USA). The eukaryotic vector has a size of 4.7 kb plus 2.6 kb

PIM1 cDNA insert. Ectopic PIM1 expression in human cell lines is driven via a strong CMV promoter. The *PIM1* cDNA clone was introduced into chemically competent *E. coli* DH5α cells for further multiplication (2.5.3). To analyze specific miR-33a targeting of *PIM1* mRNA, several *PIM1* cDNA clone mutants were generated.

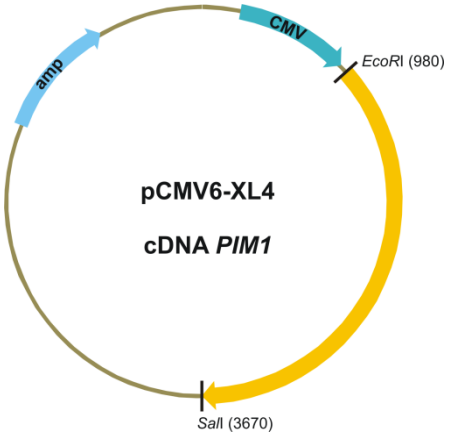

Figure 9: pCMV6-XL4 *PIM1* cDNA. Schematic overview of the *PIM1* cDNA clone; the *PIM1* cDNA (yellow arrow) is cloned behind a CMV promoter.

2.13.1.1 Δ 3'-UTR *PIM1* cDNA clone

To generate the Δ 3'-UTR *PIM1* cDNA clone, the *PIM1* full-length cDNA clone was digested with the fast digest enzyme *Hind*III (Thermo Fisher Scientific, Schwerte, Germany). The two *Hind*III restriction sites are positioned ~50 bp downstream of the PIM1 stop codon and ~400 bp upstream of the poly(A) tail (positions 1424 and 2311 in sequence NM_002648.3). After removal of the ~0.9 kb *Hind*III-fragment the vector was re-ligated and transformed into chemically competent *E. coli* DH5α cells (2.5.3). The Δ 3'-UTR *PIM1* cDNA clone lacks about two thirds of the 3'-UTR of *PIM1* which includes also the miR-33a target site. Thus this cDNA clone is important in studying the functions of miR-33a.

2.13.1.2 *PIM1* cDNA clone harboring a mutated miR-33a target site

The *PIM1* cDNA clone harboring a mutated miR-33a target site was derived from the cDNA clone lacking large parts of the *PIM1* 3'-UTR (2.13.1.1) and an already existing pGL3 control reporter construct harboring the 3'-UTR of *PIM1* with a site mutated version of the miR-33a target site (2.13.3.2). Therefore both vector constructs were digested with the restriction endonuclease *Hind*III (Thermo Fisher Scientific, Schwerte, Germany) to generate for the one hand the fragment of the *PIM1* cDNA clone lacking large parts of the *PIM1* 3'-UTR and on the other hand the *Hind*III-generated 3'-UTR insert containing the mutated miR-33a target site. After separation of the fragments by agarose gel electrophoresis (2.14.2.1) and cleaning up fragmented plasmid DNA (2.15.9), a re-ligation

step was applied, followed by its transformation into *E. coli* DH5α cells (2.15.5, 2.5.3). Correct insertion of the *Hind*III-cleaved fragments was verified via DNA sequencing (2.15.10).

2.13.2 pGL3 control reporter vector

In this thesis the commercially available pGL3 control reporter plasmid (Promega, Mannheim, Germany; vector sequence imprinted in Appendix Q; Figure 10a) was used for promoter studies and analyses of miRNA target sites via luciferase assays. This reporter vector consists of a luciferase gene strongly expressed by a SV40 promoter. For investigation of putative promoter constructs the SV40 promoter was exchanged by the promoter sequence of interest (Figure 10b). To determine miRNA-specific targeting of a protein of interest, its 3'-UTR was cloned behind the luciferase gene (Figure 10c).

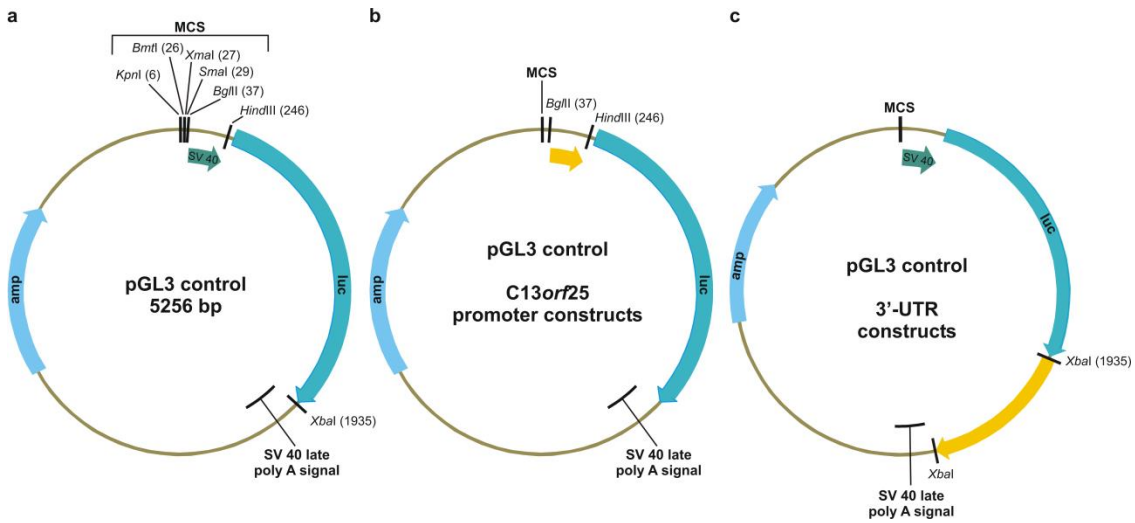

Figure 10: pGL3 control reporter vector and its derivatives. (**a**) Schematic overview of the pGL3 control reporter vector. (**b**) Schematic overview of the *C13orf25* promoter constructs; the individual sequence of the promoter construct (yellow arrow) is cloned in front of the luciferase coding region. (**c**) Schematic overview of the 3'-UTR constructs; the 3'-UTR of the protein of interest (yellow arrow) is cloned behind the luciferase coding region.

2.13.3 Cloning of different pGL3 reporter vector constructs

In the following chapters all pGL3 reporter vector constructs are described which were used in this thesis. Cloning experiments were done by several researchers and also depicted in detail elsewhere.

2.13.3.1 pGL3 control *PIM1* 3'-UTR reporter construct

In the 3'-UTR of human *PIM1* one miR-33a target site is located. To determine specific effects of a miR-33a mimic on *PIM1* mRNA, its 3'-UTR was cloned into the pGL3 control reporter vector. Human *PIM1* 3'-UTR was amplified from genomic DNA of the erythroleukemia cell line K562 using the primers listed in Appendix J. Afterwards the *PIM1* 3'-UTR was cloned into the unique *Xba*I site of the pGL3 control reporter vector located directly behind the luciferase gene. A transformation step into *E. coli* DH5α cells followed (2.5.5). Correct insertion of the *PIM1* 3'-UTR was validated via restriction digest of the plasmid and DNA sequencing (2.15.4, 2.15.10). The generated reporter construct was performed by Robert Prinz (194).

2.13.3.2 pGL3 control *PIM1* 3'-UTR mutated miR-33a target site reporter construct

To eliminate the miR-33a target site in the pGL3 control *PIM1* 3'-UTR vector, a mutagenesis PCR according to Brennecke et al. (195) was performed using primers listed in Appendix J. DNA sequencing (2.15.10) verified correctness of introduced mutations. This reporter construct was cloned by Robert Prinz (194).

2.13.3.3 pGL3 control hsa-let-7a target site reporter constructs

To introduce a hsa-let-7a site behind the luciferase coding sequence of the pGL3 control reporter vector, two complementary DNA oligonucleotides (Appendix J) encoding the let-7a target sequence (MIMAT0000062) (2.18.6) were annealed in annealing buffer (30 mM HEPES KOH pH 7.4, 100 mM KCl, 2 mM Mg_2Cl, 50 mM NH_4Ac) and cleaved with the restriction enzyme *Xba*I (2.15.4). Afterwards the DNA fragment was cloned into the unique *Xba*I site located immediately downstream of the luciferase gene of the linearized and dephosphorylated (2.15.2) pGL3 control reporter plasmid. Correct insertion of the double-stranded DNA oligonucleotide was identified through linearizing of recombinant plasmids via a unique *Blp*I site which was introduced with the annealed DNA insert. Cloning of the insert resulted in two opposite orientations that were identified by DNA sequencing (2.15.10). These clones, giving rise to RNA transcripts harboring a let-7a target site, were classified as 'forward orientation'; those with the opposite insert orientation served as negative control reporter plasmids, termed as 'inverted orientation'. Cloning studies were done by Robert Prinz (194).

2.13.3.4 pGL3 control P21 3'-UTR reporter construct

The 3'-UTR of human P21 harbors two target sites for members of the human miR-106b family, namely miR-17-5p and miR-20a. To determine the effects of LNA antiseeds directed against mature miR-106b family members on P21 protein levels, its 3'-UTR was cloned into the pGL3 control reporter vector via the *Xba*I site. Initially the 3'-UTR was amplified from human genomic DNA of K562 cells using primers listed in Appendix J. Afterwards the amplicon was subcloned into a pCR™2.1-TOPO® vector (TOPO® TA Cloning® kit, Invitrogen, Karlsruhe, Germany) prior to insertion into the pGL3 control vector. Correct introduction of the insert was applied using restriction digest as well as DNA sequencing (2.15.4, 2.15.10). Creation of the construct was performed by Robert Prinz (194).

2.13.3.5 pGL3 control P21 3'-UTR mutated miR-106b family target sites reporter construct

Mutagenesis of the two miR-106b family target sites in the P21 3'-UTR was performed via mutagenesis PCR (2.15.8.2) of the pGL3 control P21 3'-UTR reporter vector. Primers were designed according to Brennecke et al. (195) and are listed in Appendix J. The generated amplicons were cloned into *E. coli* DH5α cells (2.5.5) and correct insertion of the mutations was verified via DNA sequencing (2.15.10). This construct was generated by Robert Prinz (194).

2.13.3.6 pGL3 control *C13orf25* promoter constructs

To study the intronic AT-rich region preceding the miR-17-92 cluster, several *C13orf25* promoter constructs were cloned. These constructs include individual segments which either start ~100 nt or ~200 nt upstream of the miR-17 coding sequence. Therefore the pGL3 control reporter plasmid was used and the strong SV40 promoter deleted via restriction digest with the two enzymes *Bgl*II and *Hind*III. At this position the favored *C13orf25* segments were introduced harboring the respective restriction enzyme sites. Promoter fragments were initially amplified from human genomic K562 DNA using the primers listed in Appendix J. The amplicons were purified and digested with *Bgl*II and *Hind*III for re-introduction and ligation into the pGL3 control reporter vector (2.15.5). The vectors containing a 1.5 kb insert, a shortened insert of 625 bp or a 339 bp insert were generated by Robert Prinz (194). Similarly some promoter constructs were cloned by Dorothee Hartmann (196). One construct was designed containing 297 bp of *C13orf25*, a second one harbored only 197 bp. Additionally a 250 bp, a 190 bp and a 108 bp construct were cloned. One

construct comprised an inverted sequence of the 339 bp reporter construct and dealt as in internal control plasmid. All segments were cloned into *E. coli* DH5α cells (2.5.5) and were verified via DNA sequencing (2.15.10).

2.14 General nucleic acid techniques

Nucleic acid techniques can be used either for DNA or RNA oligonucleotides. DNA or RNA samples were stored at -20 °C for longer periods and dissolved in double-distilled water.

2.14.1 Determination of nucleic acid concentration

Nucleic acids are able to absorb light at a specific wavelength. The aromatic ring of each base can absorb light at the distinct wavelength of 260 nm. The nucleic acid concentration can be determined according to the law of Lambert-Beer (Equation 1) which relates the absorption of light to the properties of a material or solution that light has travelled through. The concentration of a sample can be determined if the absorbance is measured and the molar absorptivity as well as the path length of the cuvette are known.

Equation 1: Law of Lambert-Beer.

$$E = \varepsilon * c * l$$

[E]: extinction

[ε]: molar absorptivity (extinction coefficient) [1/(M * cm)]

[c]: molar concentration [M]

[l]: path length of the cuvette [cm]

During the laboratory work the concentration of nucleic acids was determined using double-distilled water as solvent. For absorption of 1 at 260 nm (1 A_{260}) and a cuvette path length of 1 cm following concentrations of nucleic acids can be assumed (Equation 2):

Equation 2: Concentration of nucleic acids.

1 A_{260} dsDNA → 50 µg/mL

1 A_{260} ssDNA → 37 µg/mL

1 A_{260} RNA → 40 µg/mL

The purity of nucleic acids can be estimated by measuring the ratio of A_{260}/A_{280}. The aromatic amino acids of proteins have their absorbance maximum at 280 nm. If the nucleic acid

solution is not contaminated with proteins or phenol (2.16.3) its absorbance ratio will be in between of 1.8 to 2.0 (183).

2.14.2 Nucleic acid gel electrophoresis

In 1955 O. Smithies performed the separation of serum in a gel electrophoresis (197) via starch gels for the first time. This was the beginning of an enormous and powerful method to analyze macromolecules, in particular nucleic acids. This technique is used in molecular biology to separate DNA or RNA molecules depending on their length. Because DNA and/or RNA oligonucleotides naturally contain a phosphodiester backbone, these molecules are negatively charged. This charge is a direct proportion to the amount of phosphate groups in the nucleotide chain. Thus the length of the DNA or RNA of interest can be determined.

2.14.2.1 Agarose gel electrophoresis

Separation of nucleic acids in an agarose gel matrix was established in 1964 and initially described by Tsanev et al. (198). Negatively charged nucleic acids, commonly DNA fragments or RNA oligonucleotides with a size larger than 500 nt, are able to migrate in an electric field towards the anode. During the laboratory work of this thesis analyses of DNA vectors, PCR reactions and PEI complexes were performed using agarose gel electrophoresis. To prepare agarose gels, variable amounts of agarose (Table 12) were diluted in TBE buffer (89 mM Tris-HCl, 89 mM borate, 2 mM EDTA) according to the needed separation range.

Table 12: Separation range of agarose gels.

% Agarose (w/v)	DNA fragment size (kb)
0.5	1.0-30.0
0.7	0.8-12.0
1.0	0.5-7.0
1.2	0.4-6.0
1.5	0.2-3.0
2.0	0.1-2.0

The indicated amount of agarose was added into 1x TBE buffer and was dissolved by heating it up in the microwave. After cool down of the solution ethidium bromide was complemented with a final concentration of 250 ng/mL. The gel solution was tipped into an agarose gel slide and a comb was applied before gelation of the matrix. DNA samples were mixed with 5x DNA loading dye (100 mM Tris-HCl pH 7.5, 50 mM EDTA pH 8.0, 70 %

glycerin (v/v), 0.05 % bromophenol blue (w/v), 0.05 % xylene cyanol blue (w/v)) and then loaded onto the agarose gel. Gel electrophoresis was done using TBE as running buffer. In general electrophoresis was run for 1 h at 80 mA in a PerfectBlue gel system Mini S (PEQLAB Biotechnologie, Erlangen, Germany). PEI complexes were analyzed in 1 % agarose gels for 2 h at 50 mA, after being dissolved in 5x DNA loading dye.

2.14.2.2 Polyacrylamide gel electrophoresis

PolyAcrylamide Gel Electrophoresis (PAGE) was first described in 1967 (199). The usage of a polyacrylamid matrix has several advantages in comparison to agarose matrices. The gels are much thiner, are transparent and beyond more reliable in separating smaller DNA fragments or RNA oligonucleotides up to 300 nt. In consequence of a radical polymerisation reaction acrylamide and bisacrylamide are able to cross-link, forming a structured grid that harbors a defined pore size. Polyacrylamide gel electrophoresis can be performed either in native or denaturing method and size separation is dependent on the ratio of acrylamide/bisacrylamide in the matrix (Table 13). The migration speed of single-stranded DNA can be estimated using two dyes, BromoPhenol Blue (BPB) and Xylene Cyanol Blue (XCB), during gel electrophoresis.

Table 13: Size fragmentation in PAGE.

Ratio of polyacrylamide [%]	BPB [nt]	XCB [nt]
8	19	70-80
10	12	55

Polyacrylamide gels were poured between two glass plates which were tightened with several clamps. A comb with the favored number of pockets was introduced between the plates before the gel solution was fixed. Hardening of the matrix took 30 min. The gel was placed in between an upper and lower chamber, the comb was removed and the pockets rinsed with TBE (89 mM Tris-HCl, 89 mM borate, 2 mM EDTA). PAGE was performed in self-made equipment (University of Lübeck, Germany) using 8-30 mA for 30 min to several hours depending on the percentage, conditions and size of the prepared gel. During this thesis native polyacrylamide gel electrophoresis was needed to separate amplified products of quantitative PCR which have a product length smaller than 100 bp. For this purpose polyacrylamide gel solution (10 % acrylamide/bisacrylamide (48:2) in TBE) was prepared and 0.01 volume of APS (dissolved as a 10 % solution) and 0.001 volume of TEMED were added to start radical polymerisation reaction. PCR samples were mixed with required amounts of 5x DNA loading dye (2.15.8) and were loaded onto the gel. Native PAGE was started as

described above. After finishing electrophoresis DNA fragments were detected using ethidium bromide (2.14.3.1). Denaturing polyacrylamide gel electrophoresis was performed to separate RNA. The buffer contains urea to interact with the stacking bases and destroy hydrogen bonds. This leads to a destabilization of RNA secondary structures. Analyses of total RNA were performed on 8 % denaturing PAGE (8 % acrylamide/bisacrylamide (48:2), 8 M urea in TBE). Commonly 0.5 to 1 µg of total RNA was used and mixed with 2x denaturing loading buffer (66 % (v/v) formamide, 2.6 M urea, 0.02 % (w/v) bromophenol blue, 0.02 % (w/v) xylene cyanol blue in 2x TBE). Samples were heated up to 95 °C for 2 min and were kept on ice until loading on the gel matrix. Denaturing PAGE was done as indicated above. After finishing electrophoresis RNA was stained using ethidium bromide (2.14.3.1).

2.14.3 Staining of nucleic acids

After gel electrophoresis of nucleic acids these molecules can be visualized using several staining techniques. Most commonly separated DNA or RNA samples are detected with small compounds which enable intercalation of the compound between stacked bases of DNA or RNA molecules respectively. Subsequently these compounds can be exposed to ultraviolet light (UV light) to generate fluorescence or they are visible themselves.

2.14.3.1 Ethidium bromide staining of nucleic acids

Ethidium bromide is used to detect separated nucleic acids in molecular biology (200). This fluorescent dye intercalates into double-stranded DNA or partially double-stranded RNA. When it is exposed to UV light, it shows an orange fluorescence emitting light at a wavelength of 590 nm. Staining of agarose gels was done following gel electrophoresis, while ethidium bromide was already included in the gel matrix (2.14.2.1). In case of polyacrylamide gels (2.14.2.2) DNA or RNA samples were stained after electrophoresis was finished. Therefore the gel was incubated in an appropriate volume of water containing 5 µg/mL ethidium bromide. After a 10 min shaking step at room temperature DNA or RNA bands can be detected and visualized using the gel documentation system Gerix 1000 (biostep, Jahnsdorf, Germany). Agarose or polyacrylamide gels were digitalized and recorded onto an USB flash drive for documentation.

2.14.3.2 Crystal violet staining of DNA

Crystal violet is another dye to stain DNA in agarose gels. The triarylmethane dye can be used as a non-toxic intercalating agent. It is used for detection of nucleic acids which should not be exposed to UV light to avoid destruction of DNA helices, especially DNA needed for *in vitro* cloning experiments. For staining procedure (2.14.2.1) it is applied directly into the

agarose gel matrix in a concentration of 10 µg/mL diluted in TBE buffer (89 mM Tris-HCl, 89 mM borate, 2 mM EDTA) and also the running buffer contains crystal violet in the indicated concentration. After finishing the agarose gel electrophoresis separated and dyed DNA bands were excised immediately with a sterile scalpel for further application.

2.14.3.3 Silver staining of nucleic acids

In 1973 Kerenyi and Gallyas first described the detection of proteins in gel matrices using silver ions (201). Nucleic acids are negatively charged. Positive silver ions can be chemically reduced to a silver coating at their surface and thus nucleic acids are stained. For silver staining nucleic acids were separated in agarose or polyacrylamide gels and fixed in the gel matrix using fixating solution (50 % MeOH (v/v), 12 % acetic acid (v/v)) for 15 min at room temperature on a shaker. Fixation step was repeated three times. Afterwards excessive amounts of acetic acid were washed out of the matrix with 30 % EtOH solution, again three times for 5 min at room temperature. Then the gel matrix was incubated for 45 sec in a freshly prepared coating solution (50 mL ddH_20, 33 µL HCHO 35 %, 25 µL $Na_2S_2O_3$ 43 %) and washed three times for 1 min in double-distilled water. Silver incubation (2 g/L $AgNO_3$ supplemented with 660 µL HCHO 35 %) was performed for 20 min at room temperature using a shaker. Subsequently excess of silver ions was washed out with double-distilled water for 1 min. Reduction of silver ions was done using reduction solution (60 g/L Na_2CO_3, 150 mL were supplemented with 75 µL of HCHO 35 % and 1.5 µL of $Na_2S_2O_3$ 43 %). When the expected bands had appeared, the gel was rinsed with water. Finally reduction was stopped using 7 % acetic acid. Gels were stored in 30 % EtOH solution and pictured using a Bio-Rad GS-800 Calibrated Densitometer (Munich, Germany). Pictures were digitalized onto an USB flash drive.

2.14.3.4 SYBR® Gold staining of nucleic acids

Detection of single- or double-stranded DNA or RNA oligonucleotides can be performed using SYBR® gold (Invitrogen™ Life Technologies, Darmstadt, Germany). This most sensitive fluorescent staining dye is an unsymmetrical cyanine dye that exhibits fluorescence increase upon binding to nucleic acids using standard ultraviolet transilluminators (202). The SYBR® Gold staining dye is provided as a 10.000-fold concentrate and was used for staining of DNA or RNA samples in agarose or polyacrylamide gel systems. The concentrated staining solution was diluted in TBE buffer (89 mM Tris-HCl, 89 mM borate, 2 mM EDTA) and protected from light. Gel matrices were incubated for 10-40 min at room temperature in a dish covered with an appropriate amount of solution. During this incubation step dishes were

kept in the dark or covered with aluminum foil. Afterwards 1x dilution was stored for up to one month at 4 °C and SYBR® gold stained nucleic acids were detected in UV light.

2.14.3.5 Autoradiography

Detection of nucleic acids is also possible using [^{32}P]-labeled oligonucleotides. Autoradiography of the radioactive-labeled sample can be visualized in a phosphor-imaging analyzer after a separating process in an agarose or a polyacrylamide gel matrix has occurred. Therefore the gel matrix was wrapped into transparent foil and exposed to an imaging plate for time periods between 1 min to overnight depending on the amount of radioactive material. Afterwards the imaging plate was scanned using a Fuji FLA-3000 R Phosphorimager (Fujifilm, Düsseldorf, Germany). Quantification of the DNA or RNA samples was calculated using the software AIDA (Version 3.45).

2.15 DNA techniques

2.15.1 Plasmid preparation

Plasmid preparation of overnight cultures (about 3-5 mL of culture medium) was performed using the Genejet™ Plasmid Miniprep Kit (Thermo Fisher Scientific, Schwerte, Germany) according to the manufacturer's protocol. In case of preparing larger amounts of bacterial cell culture (200-500 mL of culture medium) plasmid DNA was cleaned up using the NucleoBond® PC 500 purification kit (Macherey-Nagel, Düren, Germany). Recovered plasmid DNA was diluted in double-distilled H_2O before the resulting concentration was determined in a spectral photometer (Thermo Fisher Scientific, Schwerte, Germany).

2.15.2 Phosphorylation of 5'-OH ends of DNA oligonucleotides

Synthetic DNA primers have to be phosphorylated on the free 5'-OH end to enhance the efficiency of cloning experiments (2.13). For this purpose a recombinant T4 polynucleotide kinase from *E. coli* was obtained from Thermo Fisher Scientific (Schwerte, Germany). This enzyme is able to confer the gamma-phosphate of ATP to the free 5'-OH to phosphorylate the 5'-end of single-stranded DNA oligonucleotides. Reaction mixture was mixed as indicated at the manufacturer's protocol and is shown in Table 14.

Table 14: Phosphorylation of DNA oligonucleotides.

Ingredient	Concentration	Amount
DNA oligonucleotide	100 µM	0.5 µL
Reaction buffer A	10x	2 µL
ATP	10 mM	2 µL
T4 PNK (Thermo Fisher Scientific)	10 U/µL	1 µL
ddH_20	-	ad 20 µL
Phosphorylation reaction: 37 °C for 30-60 min Inactivation: 75 °C for 10 min		

2.15.3 Removal of 5'-phosphate groups of plasmid DNA

For cloning experiments using linearized vector DNA (2.15.4) the 5'-phosphate has to be removed to avoid re-circularization during the ligation reaction (2.15.5). This was done using the Thermo Scientific FastAP Thermosensitive Alkaline Phosphatase (Schwerte, Germany) according to the instructions given by the manufacturer (Table 15).

Table 15: Dephosphorylation of DNA.

Ingredient	Concentration	Amount
Linearized vector DNA	-	1 µg
Reaction buffer for AP	10x	2 µL
FastAP (Thermo Fisher Scientific)	1 U/µL	1 µL
ddH_20	-	ad 20 µL
Dephosphorylation reaction: 37 °C for 10 min Inactivation: 75 °C for 5 min		

2.15.4 Restriction digest of DNA

A restriction endonuclease is an enzyme that catalyzes endonucleolytic cleavage of double-stranded DNA at a specific recognition site, also termed restriction site. The recognition site is a specific sequence of 4-8 nucleotides which show a palindromic sequence arrangement. First discovered and isolated in the 1970s (203), (204), to date several hundreds of restriction enzymes are commercially available from different bacterial or archaeal organisms. They are grouped in four types, but for molecular cloning experiments, commonly type II restrictions endonucleases are used. To cleave a DNA sequence they do not require ATP. For them it is sufficient to use Mg^{2+} ions as a cofactor. Restriction endonucleases are able to generate either displaced ends on the 5'- and 3'-end (termed

sticky end generation) or cut DNA strands at the same position (termed blunt end generation). For analytical purposes and cloning experiments several restriction enzymes were used which are listed in Table 16.

Table 16: Restriction enzymes.

Restriction enzyme	Recognition sequence 5' → 3'
FastDigest *Bgl*II (Thermo Fisher Scientific)	5'- A↓GATCT
FastDigest *Blp*I (Thermo Fisher Scientific)	5'- GC↓TNAGC
FastDigest *Hind*III (Thermo Fisher Scientific)	5'- A↓AGCTT
FastDigest *Xba*I (Thermo Fisher Scientific)	5'- T↓CTAGA

Restriction digestion reactions were performed according to the manufacturer's instructions (Table 17). If possible FastDigest restriction enzymes (Thermo Fisher Scientific, Schwerte, Germany) were used. Digestion reactions were incubated for up to 30 min at 37 °C followed by a heating step to denature the enzyme. Samples were analyzed on an agarose gel (2.14.2.1) and stained with ethidium bromide. All digestion reactions needed for further cloning experiments were separated for preparative purposes and stained either with ethidium bromide or crystal violet (2.14.3.1, 2.14.3.2). After finishing gel electrophoresis DNA fragments were cut and cleaned up (2.15.9).

Table 17: Restriction digest.

Ingredient	Concentration	Amount	
		Analytical digest	Cloning
DNA	-	500 ng	up to 5 µg
Restriction buffer	10x	1 µL	5 µL
FD restriction enzyme (Thermo Fisher Scientific)	1 FDU	0.5 µL	up to 5 µL
ddH_20	-	ad 10 µL	ad 50 µL
Digestion: 5-30 min at 37 °C Heat inactivation: as indicated by the manufacturer			

2.15.5 Ligation of DNA fragments

In molecular biology ligation of DNA fragments is an enzymatic linking of a 5'-phosphate and a 3'-hydroxyl termini of one or two DNA fragment(s) to form a new phosphodiester bond. This

reaction is catalyzed by the enzyme T4 DNA ligase (205). For cloning experiments either DNA vectors or amplified DNA of PCR reactions were digested with the favored restriction enzymes to generate a distinct 5'- or 3'-end. Afterwards two fragments having the same restricted ends, blunt ends or sticky ends, were incubated for up to 4 h at room temperature with T4 DNA ligase (Thermo Fisher Scientific, Schwerte, Germany) as shown in Table 18. The ligation reaction was used for transformation reactions into bacterial *E. coli* DH5α cells (2.5.3).

Table 18: Ligation reaction.

Ingredients	Concentration	Amount
Plasmid DNA	-	1-100 ng
Insert DNA	-	500 ng
Reaction buffer	10x	2 µL
T4 DNA ligase (Thermo Fisher Scientific)	5 Weiss U/µL	2 µL
ddH_20	-	ad 20 µL
Ligation: 1-4 hours, RT		

2.15.6 Human genomic DNA preparation

Human genomic DNA (gDNA) was prepared for cloning experiments of respective pGL3 control vector constructs. Therefore the human erythroleukemia cell line K562 was used. Preparation of human total DNA was done with the DNeasy® Blood & Tissue Kit (Quiagen, Hilden, Germany). 5 * 10^6 K562 cells were centrifuged and washed with PBS until the total DNA was prepared according to the manufacturer's protocol using the 'Spin-Column Protocol' for purification of total DNA from human cells. After elution of total DNA its concentration was determined in a spectral photometer (Thermo Fisher Scientific, Schwerte, Germany) and DNA was prepared for following PCR amplification reactions (2.15.8.1). The preparation of human genomic DNA was performed by Robert Prinz (194).

2.15.7 Reverse transcription

Reverse transcriptase (RT) is an RNA-dependent DNA polymerase which allows generation of complementary DNA (cDNA) from an RNA template. Reverse transcriptase is needed for the replication of retroviruses. In 1970 two independent researchers (206), (207) found this enzyme. Since this discovery the door was open to create single-stranded DNA from RNA templates to further study the transcriptome of different organisms. For this thesis cDNA was arisen from total RNA or RNA, which was enriched for RNA transcripts smaller than 200 nt.

Therefore the RevertAid H Minus reverse transcriptase (Thermo Fisher Scientific, Schwerte, Germany) was used. This transcriptase is a recombinant variant of the M-MuLV RT lacking the RNaseH activity to increase the yield of full-length cDNA. In general 250-1000 ng of RNA were transcribed using 5-10 pmol of a specific reverse primer or 100 pmol of random hexamer primer according to the manufacturer's protocol (Table 19). In addition a negative control for each RNA sample in the absence of reverse transcriptase was produced to check for DNA contamination of the samples.

Table 19: Reverse transcription.

Ingredient		Concentration	Amount +RT	Amount -RT
RNA		-	250-1000 ng	250-1000 ng
Primer	gene-specific	10 µM	0.5 µL	0.5 µL
	random hexamer (Thermo Fisher Scientific)	100 µM	1 µL	1 µL
ddH_20		-	ad 11 µL	ad 12 µL
Heating Step: 80 °C for 10 min place samples on ice				
RT buffer (Thermo Fisher Scientific)		5x	4 µL	4 µL
dNTPs		10 mM (2.5 mM each)	2 µL	2 µL
ddH_20		-	2 µL	2 µL
RevertAid H Minus reverse transcriptase (Thermo Fisher Scientific)		200 U/µL	1 µL	-
reverse transcription: 42 °C for 60 min inactivation of RT: 70 °C for 10 min				

In the following the samples were prepared for quantitative real-time PCR measurements (2.15.8.3). The cDNA sample was diluted 1:5 or 1:10 with double-distilled water depending on the number of RNA transcripts that should be detected. QPCR was performed either straight after cDNA synthesis or samples were stored at -20 °C until usage.

2.15.8 PCR

PCR (Polymerase Chain Reaction) has been developed in 1983 by Kary Mullis (208). It is a technique to amplify DNA in an exponential manner. Used as a common procedure in molecular biology e. g. for cloning experiments, to date it can also be used for quantifying multiplied DNA sequences.

2.15.8.1 Amplification of genomic DNA

Purified human genomic DNA (gDNA) of K562 cells was used for amplification of the *PIM1* 3'-UTR, the P21 3'-UTR or the *C13orf25* promoter region. The primers needed for amplification reaction of the respective constructs are depicted in Appendix J. The reaction set up was mixed (Table 20) and after multiplication of gDNA (Table 21) the products are used for cloning into the pGL3 control vector (194).

Table 20: Reaction mixture gDNA.

Ingredient	Concentration	Amount
gDNA (K562)	-	300 ng
Taq buffer with KCl	10x	5 µL
dNTP mix	2.5 mM each	1 µL
Primer fwd	100 µM	0.5 µL
Primer rev	100 µM	0.5 µL
$MgCl_2$	25 mM	2 µL
Taq DNA polymerase (Thermo Fisher Scientific)	5 U/µL	0.5 µL
ddH_20	-	ad 50 µL

Table 21: Amplification gDNA.

Step	Temperature [°C]	Time [sec]	Repeat
Denaturation	94	300	1
Amplification cycle	94	45	30
	56	60	
	72	90	
Fill up cycle	72	420	1
Cooling	10	∞	-

2.15.8.2 Mutagenesis PCR for cloning experiments

To generate mutations into the seed region of miRNA target sequences in the pGL3 3'-UTR constructs mutagenesis PCR was performed. Therefore primers were designed according to Brennecke et al. (195) in case of mutating miRNA target sequences or by hand for all other introduced mutations. Nucleotides which should be exchanged in mutagenesis PCR were introduced in the forward primer sequence (Appendix J). Additionally a fully complementary reverse primer was designed (Appendix J). Mutations are positioned in the middle of the primer and flanked by approximately 10-15 nt on each site. As a template individual pGL3 control 3'-UTR or *C13orf25* promoter constructs were used for PCR reaction

(Table 22). After a phosphorylation reaction of the two respective primers (2.15.2), the amplification of the template was performed as indicated in mutagenesis PCR reaction (Table 23). Amplification program is dependent on the length of the amplicon.

Table 22: Reaction mixture mutagenesis PCR.

Ingredient	Concentration	Amount
Template	-	100 ng | 1 ng
Pfu buffer with $MgSO_4$	10x	10 µL | 5 µL
dNTP mix	2.5 mM each	1.6 µL | 1 µL
Primer fwd, phosphorylated	2.5 µM	2.5 µL | 4 µL
Primer rev, phosphorylated	2.5 µM	2.5 µL | 4 µL
$MgSO_4$	25 mM	12 µL | 5 µL
Pfu DNA Polymerase (Thermo Fisher Scientific)	2.5 U/µL	1 µL | 1 µL
ddH_2O	-	ad 100 µL | 50 µL

Table 23: Amplification mutagenesis PCR.

Step	Temperature [°C]	Time [sec]	Repeat
Denaturation	95	180-300	1
Amplification cycle	95	30-60	15-30
	50-60	40-90	
	72	30-840	
Fill up cycle	72	600	1
Cooling	8-10	∞	-

2.15.8.3 Quantitative real-time PCR

Quantitative real-time PCR (qPCR) is a technique to amplify DNA and simultaneously determine arising amounts of a target DNA or cDNA of interest. During this thesis several mRNAs or ncRNAs were analyzed using SYBR Green (Thermo Fisher Scientific, Schwerte, Germany). This DNA binding dye causes fluorescence upon interfering with the amplified dsDNA, but also including non-specific products. Increasing amounts of DNA lead to an increase of fluorescence which can be detected at each amplification cycle. Thus the amount of DNA can be measured. For quantification of miRNAs, generated miRNA-specific cDNA (2.15.7) was diluted and qPCR measurements performed using primers listed in Table 3. To determine human RNA levels of mRNAs or pri-mir-17-92, cDNA was diluted in the same manner and for quantification reactions primers depicted in Table 1 were used. Quantitative

PCR reactions were applied as described in Table 24 using freshly prepared or frozen cDNA samples. Amplification was done using either a LightCycler® 2.0 from Roche (Mannheim, Germany) or a MyiQ™5 Real-Time PCR Detection System (Bio-Rad, Munich, Germany) according to the instructions depicted in Table 25 and Table 26. Analyses of generated data was performed with the applied software iQ™5 (version 2.0) and 2^{-Cp}, $2^{-\Delta Cp}$ and $2^{-\Delta\Delta Cp}$ values evaluated according to Schmittgen and Livak (209).

Table 24: Quantitative real-time PCR.

Ingredient	Concentration	Amount
cDNA	1:5 or 1:10 dilution	4 µL
Absolute qPCR SYBR Green Mix (Thermo Fisher Scientific)	2x	10 µL
Primer fwd	5 µM	0.5 µL
Primer rev	5 µM	0.5 µL
ddH_2O	-	5 µL

Table 25: Amplification qPCR of mRNAs.

Step	Temperature [°C]	Time [sec]	Repeat
Initial Denaturation	95	900	1
Amplification cycle	95	10	55
	55	10	
	72	10	
Melting Curve	55 → 95	15	1 °C per sec
Cooling	40	30	-

Table 26: Amplification qPCR of miRNAs.

Step	Temperature [°C]	Time [sec]	Repeat
Initial Denaturation	95	900	1
Amplification cycle	95	10	55
	60	20	
	72	12	
Melting Curve	55 → 95	10	1 °C per sec
Cooling	40	10	-

2.15.9 Purification of PCR reactions

Purification of PCR reactions was applied to remove remaining template DNA, primers and/or dNTPs which were used in the amplification reaction. This either can be performed after the amplification step of the PCR reaction (2.15.8) or can be done after separation of the amplified PCR product in an agarose gel (2.14.2.1). The Wizard® SV Gel and PCR Clean-Up System (Promega, Mannheim, Germany) was used for purification. In case of purifying the PCR reaction the whole volume of PCR mixture was incubated with the indicated amount of Membrane Binding Solution before binding to the silica membrane of the Wizard® SV Minicolumns. If the amplicon was initially separated in an agarose gel, the band of interest was excised and dissolved in Membrane Binding Solution according to the manufacturer's protocol. In both cases DNA was eluted from the columns in a centrifugation step and used for further experiments.

2.15.10 DNA sequencing

DNA sequencing reactions were sent out and performed at eurofins mwg|operon (Ebersberg, Germany). Samples were prepared according to the company's instructions. Purified plasmid DNA was diluted in double-distilled water to a volume of 15 µL possessing a concentration of about 50-100 ng/µL. In some cases a specific primer (2 pmol/µL in a minimum volume of 15 µL) was sent out together with the sample (Appendix K). Several days later the sequencing analyses could be checked at the web page of eurofins (www.eurofinsdna.com) and data could be aligned to the vector sequence for validity and integrity.

2.15.11 ChIP assay

Chromatin ImmunoPrecipitation (ChIP) is a method to determine interactions between specific proteins and specific genomic regions such as promoter elements or DNA binding sites. Cross-linked ChIP (ChIPX) is mainly suited for mapping of the DNA target of chromatin-associated proteins. Thus proteins are reversibly cross-linked to their associated chromatin regions via formaldehyde or UV-light. These temporarily bonded DNA/protein complexes are shared and the protein of interest is selectively immunoprecipitated. After purification of the associated DNA fragments their sequences can be determined and be referred to the respective chromatin region. For this thesis, chromatin immunoprecipitation was performed according to a protocol from the Or Gozani lab (http://www.stanford.edu/group/gozani) at Stanford University with some modifications. $2 * 10^7$ K562 cells in 13 mL RPMI medium were cross-linked with 1 % formaldehyde for 10 min at 37 °C. Reactions were stopped by adjusting to 0.125 M glycine and cells were

collected by centrifugation at 400 *g* for 5 min at room temperature. For cell lysis cells were resuspended in 750 µL RIPA-buffer (10 mM Tris-HCl pH 7.4, 150 mM NaCl, 1 % deoxycholate, 1 % NP-40, 0.1 % SDS, 0.2 mM PMSF) supplemented with the cOmplete Mini Protease Inhibitor Cocktail from Roche (Mannheim, Germany) according to the manufacturer's instructions. Lyzed cells were sonicated in a Branson Sonifier 250 (duty cycle 50 %, output control 2, for 3.5 min on ice water) (Heinemann, Schwäbisch Gmünd, Germany) and centrifuged at maximum speed (13.000 rpm, 10 min at 4 °C). The supernatant was pre-cleared with 10 µL of blocked *Staphylococcus aureus* cells (PANSORBIN® Cells, Calbiochem/Merck, Darmstadt, Germany) for 15 min at 4 °C on a rotor wheel. After a second centrifugation step (13.0000 rpm, 5 min, RT), the supernatant was split into two samples (each ~350 µL, representing + and - specific antibody (AB)) which were adjusted to buffer D (16.7 mM Tris-HCl pH 8.1, 167 mM NaCl, 1.2 mM EDTA, 1.1 % Triton-X 100, 0.01 % SDS) and a total volume of 500 µL. 1 µg (1 to 5 µL) of the respective antibody was added to + AB samples, whereas the same volume buffer D was added to - AB samples. At this point also the mock control was prepared, consisting of 500 µL buffer D. + AB, - AB and mock samples were then incubated for at least 3 h at 4 °C. The following antibodies were used: monoclonal anti-c-Myc (sc-40), anti-Pim-1 (sc-13513) and anti-phospho-HP1G (Ser83) antibody (2600S); Table 8). In the case of mouse monoclonal antibodies samples were additionally incubated for 1 h with a second monoclonal goat anti-mouse IgG antibody (sc-2005, Table 9). Immunoprecipitation was initiated by adding 10 µL of Pansorbin® cells to the + AB, - AB and mock samples, followed by incubation for 15 min at room temperature. Samples were centrifuged (13.0000 rpm, 3 min, RT); the supernatant of the - AB sample was saved, later serving as the input control. Pellets were washed twice with dialysis buffer (50 mM Tris-HCl pH 8.0, 2 mM EDTA) and four times with IP-wash buffer (100 mM Tris-HCl pH 9.0, 500 mM LiCl, 1 % NP40, 1 % deoxycholate). Antibody-bound material was eluted from Pansorbin® cells by adding 150 µL elution buffer (50 mM $NaHCO_3$, 1 % SDS), vortexing and centrifugation (13.000 rpm, 3 min, RT). The supernatant was collected and the procedure was repeated. Reverse cross-linking and RNA digestion was performed in 280 µL buffer (0.3 M NaCl, and 1 µL RNaseA (10 mg/mL, Thermo Fisher Scientific, Schwerte, Germany)) for 5 h at 67 °C in a hybridization oven (Biometra, Goettingen, Germany). Chromatin was precipitated with 2.5 volumes of ethanol, followed by a ProteinaseK (Thermo Fisher Scientific, Schwerte, Germany) digest that was done according to the manufacturer's protocol. DNA was purified by phenol/chloroform extraction (2.16.3) and ethanol precipitation in the presence of 0.3 M NaOAc pH 5.2. PCR amplification using *Taq* DNA polymerase and the co-immunoprecipitated DNA as template was done under the following conditions: 2 min

at 95 °C in the absence of enzyme, followed by 35 amplification cycles of 45 sec at 95 °C, 45 sec at 60 °C, 45 sec at 72 °C using primers listed in Table 27.

Table 27: Primers for ChIP assay.

Name of Primer	Sequence 5' → 3'	Product length [bp]
A1 forward	5'- AAA GGC AGG CTC GTC GTT G	93
A1 reverse	5'- CGG GAT AAA GAG TTG TTT CTC CAA	
A2 forward	5'- ACA TGG ACT AAA TTG CCT TTA AAT G	367
A2 reverse	5'- AAT CTT CAG TTT TAC AAG GTG ATG	
A3 forward	5'- ACT GCA GTG AAG GCA CTT GT	167
A3 reverse	5'- TGC CAG AAG GAG CAC TTA GG	
A4 forward	5'- CCA ATA ATT CAA GCC AAG CAA	137
A4 reverse	5'- AAA TAG CAG GCC ACC ATC AG	
A5 forward	5'- GCC CAA TCA AAC TGT CCT GT	212
A5 reverse	5'- CGG GAC AAG TGC AAT ACC AT	

2.16 RNA techniques

2.16.1 RNA extraction for small RNAs of mammalian cell lines

Characterization of small RNAs such as miRNAs has been raised in the last decades. Playing important roles in gene regulation and developmental processes, these small non-coding RNAs are of enormous interest in many research topics. For this thesis isolation of small RNA molecules was done using the *mir*Vana™ miRNA Isolation Kit purchased from Ambion (Life Technologies, Darmstadt, Germany). All extractions were done according to the given manufacturer's protocol. Small RNA isolation was performed with about $5 * 10^6$ cells growing in suspension or under adherent conditions. After a washing step with PBS cells were lyzed in about 500 µL Lysis/Binding Solution supplemented in the Isolation Kit. An acid phenol/chloroform extraction followed which provides a robust purification to remove large amounts of DNA (210). Therefore one volume of Acid Phenol:Chloroform solution was added, the mixture vortexed and centrifuged. The upper aqueous phase was loaded onto a glass-fiber filter and after a centrifugation step, a second filter was included and enriched small RNAs were eluted in 10-20 µL ddH_2O. Afterwards concentration of RNA was determined in a spectral photometer (Thermo Fisher Scientific, Schwerte, Germany) and small RNAs were used to generate cDNA for quantification of miRNA levels (2.15.7).

2.16.2 Total RNA extraction of mammalian cell lines

Total RNA extraction of different mammalian cell lines was applied to quantitate the cellular activity at different time points or after different treatments of the cells. Thus different levels in gene expression and regulation can be determined. For this purpose total cellular RNA of mammalian cells was purified using a variation of the guanidinium thiocyanate-phenol-chloroform extraction method described in 1987 by Piotr Chomczynski and Nicoletta Sacchi (210). For purification about $5 * 10^6$ cells were counted and washed with PBS. Afterwards they were lyzed by pipetting up and down in 750 µL of Tri-lysing buffer (0.8 M guanidinium thiocyanate, 0.4 M ammonium thiocyanate, 0.1 M sodium acetate pH 5.0, 5 % glycerin, 48 % aqua-phenol pH < 5.0). The solution was incubated for 5 min at room temperature and 200 µL of chloroform was added. A shaking step for 30 sec using a vortex mixer followed. Subsequently the solution was incubated for 10 min at room temperature and organic and aqueous phase separated via a centrifugation step for 20 min at room temperature and 13.300 rpm. The upper aqueous phase was shaken out a second time with one volume of chloroform to enrich purity of RNA and to discard as much DNA and protein contamination as possible. After the solution was shaken out for 15 sec using a vortex mixer the sample was separated again and spun down at 13.300 rpm for 5 min. In the following the aqueous phase was transferred into a new tube and total RNA precipitated with one to two volume(s) of isopropanol for 10-30 min at room temperature. Total RNA was pelleted via centrifugation at 13.300 rpm for 30 min at 4 °C and the pellet washed with 75 % ethanol. Finally RNA concentration was measured in a spectral photometer (Thermo Fisher Scientific, Schwerte, Germany) following either a DNaseI treatment (2.16.4) or total RNA was prepared for quantitative PCR measurements (2.15.8.3).

2.16.3 Phenol/chloroform extraction of RNA

DNaseI digested total RNA extracts (2.16.4) have to be purified via phenol/chloroform extraction to get rid of protein and salt impurity. Sample material after DNaseI digestion was formulated in a volume of 200 µL which is the minimum amount of starting volume. This solution was mixed with one volume of aqua-phenol pH < 5.0 for RNA preparation. The sample was shaken vigorously for 30-60 sec and then incubated for 5 min at room temperature. Subsequently the sample was centrifuged for 5 min at 13.000 rpm using a centrifuge and the upper aqueous phase transferred to a new tube. One volume of chloroform was added and again the sample was shaken for 15 sec using a vortex mixer. Another centrifugation step follows (5 min, 13.000 rpm, RT). Once again the upper aqueous phase was pipetted into a new tube. RNA was precipitated by adding 1-2.5 volume(s) of

isopropanol right after sodium acetate had been added to the sample to reach a final concentration of 0.3 M NaAc. Precipitation was performed for 10 min at room temperature and RNA pelleted for 30 min at 4 °C and 13.000 rpm. To free the RNA pellet of salt ions, a washing step with 75 % EtOH was included, followed by another centrifugation step. RNA pellet was dried for 5 min and dissolved in 10-20 µL of double-distilled water. RNA concentration was determined and calculated in a spectral photometer (Thermo Fisher Scientific, Schwerte, Germany).

2.16.4 DNaseI digestion

To get rid of any DNA contamination, extracted total RNA (2.16.2) was digested with DNaseI (Thermo Fisher Scientific, Schwerte, Germany). RNase-free DNaseI is able to digest single- and double-stranded DNA by hydrolyzing phosphodiester bonds. Enzymatic activity and thus cleavage efficiency is dependent on Ca^{2+} ions. For digestion of DNA in total RNA prepared samples 1 µg of RNA was mixed with 1 U DNaseI and incubated for 30 min at 37 °C as described by the manufacturer's protocol (Table 28). Afterwards DNaseI enzyme was heat deactivated and an additional DNaseI digestion step was included, followed by another phenol/chloroform extraction (2.16.3) to remove hydrolyzed DNA fragments, DNaseI enzyme and salt ions.

Table 28: DNaseI digestion.

Ingredient	Concentration	Amount
RNA	-	1 µg
DNaseI buffer	10x	10 µL
DNaseI, RNase-free (Thermo Fisher Scientific)	50 U/µL	1 U
ddH_20	-	ad 100 µL
DNA digestion: 37 °C for 30 min Inactivation of DNaseI: 65 °C for 10 min		
DNaseI buffer	1x	25 µL
DNaseI, RNase-free (Thermo Fisher Scientific)	50 U/µL	1 U
ddH_20	-	ad 250 µL
DNA digestion: 37 °C for 30 min Phenol/chloroform extraction		

2.16.5 Radiolabeling of the 5'-end of RNA

5'-end labeling of double-stranded siRNA or small single-stranded RNA oligonucleotides (Table 29) was performed using the T4 polynucleotide kinase (Thermo Fisher Scientific,

Schwerte, Germany) isolated from *E. coli* T4 bacteriophage. This enzyme catalyzes the transfer of a gamma-phosphate from [γ-^{32}P]-ATP to the 5'-OH end of single- or double-stranded nucleic acids.

Table 29: Oligonucleotides for 5'-end labeling.

Name of oligonucleotide	Sequence 5' → 3'	
VR1 siRNA (179)	sense	5'- GCG CAU CUU CUA CUU CAA CdTdT
	antisense	5'- GUU GAA GUA GAA GAU GCG CdTdT
pRNA 14-mer (211)	5'- GUU CGG UCA AAA CU	
pRNA 8-mer (212)	5'- GUU CGG UC	

The phosphorylation mixture was prepared as indicated in Table 30 using radiolabeled ATP purchased at Hartmann Analytic GmbH (Braunschweig, Germany).

Table 30: Radiolabeling mixture.

Ingredient	Concentration	Amount
RNA oligonucleotide	-	30 pmol
Reaction buffer A	10x	2 µL
[γ-^{32}P]-ATP	3000 Ci/mmol	3 µL
T4 PNK (Thermo Fisher Scientific)	10 U/µL	1.5 µL
ddH_20	-	ad 20 µL
Phosphorylation reaction: 37 °C for 60 min Purification: illustra MicroSpin G-25 spin columns		

Afterwards the phosphorylation reaction was purified from unincorporated nucleotides using illustra MicroSpin G-25 spin columns (GE Healthcare Life Sciences, Freiburg, Germany) according to the manufacturer's protocol. The radiolabeled RNA was eluted and the amount of radioactivity and the efficiency of labeling reaction were measured in a 1900 CA TRI-CARB® Liquid Scintillation Analyzer (Perkin Elmer, MA, USA). Radiolabeled RNA oligonucleotides were used to perform radioactive studies on PEI complexes (2.8.2.2, 2.16.6).

2.16.6 Determination of PEI complex formation efficacy

To determine the efficacy of PEI F25 LMW complex formation with nucleic acids or LNA antiseeds, a radioactive assay was employed as described previously (213). 500 ng of single-stranded RNA, 14- or 8-meric, or double-stranded siRNA were used, mixed with trace amounts (10^4 Cerenkov cpm) of 5'-[^{32}P]-end labeled siRNA, RNA 14-mer or RNA 8-mer

(Table 29) respectively. Complex formation was performed with the indicated amounts of PEI F25 LMW (2.8.2.2). Samples were mixed with 5x DNA loading dye (10 mM Tris-HCl pH 7.6), 80 % glycerol, 0.03 % bromophenol blue, 0.03 % xylene cyanol blue) and analyzed in agarose gel electrophoresis (2.14.2.1). Complex formation was analyzed by autoradiography (2.14.3.5) of the agarose gel for 3 h using a Fuji FLA-3000 R Phosphorimager (Fujifilm, Germany). The ratio of free to partially and fully complexed RNA was calculated using AIDA software (Version 3.45).

2.17 Atomic force microscopy

Atomic Force Microscopy (AFM) is a high-resolution type of scanning probe microscopy first described in the 1980s by Binnig and Rohrer (214) as a technique to detect surfaces at an atomic level. The technique uses piezoelectric elements that are able to facilitate tiny and precise movements. This enables a very powerful and accurate measurement. PEI/LNA complexes were analyzed by atomic force microscopy and were done with the help of the working team of Prof. Dr. Bakowsky at the Institute of Pharmaceutical Technology and Biopharmaceutics, Philipps-Universität Marburg, Germany. Complexes were prepared (2.8.2.2) with 500 ng of LNA 14-mer 17-5p or LNA 8-mer (PS) and increasing amounts of PEI F25 LMW. Complexes were directly transferred onto a silicon chip by dipping the chip into the complex solution. AFM was performed on a vibration-damped NanoWizard (JPK instruments, Berlin, Germany) as described in detail elsewhere (215). Commercially available pyramidal Si_3N_4 tips (NSC16 AIBS, Micromasch, Estonia) mounted to a cantilever with a length of 230 µm. A resonance frequency of about 170 kHz and a nominal force constant of about 40 N/m were used. To avoid damage of the sample surface, measurements were performed in intermitted contact. The scan speed was proportional to the scan size and the scan frequency was between 0.5 and 1.5 Hz. Images were obtained by displaying the amplitude signal of the cantilever in the trace direction and the height signal in the retrace direction, both signals were simultaneously recorded. The complexes were visualized either in height or in amplitude mode (512 x 512 pixels).

2.18 Bioinformatics and software tools

In this chapter important bioinformatical methods and software tools are listed which were used throughout the complete work for this thesis.

2.18.1 GraFit™

The program GraFit™ (Version 5.0) is a data analysis software for Microsoft© Windows™ and was needed for creating scientific graphs depicted in most figures. GraFit™ is programed by Robin J. Leatherbarrow (216) for Erithacus Software Ltd. (Horley, U.K.) and provides the experimental scientist with a tool for visualization and analyses of existing data.

2.18.2 CorelDRAW® Graphics Suite

CorelDRAW® Graphics Suite is a graphic and image editing collection of the Corel™ Corporation (Ottawa, Canada). In 1989 version 1.2 was released for Microsoft© Windows™ computer systems and for this thesis version CorelDRAW® release 11.0 was used. The software is based on vector graphics construction and was applied for figure drawing.

2.18.3 Statistical analyses

2.18.3.1 R

Since 1993 the open source programming language R is available to use it for statistical computing. This software was used to generate two-sided t-test analyses to identify significant data in between the obtained values.

2.18.3.2 GraphPad Prism®

Another software program used for statistical analyses was GraphPad Prism® (Version 4.0) available for Microsoft© Windows™. This tool was used by the group of Prof. Dr. Achim Aigner to calculate Student's t-test, 1-way ANOVA/Tukey's multiple comparison posttests and 2-way ANOVA/Bonferroni posttests.

2.18.4 NCBI

The National Center for Biotechnology Information (NCBI) was founded in 1988 through legislation and harbors relevant information to biotechnology such as an index of biomedical research articles in PubMed or PubMed Central, the genome sequencing data or the GenBank. All researchers working in the field of biotechnology or molecular biochemistry use the different information tools offered by the NCBI (http://www.ncbi.nlm.nih.gov/). Another important tool being part of the NCBI is the BLAST sequence alignment tool. Designed in 1990 the Basic Local Alignment Search Tool (BLAST) (217) is a powerful program to search for local alignments in different organisms comparing protein or DNA sequences which are

part of the GenBank with those being experimentally validated. To date it is the most often used software tool worldwide analyzing biological data of sequenced material.

2.18.5 TargetScan

MiRNA target sites were predicted using the online software tool TargetScan Release 5.1 (http://www.targetscan.org/vert_50/) which is provided by the Massachusetts Institute of Technology. The search page of TargetScan is available for searching target sites in mammals or mouse sequences, but is also at hand for worm, fly and fish based data search. Therefore the software is searching for the presence of conserved 8- or 7-mer nucleotide sites which match the seed region of individual miRNAs (218). The program also includes the identification of seed sequences that have included mismatch positions, but only if this mismatches can be compensated by a conserved 3'-pairing of the miRNA (219). For searching in mammals the program ranks hits based on the predicted efficacy of targeting which is calculated by using the context score of the sites including site-type, 3'-pairing, local AU and position contribution (69). The software is permanently improved and now version 6.2 is available.

2.18.6 MiRBase

The bioinformatical software program miRBase is available as an archive of microRNA sequences and annotations (http://www.mirbase.org/). The biological database is hosted and maintained at the University of Manchester and had been set up by the microRNA registry of Sam Griffiths-Jones in 2004 (180). The miRBase registry provides the inclusion of novel miRNA genes and helps to assign names (220). MiRBase can be used to search for annotated miRNAs, while each entry represents a predicted hairpin of a miRNA transcript, giving information about the location and sequence of the mature miRNA. This software tool was used to search for mammalian miRNAs of interest e.g. to establish primer design for miRNA quantification.

2.18.7 ClustalW and WebLogo

The Clustal series is a software tool for doing multiple sequence alignments of three or more protein or DNA sequences (221). Started in 2003 ClustalW can be used to generate phylogenetic trees and is available at the webserver of the European Bioinformatics Institute (http://www.ebi.ac.uk/Tools/msa/clustalw2/). For the purpose needed in this thesis ClustalW was used to generate multiple sequence alignments of promoter regions or of selected 3'-UTRs of different organisms to check sequence conservation of miRNA target sites. To

create a defined picture of conserved regions a WebLogo (222) was compiled. The WebLogo software is designed to make sequence logos as easy as possible. They are pictured as a graphical representation of amino acids or nucleic acids. In the WebLogo the stack of each symbol and its corresponding height is dependent on the conservation of the amino acid or nucleotide in the respective alignment.

2.18.8 PromPredict

To identify putative promoter sequence elements within the AT-rich region of *C13orf25*, the software tool PromPredict (http://nucleix.mbu.iisc.ernet.in/prompredict/prompredict.html) was used. This tool was designed in the Manju Bansal lab (223) to identify promoter regions in genomic DNA sequences based on differences in DNA stability between neighboring regions.

2.18.9 Neural Network Promoter Prediction

The Neural Network Promoter Prediction software tool is a program of the Berkeley Drosophila Genome Project (http://www.fruitfly.org/seq_tools/promoter.html). In 2001 the software was generated by M.G. Reese (224). For this thesis the program was used for promoter predictions of the AT-rich region within *C13orf25* and helps to find putative promoter elements.

2.18.10 McPromoter 006

McPromoter 006 is a statistical tool for the prediction of transcription start sites in eukaryotic DNA and was initially developed by Uwe Ohler (225) in 1999 (http://tools.genome.duke.edu/generegulation/McPromoter/). The software tool was used to predict intronic promoter regions within *C13orf25*.

2.18.11 Promoter 2.0 Prediction Server

Promoter 2.0 predicts is a software tool to predict transcription start sites of vertebrates (http://www.cbs.dtu.dk/services/Promoter/) that was developed in 1998 by Steen Knudsen (226) and was used search for transcription start sites within *C13orf25*.

2.18.12 CorePromoter

CorePromoter is a prediction program for transcription start sites based on a Quadratic Discrimination Analysis of human core-promoters. The software tool was developed in 1998

by Michael Zhang (227) and the web-based software (http://rulai.cshl.org/tools/genefinder/CPROMOTER/human.htm) was used to search for promoter elements within the human *C13orf25* AT-rich intronic region.

3 Results and Discussion

The following section is a summary of the scientific publications resulting from my research work. The publications will be briefly resumed by topic in single chapters including a short discussion about the results obtained. Detailed information concerning the results, materials, and methods are given in the respective publications.

3.1 Project 1: The proto-oncogene PIM1 is a target of miR-33a *in vitro* and *in vivo* (publication I and II)

Introduction

The PIM1 kinase belongs to a family of constitutively active serine/threonine kinases (133) which fulfills important functions in cellular processes that are involved in malignant transformation of cells (137) and as a consequence PIM1 is classified as a proto-oncogene. Overexpression of this kinase is correlated with a poor prognosis in almost all hematopoietic malignancies and solid cancers (133), in our study represented by the chronic myelogenous leukemia cell line K562 and the colorectal adenocarcinoma cell line LS174T. PIM1 is a promising target for therapeutic strategies in the treatment of cancer (133) because a large number of PIM1 targets are involved in proliferation, differentiation and apoptosis to promote tumorigenesis (138). To date small molecular compounds which compete for ATP-binding have been designed to mediate post-translational regulation of the PIM1 kinase (160).

In our study, we revealed to use RNAi-mediated protein knockdown of PIM1 through PIM1-specific siRNA and miRNA as a novel therapeutic approach for targeting PIM1 at the mRNA level.

Results

For this purpose, we initially performed *in silico* screenings using bioinformatical tools to search for putative miRNA binding sites within the *PIM1* 3'-UTR and indeed several of such sites could be identified for the binding of e.g. the miRNAs miR-15a, miR-16-1 and miR-33a. These three miRNAs have been further considered in the following *in vitro* experiments because (i) miR-15a and miR-16-1, which are characterized by the same seed sequence, are known as tumor suppressors via targeting of the anti-apoptotic B-cell lymphoma 2 (BCL2) protein and thus inducing apoptosis (80) and (ii) the highest conservation within the putative miRNA binding sites in the *PIM1* 3'-UTR was shown for miR-33a including the seed region as well as nt 13-17 of the miRNA.

Low expression levels of miR-33a in normal and cancer cell lines such as K562, LS174T, Skov-3, HEK293, HUH7 or HepG2 do not refer to a direct correlation between a tumor-suppressive function of endogenously expressed miR-33a in the regulation of *PIM1* mRNA. However the high conservation of the miR-33a binding site in the *PIM1* 3'-UTR and the overall low expression levels of this miRNA in the tested cancer cell lines suggested the possibility to reduce PIM1 levels in tumor cells by transfection of commercially available

miRNA mimics (Dharmacon/Thermo Fisher Scientific). Indeed the transfection of miR-33a mimics decreased PIM1 protein levels in the two tested cell lines K562 and LS174T about 40-60 %, whereas miR-15a and miR-16-1 miRNA mimics failed in the downregulation of PIM1 (Figure 11a).

Another highly ranked putative target of miR-33a is the cell cycle regulator cyclin dependent kinase 6 (CDK6) harboring two conserved putative miR-33a binding sites within the *PIM1* 3'-UTR. CDK6 is associated with D-type cyclins and involved in cell cycle progression by regulating G1/S transition (228). We asked if CDK6 is also regulated by miR-33a, but we could not validate CDK6 as a target of miR-33a in K562 cells (Figure 11b). In a mouse system, the tumor suppressor p53 (TP53) (229) was found to be a target of miR-33a. However we could not confirm this result in LS174T cells (Figure 11c). Another published target of miR-33a is the ATP-binding cassette transporter A1 (ABCA1) (230), (231). Reduction of ABCA1 protein levels could not be tested in the two cell lines due to an overall too low endogenous expression of ABCA1 protein.

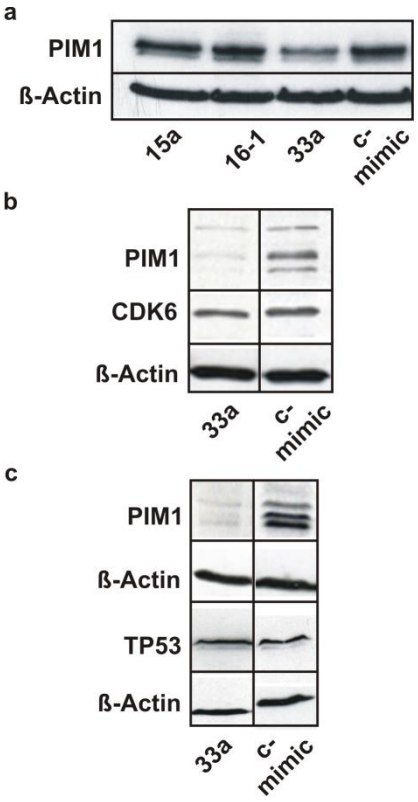

Figure 11: Human PIM1 is a target of miR-33a. (**a**) In K562 cells *PIM1* is downregulated by a miR-33a mimic, while miR-15a and miR-16-1 mimics as well as the control mimic have no measurable effects on PIM1 protein expression levels. ß-Actin serves as an internal loading control. (**b**) Knockdown efficacy of a miR-33a mimic after transfection into K562 cells. PIM1 expression levels are substantial decreased, whereas no effect was detected for the highly predicted target CDK6. ß-Actin serves as an internal loading control. (**c**) In LS174T cells knockdown efficacy of a miR-33a mimic was detected. A substantial decrease of protein expression was observed for PIM1. Although TP53 was reported to be a target of miR-33a in the mouse system (229), we were unable to detect a significant repression of human TP53. ß-Actin serves as an internal loading control.

The specificity of miR-33a binding to the 3'-UTR of *PIM1* was shown (i) by luciferase reporter assays as well as (ii) ectopic PIM1 expression in PIM1 negative cells. (i) A reporter vector containing the *PIM1* 3'-UTR behind a firefly luciferase showed substantial downregulation of luciferase activity after co-transfection with a miR-33a mimic, whereas the repression effects were abrogated when using a seed-mutagenized variant of the reporter (Figure 12a). (ii) Ectopic PIM1 expression was performed in the ovarian carcinoma cell line Skov-3 to further substantiate that miR-33a specifically and directly represses PIM1 expression. In fact, Western Blot experiments confirmed downregulation of ectopic expressed PIM1 protein levels by miR-33a. A loss of responsiveness was seen either for a seed-mutagenized construct or a *PIM1* cDNA clone lacking large parts of the *PIM1* 3'-UTR (Figure 12b).

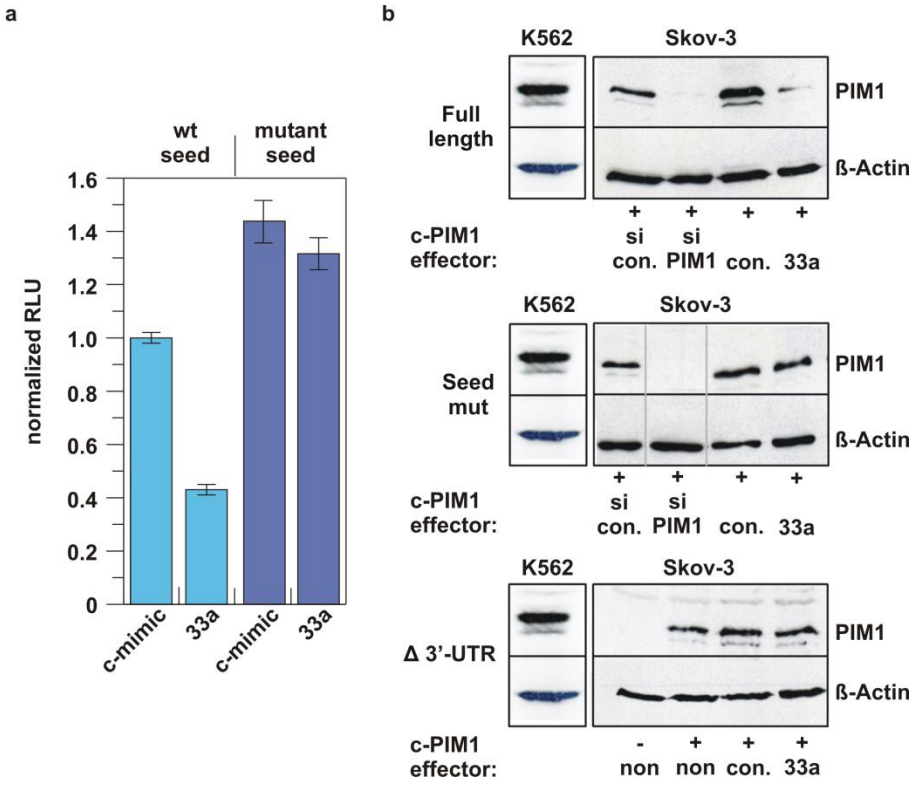

Figure 12: MiR-33a-specific regulation of PIM1 expression. (**a**) K562 cells were co-transfected with the control mimic or a miR-33a mimic and a reporter plasmid containing the *PIM1* 3'-UTR or a seed-mutagenized variant fused to the luciferase coding region respectively. Data represent mean values derived from at least three independent experiments (+/- S.E.M.). (**b**) Effects of the miR-33a mimic and a PIM1-specific siRNA on ectopic PIM1 expression were detected in Western Blot experiments. Therefore a full-length *PIM1* cDNA clone, a miR-33a target site mutagenized variant (seed mut) or a vector lacking large parts of the 3'-UTR of *PIM1* (Δ 3'-UTR) were co-transfected with a control siRNA (si con.), a PIM1-specific siRNA (si PIM1), a control mimic (c-mimic) or a miR-33a mimic into Skov-3 cells. ß-Actin serves as an internal loading control.

To further characterize the miR-33a-dependent downregulation of PIM1 protein levels, we compared the observed effect with a knockdown mediated by a PIM1-specific siRNA. Although the siRNA transfection resulted in an even more efficient knockdown of PIM1, the time-dependent decrease of protein levels of miR-33a and a PIM1-specific siRNA in K562 cells were similar and still present after 96 h post-transfection (Figure 13).

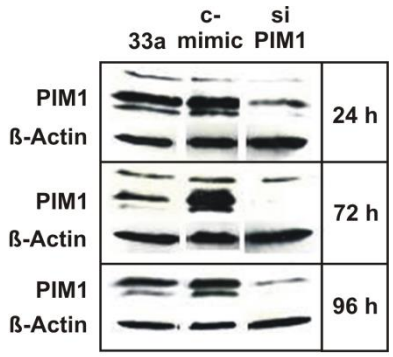

Figure 13: Long-term effects of PIM1 knockdown by the miR-33a mimic. Comparison of the PIM1 knockdown persistence for the miR-33a mimic versus the PIM1-specific siRNA detected 24, 72 and 96 h post-transfection.

As it has been reported that PIM1 is involved in the regulation of cell proliferation in K562 cells (157), we hypothesized that a negative effect on proliferation might be associated with the biological relevance of the observed miR-33a effects. Indeed an anti-proliferative effect could be verified in the two investigated cell lines K562 and LS174T either for a PIM1-specific siRNA or the miR-33a mimic (data not shown).

So far we have established PIM1 as a target of miR-33a, thus opening up the possibility to further investigate the proto-oncogene PIM1 in an anti-cancer approach using the tumor-suppressive miR-33a for miRNA replacement therapy. For this reason we started formulation of miR-33a with the cationic branched polyethylenimine PEI F25 LMW which has been previously established as excellent *in vivo* delivery agent for siRNAs in mouse tumor models (176). To assess the therapeutic anti-tumor activity of miR-33a, a subcutaneous LS174T colon carcinoma xenograft mouse model was generated and treated by systemic injection of the PEI/miR-33a complexes. The systemic PEI/miR-33a replacement therapy resulted in a significant reduction in tumor growth of about 40 % (Figure 14a,c). Consistent with the inhibition of tumor growth, a reduction of PIM1 protein levels could be determined during the analysis of the tumors after termination of the experiment (Figure 14b). During the experimental period of PEI/miR-33a treatment no reduction in body weight of the mice was

detectable. Furthermore induction of immune responses, any hepatotoxicity or other unwanted side effects of miR-33a replacement therapy was not observed.

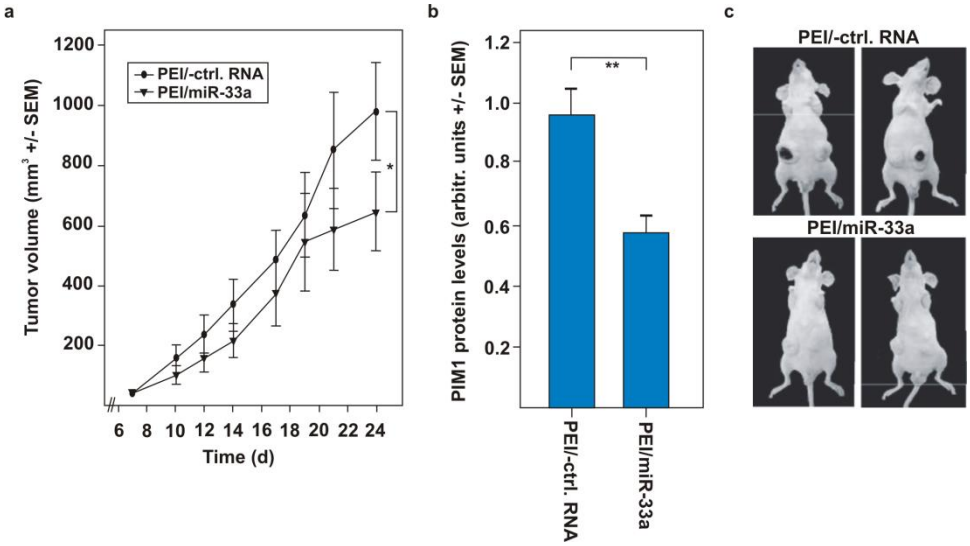

Figure 14: Antitumor effects of systemic PEI/miR-33a treatment in LS174T tumor xenografts. (**a**) Inhibition of tumor growth of systemically injected PEI/miR-33a complexes compared with negative control treated mice. (**b**) Analysis of the tumor xenografts upon termination of the experiment reveals a reduction of PIM1 protein levels upon PEI/miR-33a treatment in comparison to a control treatment. (**c**) Representative examples of treated mice.

Discussion

In our study miR-33a has been established as a miRNA being implicated in tumor progression *in vitro* and *in vivo*. It was shown in luciferase reporter assays as well as in Western Blot experiments that the oncogenic kinase PIM1 is a specific target of tumor-suppressive miR-33a. Likewise transfection of miR-33a mimics decelerated proliferation and polyethylenimine-based miRNA replacement therapy successfully reduced tumor growth without unwanted side effects in a xenograft mouse model of colon cancer.

Human miR-33a and related miR-33b are encoded in the intron of human sterol regulatory element binding protein 2 (SREBP2) on chromosome 22 and SREBP1 on chromosome 17 and are transcribed together with the host gene respectively. SREBPs are key regulators in lipid metabolism and homeostasis. Recently it was reported that both, miR-33a and miR-33b, are involved in the regulation of cholesterol biosynthesis and uptake, repressing proteins like ABCA1 (230), (231) which is involved in cholesterol efflux. Antagonism of miR-33a/b with antisense oligonucleotides has been shown to mediate reverse cholesterol transport and regression of atherosclerosis in mice (232). In non-human

primates a study was initiated to establish a therapeutic approach against dyslipidemia in cardiovascular disease risk. After inhibition of miR-33a/b with a 2'-F/MOE modified phosphorothioate antisense oligonucleotide, plasma high-density lipoprotein (HDL) levels of the monkeys were raised and very-low-density-lipoprotein (VLDL) triglycerides were lowered (233). However a long-term antimiR-33 study in high-fat, high-cholesterol-fed $Ldlr^{-/-}$ mice failed to prevent progression of atherosclerosis (234), maybe due to the absence of miR-33b in rodents.

In our study we have demonstrated that PIM1 is a genuine target of miR-33a, although we have not yet identified the biological constellation(s) under which miR-33a levels are overexpressed to directly repress endogenous PIM1. Expression of miR-33a/b is generally low (230) either in normal or cancer tissues and is associated with SREBP transcription.

Therefore a linkage between cholesterol homeostasis and cell proliferation seems to be the most obvious constellation to identify a natural context of miR-33a-dependent PIM1 regulation. There are also other biological circumstances where PIM1 is upregulated. For example PIM1 has cardioprotective effects which are mediated through an overexpression in cardiac progenitor cells (235), (236). As another example PIM1 is induced during the development of monocytes to macrophages (own observations). However miR-33a has not been analyzed under these conditions. The tumor suppressor activity of miR-33a/b has also been shown for the regulation of the oncogene MYC (237). In medulloblastoma cells a statin-induced upregulation of miR-33b substantially decreased cellular MYC protein levels and for this reason presents a promising therapeutic option against cancers involving MYC overexpression (237). SREBP expression has also been implicated in the regulation of the cell cycle (238) and thus a connection between miR-33a and cell cycle progression has been reported in the liver cell line HUH7. In this context CDK6 and cyclin D1 (CCND1) have been established as targets of miR-33a reducing cell proliferation and arresting the cell cycle in G1 phase (239).

Taken together, these findings emphasize an essential role of miR-33a in the cellular connection of several molecular pathways. In addition cell-type and tissue-specific regulatory pathways as well as expression levels of miR-33a seem to be crucial and regulation of miR-33a/b in therapeutic approaches has to be well-balanced. However our PEI/miR-33a replacement strategy showed antitumor effects *in vivo* and an accumulation of delivered miRNAs in tumor tissues has been shown (28). Ultimately personalized therapy and targeted delivery is preferable in order to reduce side effects and extensive research in this field should be promoted.

3.2 Project 2: Novel seed-directed LNA antimiRs as potent miRNA inhibitors *in vitro* (publication III)

Introduction

MiRNA expression differs in normal and cancer tissues (39) and overexpression of oncogenic miRNAs is often associated with malignant transformation and tumorigenesis (100). One important oncogenic miRNA cluster is the miR-17-92 cluster that can promote proliferation and is involved in the inhibition of apoptosis (88). MiRNAs of this cluster, miR-17 and miR-20a, have been reported to post-transcriptionally control the cell cycle regulator P21 (240), an important and well-characterized cyclin-dependent kinase inhibitor with tumor suppressor activity (241). The inhibition of oncogenic miRNAs to modulate oncogenic pathways is a promising therapeutic strategy in the prevention and treatment of cancer. AntimiR design is a challenging task because there are several chemical modifications available to enhance resistance against cellular nucleases and to increase the binding affinity to the target miRNA of interest (109). To date a safe and efficient delivery of antimiRs is still the main bottleneck. Successful *in vivo* delivery of antagomiRs (124) which are conjugated with cholesterol to improve their cellular uptake has been reported. Moreover *tiny LNAs* (126) which harbor a phosphorothioate (PS) backbone can also be delivered without any formulation in a mouse tumor model. A formulated delivery of unconjugated antimiRs has not been explored so far.

In our study we scrutinized a novel class of potent miRNA inhibitors: single-stranded short LNA oligonucleotides harboring a natural phosphodiester backbone (PO), henceforth termed LNA antiseeds (PO). We tested length-dependent miRNA inhibition of several LNA antiseeds to explore even miRNA family targeting. Furthermore we established complex and nanoparticle formation of the LNA antiseeds with the cationic branched polyethylenimine PEI F25 LMW to enable the delivery into a broad spectrum of tissues and organs.

Results

As a first experimental approach we determined the minimum LNA antiseed (PO) length which is needed for the inhibition of miRNA function. Thus we investigated inhibitory effects of 8-, 10-, 12-, and 14-meric LNA antiseeds (PO) against miRNA let-7a. For this purpose we cloned a hsa-let-7a target sequence in the 3'-UTR of a luciferase reporter gene (Promega); as a control we replaced the sequence by an inverted hsa-let-7a target sequence. The inhibitory effect of miRNA let-7a in HeLa cells was shown by a derepression of the luciferase

activity. Only weak effects were obtained with the 8- or 10-meric LNA antiseeds (PO) (data not shown), whereas 12- and 14-meric LNA antiseeds (PO) efficiently derepressed the luciferase reporter even in low concentration ranges of 1-20 nM (Figure 15). As a negative control we used an unspecific and unrelated 14-mer LNA oligonucleotide directed against bacterial RNaseP (182). A commercially available antimiR against let-7a, designed as a miRNA hairpin inhibitor (181), served as in internal positive control for derepression of the reporter system (Figure 15).

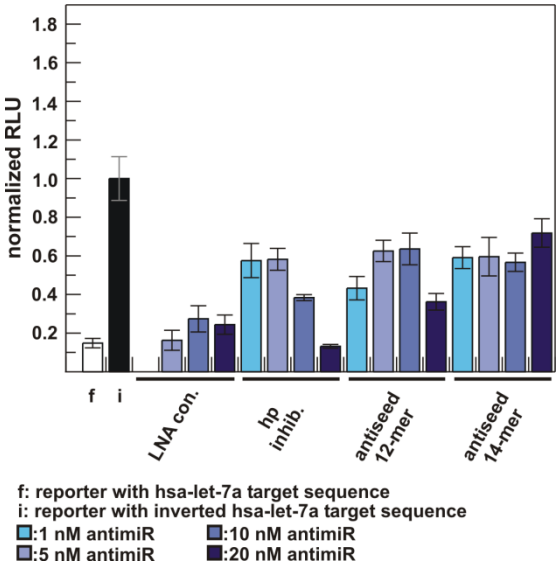

Figure 15: LNA antiseeds (PO) as miRNA inhibitors. Comparison of 12- and 14-meric LNA antiseeds (PO) with a commercially available hairpin inhibitor (hp inhib.) targeting a hsa-let-7a luciferase reporter at the indicated concentrations. As a control an unrelated LNA 14-mer (LNA con.) was used. Values are derived from at least three independent experiments (+/- S.E.M.) after co-transfection into HeLa cells.

In a second approach we determined derepression activity of LNA antiseeds (PO) by the investigation of an endogenously expressed target gene. Therefore derepression of basal protein levels of the tumor suppressor P21 was analyzed in the erythroleukemia cell line K562. This cell line expresses P21 mRNA, but protein levels are barely sufficient for the detection in Western Blot experiments. Recently it has been reported that P21 is post-transcriptionally regulated by miRNAs of the miR-106b family (240) e.g. miR-17 and miR-20a. We therefore hypothesized that miR-17 and miR-20a, which are overexpressed in K562 cells (103), repress endogenous P21 protein levels in the indicated cell line. To test this, 14-meric LNA antiseeds (PO) directed against the two miRNAs were transfected into K562 cells, and indeed caused substantial increase of P21 protein levels in comparison to an unrelated LNA control. The effect of raised P21 protein levels mediated by the LNA antiseeds (PO) was persistent and could still be detected 120 h after a single transfection of the LNA antiseeds (PO) (Figure 16a). The specificity of the observed LNA antiseed (PO) effect was analyzed with a luciferase reporter vector (Promega). For this purpose, the 3'-UTR of P21 and a seed-mutagenized variant were cloned behind the firefly

luciferase of the reporter vector. As a positive control, commercially available miRNA hairpin inhibitors (181) were compared with the LNA antiseeds (PO). At a concentration of 10 nM the derepression of luciferase activity was not as substantial as it was observed with the LNA antiseeds (PO) directed against miR-17 and miR-20a. Moreover the combination of equimolar concentrations of the hairpin inhibitors enhanced derepression of the reporter that was now comparable to the effect of the single LNA antiseeds (PO) (Figure 16b). These findings implied that LNA antiseeds (PO) are able to inhibit and block miRNAs of the same family, whereas miRNA inhibitors are more specific to a single miRNA. As a further positive control, we tested a *tiny LNA* directed against the seed region of miR-17/20a, and indeed found highly efficient derepression of the reporter system (Figure 16b), but also a slight increase in luciferase activity for the seed-mutagenized reporter construct (Figure 16c) implicating slight non-specific effects.

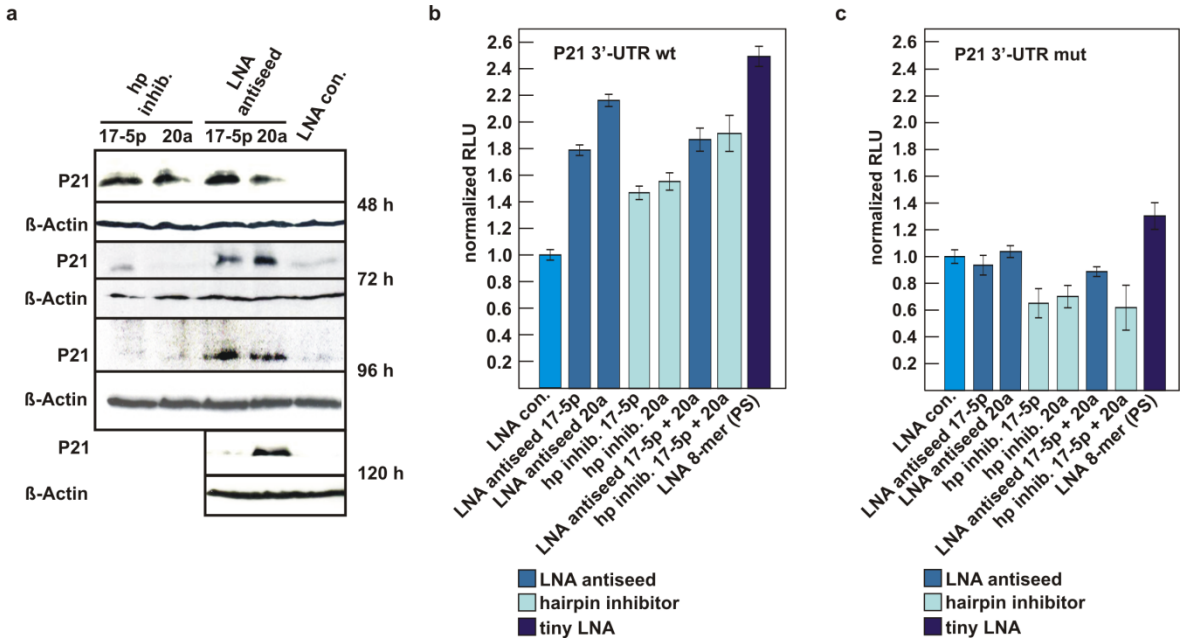

Figure 16: Specific inhibitory effects of LNA antiseeds (PO) against the miR-106b family. (**a**) Duration of P21 derepression by LNA antiseeds (PO) versus hairpin inhibitors (hp inhib.). Expression of basal P21 protein levels were analyzed by Western Blot after transfection of the antimiRs into K562 cells. (**b**) Specific derepression activity of the indicated miRNA inhibitors after co-transfection with the P21 3'-UTR luciferase reporter into HeLa cells. Luciferase activity values are derived from at least three independent experiments (+/- S.E.M.). (**c**) Effects of the indicated miRNA inhibitors on luciferase expression using the seed-mutated version of the reporter in HeLa cells. Values are derived from at least three independent experiments (+/- S.E.M.).

As the delivery of antisense oligonucleotides is the major bottleneck for therapeutic applications, unconjugated LNA antiseeds with a PO backbone have to be formulated e.g. with polyethylenimine for the use in *in vivo* studies to enable uptake into cells and tissues. Previously we have established the use of the branched cationic polyethylenimine PEI F25 LMW for systemic delivery of siRNA (176) or for miRNA replacement therapy (28). To explore efficient LNA antiseed complex formation with PEI F25 LMW, we performed atomic force microscopy (AFM) to visualize the shaped nanoparticles. In fact formation of polymeric nanoparticles was observed upon mixing of PEI F25 LMW with an LNA antiseed (PO) (Figure 17a). After demonstrating the efficient formation of homogenous nanoparticles, we analyzed PEI/LNA let-7a (PO) complexes in the hsa-let-7a-specific luciferase reporter assay in HeLa cells. This PEI-based delivery strategy mediated substantial derepression of luciferase activity *in vitro* (Figure 17b), thus providing the basis for future research of LNA antiseeds also in mouse tumor models.

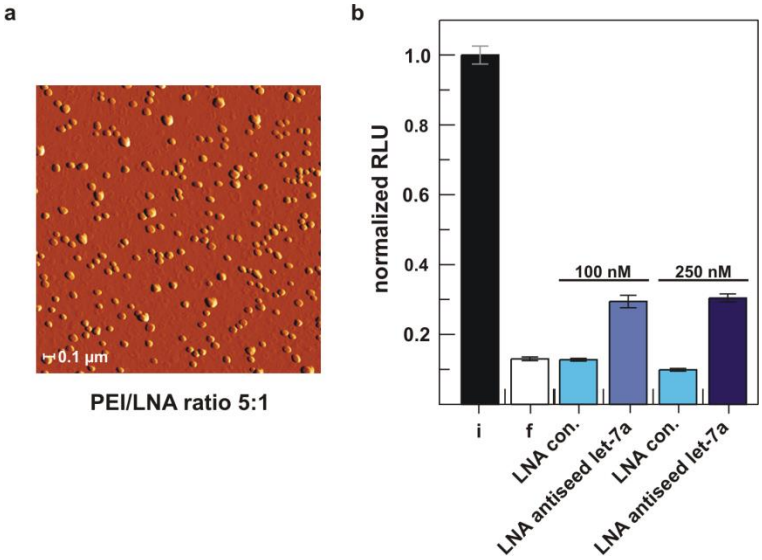

Figure 17: Functional delivery of PEI/LNA antiseed (PO) nanoparticles. (**a**) Detection of PEI F25 LMW/LNA nanoparticles using atomic force microscopy. (**b**) In HeLa cells co-transfection of the hsa-let-7a luciferase reporter with PEI/LNA antiseed let-7a (PO) nanoparticles leads to derepression of luciferase activity. Values are derived from at least three independent experiments (+/- S.E.M.).

Discussion

The advantages of antimiR-based applications are (i) to analyze important cellular functions of miRNAs by blocking them and thereby preventing post-transcriptional regulation or (ii) to inhibit overexpressed and oncogenic miRNAs in several disease states. To date antimiR-based therapy has been successfully established *in vitro* and *in vivo* using several different modifications either in the backbone or the sugar positions of the oligonucleotides. One of the most important variations is the introduction of LNA sugar modifications, where the ribose is sterically stabilized and locked in the C3'-endo conformation. LNA modifications

enable an increase of target affinity by enhancing the melting temperature (T_m) of the oligonucleotide (115),(242). It has been reported that the dissociation constant of LNA/RNA hybrids, which can be determined as k_{off} value, is dramatically reduced (243), and thus LNA oligonucleotides are very efficient and persistent in blocking RNA functionality. A better resistance against cellular nucleases has been shown that is further increased by the introduction of phosphorothioate linkages (105), (244). Despite this advantage, a phosphorothioate modified antisense oligonucleotide has some disadvantages such as a non-specific binding to cellular proteins associated with toxic side effects (245), (244). Preferentially oligonucleotides harboring a natural phosphodiester backbone should be used for systemic application because they show no toxicity or any side effects (28), (244). However antimiRs with a phosphorothioate backbone can be delivered unconjugated; nevertheless a formulation of the LNA antiseeds (PO) with the cationic branched polyethyleneimine PEI F25 LMW has many advantages. PEI polymers are able to (i) protect the incorporated nucleic acids against nucleases, (ii) mediate the cellular uptake and (iii) trigger the release of the oligonucleotides into the cytoplasm via a proton/sponge effect (246). Furthermore in miRNA replacement therapy the cationic branched PEI F25 LMW has proven a targeted delivery of the nucleic acids into tumor tissues causing neither toxicity nor an increase of hepatic enzymes or any immunostimulatory effects (28). Thus polyethyleneimine formulated miRNA-based LNA antiseed (PO) therapy is a promising option to inhibit oncogenic miRNAs and should be further investigated in *in vivo* tumor mouse models of different cancer types.

3.3 Project 3: Transcriptional regulation of the human miR-17-92 cluster (manuscript in preparation IV)

Introduction

The oncogenic miRNA cluster miR-17-92 is one of the best characterized human miRNA clusters and encodes six miRNAs, namely miR-17, miR-18a, miR-19a, miR-20a, miR-19b and miR-92a. Also referred to as oncomiR-1 or *C13orf25*, miR-17-92 is associated with hematopoietic malignancies and solid cancers (96). Overexpression of the cluster promotes proliferation, inhibits apoptosis and accelerates angiogenesis (88). Analyses to study transcriptional regulation of miRNAs or miRNA clusters are necessary and relevant to develop novel strategies aiming at cancer prevention. Unfortunately only few miRNA promoters have been identified or closer characterized to date (169). Transcription of the polycistronic miR-17-92 cluster has been shown to be in part controlled by an E2F-regulated host gene promoter with E2F3 being the main E2F variant associated with the host gene promoter (167), (166). Additionally transcription originates from an intronic AT-rich region directly upstream of the miRNA coding region (169) which had been determined by nucleosome mapping combined with chromatin signatures to identify transcriptionally active promoters (247), (248), (249). Cluster expression originating from the intronic AT-rich region is activated by the transcription factor MYC that binds to a conserved E-box element (E3) approximately 1.5 kb upstream of the miR-17-92 coding sequence (87), (91), (248).

In our study we scrutinized promoter activity emanating from the intronic AT-rich region. ChIP experiments identified the proto-oncogene PIM1 and one of its phosphorylation targets HP1G (155) to be associated with the chromatin region comprising the functional MYC-binding site. SiRNA-mediated knockdown of PIM1 protein resulted in decreased levels of pri-mir-17-92 transcript levels. Both results provide evidence that the miR-17-92 cluster belongs to those 20 % of all MYC regulated genes that show a synergism with the oncogenic kinase PIM1 (159).

Results

As a first experimental approach we analyzed MYC-dependent transcriptional activation of the intronic AT-rich sequence. Therefore we cloned several pGL3 control luciferase reporter constructs (Promega) that were generated from the intronic AT-rich promoter region (Figure 18a). After transfection into K562 and HeLa cells, expressing the miR-17-92 cluster at very high and high levels (data not shown), we evaluated transcriptional activity of this putative

promoter region. Indeed we showed MYC-dependent transcriptional activity emanating from the intronic AT-rich region (1.5 kb construct). A knockdown of MYC protein levels (K562 cells) or a truncated reporter variant lacking the functional MYC binding site E3 (625 bp construct) caused substantial downregulation of luciferase activity of about 4.5-fold in K562 and almost 20-fold in HeLa (Figure 18b). This finding supports the assumption that MYC binding to the E3 site plays a central role in activating transcription of miR-17-92. We further shortened the promoter constructs including elements with their 3'-boundary approximately 290 bp upstream of the mature miR-17-5p coding sequence due to basal promoter activity obtained with the 625 bp construct. As controls we included the pGL3 control reporter vector lacking the SV40 promoter sequence as well as a construct with comparable AT-content (inverted 339 bp construct) (Figure 18a,b). In contrast to the inverted 339 bp construct all fragments which are shorter than ~340 bp conferred residual promoter activity indicating that parts of the intronic promoter region promote specific transcriptional activity (Figure 18b).

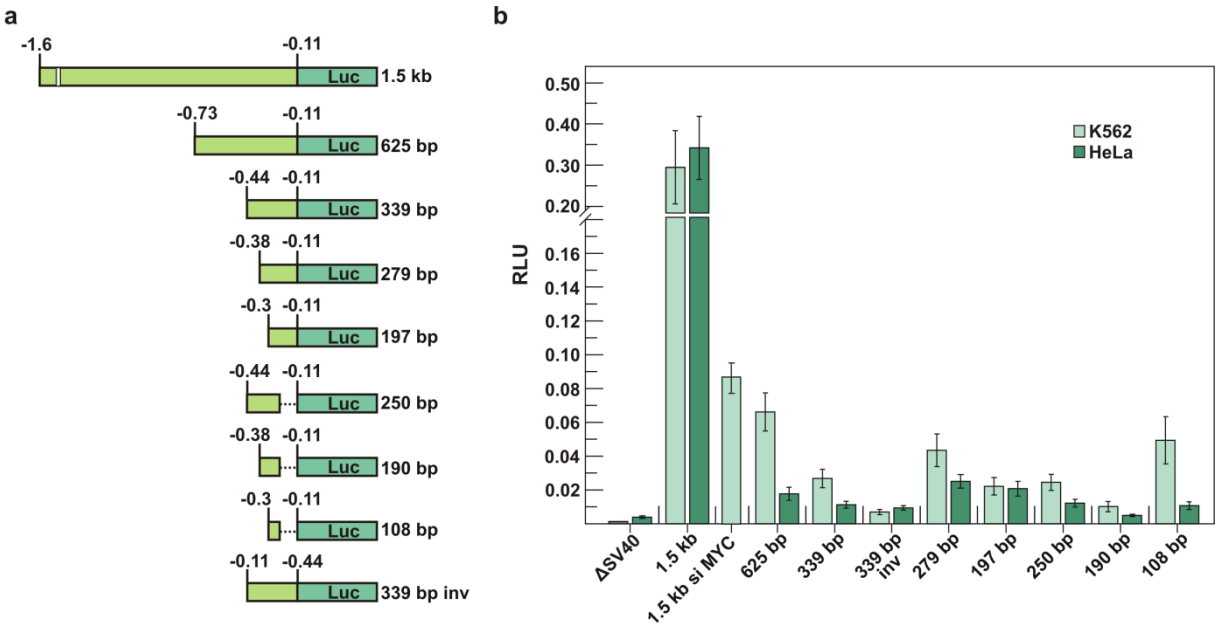

Figure 18: MYC-dependent intronic transcriptional activity of the human *C13orf25* locus. (**a**) Schematic representation of different *C13orf25* segments fused to the luciferase gene. The functional MYC binding site (E3) is indicated in the 1.5 kb construct (white box). (**b**) Promoter activities of the different promoter reporter constructs in K562 and HeLa cells. Obtained luciferase activities were normalized to the pGL3 control vector (Promega). RLU values of the individual constructs were derived from 5 to 16 experiments (+/- S.E.M.).

Next we considered if other factors beyond MYC may be involved in transcriptional regulation of the human miR-17-92 cluster. Indeed ChIP assays of the functional MYC binding site in the AT-rich promoter region confirmed not only association of MYC to this chromosomal area. Further we identified the oncogenic kinase PIM1 as well as its phosphorylation target

HP1G to be associated with this chromatin region (Figure 19). Additionally we were able to identify HP1G association along the miRNA coding region indicating that HP1G participates in active transcription of the miR-17-92 cluster (data not shown).

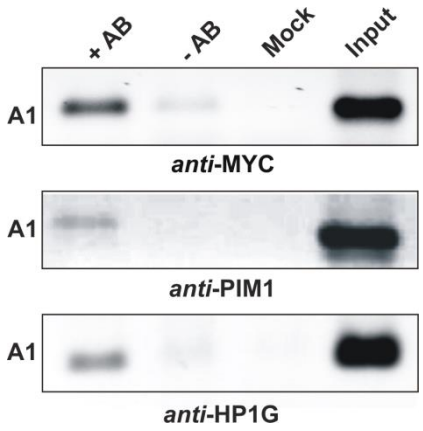

Figure 19: ChIP analysis of the functional MYC binding site in the intronic region of *C13orf25*. In K562 cells ChIP analysis identified MYC, PIM1 and HP1G association with this chromatin region. + AB: with antibody; - AB: without antibody; Mock: buffer without cell lysate; Input: supernatant of the - AB sample.

To scrutinize the role of PIM1 in miR-17-92 expression, we determined cellular pri-mir-17-92 transcription levels by qPCR after siRNA-mediated knockdown experiments of E2F3, MYC and PIM1 in the two different cell lines. K562 and HeLa cells were selected due to very high and high expression levels of the miR-17-92 cluster as well as PIM1 protein levels respectively. Single knockdown experiments of MYC, E2F3 or PIM1 decreased the pri-mir-17-92 levels to about 40, 60 and 60 % in HeLa cells and to 30, 30 and 45 % in K562 cells respectively (Figure 20a,b). Double-knockdown experiments had additive suppression effects for a MYC/E2F3 knockdown in both cell lines (~20 % remaining pri-mir-17-92 levels). In case of MYC/PIM1 and E2F3/PIM1 double-knockdowns cooperative suppression was only obtained in HeLa resulting in decreased transcript levels to about 20 and 30 % (Figure 20a,b).

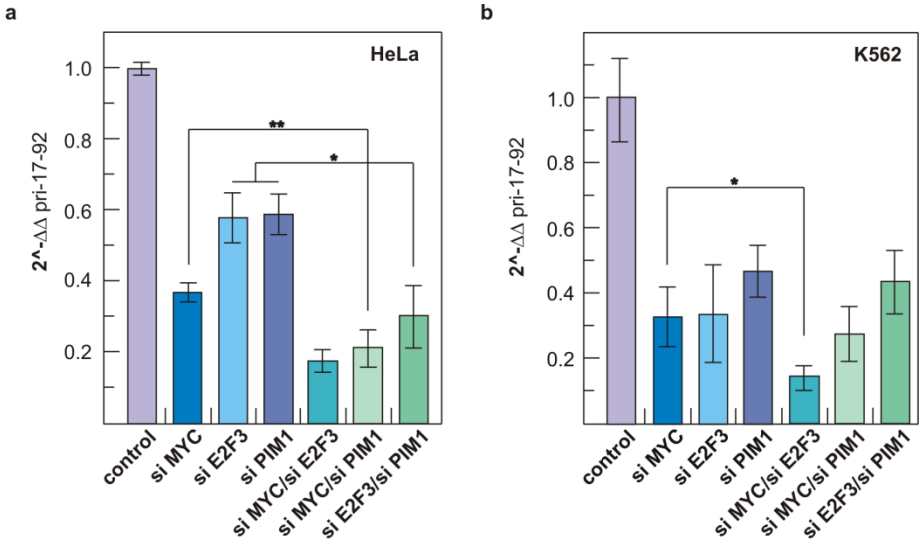

Figure 20: Transcriptional activity of the human miR-17-92 cluster after RNAi-mediated knockdown of regulatory proteins. (**a**) Quantitative PCR of pri-mir-17-92 levels in HeLa cells after single- and double-knockdown experiments of MYC, E2F3 and PIM1. 2^-ΔΔpri-mir-17-92 values were normalized against 5S rRNA and an internal control siRNA (179) and were obtained from at least three independent experiments (+/- S.E.M.). Statistical analyses were done using the software R (250). (**b**) Transcription levels of pri-mir-17-92 levels in K562 after single- and double-knockdown experiments of the respective proteins. QPCR results were normalized against 5S rRNA and an internal control siRNA (179) and were obtained from at least three independent experiments (+/- S.E.M.). Statistical analysis was done using the software R (250).

Discussion

In our study the intronic AT-rich region preceding the miR-17-92 cluster was scrutinized in more detail than it was done in previous work (169), (248), (249) additionally regarding an siRNA-mediated knockdown of MYC protein on transcription. The obtained effect was similar to the one observed after truncation of the functional MYC binding site E3. These findings substantiate the conception that the E3 site plays an important role in activating transcription emanating from the intronic promoter region of *C13orf25*. However even smaller promoter fragments still showed substantial, but specific transcriptional activation being independent of the functional MYC site. This MYC-independent activation was more pronounced in K562 cells due to the particularly high miR-17-92 cluster expression indicating cell type-specific differences in cluster expression. Our reporter assay data suggest multiple TSSs within this AT-rich region, although the predicted transcription initiation region approximately 0.2 kb downstream of the E3 box (169) may well be the major one.

Colocalization of MYC, the proto-oncogene PIM1 and its phosphorylation target HP1G to the chromatin region harboring the functional MYC binding site was shown in ChIP analysis. Importantly it has been reported that PIM1-catalyzed phosphorylation of H3S10 at MYC

activated target genes is required for MYC-dependent oncogenic transformation (251). Three paralogs of HP1 proteins in mammals regulate heterochromatin formation, gene silencing or gene activation (252), (156). The role of HP1G has not been fully understand, but it has been reported that HP1G is found in association with euchromatin (253), active genes (156) and can further be recruited to inducible promoters where it replaces HP1B to induce a switch from the repressive to the active transcriptional state (254). The replacement by HP1G requires H3 phospho-acetylation and a transient phosphorylation of H3S10 via aurora kinase B (AURKB) was shown to be essential for dissociation of HP1 proteins from chromatin during M-phase of the cell cycle (255). Our ChIP data of HP1G provide evidence for an activating role of HP1G during transcription. The identification of HP1G along the miR-17-92 coding region is to our knowledge the first indication that HP1G is involved in the activation of miRNA gene transcription. Recently it has been reported that HP1G can also be localized within coding regions of protein genes together with elongating RNA polymerase II (POLR2) (254).

Association of PIM1 with the E3 site in the intronic chromosomal region of *C13orf25* gave rise to the assumption that PIM1 plays a crucial role in transcriptional activation of the miR-17-92 cluster. RNAi-mediated knockdown experiments including MYC, PIM1 and E2F3 downregulation indicate that all three proteins are important for cluster expression. Transcription is affected either from the host gene promoter by E2F3 or the intronic promoter region regulated by MYC and PIM1. Of course, we cannot exclude indirect effects that have contributed as well such as effects originating from inhibition of cell proliferation (PIM1), changes in the kinetics of miRNA processing and global changes in transcriptional networks or mutual transactivation (E2F3 and MYC) (256), (257), (258). Besides it has been reported that miR-17-5p and miR-20a are negative regulators of *E2F1-3* mRNAs (91), (166). A major finding of our study is the involvement of the oncogenic kinase PIM1 in the regulation of miR-17-92 expression. This is inferred from its MYC-dependent recruitment to the E3 site in the intronic promoter region and a strong negative effect of a PIM1 knockdown on endogenous cluster expression. Moreover double-knockdown experiments revealed a synergistic effect compared to individual MYC and PIM1 knockdowns in HeLa cells.

Further investigations and extended research regarding transcriptional control of miRNA promoters could provide profound evidences for better understanding the complex network between miRNA expression and the development of cancer.

4 References

1. Hanahan, D. and Weinberg, R. A. (2011) Hallmarks of cancer: the next generation. *Cell* **144**, 646–74
2. Hanahan, D. and Weinberg, R. A. (2000) The Hallmarks of Cancer. *Cell* **100**, 57–70
3. Nowell, P. C. (1976) The clonal evolution of tumor cell populations. *Science* **194**, 23–8
4. Visvader, J. E. (2011) Cells of origin in cancer. *Nature* **469**, 314–22
5. David, A. R. and Zimmerman, M. R. (2010) Cancer: an old disease, a new disease or something in between? *Nature Reviews.Cancer* **10**, 728–33
6. Sandison, A. T. (1967) Diseases in Anitquity. *American Journal of Physical Anthropology*, 105–106
7. Merlo, L. M. F., Pepper, J. W., Reid, B. J. and Maley, C. C. (2006) Cancer as an evolutionary and ecological process. *Nature Reviews.Cancer* **6**, 924–35
8. Lazebnik, Y. (2010) What are the hallmarks of cancer? *Nature Reviews.Cancer* **10**, 232–233
9. www.cancer.gov
10. *Krebs in Deutschland 2007/2008 8. Ausgabe* (2012) Robert Koch Institut; Gesellschaft der epidemiologischen Krebsregister in Deutschland e.V.
11. Doll, R. and Peto, R. (1981) The causes of cancer: quantitative estimates of avoidable risks of cancer in the United States today. *Journal of the National Cancer Institute* **66**, 1191–308
12. Colditz, G. A., Sellers, T. A. and Trapido, E. (2006) Epidemiology - identifying the causes and preventability of cancer? *Nature Reviews.Cancer* **6**, 75–83
13. Renan, M. J. (1993) How many mutations are required for tumorigenesis? Implications from human cancer data. *Molecular Carcinogenesis* **7**, 139–46
14. Hollstein, M., Sidransky, D., Vogelstein, B. and Harris, C. C. (1991) p53 Mutations in Human Cancers. *Science* **253**, 49–53
15. Croce, C. M. (2008) Oncogenes and cancer. *The New England Journal of Medicine* **358**, 502–11
16. http://www.enzyklo.de/Begriff/Tumorsuppressorgene
17. http://www.krebsgesellschaft.de/krebsentstehung
18. Kasinski, A. L. and Slack, F. J. (2011) MicroRNAs en route to the clinic: progress in validating and targeting microRNAs for cancer therapy. *Nature Reviews.Cancer* **11**, 849–64
19. Esquela-Kerscher, A. and Slack, F. J. (2006) Oncomirs - microRNAs with a role in cancer. *Nature Reviews.Cancer* **6**, 259–69
20. Grubbe, E. (1957) Pioneer in X-ray therapy. *Science* **125**, 18–19
21. Cao, Y., DePinho, R. A., Ernst, M. and Vousden, K. (2011) Cancer research: past, present and future. *Nature Reviews.Cancer* **11**, 749–54
22. De Bono, J. S. and Ashworth, A. (2010) Translating cancer research into targeted therapeutics. *Nature* **467**, 543–9
23. Sawyers, C. (2004) Targeted cancer therapy. *Nature* **432**, 294–7
24. Imai, K. and Takaoka, A. (2006) Comparing antibody and small-molecule therapies for cancer. *Nature Reviews.Cancer* **6**, 714–27
25. Scott, A. M., Wolchok, J. D. and Old, L. J. (2012) Antibody therapy of cancer. *Nature Reviews.Cancer* **12**, 278–87

26. Lu, J., Getz, G., Miska, E. A., Alvarez-Saavedra, E., Lamb, J., Peck, D., Sweet-Cordero, A., Ebert, B. L., Mak, R. H., Ferrando, A. A., Downing, J. R., Jacks, T., Horvitz, H. R. and Golub, T. R. (2005) MicroRNA expression profiles classify human cancers. *Nature* **435**, 834–8
27. Ryan, B. M., Robles, A. I. and Harris, C. C. (2010) Genetic variation in microRNA networks: the implications for cancer research. *Nature Reviews.Cancer* **10**, 389–402
28. Ibrahim, A. F., Weirauch, U., Thomas, M., Grünweller, A., Hartmann, R. K. and Aigner, A. (2011) MicroRNA replacement therapy for miR-145 and miR-33a is efficacious in a model of colon carcinoma. *Cancer Research* **71**, 5214–24
29. Lindow, M. and Kauppinen, S. (2012) Discovering the first microRNA-targeted drug. *The Journal of Cell Biology* **199**, 407–12
30. He, L. and Hannon, G. J. (2004) MicroRNAs: small RNAs with a big role in gene regulation. *Nature Reviews.Genetics* **5**, 522–31
31. Fire, A., Xu, S., Montgomery, M. K., Kostas, S. A., Driver, S. E. and Mello, C. C. (1998) Potent and specific genetic interference by double-stranded RNA in Caenorhabitis elegans. *Nature* **391**, 806–811
32. Sharp, P. A. (2001) RNA interference - 2001. *Genes & Development* **15**, 485–90
33. Lee, R. C., Feinbaum, R. L. and Ambros, V. (1993) The C. elegans heterochronic gene lin-4 encodes small RNAs with antisense complementarity to lin-14. *Cell* **75**, 843–54
34. Reinhart, B. J., Slack, F. J., Basson, M., Pasquinelli, A. E., Bettinger, J. C., Rougvie, A. E., Horvitz, H. R. and Ruvkun, G. (2000) The 21-nucleotide let-7 RNA regulates developmental timing in Caenorhabditis elegans. *Nature* **403**, 901–6
35. Lagos-Quintana, M., Rauhut, R., Lendeckel, W. and Tuschl, T. (2001) Identification of novel genes coding for small expressed RNAs. *Science* **294**, 853–8
36. Lee, R. C. and Ambros, V. (2001) An extensive class of small RNAs in Caenorhabditis elegans. *Science* **294**, 862–4
37. Lau, N. C., Lim, L. P., Weinstein, E. G. and Bartel, D. P. (2001) An abundant class of tiny RNAs with probable regulatory roles in Caenorhabditis elegans. *Science* **294**, 858–62
38. Kozomara, A. and Griffiths-Jones, S. (2011) miRBase: integrating microRNA annotation and deep-sequencing data. *Nucleic Acids Research* **39**, D152–7
39. Iorio, M. V and Croce, C. M. (2009) MicroRNAs in cancer: small molecules with a huge impact. *Journal of Clinical Oncology* **27**, 5848–56
40. Krol, J., Loedige, I. and Filipowicz, W. (2010) The widespread regulation of microRNA biogenesis, function and decay. *Nature Reviews.Genetics* **11**, 597–610
41. Carthew, R. W. and Sontheimer, E. J. (2009) Origins and Mechanisms of miRNAs and siRNAs. *Cell* **136**, 642–55
42. Rodriguez, A., Griffiths-Jones, S., Ashurst, J. L. and Bradley, A. (2004) Identification of Mammalian microRNA Host Genes and Transcription Units. *Genome Research* **14**, 1902–1910
43. Lee, Y., Jeon, K., Lee, J.-T., Kim, S. and Kim, V. N. (2002) MicroRNA maturation: stepwise processing and subcellular localization. *The EMBO Journal* **21**, 4663–70
44. Saini, H. K., Griffiths-Jones, S. and Enright, A. J. (2007) Genomic analysis of human microRNA transcripts. *Proceedings of the National Academy of Sciences of the United States of America* **104**, 17719–17724
45. Griffiths-Jones, S., Saini, H. K., Van Dongen, S. and Enright, A. J. (2008) miRBase: tools for microRNA genomics. *Nucleic Acids Research* **36**, D154–8

46. Mourelatos, Z., Dostie, J., Paushkin, S., Sharma, A., Charroux, B., Abel, L., Rappsilber, J., Mann, M. and Dreyfuss, G. (2002) miRNPs: a novel class of ribonucleoproteins containing numerous microRNAs. *Genes & Development* **16**, 720–8
47. Okamura, K., Hagen, J. W., Duan, H., Tyler, D. M. and Lai, E. C. (2007) The mirtron pathway generates microRNA-class regulatory RNAs in Drosophila. *Cell* **130**, 89–100
48. Lee, Y., Kim, M., Han, J., Yeom, K.-H., Lee, S., Baek, S. H. and Kim, V. N. (2004) MicroRNA genes are transcribed by RNA polymerase II. *The EMBO Journal* **23**, 4051–60
49. Bartel, D. P. (2004) MicroRNAs: Genomics, Biogenesis, Mechanism, and Function. *Cell* **116**, 281–297
50. Denli, A. M., Tops, B. B. J., Plasterk, R. H. A., Ketting, R. F. and Hannon, G. J. (2004) Processing of primary microRNAs by the Microprocessor complex. *Nature* **432**, 231–5
51. Lee, Y., Ahn, C., Han, J., Choi, H., Kim, J., Yim, J., Lee, J., Provost, P., Rådmark, O., Kim, S. and Kim, V. N. (2003) The nuclear RNase III Drosha initiates microRNA processing. *Nature* **425**, 415–9
52. Landthaler, M., Yalcin, A. and Tuschl, T. (2004) The Human DiGeorge Syndrome Critical Region Gene 8 and Its D . melanogaster Homolog Are Required for miRNA Biogenesis. *Current Biology* **14**, 2162–2167
53. Basyuk, E. (2003) Human let-7 stem-loop precursors harbor features of RNase III cleavage products. *Nucleic Acids Research* **31**, 6593–6597
54. Yi, R., Qin, Y., Macara, I. G. and Cullen, B. R. (2003) Exportin-5 mediates the nuclear export of pre-microRNAs and short hairpin RNAs. *Genes & Development* **17**, 3011–6
55. Lund, E., Güttinger, S., Calado, A., Dahlberg, J. E. and Kutay, U. (2004) Nuclear export of microRNA precursors. *Science* **303**, 95–8
56. Gwizdek, C., Ossareh-Nazari, B., Brownawell, A. M., Doglio, A., Bertrand, E., Macara, I. G. and Dargemont, C. (2003) Exportin-5 mediates nuclear export of minihelix-containing RNAs. *The Journal of Biological Chemistry* **278**, 5505–8
57. Hutvágner, G., McLachlan, J., Pasquinelli, A. E., Bálint, E., Tuschl, T. and Zamore, P. D. (2001) A cellular function for the RNA-interference enzyme Dicer in the maturation of the let-7 small temporal RNA. *Science* **293**, 834–8
58. Ketting, R. F., Fischer, S. E., Bernstein, E., Sijen, T., Hannon, G. J. and Plasterk, R. H. (2001) Dicer functions in RNA interference and in synthesis of small RNA involved in developmental timing in C. elegans. *Genes & Development* **15**, 2654–9
59. Hutvágner, G. and Zamore, P. D. (2002) A microRNA in a multiple-turnover RNAi enzyme complex. *Science* **297**, 2056–60
60. Yan, K. S., Yan, S., Farooq, A., Han, A., Zeng, L. and Zhou, M.-M. (2003) Structure and conserved RNA binding of the PAZ domain. *Nature* **426**, 468–74
61. Song, J.-J., Liu, J., Tolia, N. H., Schneiderman, J., Smith, S. K., Martienssen, R. A., Hannon, G. J. and Joshua-Tor, L. (2003) The crystal structure of the Argonaute2 PAZ domain reveals an RNA binding motif in RNAi effector complexes. *Nature Structural Bology* **10**, 1026–32
62. Khvorova, A., Reynolds, A. and Jayasena, S. D. (2003) Functional siRNAs and miRNAs Exhibit Strand Bias. *Cell* **115**, 209–216
63. Hammond, S. M., Bernstein, E., Beach, D. and Hannon, G. J. (2000) An RNA-directed nuclease mediates post-transcriptional gene silencing in Drosophila cells. *Nature* **404**, 293–6
64. Bernstein, E., Caudy, A. A., Hammond, S. M. and Hannon, G. J. (2001) Role for a bidentate ribonuclease in the initiation step of RNA interference. *Nature* **409**, 363–6

65. Maniataki, E. and Mourelatos, Z. (2005) A human, ATP-independent, RISC assembly machine fueled by pre-miRNA. *Genes & Development* **19**, 2979–90

66. Wightman, B., Ha, I. and Ruvkun, G. (1993) Posttranscriptional regulation of the heterochronic gene lin-14 by lin-4 mediates temporal pattern formation in C. elegans. *Cell* **75**, 855–62

67. Doench, J. G., Petersen, C. P. and Sharp, P. A. (2003) siRNAs can function as miRNAs. *Genes & Development* **17**, 438–42

68. Doench, J. G. and Sharp, P. A. (2004) Specificity of microRNA target selection in translational repression. *Genes & Development* **18**, 504–11

69. Grimson, A., Farh, K. K.-H., Johnston, W. K., Garrett-Engele, P., Lim, L. P. and Bartel, D. P. (2007) MicroRNA targeting specificity in mammals: determinants beyond seed pairing. *Molecular Cell* **27**, 91–105

70. Lytle, J. R., Yario, T. A. and Steitz, J. A. (2007) Target mRNAs are repressed as efficiently by microRNA-binding sites in the 5’ UTR as in the 3' UTR. *Proceedings of the National Academy of Sciences of the United States of America* **104**, 9667–72

71. Tay, Y., Zhang, J., Thomson, A. M., Lim, B. and Rigoutsos, I. (2008) MicroRNAs to Nanog, Oct4 and Sox2 coding regions modulate embryonic stem cell differentiation. *Nature* **455**, 1124–8

72. Place, R. F., Li, L.-C., Pookot, D., Noonan, E. J. and Dahiya, R. (2008) MicroRNA-373 induces expression of genes with complementary promoter sequences. *Proceedings of the National Academy of Sciences of the United States of America* **105**, 1608–13

73. Hwang, H.-W., Wentzel, E. A. and Mendell, J. T. (2007) A hexanucleotide element directs microRNA nuclear import. *Science* **315**, 97–100

74. Kunej, T., Godnic, I., Horvat, S., Zorc, M. and Calin, G. A. (2012) Cross talk between microRNA and coding cancer genes. *Cancer Journal* **18**, 223–31

75. Sassen, S., Miska, E. A. and Caldas, C. (2008) MicroRNA: implications for cancer. *Virchows Archiv: an international Journal of Pathology* **452**, 1–10

76. Calin, G. A., Sevignani, C., Dumitru, C. D., Hyslop, T., Noch, E., Yendamuri, S., Shimizu, M., Rattan, S., Bullrich, F., Negrini, M. and Croce, C. M. (2004) Human microRNA genes are frequently located at fragile sites and genomic regions involved in cancers. *Proceedings of the National Academy of Sciences of the United States of America* **101**, 2999–3004

77. Calin, G. A. and Croce, C. M. (2006) MicroRNA signatures in human cancers. *Nature Reviews.Cancer* **6**, 857–66

78. Kong, Y. W., Ferland-McCollough, D., Jackson, T. J. and Bushell, M. (2012) microRNAs in cancer management. *The Lancet Oncology* **13**, e249–58

79. Calin, G. A., Dumitru, C. D., Shimizu, M., Bichi, R., Zupo, S., Noch, E., Aldler, H., Rattan, S., Keating, M., Rai, K., Rassenti, L., Kipps, T., Negrini, M., Bullrich, F. and Croce, C. M. (2002) Frequent deletions and down-regulation of micro- RNA genes miR15 and miR16 at 13q14 in chronic lymphocytic leukemia. *Proceedings of the National Academy of Sciences of the United States of America* **99**, 15524–9

80. Cimmino, A., Calin, G. A., Fabbri, M., Iorio, M. V, Ferracin, M., Shimizu, M., Wojcik, S. E., Aqeilan, R. I., Zupo, S., Dono, M., Rassenti, L., Alder, H., Volinia, S., Liu, C., Kipps, T. J., Negrini, M. and Croce, C. M. (2005) miR-15 and miR-16 induce apoptosis by targeting BCL2. *Proceedings of the National Academy of Sciences of the United States of America* **102**, 13944–13949

81. Calin, G. A., Ferracin, M., Cimmino, A., Di Leva, G., Shimizu, M., Wojcik, S. E., Iorio, M. V, Visone, R., Sever, N. I., Fabbri, M., Iuliano, R., Palumbo, T., Pichiorri, F., Roldo, C., Garzon, R., Sevignani, C., Rassenti, L., Alder, H., Volinia, S., Liu, C., Kipps, T. J., Negrini, M. and Croce, C. M. (2005) A MicroRNA signature associated with prognosis and progression in chronic lymphocytic leukemia. *The New England Journal of Medicine* **353**, 1793–801

82. Kohlhaas, S., Garden, O. A., Scudamore, C., Turner, M., Okkenhaug, K. and Vigorito, E. (2009) Cutting edge: the Foxp3 target miR-155 contributes to the development of regulatory T cells. *Journal of Immunology* **182**, 2578–82

83. Iorio, M. V, Ferracin, M., Liu, C.-G., Veronese, A., Spizzo, R., Sabbioni, S., Magri, E., Pedriali, M., Fabbri, M., Campiglio, M., Ménard, S., Palazzo, J. P., Rosenberg, A., Musiani, P., Volinia, S., Nenci, I., Calin, G. A., Querzoli, P., Negrini, M. and Croce, C. M. (2005) MicroRNA gene expression deregulation in human breast cancer. *Cancer Research* **65**, 7065–70

84. Meng, F., Henson, R., Wehbe-Janek, H., Ghoshal, K., Jacob, S. T. and Patel, T. (2007) MicroRNA-21 regulates expression of the PTEN tumor suppressor gene in human hepatocellular cancer. *Gastroenterology* **133**, 647–58

85. Wickramasinghe, N. S., Manavalan, T. T., Dougherty, S. M., Riggs, K. A., Li, Y. and Klinge, C. M. (2009) Estradiol downregulates miR-21 expression and increases miR-21 target gene expression in MCF-7 breast cancer cells. *Nucleic Acids Research* **37**, 2584–95

86. Kim, Y. J., Hwang, S. J., Bae, Y. C. and Jung, J. S. (2009) MiR-21 regulates adipogenic differentiation through the modulation of TGF-beta signaling in mesenchymal stem cells derived from human adipose tissue. *Stem Cells (Dayton, Ohio)* **27**, 3093–102

87. He, L., Thomson, J. M., Hemann, M. T., Hernando-Monge, E., Mu, D., Goodson, S., Powers, S., Cordon-Cardo, C., Lowe, S. W., Hannon, G. J. and Hammond, S. M. (2005) A microRNA polycistron as a potential human oncogene. *Nature* **435**, 828–33

88. Olive, V., Jiang, I. and He, L. (2010) mir-17-92, a cluster of miRNAs in the midst of the cancer network. *The international Journal of Biochemistry & Cell Biology* **42**, 1348–54

89. Chang, T.-C., Wentzel, E. A., Kent, O. A., Ramachandran, K., Mullendore, M., Lee, K. H., Feldmann, G., Yamakuchi, M., Ferlito, M., Lowenstein, C. J., Arking, D. E., Beer, M. A., Maitra, A. and Mendell, J. T. (2007) Transactivation of miR-34a by p53 broadly influences gene expression and promotes apoptosis. *Molecular Cell* **26**, 745–52

90. Corney, D. C., Flesken-Nikitin, A., Godwin, A. K., Wang, W. and Nikitin, A. Y. (2007) MicroRNA-34b and MicroRNA-34c are targets of p53 and cooperate in control of cell proliferation and adhesion-independent growth. *Cancer Research* **67**, 8433–8

91. O'Donnell, K. A., Wentzel, E. A., Zeller, K. I., Dang, C. V and Mendell, J. T. (2005) c-Myc-regulated microRNAs modulate E2F1 expression. *Nature* **435**, 839–43

92. Chang, T.-C., Zeitels, L. R., Hwang, H.-W., Chivukula, R. R., Wentzel, E. A., Dews, M., Jung, J., Gao, P., Dang, C. V, Beer, M. A., Thomas-Tikhonenko, A. and Mendell, J. T. (2009) Lin-28B transactivation is necessary for Myc-mediated let-7 repression and proliferation. *Proceedings of the National Academy of Sciences of the United States of America* **106**, 3384–9

93. Chin, L. J., Ratner, E., Leng, S., Zhai, R., Nallur, S., Babar, I., Muller, R.-U., Straka, E., Su, L., Burki, E. A., Crowell, R. E., Patel, R., Kulkarni, T., Homer, R., Zelterman, D., Kidd, K. K., Zhu, Y., Christiani, D. C., Belinsky, S. A., Slack, F. J. and Weidhaas, J. B. (2008) A SNP in a let-7 microRNA complementary site in the KRAS 3' untranslated region increases non-small cell lung cancer risk. *Cancer Research* **68**, 8535–40

94. Blenkiron, C., Goldstein, L. D., Thorne, N. P., Spiteri, I., Chin, S.-F., Dunning, M. J., Barbosa-Morais, N. L., Teschendorff, A. E., Green, A. R., Ellis, I. O., Tavaré, S., Caldas, C. and Miska, E. A. (2007) MicroRNA expression profiling of human breast cancer identifies new markers of tumor subtype. *Genome Biology* **8**, R214

95. Karim, B. O., Ali, S. Z., Landolfi, J. A., Mann, J. F., Liu, G., Christian, A., Dicello, J. F., Rosenthal, D. L. and Huso, D. L. (2008) Cytomorphologic differentiation of benign and malignant mammary tumors in fine needle aspirate specimens from irradiated female Sprague–Dawley rats. *Veterinary Clinical Pathology* **37**, 229–236

96. Ota, A., Tagawa, H., Karnan, S., Tsuzuki, S., Karpas, A., Kira, S., Yoshida, Y. and Seto, M. (2004) Identification and Characterization of a Novel Gene, C13orf25, as a Target for 13q31-q32 Amplification in Malignant Lymphoma. *Cancer Research* **64**, 3087–3095

97. Garzon, R., Garofalo, M., Martelli, M. P., Briesewitz, R., Wang, L., Fernandez-Cymering, C., Volinia, S., Liu, C.-G., Schnittger, S., Haferlach, T., Liso, A., Diverio, D., Mancini, M., Meloni, G., Foa, R., Martelli, M. F., Mecucci, C., Croce, C. M. and Falini, B. (2008) Distinctive microRNA signature of acute myeloid leukemia bearing cytoplasmic mutated nucleophosmin. *Proceedings of the National Academy of Sciences of the United States of America* **105**, 3945–50

98. Akao, Y., Nakagawa, Y. and Naoe, T. (2006) let-7 MicroRNA Functions as a Potential Growth Suppressor in Human Colon Cancer Cells. *Biological & Pharmaceutical Bulletin* **29**, 903–906

99. Radisky, D. C. (2011) miR-200c at the nexus of epithelial-mesenchymal transition, resistance to apoptosis, and the breast cancer stem cell phenotype. *Breast Cancer Research* **13**, 110

100. Garzon, R., Marcucci, G. and Croce, C. M. (2010) Targeting microRNAs in cancer: rationale, strategies and challenges. *Nature Reviews.Drug Discovery* **9**, 775–89

101. Chang, T.-C., Yu, D., Lee, Y.-S., Wentzel, E. A., Arking, D. E., West, K. M., Dang, C. V, Thomas-Tikhonenko, A. and Mendell, J. T. (2008) Widespread microRNA repression by Myc contributes to tumorigenesis. *Nature Genetics* **40**, 43–50

102. Gumireddy, K., Young, D. D., Xiong, X., Hogenesch, J. B., Huang, Q. and Deiters, A. (2008) Small-molecule inhibitors of microrna miR-21 function. *Angewandte Chemie* **47**, 7482–4

103. Thomas, M., Lange-Grünweller, K., Weirauch, U., Gutsch, D., Aigner, A., Grünweller, A. and Hartmann, R. K. (2012) The proto-oncogene Pim-1 is a target of miR-33a. *Oncogene* **31**, 918–28

104. Thomas, M., Lange-Grünweller, K., Dayyoub, E., Bakowsky, U., Weirauch, U., Aigner, A., Hartmann, R. K. and Grünweller, A. (2012) PEI-complexed LNA antiseeds as miRNA inhibitors. *RNA Biology* **9**, 1088–98

105. Thorsen, S. B., Obad, S., Jensen, N. F., Stenvang, J. and Kauppinen, S. (2012) The therapeutic potential of microRNAs in cancer. *Cancer Journal* **18**, 275–84

106. Kota, J., Chivukula, R. R., O'Donnell, K. A., Wentzel, E. A., Montgomery, C. L., Hwang, H.-W., Chang, T.-C., Vivekanandan, P., Torbenson, M., Clark, K. R., Mendell, J. R. and Mendell, J. T. (2009) Therapeutic microRNA delivery suppresses tumorigenesis in a murine liver cancer model. *Cell* **137**, 1005–17

107. Trang, P., Medina, P. P., Wiggins, J. F., Ruffino, L., Kelnar, K., Omotola, M., Homer, R., Brown, D., Bader, A. G., Weidhaas, J. B. and Slack, F. J. (2010) Regression of murine lung tumors by the let-7 microRNA. *Oncogene* **29**, 1580–7

108. Bader, A. G., Brown, D. and Winkler, M. (2010) The promise of microRNA replacement therapy. *Cancer Research* **70**, 7027–30

109. Stenvang, J., Petri, A., Lindow, M., Obad, S. and Kauppinen, S. (2012) Inhibition of microRNA function by antimiR oligonucleotides. *Silence* **3**, 1

110. Geary, R. S., Watanabe, T. A., Truong, L., Freier, S., Lesnik, E. A., Sioufi, N. B., Sasmor, H., Manoharan, M. and Levin, A. A. (2001) Pharmacokinetic properties of 2'-O-(2-methoxyethyl)-modified oligonucleotide analogs in rats. *The Journal of Pharmacology and Experimental Therapeutics* **296**, 890–7
111. Hutvágner, G., Simard, M. J., Mello, C. C. and Zamore, P. D. (2004) Sequence-specific inhibition of small RNA function. *PLoS Biology* **2**, E98
112. Davis, S., Lollo, B., Freier, S. and Esau, C. (2006) Improved targeting of miRNA with antisense oligonucleotides. *Nucleic Acids Rresearch* **34**, 2294–304
113. Koshkin, A. A., Singh, S. K., Nielsen, P., Rajwanshi, V. K., Kumar, R., Meldgaard, M., Olsen, C. E. and Wengel, J. (1998) LNA (Locked Nucleic Acids): Synthesis of the Adenine, Cytosine, Guanine, 5-Methylcytosine, Thymine and Uracil Bicyclonucleoside Monomers, Oligomerisation, and Unprecedented Nucleic Acid Recognition. *Tetrahedron* **54**, 3607–3630
114. Koshkin, A. A., Rajwanshi, V. K. and Wengel, J. (1998) Novel Convenient Syntheses of LNA [2.2.1] Bicyclo Nueleosides. *Tetrahedron* **39**, 4381–4384
115. Braasch, D. A. and Corey, D. R. (2001) Locked nucleic acid (LNA): fine-tuning the recognition of DNA and RNA. *Chemistry & Biology* **8**, 1–7
116. Summerton, J. and Weller, D. (1997) Morpholino Antisense Oligomers: Design, Preparation, and Properties. *Antisense & Nucleic Acid Drug Development* **7**, 187–195
117. Flynt, A. S., Li, N., Thatcher, E. J., Solnica-Krezel, L. and Patton, J. G. (2007) Zebrafish miR-214 modulates Hedgehog signaling to specify muscle cell fate. *Nature Genetics* **39**, 259–63
118. Esquela-Kerscher, A., Trang, P., Wiggins, J. F., Patrawala, L., Cheng, A., Ford, L., Weidhaas, J. B., Brown, D., Bader, A. G. and Slack, F. J. (2008) The let-7 microRNA reduces tumor growth in mouse models of lung cancer. *Cell Cycle* **7**, 759–764
119. Wiggins, J. F., Ruffino, L., Kelnar, K., Omotola, M., Patrawala, L., Brown, D. and Bader, A. G. (2010) Development of a lung cancer therapeutic based on the tumor suppressor microRNA-34. *Cancer Research* **70**, 5923–30
120. Takeshita, F., Patrawala, L., Osaki, M., Takahashi, R., Yamamoto, Y., Kosaka, N., Kawamata, M., Kelnar, K., Bader, A. G., Brown, D. and Ochiya, T. (2010) Systemic delivery of synthetic microRNA-16 inhibits the growth of metastatic prostate tumors via downregulation of multiple cell-cycle genes. *Molecular Therapy* **18**, 181–7
121. Kitade, Y. and Akao, Y. (2010) MicroRNAs and Their Therapeutic Potential for Human Diseases: MicroRNAs, miR-143 and -145, Function as Anti-oncomirs and the Application of Chemically Modified miR-143 as an Anti-cancer Drug. *Journal of Pharmacological Sciences* **114**, 276–280
122. Pramanik, D., Campbell, N. R., Karikari, C., Chivukula, R., Kent, O. A., Mendell, J. T. and Maitra, A. (2011) Restitution of tumor suppressor microRNAs using a systemic nanovector inhibits pancreatic cancer growth in mice. *Molecular Cancer Therapeutics* **10**, 1470–80
123. Esau, C. C. (2008) Inhibition of microRNA with antisense oligonucleotides. *Methods* **44**, 55–60
124. Krützfeldt, J., Rajewsky, N., Braich, R., Rajeev, K. G., Tuschl, T., Manoharan, M. and Stoffel, M. (2005) Silencing of microRNAs in vivo with "antagomirs". *Nature* **438**, 685–9
125. Elmén, J., Lindow, M., Schütz, S., Lawrence, M., Petri, A., Obad, S., Lindholm, M., Hedtjärn, M., Hansen, H. F., Berger, U., Gullans, S., Kearney, P., Sarnow, P., Straarup, E. M. and Kauppinen, S. (2008) LNA-mediated microRNA silencing in non-human primates. *Nature* **452**, 896–9

126. Obad, S., Dos Santos, C. O., Petri, A., Heidenblad, M., Broom, O., Ruse, C., Fu, C., Lindow, M., Stenvang, J., Straarup, E. M., Hansen, H. F., Koch, T., Pappin, D., Hannon, G. J. and Kauppinen, S. (2011) Silencing of microRNA families by seed-targeting tiny LNAs. *Nature Genetics* **43**, 371–8

127. Esau, C., Davis, S., Murray, S. F., Yu, X. X., Pandey, S. K., Pear, M., Watts, L., Booten, S. L., Graham, M., McKay, R., Subramaniam, A., Propp, S., Lollo, B. A., Freier, S., Bennett, C. F., Bhanot, S. and Monia, B. P. (2006) miR-122 regulation of lipid metabolism revealed by in vivo antisense targeting. *Cell Metabolism* **3**, 87–98

128. Jopling, C. L., Yi, M., Lancaster, A. M., Lemon, S. M. and Sarnow, P. (2005) Modulation of hepatitis C virus RNA abundance by a liver-specific MicroRNA. *Science* **309**, 1577–81

129. Ji, Q., Hao, X., Zhang, M., Tang, W., Yang, M., Li, L., Xiang, D., Desano, J. T., Bommer, G. T., Fan, D., Fearon, E. R., Lawrence, T. S. and Xu, L. (2009) MicroRNA miR-34 inhibits human pancreatic cancer tumor-initiating cells. *PloS One* **4**, e6816

130. Cuypers, H. T., Selten, G., Quint, W., Zijlstra, M., Maandag, E. R., Boelens, W., Van Wezenbeek, P., Melief, C. and Berns, A. (1984) Murine leukemia virus-induced T-cell lymphomagenesis: integration of proviruses in a distinct chromosomal region. *Cell* **37**, 141–50

131. Allen, J. D. and Berns, A. (1996) Complementation tagging of cooperating oncogenes in knockout mice. *Seminars in Cancer Biology* **7**, 299–306

132. Mikkers, H., Nawijn, M., Allen, J., Verhoeven, E., Jonkers, J., Berns, A. and Brouwers, C. (2004) Mice Deficient for All PIM Kinases Display Reduced Body Size and Impaired Responses to Hematopoietic Growth Factors. *Molecular and Cellular Biology* **24**, 6101–6115

133. Nawijn, M. C., Alendar, A. and Berns, A. (2011) For better or for worse: the role of Pim oncogenes in tumorigenesis. *Nature Reviews.Cancer* **11**, 23–34

134. Eichmann, A., Yuan, L., Bréant, C., Alitalo, K. and Koskinen, P. J. (2000) Developmental expression of pim kinases suggests functions also outside of the hematopoietic system. *Oncogene* **19**, 1215–24

135. Wingett, D., Long, A., Kelleher, D. and Magnuson, N. S. (1996) Pim-1 Proto-Oncogene Expression in Anti-CD3-Mediated T Cell Activation Is Associated with Protein Kinase C Activation and Is Independent of Raf-1. *Journal of Immunology* **156**, 549–557

136. Amson, R., Sigaux, F., Przedborski, S., Flandrin, G., Givol, D. and Telerman, A. (1989) The human protooncogene product p33pim is expressed during fetal hematopoiesis and in diverse leukemias. *Proceedings of the National Academy of Sciences of the United States of America* **86**, 8857–61

137. Bachmann, M. and Möröy, T. (2005) The serine/threonine kinase Pim-1. *The international Journal of Biochemistry & Cell Biology* **37**, 726–30

138. Wang, Z., Bhattacharya, N., Weaver, M., Petersen, K., Meyer, M., Gapter, L. and Magnuson, N. S. (2001) Pim-1: a serine/threonine kinase with a role in cell survival, proliferation, differentiation and tumorigenesis. *Journal of Veterinary Science* **2**, 167–79

139. Alizadeh, A. A., Eisen, M. B., Davis, R. E., Ma, C., Lossos, I. S., Rosenwald, A., Boldrick, J. C., Sabet, H., Tran, T., Yu, X., Powell, J. I., Yang, L., Marti, G. E., Moore, T., Jr, J. H., Lu, L., Lewis, D. B., Tibshirani, R., Sherlock, G., Chan, W. C., Greiner, T. C., Weisenburger, D. D., Armitage, J. O., Warnke, R., Levy, R., Wilson, W., Grever, M. R., Byrd, J. C., Botstein, D., Brown, P. O. and Staudt, L. M. (2000) Distinct types of diffuse large B-cell lymphoma identified by gene expression profiling. *Nature* **403**, 503–511

140. Ayala, G. E., Dai, H., Ittmann, M., Li, R., Powell, M., Frolov, A., Wheeler, T. M., Thompson, T. C. and Rowley, D. (2004) Growth and survival mechanisms associated with perineural invasion in prostate cancer. *Cancer Research* **64**, 6082–90

141. Domen, J., Van der Lugt, N. M., Laird, P. W., Saris, C. J., Clarke, A. R., Hooper, M. L. and Berns, A. (1993) Impaired interleukin-3 response in Pim-1-deficient bone marrow-derived mast cells. *Blood* **82**, 1445–52

142. Domen, J., Van der Lugt, N. M. T., Acton, D., Laird, P. W., Linders, K. and Berns, A. (1993) Pim-1 Levels Determine the Size o f Early B Lymphoid Compartments in Bone Marrow. *The Journal of Experimental Medicine* **178**, 1665–1673

143. Saris, C. J. M., Domen, J. and Berns, A. (1991) The pim-1 oncogene encodes two related protein-serine/threonine kinases by alternative initiation at AUG and CUG. *The EMBO Journal* **10**, 655–664

144. Nasser, M. W., Datta, J., Nuovo, G., Kutay, H., Motiwala, T., Majumder, S., Wang, B., Suster, S., Jacob, S. T. and Ghoshal, K. (2008) Down-regulation of micro-RNA-1 (miR-1) in lung cancer. Suppression of tumorigenic property of lung cancer cells and their sensitization to doxorubicin-induced apoptosis by miR-1. *The Journal of Biological Chemistry* **283**, 33394–405

145. Eiring, A. M., Harb, J. G., Neviani, P., Garton, C., Oaks, J. J., Spizzo, R., Liu, S., Schwind, S., Santhanam, R., Hickey, C. J., Becker, H., Chandler, J. C., Andino, R., Cortes, J., Hokland, P., Huettner, C. S., Bhatia, R., Roy, D. C., Liebhaber, S. A., Caligiuri, M. A., Marcucci, G., Garzon, R., Croce, C. M., Calin, G. A. and Perrotti, D. (2010) miR-328 functions as an RNA decoy to modulate hnRNP E2 regulation of mRNA translation in leukemic blasts. *Cell* **140**, 652–65

146. Hoover, D. S., Wingett, D. G., Zhang, J., Reeves, R. and Magnuson, N. S. (1997) Pim-1 Protein Expression Is Regulated by Its 5'-Untranslated Region and Translation Initiation Factor eIF-4E. *Cell Growth & Differentiation* **8**, 1371–1380

147. Culjkovic, B., Topisirovic, I., Skrabanek, L., Ruiz-Gutierrez, M. and Borden, K. L. B. (2006) eIF4E is a central node of an RNA regulon that governs cellular proliferation. *The Journal of Cell Biology* **175**, 415–26

148. Mizuno, K., Shirogane, T., Shinohara, A., Iwamatsu, A., Hibi, M. and Hirano, T. (2001) Regulation of Pim-1 by Hsp90. *Biochemical and Biophysical Research Communications* **281**, 663–9

149. Losman, J. A., Chen, X. P., Vuong, B. Q., Fay, S. and Rothman, P. B. (2003) Protein phosphatase 2A regulates the stability of Pim protein kinases. *The Journal of Biological Chemistry* **278**, 4800–5

150. Wang, Z., Bhattacharya, N., Mixter, P. F., Wei, W., Sedivy, J. and Magnuson, N. S. (2002) Phosphorylation of the cell cycle inhibitor p21 Cip1/WAF1 by Pim-1 kinase. *Biochimica et Biophysica ACTA* **1593**, 45–55

151. Morishita, D., Katayama, R., Sekimizu, K., Tsuruo, T. and Fujita, N. (2008) Pim kinases promote cell cycle progression by phosphorylating and down-regulating p27Kip1 at the transcriptional and posttranscriptional levels. *Cancer Research* **68**, 5076–85

152. Mochizuki, T., Kitanaka, C., Noguchi, K., Muramatsu, T., Asai, A. and Kuchino, Y. (1999) Physical and Functional Interactions between Pim-1 Kinase and Cdc25A Phosphatase. *The Journal of Biological Chemistry* **274**, 18659–18666

153. Bachmann, M., Hennemann, H., Xing, P. X., Hoffmann, I. and Möröy, T. (2004) The oncogenic serine/threonine kinase Pim-1 phosphorylates and inhibits the activity of Cdc25C-associated kinase 1 (C-TAK1): a novel role for Pim-1 at the G2/M cell cycle checkpoint. *The Journal of Biological Chemistry* **279**, 48319–28

154. Aho, T. L. T., Sandholm, J., Peltola, K. J., Mankonen, H. P., Lilly, M. and Koskinen, P. J. (2004) Pim-1 kinase promotes inactivation of the pro-apoptotic Bad protein by phosphorylating it on the Ser112 gatekeeper site. *FEBS Letters* **571**, 43–9

155. Koike, N., Maita, H., Taira, T., Ariga, H. and Iguchi-Ariga, S. M. M. (2000) Identification of heterochromatin protein 1 (HP1) as a phosphorylation target by Pim-1 kinase and the effect of phosphorylation on the transcriptional repression function of HP1. *FEBS Letters* **467**, 17–21

156. Vakoc, C. R., Mandat, S. A., Olenchock, B. A. and Blobel, G. A. (2005) Histone H3 lysine 9 methylation and HP1gamma are associated with transcription elongation through mammalian chromatin. *Molecular Cell* **19**, 381–91

157. Zhang, Y., Wang, Z., Li, X. and Magnuson, N. S. (2008) Pim kinase-dependent inhibition of c-Myc degradation. *Oncogene* **27**, 4809–19

158. Verbeek, S., Van Lohuizen, M., Van der Valk, M., Domen, J., Kraal, G. and Berns, A. (1991) Mice bearing the E mu-myc and E mu-pim-1 transgenes develop pre-B-cell leukemia prenatally. *Molecular and Cellular Biology* **11**, 1176–9

159. Zippo, A., De Robertis, A., Serafini, R. and Oliviero, S. (2007) PIM1-dependent phosphorylation of histone H3 at serine 10 is required for MYC-dependent transcriptional activation and oncogenic transformation. *Nature Cell Biology* **9**, 932–44

160. Merkel, A. L., Meggers, E. and Ocker, M. (2012) PIM1 kinase as a target for cancer therapy. *Expert Opinion on Investigational Drugs* **21**, 425–36

161. Bullock, A. N., Debreczeni, J. E., Fedorov, O. Y., Nelson, A., Marsden, B. D. and Knapp, S. (2005) Structural basis of inhibitor specificity of the human protooncogene proviral insertion site in moloney murine leukemia virus (PIM-1) kinase. *Journal of Medicinal Chemistry* **48**, 7604–14

162. Bregman, H. and Meggers, E. (2006) Ruthenium half-sandwich complexes as protein kinase inhibitors: an N-succinimidyl ester for rapid derivatizations of the cyclopentadienyl moiety. *Organic Letters* **8**, 5465–8

163. Nishiguchi, G. A., Atallah, G., Bellamacina, C., Burger, M. T., Ding, Y., Feucht, P. H., Garcia, P. D., Han, W., Klivansky, L. and Lindvall, M. (2011) Discovery of novel 3,5-disubstituted indole derivatives as potent inhibitors of Pim-1, Pim-2, and Pim-3 protein kinases. *Bioorganic & Medicinal Chemistry Letters* **21**, 6366–9

164. Tanzer, A. and Stadler, P. F. (2004) Molecular evolution of a microRNA cluster. *Journal of Molecular Biology* **339**, 327–35

165. Volinia, S., Calin, G. A., Liu, C.-G., Ambs, S., Cimmino, A., Petrocca, F., Visone, R., Iorio, M., Roldo, C., Ferracin, M., Prueitt, R. L., Yanaihara, N., Lanza, G., Scarpa, A., Vecchione, A., Negrini, M., Harris, C. C. and Croce, C. M. (2006) A microRNA expression signature of human solid tumors defines cancer gene targets. *Proceedings of the National Academy of Sciences of the United States of America* **103**, 2257–61

166. Sylvestre, Y., De Guire, V., Querido, E., Mukhopadhyay, U. K., Bourdeau, V., Major, F., Ferbeyre, G. and Chartrand, P. (2007) An E2F/miR-20a autoregulatory feedback loop. *The Journal of Biological Chemistry* **282**, 2135–43

167. Woods, K., Thomson, J. M. and Hammond, S. M. (2007) Direct regulation of an oncogenic micro-RNA cluster by E2F transcription factors. *The Journal of Biological Chemistry* **282**, 2130–4

168. Matsubara, H., Takeuchi, T., Nishikawa, E., Yanagisawa, K., Hayashita, Y., Ebi, H., Yamada, H., Suzuki, M., Nagino, M., Nimura, Y., Osada, H. and Takahashi, T. (2007) Apoptosis induction by antisense oligonucleotides against miR-17-5p and miR-20a in lung cancers overexpressing miR-17-92. *Oncogene* **26**, 6099–105

169. Ozsolak, F., Poling, L. L., Wang, Z., Liu, H., Liu, X. S., Roeder, R. G., Zhang, X., Song, J. S. and Fisher, D. E. (2008) Chromatin structure analyses identify miRNA promoters. *Genes & Development* **22**, 3172–83

170. Olive, V., Bennett, M. J., Walker, J. C., Ma, C., Jiang, I., Cordon-Cardo, C., Li, Q.-J., Lowe, S. W., Hannon, G. J. and He, L. (2009) miR-19 is a key oncogenic component of mir-17-92. *Genes & Development* **23**, 2839–49
171. Mu, P., Han, Y.-C., Betel, D., Yao, E., Squatrito, M., Ogrodowski, P., De Stanchina, E., D'Andrea, A., Sander, C. and Ventura, A. (2009) Genetic dissection of the miR-17~92 cluster of microRNAs in Myc-induced B-cell lymphomas. *Genes & Development* **23**, 2806–11
172. Xiao, C., Srinivasan, L., Calado, D. P., Patterson, H. C., Zhang, B., Wang, J., Henderson, J. M., Kutok, J. L. and Rajewsky, K. (2008) Lymphoproliferative disease and autoimmunity in mice with increased miR-17-92 expression in lymphocytes. *Nature Immunology* **9**, 405–14
173. Ventura, A., Young, A. G., Winslow, M. M., Lintault, L., Meissner, A., Erkeland, S. J., Newman, J., Bronson, R. T., Crowley, D., Stone, J. R., Jaenisch, R., Sharp, P. A. and Jacks, T. (2008) Targeted deletion reveals essential and overlapping functions of the miR-17 through 92 family of miRNA clusters. *Cell* **132**, 875–86
174. Petrocca, F., Vecchione, A. and Croce, C. M. (2008) Emerging role of miR-106b-25/miR-17-92 clusters in the control of transforming growth factor beta signaling. *Cancer Research* **68**, 8191–4
175. Dews, M., Homayouni, A., Yu, D., Murphy, D., Sevignani, C., Wentzel, E., Furth, E. E., Lee, W. M., Enders, G. H., Mendell, J. T. and Thomas-Tikhonenko, A. (2006) Augmentation of tumor angiogenesis by a Myc-activated microRNA cluster. *Nature Genetics* **38**, 1060–5
176. Höbel, S., Koburger, I., John, M., Czubayko, F., Hadwiger, P., Vornlocher, H.-P. and Aigner, A. (2010) Polyethylenimine / small interfering RNA-mediated knockdown of vascular endothelial growth factor in vivo exerts anti-tumor effects synergistically with Bevacizumab. *The Journal of Gene Medicine* **12**, 287–300
177. Fernandez, P. C., Frank, S. R., Wang, L., Schroeder, M., Liu, S., Greene, J., Cocito, A. and Amati, B. (2003) Genomic targets of the human c-Myc protein. *Genes & Development* **17**, 1115–29
178. Chen, C., Ridzon, D. A., Broomer, A. J., Zhou, Z., Lee, D. H., Nguyen, J. T., Barbisin, M., Xu, N. L., Mahuvakar, V. R., Andersen, M. R., Lao, K. Q., Livak, K. J. and Guegler, K. J. (2005) Real-time quantification of microRNAs by stem-loop RT-PCR. *Nucleic Acids Research* **33**, e179
179. Grünweller, A., Gillen, C., Erdmann, V. A. and Kurreck, J. (2003) Cellular uptake and localization of a Cy3-labeled siRNA specific for the serine/threonine kinase Pim-1. *Oligonucleotides* **13**, 345–52
180. Griffiths-Jones, S. (2004) The microRNA Registry. *Nucleic Acids Research* **32**, D109–11
181. Vermeulen, A., Robertson, B., Dalby, A. B., Marshall, W. S., Karpilow, J. O. N., Leake, D., Khvorova, A. and Baskerville, S. (2007) Double-stranded regions are essential design components of potent inhibitors of RISC function. *RNA* **13**, 723–730
182. Gruegelsiepe, H., Brandt, O. and Hartmann, R. K. (2006) Antisense inhibition of RNase P: mechanistic aspects and application to live bacteria. *The Journal of Biological Chemistry* **281**, 30613–20
183. Sambrook, J., Fritsch, E. and Maniatis, T. (1989) *Molecular Cloning. A laboratory manual.*, Cold Spring Harbor Laboratory, Cold Spring Harbor, N.Y.
184. Bertani, G. (1951) Studies on lysogenesis. The mode of phage liberation by lysogenic Escherichia coli. *Journal of Bacteriology* **62**, 293–300
185. Griffith, F. (1928) The significance of Pneumococcal Types. *Journal of Hygiene* **XXVII**, 113–159

186. Lozzio, C. B. and Lozzio, B. B. (1975) Human chronic myelogenous leukemia cell-line with positive Philadelphia chromosome. *Blood* **45**, 321–34

187. Gey, G. O., Coffman, W. D. and Kubicek, M. T. (1952) Tissue culture studies of the proliferative capacity of cervical carcinoma and normal epithelium. *Cancer Research* **12**, 264–265

188. Tom, B. H., Rutzky, L. P., Oyasu, R., Tomlta, J. T., Goldenberg, D. M. and Barry, D. (1977) Human Colon Adenocarcinoma Cells. *Journal of the National Cancer Institute* **58**, 1507–1512

189. Fogh, J., Fogh, J. M. and Orfeo, T. (1977) One hundred and twenty-seven cultured human tumor cell lines producing tumors in nude mice. *Journal of the National Cancer Institute* **59**, 221–6

190. Werth, S., Urban-Klein, B., Dai, L., Höbel, S., Grzelinski, M., Bakowsky, U., Czubayko, F. and Aigner, A. (2006) A low molecular weight fraction of polyethylenimine (PEI) displays increased transfection efficiency of DNA and siRNA in fresh or lyophilized complexes. *Journal of Controlled Release* **112**, 257–70

191. Tulchin, N., Ornstein, L. and Davis, B. J. (1976) A microgel system for disc electrophoresis. *Analytical Biochemistry* **72**, 485–90

192. Towbin, H., Staehelin, T. and Gordon, J. (1992) Electrophoretic transfer of proteins from polyacrylamide gels to nitrocellulose sheets: procedure and some applications. 1979. *Biotechnology* **24**, 145–9

193. Kerr, J. F. R., Wyllie, A. H. and Currie, A. R. (1972) APOPTOSIS: A BASIC BIOLOGICAL PHENOMENON WITH WIDE-RANGING IMPLICATIONS IN TISSUE KINETICS. *British Journal of Cancer* **26**, 239–257

194. Prinz, R. (2009) Regulation of proto-oncogenic Pim-1 kinase and miR-17-92 microRNA cluster in the human leukemia cell line K562.

195. Brennecke, J., Stark, A., Russell, R. B. and Cohen, S. M. (2005) Principles of microRNA-target recognition. *PLoS Biology* **3**, e85

196. Hartmann, D. (2010) Transkriptionelle Regulation des microRNA-Clusters miR-17-92 in Tumorzelllinien unter Berücksichtigung der onkogenen Kinase Pim-1.

197. Smithies, O. (1955) Zone electrophoresis in starch gels: group variations in the serum proteins of normal human adults. *The Biochemical Journal* **61**, 629–41

198. Tsanev, R. (1964) Direct spectropeotometric analysis of ribonucleic acid fractionation by agar-gelelectrophoresis. *Biochimica et Biophysica ACTA* **3**, 374–382

199. Loening, U. E. (1967) The fractionation of high-molecular-weight ribonucleic acid by polyacrylamide-gel electrophoresis. *The Biochemical Journal* **102**, 251–7

200. Sharp, P. A., Sugden, B. and Sambrook, J. (1973) Detection of Two Restriction Endonuclease Activities in Haemophilus parainfluenzae Using Analytical Agarose-Ethidium Bromide Electrophoresis. *Biochemistry* **12**, 3055–3063

201. Kerenyi, L. and Gallyas, F. (1973) Über Probleme der quantitativen Auswertung der mit physikalischer Entwicklung versilberten Agarelektrophoretogramme. *Clinica Chimica Acta* **47**, 425–436

202. Tuma, R. S., Beaudet, M. P., Jin, X., Jones, L. J., Cheung, C. Y., Yue, S. and Singer, V. L. (1999) Characterization of SYBR Gold nucleic acid gel stain: a dye optimized for use with 300-nm ultraviolet transilluminators. *Analytical Biochemistry* **268**, 278–88

203. Smith, H. O. and Wilcox, K. W. (1970) A Restriction Enzyme from Hemophilus influenzae. *Journal of Molecular Biology* **51**, 379–391

204. Danna, K. and Nathans, D. (1971) Specific cleavage of simian virus 40 DNA by restriction endonuclease of Hemophilus influenzae. 1971. *Reviews in Medical Virology* **9**, 75–81

205. Pheiffer, B. H. and Zimmerman, S. B. (1983) Polymer-stimulated ligation: enhanced blunt- or cohesive-end ligation of DNA or deoxyribooligonucleotides by T4 DNA ligase in polymer solutions. *Nucleic Acids Research* **11**, 7853–7871
206. Temin, H. M. and Mizutani, S. (1970) RNA-dependent DNA Polymerase in Virions of Rous Sarcoma Virus. *Nature* **226**, 1211–1213
207. Baltimore, D. (1970) Viral RNA-dependent DNA Polymerase. *Nature* **226**, 1209–1211
208. Saiki, R. K., Scharf, S., Faloona, F., Mullis, K. B., Horn, G. T., Erlich, H. A. and Arnheim, N. (1985) Enzymatic amplification of beta-globin genomic sequences and restriction site analysis for diagnosis of sickle cell anemia. 1985. *Science* **230**, 1350–1354
209. Schmittgen, T. D. and Livak, K. J. (2008) Analyzing real-time PCR data by the comparative CT method. *Nature Protocols* **3**, 1101–1108
210. Chomczynski, P. (1987) Single-Step Method of RNA Isolation by Acid Guanidinium Extraction. **159**, 156–159
211. Beckmann, B. M., Grünweller, A., Weber, M. H. W. and Hartmann, R. K. (2010) Northern blot detection of endogenous small RNAs (approximately14 nt) in bacterial total RNA extracts. *Nucleic Acids Research* **38**, e147
212. Beckmann, B. M., Hoch, P. G., Marz, M., Willkomm, D. K., Salas, M. and Hartmann, R. K. (2012) A pRNA-induced structural rearrangement triggers 6S-1 RNA release from RNA polymerase in Bacillus subtilis. *The EMBO Journal* **31**, 1727–38
213. Malek, A., Czubayko, F. and Aigner, A. (2008) PEG grafting of polyethylenimine (PEI) exerts different effects on DNA transfection and siRNA-induced gene targeting efficacy. *Journal of Drug Targeting* **16**, 124–39
214. Binnig, G. and Rohrer, H. (1986) Scanning tunneling microscopy. *IBM J. Res. Dev.* **30**, 355–369
215. Sitterberg, J., Ozcetin, A., Ehrhardt, C. and Bakowsky, U. (2010) Utilising atomic force microscopy for the characterisation of nanoscale drug delivery systems. *European Journal of Pharmaceutics and Biopharmaceutics* **74**, 2–13
216. Leatherbarrow, R. J. (2001) GraFit Version 5, Erithacus Software Ltd.
217. Altschul, S. F., Gish, W., Miller, W., Myers, E. W. and Lipman, D. J. (1990) Basic local alignment search tool. *Journal of Molecular Biology* **215**, 403–10
218. Lewis, B. P., Burge, C. B. and Bartel, D. P. (2005) Conserved seed pairing, often flanked by adenosines, indicates that thousands of human genes are microRNA targets. *Cell* **120**, 15–20
219. Friedman, R. C., Farh, K. K.-H., Burge, C. B. and Bartel, D. P. (2009) Most mammalian mRNAs are conserved targets of microRNAs. *Genome Research* **19**, 92–105
220. Griffiths-Jones, S., Grocock, R. J., Van Dongen, S., Bateman, A. and Enright, A. J. (2006) miRBase: microRNA sequences, targets and gene nomenclature. *Nucleic Acids Research* **34**, D140–4
221. Chenna, R. (2003) Multiple sequence alignment with the Clustal series of programs. *Nucleic Acids Research* **31**, 3497–3500
222. Crooks, G. E., Hon, G., Chandonia, J. and Brenner, S. E. (2004) WebLogo : A Sequence Logo Generator. *Genome Research* **14**, 1188–1190
223. Rangannan, V. and Bansal, M. (2009) Relative stability of DNA as a generic criterion for promoter prediction: whole genome annotation of microbial genomes with varying nucleotide base composition. *Molecular BioSystem* **5**, 1758–1769
224. Reese, M. G. (2001) Application of a time-delay neural network to promoter annotation in the Drosophila melanogaster genome. *Computers & Chemistry* **26**, 51–6

225. Ohler, U. (2006) Identification of core promoter modules in Drosophila and their application in accurate transcription start site prediction. *Nucleic Acids Research* **34**, 5943–50

226. Knudsen, S. (1999) Promoter2.0: for the recognition of PolII promoter sequences. *Bioinformatics* **15**, 356–61

227. Zhang, M. Q. (1998) Identification of human gene core promoters in silico. *Genome Research* **8**, 319–26

228. Meyersono, M. and Harlow, E. (1994) Identification of G1 Kinase Activity for cdk6 , a Novel Cyclin D Partner. *Molecular and Cellular Biology* **14**, 2077–2086

229. Herrera-Merchan, A., Cerrato, C., Luengo, G., Dominguez, O., Piris, M. A., Serrano, M. and Gonzalez, S. (2010) miR-33-mediated downregulation of p53 controls hematopoietic stem cell self-renewal. *Cell Cycle* **9**, 3277–85

230. Najafi-Shoushtari, S. H., Kristo, F., Li, Y., Shioda, T., Cohen, D. E., Gerszten, R. E. and Näär, A. M. (2010) MicroRNA-33 and the SREBP host genes cooperate to control cholesterol homeostasis. *Science* **328**, 1566–9

231. Rayner, K. J., Suárez, Y., Dávalos, A., Parathath, S., Fitzgerald, M. L., Tamehiro, N., Fisher, E. A., Moore, K. J. and Fernández-Hernando, C. (2010) MiR-33 contributes to the regulation of cholesterol homeostasis. *Science* **328**, 1570–3

232. Rayner, K. J., Sheedy, F. J., Esau, C. C., Hussain, F. N., Temel, R. E., Parathath, S., Gils, J. M. Van, Rayner, A. J., Chang, A. N., Suarez, Y., Fernandez-Hernando, C., Fisher, E. A. and Moore, K. J. (2011) Antagonism of miR-33 in mice promotes reverse cholesterol transport and regression of atherosclerosis. *The Journal of Clinical Investigation* **121**, 2921–31

233. Rayner, K. J., Esau, C. C., Hussain, F. N., McDaniel, A. L., Marshall, S. M., Van Gils, J. M., Ray, T. D., Sheedy, F. J., Goedeke, L., Liu, X., Khatsenko, O. G., Kaimal, V., Lees, C. J., Fernandez-Hernando, C., Fisher, E. a, Temel, R. E. and Moore, K. J. (2011) Inhibition of miR-33a/b in non-human primates raises plasma HDL and lowers VLDL triglycerides. *Nature* **478**, 404–7

234. Marquart, T. J., Wu, J., Lusis, A. J. and Baldán, A. (2013) AntimiR-33 Therapy Does Not Alter the Progression of Atherosclerosis in Low-Density Lipoprotein Receptor-Deficient Mice. *Arteriosclerosis, Thrombosis, and Vascular Biology* **33**

235. Muraski, J. A., Rota, M., Misao, Y., Fransioli, J., Cottage, C., Gude, N., Esposito, G., Delucchi, F., Arcarese, M., Alvarez, R., Siddiqi, S., Emmanuel, G. N., Wu, W., Fischer, K., Martindale, J. J., Glembotski, C. C., Leri, A., Kajstura, J., Magnuson, N., Berns, A., Beretta, R. M., Houser, S. R., Schaefer, E. M., Anversa, P. and Sussman, M. A. (2007) Pim-1 regulates cardiomyocyte survival downstream of Akt. *Nature Medicine* **13**, 1467–75

236. Cottage, C. T., Bailey, B., Fischer, K. M., Avitable, D., Collins, B., Tuck, S., Quijada, P., Gude, N., Alvarez, R., Muraski, J. and Sussman, M. A. (2010) Cardiac progenitor cell cycling stimulated by pim-1 kinase. *Circulation Research* **106**, 891–901

237. Takwi, A. A. L., Li, Y., Becker Buscaglia, L. E., Zhang, J., Choudhury, S., Park, A. K., Liu, M., Young, K. H., Park, W.-Y., Martin, R. C. G. and Li, Y. (2012) A statin-regulated microRNA represses human c-Myc expression and function. *EMBO Molecular Medicine* **145**, 1–14

238. Slack, F. J. (2012) A role of miR-33 for cell cycle progression and cell proliferation. *Cell cycle* **11**, 1057–1058

239. Cirera-Salinas, D., Pauta, M., Allen, R. M., Salerno, A. G., Ramírez, C. M., Chamorro-Jorganes, A., Wanschel, A. C., Lasunción, M. A., Morales-Ruiz, M., Suárez, Y., Baldán, Á., Esplugues, E. and Fernández-Hernando, C. (2012) Mir-33 regulates cell proliferation and cell cycle progression. *Cell cycle* **11**, 922–933

240. Ivanovska, I., Ball, A. S., Diaz, R. L., Magnus, J. F., Kibukawa, M., Schelter, J. M., Kobayashi, S. V, Lim, L., Burchard, J., Jackson, A. L., Linsley, P. S. and Cleary, M. A. (2008) MicroRNAs in the miR-106b family regulate p21/CDKN1A and promote cell cycle progression. *Molecular and Cellular Biology* **28**, 2167–74

241. Gartel, A. L. and Radhakrishnan, S. K. (2005) Lost in transcription: p21 repression, mechanisms, and consequences. *Cancer Research* **65**, 3980–5

242. Kurreck, J., Wyszko, E., Gillen, C. and Erdmann, V. A. (2002) Design of antisense oligonucleotides stabilized by locked nucleic acids. *Nucleic Acids Research* **30**, 1911–8

243. Christensen, U., Jacobsen, N., Rajwanshi, V. K., Wengel, J. and Koch, T. (2001) Stopped-flow kinetics of locked nucleic acid (LNA)-oligonucleotide duplex formation: studies of LNA-DNA and DNA-DNA interactions. *Biochemical Journal* **354**, 481–484

244. Wahlestedt, C., Salmi, P., Good, L., Kela, J., Johnsson, T., Ho, T., Broberger, C., Porreca, F., Lai, J., Ren, K., Ossipov, M., Koshkin, A., Jakobsen, N., Skouv, J., Oerum, H., Jacobsen, M. H. and Wengel, J. (2000) Potent and nontoxic antisense oligonucleotides containing locked nucleic acids. *PNAS* **97**, 5633–5638

245. Brown, D. A., Kang, S. H., Gryaznov, S. M., DeDionisio, L., Heidenreich, O., Sullivan, S., Xu, X. and Nerenberg, M. I. (1994) Effect of phosphorothioate modification of oligodeoxynucleotides on specific protein binding. *The Journal of Biological Chemistry* **269**, 26801–5

246. Boussif, O., Lezoualc'h, F., Zanta, M. A., Mergny, M. D., Scherman, D., Demeneix, B. and Behr, J. P. (1995) A versatile vector for gene and oligonucleotide transfer into cells in culture and in vivo: polyethylenimine. *Proceedings of the National Academy of Sciences of the United States of America* **92**, 7297–301

247. Guenther, M. G., Levine, S. S., Boyer, L. A., Jaenisch, R. and Young, R. A. (2007) A Chromatin Landmark and Transcription Initiation at Most Promoters in Human Cells. *Cell* **130**, 77–88

248. Ji, M., Rao, E., Ramachandrareddy, H., Shen, Y., Jiang, C., Chen, J., Hu, Y., Rizzino, A., Chan, W. C., Fu, K. and McKeithan, T. W. (2011) The miR-17-92 microRNA cluster is regulated by multiple mechanisms in B-cell malignancies. *The American Journal of Pathology* **179**, 1645–56

249. Pospisil, V., Vargova, K., Kokavec, J., Rybarova, J., Savvulidi, F., Jonasova, A., Necas, E., Zavadil, J., Laslo, P. and Stopka, T. (2011) Epigenetic silencing of the oncogenic miR-17-92 cluster during PU.1-directed macrophage differentiation. *The EMBO Journal* **30**, 4450–64

250. R Core Team (2012) R: A Language and Environment for Statistical Computing. *R Foundation for Statistical Computing*

251. Venturini, L., Battmer, K., Castoldi, M., Schultheis, B., Hochhaus, A., Muckenthaler, M. U., Ganser, A., Eder, M. and Scherr, M. (2007) Expression of the miR-17-92 polycistron in chronic myeloid leukemia (CML) CD34+ cells. *Blood* **109**, 4399–405

252. Kwon, S. H. and Workman, J. L. (2011) HP1c casts light on dark matter. *Cell Cycle* **10**, 625–630

253. Minc, E., Allory, Y., Worman, H. J., Courvalin, J. and Buendia, B. (1999) Localization and phosphorylation of HP1 proteins during the cell cycle in mammalian cells. *Chromosoma* **108**, 220–234

254. Mateescu, B., Bourachot, B., Rachez, C., Ogryzko, V. and Muchardt, C. (2008) Regulation of an inducible promoter by an HP1beta-HP1gamma switch. *EMBO Reports* **9**, 267–72

255. Fischle, W., Tseng, B. S., Dormann, H. L., Ueberheide, B. M., Garcia, B. A., Shabanowitz, J., Hunt, D. F., Funabiki, H. and Allis, C. D. (2005) Regulation of HP1-chromatin binding by histone H3 methylation and phosphorylation. *Nature* **438**, 1116–22

256. Adams, M. R., Sears, R., Nuckolls, F., Leone, G. and Nevins, J. R. (2000) Complex Transcriptional Regulatory Mechanisms Control Expression of the E2F3 Locus. *Molecular and Cellular Biology* **20**, 3633–3639

257. Thalmeier, K., Synovzik, H., Mertz, R., Winnacker, E. L. and Lipp, M. (1989) Nuclear factor E2F mediates basic transcription and trans-activation by E1a of the human MYC promoter. *Genes & Development* **3**, 527–536

258. Wong, J. V., Dong, P., Nevins, J. R., Mathey-Prevot, B. and You, L. (2011) Network calisthenics: Control of E2F dynamics in cell cycle entry. *Cell Cycle* **10**, 3086–3094

259. Wain, H. M., Bruford, E. A., Lovering, R. C., Lush, M. J., Wright, M. W. and Povey, S. (2002) Guidelines for human gene nomenclature. *Genomics* **79**, 464–70

APPENDIX

A. Publication I

The proto-oncogene Pim-1 is a target of miR-33a.

Oncogene (2012), *31*, 918-928

Impact Factor 2011: 6.37*

**2011 Journal Citation Reports* (Thomson Reuters, 2012)

Author contributions:

Research design: 35 %

Experimental work: 65 %

Data analysis and evaluation: 70 %

Manuscript writing: 30 %

Oncogene (2012) 31, 918–928
© 2012 Macmillan Publishers Limited All rights reserved 0950-9232/12
www.nature.com/onc

ORIGINAL ARTICLE

The proto-oncogene Pim-1 is a target of miR-33a

M Thomas[1], K Lange-Grünweller[1], U Weirauch[2], D Gutsch[2], A Aigner[2], A Grünweller[1] and RK Hartmann[1]

[1]*Institute of Pharmaceutical Chemistry, Faculty of Pharmacy, Philipps-University Marburg, Marburg, Germany and* [2]*Institute of Pharmacology, Faculty of Medicine, Philipps-University Marburg, Marburg, Germany*

The constitutively active serine/threonine kinase Pim-1 is upregulated in different cancer types, mainly based on the action of several interleukines and growth factors at the transcriptional level. So far, a regulation of oncogenic Pim-1 by microRNAs (miRNAs) has not been reported. Here, we newly establish miR-33a as a miRNA with potential tumor suppressor activity, acting through inhibition of Pim-1. A screen for miRNA expression in K562 lymphoma, LS174T colon carcinoma and several other cell lines revealed generally low endogenous miR-33a levels relative to other miRNAs. Transfection of K562 and LS174T cells with a miR-33a mimic reduced Pim-1 levels substantially. In contrast, the cell-cycle regulator cyclin-dependent kinase 6 predicted to be a conserved miR-33a target, was not downregulated by the miR-33a mimic. Seed mutagenesis of the Pim-1 3′-untranslated region in a luciferase reporter construct and in a Pim-1 cDNA expressed in Pim-1-deficient Skov-3 cells demonstrated specific and direct downregulation of Pim-1 by the miR-33a mimic. The persistence of this effect was comparable to that of a small interfering RNA-mediated knockdown of Pim-1, resulting in decelerated cell proliferation. In conclusion, we demonstrate the potential of miR-33a to act as a tumor suppressor miRNA, which suggests miR-33a replacement therapy through delivery of miR mimics as a novel therapeutic strategy.
Oncogene (2012) **31,** 918–928; doi:10.1038/onc.2011.278; published online 11 July 2011

Keywords: Pim-1; microRNA; miR-33a; proliferation; RNAi; siRNA

Introduction

MicroRNAs (miRNAs) are important regulators of gene expression, controlling developmental processes like embryonic stem cell differentiation, several metabolic pathways, cell proliferation, apoptosis and stress responses (for reviews see Bartel, 2004; Gangaraju and Lin, 2009). Like small interfering RNAs (siRNAs), miRNAs are loaded into Argonaute-containing 'RNA-induced silencing complexes' called miRNA ribonucleoprotein complexes (miRNPs) (Wang *et al*., 2009). In general, miRNAs have partial complementarity to their target mRNAs leading to translational inhibition or degradation of the respective mRNA in P-bodies (Liu *et al*., 2005; Rehwinkel *et al*., 2005). A prerequisite for miRNA interaction with mRNA targets is the so-called 'seed region' covering nucleotides (nt) 2–8 of the mature miRNA strand. This region usually forms a continuous duplex with the target followed by an unpaired region and a second less stringent base-pairing interaction (Lewis *et al*., 2005; Grimson *et al*., 2007; Bartel, 2009).

Many miRNAs have been identified to be involved in the development of cancer or metastasis, for example miR-21, members of the miR-17-92 cluster or miR-155, and are therefore called oncogenic miRNAs (Esquela-Kerscher and Slack, 2006). These miRNAs can downregulate targets that are involved in the regulation of apoptosis or cell-cycle progression, such as the phosphatase and tensin homolog (Pten), the transcription factor E2F1 or the apoptotic regulator Bim (for review see Croce, 2009). On the other hand, certain oncogenes like the transcription factor c-Myc are involved in the transcriptional regulation of miRNAs (O'Donnell *et al*., 2005).

Other miRNAs, for example miR-15a, miR-16-1, let-7a and miR-145, have been reported to be able to exert tumor suppressor activity by controlling targets that can inhibit apoptosis or promote cell-cycle progression. The tumor suppressor function of miRNAs is mainly directed against classical oncogenes, including the small G-protein Ras, the transcription factor c-Myc, Bcl-2, or cell cycle-dependent kinases like Cdk4 and Cdk6 (Cimmino *et al*., 2005; Iorio *et al*., 2005; Johnson *et al*., 2005; Croce, 2009). Consequently, in several tumors, these miRNAs are downregulated or not expressed at all (Garzon *et al*., 2009). For example, miR-15a and miR-16-1 are encoded in the chromosomal region 13q14.3 and loss of this region is the most common genomic aberration in chronic lymphocytic leukemia (Calin *et al*., 2002). Likewise, downregulation or loss of expression of these two miRNAs are frequently observed in prostata carcinomas (Bonci *et al*., 2008).

Beyond Cdk4 and Cdk6, we are not aware of any other examples of oncogenic kinases regulated by miRNAs, despite the fact that the activities of oncogenic

Correspondence: Dr A Grünweller or Professor RK Hartmann, Institute of Pharmaceutical Chemistry, Philipps-University Marburg, Marbacher Weg 6, AG Hartmann, Marburg 35037 Germany.
E-mails: arnold.gruenweller@staff.uni-marburg.de or roland.hartmann@staff.uni-marburg.de
Received 14 July 2010; revised 2 June 2011; accepted 4 June 2011; published online 11 July 2011

kinases are often deregulated in cancer cells (Amaravadi and Thompson, 2005). So-called survival kinases such as Akt, which promote anti-apoptotic responses or execute crucial steps in cell cycle progression, have received attention as therapeutic targets (Crowell *et al*., 2007; Martelli *et al*., 2007). This is also true for the Pim-1 kinase that can function in a synergistic manner with c-Myc to establish severe forms of B-cell lymphomas (van Lohuizen *et al*., 1989; Verbeek *et al*., 1991; Zippo *et al*., 2007; Zhang *et al*., 2008).

Pim kinases belong to the small group of constitutively active kinases (Amaravadi and Thompson, 2005; Qian *et al*., 2005), and thus their activity correlates with their cellular expression levels. PIM oncogenes are frequently overexpressed in human hematological malignancies and in several solid tumors, for example in prostate and breast cancer. PIM kinases exert their oncogenic potential through regulating MYC transcriptional activity, cap-dependent protein translation, cell-cycle progression as well as through suppression of apoptosis by means of BCL2-associated agonist of cell death (Bad) phosphorylation (for review, see Brault *et al*., 2010; Nawijn *et al*., 2011). Isoforms of Pim kinases include Pim-1, -2 and -3 (each $\sim$33 kDa), and utilization of alternative start codons gives rise to additional size variants, that is, 44 kDa (Pim-1; Xie *et al*., 2006) or 37 and 40 kDa (Pim-2; Fox *et al*., 2003), respectively (Amaravadi and Thompson, 2005). For Pim-1, several phosphorylation targets have been identified, such as Cdc25A (Mochizuki *et al*., 1999) and p21 (Wang *et al*., 2002) among others (for review see Bachmann and Möröy, 2005). So far, the expression of Pim-1 has been found to be regulated mainly at the transcriptional level by the action of several interleukines and growth factors that activate STAT3 and/or STAT5 via Janus kinases (Bachmann and Möröy, 2005). In contrast, a regulation of Pim-1 by miRNAs, which may well add to the differential expression in tumor versus normal cells, has not been reported.

In this study, we establish Pim-1 as a target of miR-33a, a miRNA that has not been implicated in tumor progression so far. Levels of miR-33a were observed to be low in a variety of tested cancer cell lines. Transfection of the myeloid leukemia suspension cell line K562 and the colon cancer adhesion cell line LS174T with a miR-33a mimic resulted in an anti-proliferative effect through reduced expression of Pim-1. The potential tumor suppressor activity of miR-33a would extend its hitherto known physiological functions in cholesterol metabolism (Najafi-Shoushtari *et al*., 2010; Rayner *et al*., 2010), and may offer novel options in miRNA-based tumor therapy.

Results

For the present study, we chose the following cell lines: (1) the suspension cell line K562 as a model for high endogenous Pim-1 expression; (2) adherent LS174T cells with moderate Pim-1 levels and representing solid tumors, which can be used for the induction of colon carcinomas in nude mice; and (3) Pim-1-negative Skov-3 cells for ectopic Pim-1 overexpression.

The 3′-untranslated region of Pim-1 harbors a conserved binding site for miR-33a

Here, we asked the question if the oncogenic kinase Pim-1 might be a target of miRNAs. The analysis of human Pim-1 mRNA for putative miRNA-binding sites by TargetScan 5.1 (Whitehead Institute for Biomedical Research, Cambridge, MA, USA) predicted conserved binding sites for miR-124/506, miR-26a/b, miR-15a/-16-1, miR-24, miR-33a and miR-144 (Figure 1a). Among those, the highest context score percentile of 98 was predicted for miR-33a. For this miRNA, the seed region from position 2–8 nt and the anchor A (Grimson *et al*., 2007) are almost completely conserved between human, mouse, rabbit, dog and chicken. Also conserved among all five eukaryotes is an unpaired nucleotide stretch (positions 10–12 nt) following the seed, as well as a second stretch (nt 13–17) complementary to the target, thus perfectly matching the 'Grimson rules' (Grimson *et al*., 2007; Figures 1b and c, right panels). We further considered miR-15a/-16-1 as candidate regulators of Pim-1 expression owing to their well-characterized tumor suppressor activities (Cimmino *et al*., 2005; Aqeilan *et al*., 2010). However, both miRNAs were ranked much lower by TargetScan 5.1 (percentile of 50 for miR-15a and 67 for miR-16-1) correlating with a lower adherence to the 'Grimson rules' and a lower evolutionary conservation of the putative miR-15a/-16-1 target site in the Pim-1 3′-untranslated region (3′-UTR) (Figures 1b and c, left panels). MiR-124/506, miR-26a/b, miR-24 and miR-144 were considered less promising (see Supplementary Information and Supplementary Figure S1), thus prompting us to mainly focus our studies on the potential Pim-1 targeting by miR-33a.

Profiling of selected miRNAs in K562 and LS174T cells

We next quantified the levels of miR-33a in K562 and LS174T cells by the stem-loop primer reverse transcriptase qPCR technique (Chen *et al*., 2005a). Our analysis also included the closely related miR-33b, other miRNAs predicted to target the Pim-1 3′-UTR (miR-15a/-16-1, miR-24, miR-26a, miR-144; see above), miR-17-5p/-20a highly expressed in K562 cells (Venturini *et al*., 2007), and miR-374a as a reference miRNA that shows minimal variability in cell lines, as recommended by Applied Biosystems (Foster City, CA, USA) for TaqMan MicroRNA Assays. Among the analyzed miRNAs with seeds in the Pim-1 3′-UTR, expression levels in K562 cells decreased in the order miR-16-1 > miR-26a > miR-24 > miR-15a >> miR-33a >> miR-144 >> miR-33b, and a comparable order (miR-16-1 > miR-24 > miR-26a > miR-15a >> miR-33a >> miR-144, miR-33b) was observed in LS174T cells (Figures 2a and b). Notably, miR-33a expression was comparably low in both cell lines. Conversely, miR-16-1, to which tumor suppressor functions have been assigned (Cimmino *et al*., 2005; Aqeilan *et al*., 2010), showed relatively high expression

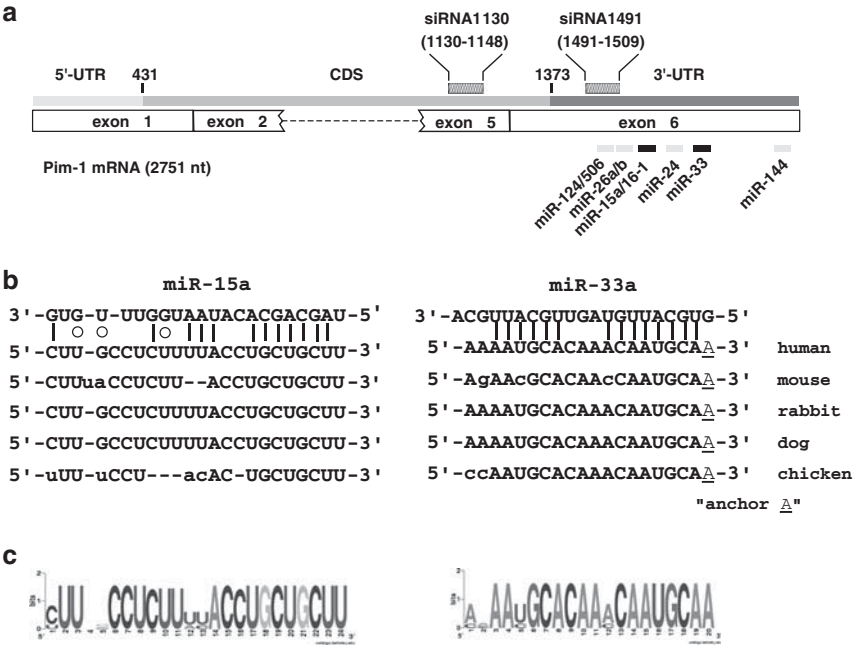

Figure 1 Predicted miRNA-binding sites in the 3′-UTR of Pim-1. (**a**) Schematic presentation of the human Pim-1 mRNA (5′-UTR in light gray, coding sequence in gray and 3′-UTR in black) based on the updated National Center for Biotechnology Information (NCBI) Reference Sequence NM_002648.3. The coding region ranges from position 431–1372. Six conserved target sites for miRNAs (light gray and dark gray boxes below the 3′-UTR) are predicted in the 3′-UTR by TargetScan 5.1. The target sites of the Pim-1-specific siRNAs used in this study are marked by the gray-shaded boxes above exons 5 and 6, respectively. The predicted miRNA target sites for miR-15a and miR-33a (dark gray boxes below the 3′-UTR) are detailed in (**b**). (**b**) Sequence alignments of miR-15a and miR-33a target sites in different vertebrates. MiR-33a is in a sequence context predicted to be optimal for miRNA binding (context score percentile of 98 out of 100). The seed region (nt 2–8), the central loop region (nt 10–12) and the second pairing region are fully conserved from human to chicken, except for two base exchanges in the mouse target sequence (indicated by lowercase letters). For comparison, the predicted miR-15a target sequence in the Pim-1 3′-UTR is less conserved. (**c**) Weblogos to illustrate the phylogenetic conservation of miR-15a and miR-33a target sites in the Pim-1 3′-UTR based on the sequence alignment shown in (**b**).

levels in both cell lines. As expected, high levels of the oncogenic miR-17-5p and miR-20a, encoded in the miR-17-92 cluster, were found in K562 and LS174T cells. To address the question if miR-33a levels also tend to be low in other cell lines than K562 and LS174T, we further tested HepG2 and Huh7 (liver carcinoma), Skov-3 (ovarian carcinoma) and Hek293 (embryonic kidney) as a nontumor cell line for miR-33a expression. HepG2 and Huh7 cells were included, since miR-33 was recently reported to contribute to the regulation of cholesterol homeostasis in liver cells (Najafi-Shoushtari *et al*., 2010; Rayner *et al*., 2010). Skov-3 cells were chosen because we considered this cell line as a host for ectopic Pim-1 expression (see below). However, all the additionally tested human cell lines had low miR-33a levels (Figure 2c), only HepG2 cells showed substantial Pim-1 protein expression (data not shown). Thus, at least for the cell types analyzed so far under standard growth conditions, a direct correlation between miR-33a and Pim-1 levels is not evident. Our finding of similarly low miR-33a levels in Hek293 cells relative to the tested cancer cell lines does not support the idea that tumor cells may further downregulate their miR-33a levels (own observations and Willemijn Gommans, personal communication).

Pim-1, but not Cdk6, is a target of miR-33a

The high conservation of the miR-33a-binding site in the 3′-UTR of Pim-1 and the relatively low levels of miR-33a in all tested cell lines suggested the possibility to reduce Pim-1 overexpression in tumors by transfection of cells with a commercially available modified miR-33a mimic. Indeed, western blots demonstrated a substantial downregulation of Pim-1 by the miR-33a mimic in K562 cells. Notably, no change in Pim-1 expression was observed upon transfection with miR-15a or miR-16-1 mimics, or a nonspecific control mimic (Figure 3a). Next, we compared an unmodified synthetic miR-33a mimic, which represents the Dicer processing product of pre-miR-33a (see Figure 3b and http://www.mirbase.org) with the commercial mimic (miR-33a modified) from Thermo Scientific (Schwerte, Germany). The unmodified mimic was also capable of downregulating Pim-1 in K562 cells, but less efficiently than the modified mimic (Figure 3c). Consistent with this finding, the unmodified miR-33a mimic led to an only moderate reduction in Pim-1 expression in LS174T cells, while the modified miR-33a mimic resulted in a substantial downregulation of Pim-1 protein levels (Figure 3d).

We further asked the question if miR-33a, beyond Pim-1, may also target another cell-cycle regulator,

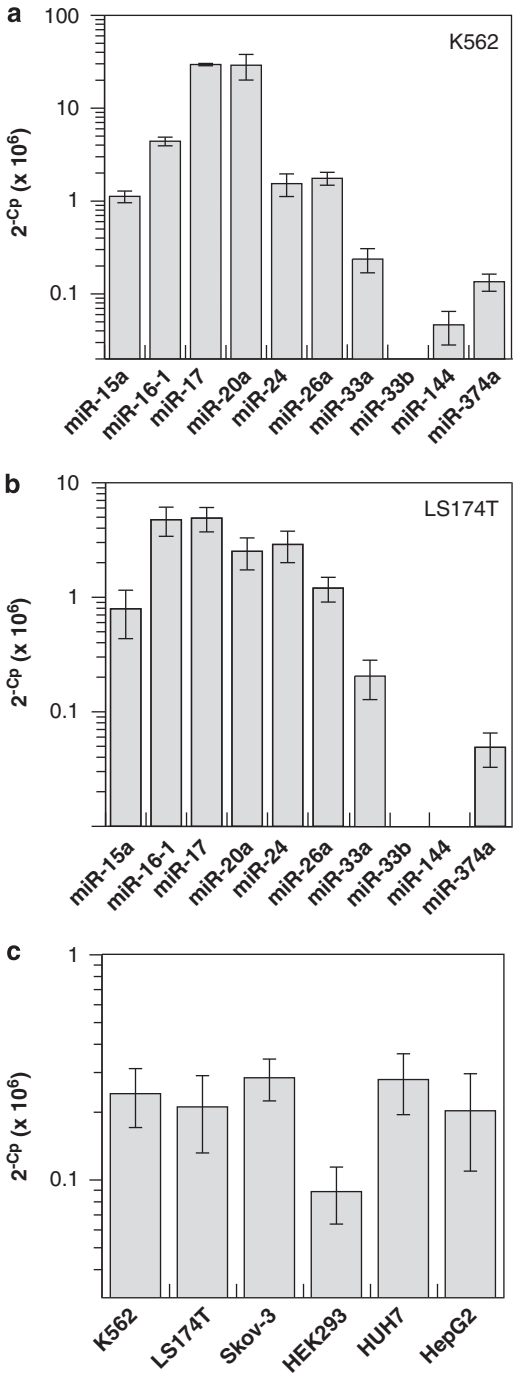

Figure 2 miRNA profiling in K562 and LS174T cells. (**a**) Expression profiling of 10 human miRNAs in K562 cells using the stem-loop primer reverse transcriptase qPCR technique. Values are based on Cp values (see Supplementary Information) derived from three independent experiments each performed in triplicate (± s.e.m.). (**b**) Expression profiling for the same set of miRNAs in LS174T cells. (**c**) Levels of miR-33a in a set of selected cell lines, demonstrating its generally low expression.

cyclin-dependent kinase 6 (Cdk6), since Targetscan 5.1 had ranked Cdk6 position three among putative miR-33a targets owing to the presence of two conserved target sites in its 3′-UTR (Supplementary Figure S2); the context score percentile was 98 for target site 1 and 20 for site 2). For comparison, Pim-1 was ranked position 56. Cdk6, as Cdk4, promotes the G1/S transition of the cell cycle in conjunction with D-type cyclins through phosphorylation and thus inactivation of the tumor suppressor protein Rb (Meyerson and Harlow, 1994). Western blot analysis after transfection of K562 cells with the modified and unmodified miR-33a mimics, however, provided no evidence for downregulation of Cdk6 by miR-33a mimics (Figure 3c). Recently, p53 and ATP-binding cassette transporter A1 (ABCA1) were published as targets of miR-33a (Herrera-Merchan *et al*., 2010; Najafi-Shoushtari *et al*., 2010; Rayner *et al*., 2010). Since K562 is a p53-deficient cell line (Zhang *et al*., 1993), we were only able to test if p53 may also be downregulated by miR-33a mimics in LS174T cells. However, transfection of miR-33a mimics in several independent experiments provided no evidence for a downregulation of p53 in LS174T cells (Figure 3d). This observation deviates from the findings of Herrera-Merchan *et al*. (2010) obtained in the mouse system, but is consistent with the fact that, in the human system, the two predicted target sites of miR-33a in the p53 3′-UTR (Herrera-Merchan *et al*., 2010) would each include two seed mismatches when paired to miR-33a. Unfortunately, the ABCA1 transporter was hardly detec table in K562 and LS174T cells (data not shown), which also disfavored the use of ABCA1 as a straightforward second model target to demonstrate inhibition by miR-33a in K562 cells.

Pim-1 knockdown by the miR-33a mimic versus siRNA

Next, we compared the miR-33a-dependent downregulation of Pim-1 with the knockdown mediated by a Pim-1-specific siRNA (siRNA1130 directed against exon 5, Figure 1a). While the siRNA transfection resulted in a very efficient knockdown of Pim-1 (Figures 4a and b), the reduction in Pim-1 protein levels mediated by the modified miR-33a mimic was less profound (Figure 4b). However, the time dependence of Pim-1 knockdown was similar for the Pim-1-specific siRNA and the miR-33a mimic, with decreased protein levels already visible after 24 h, a maximum reduction being reached after 72 h and lower Pim-1 levels still present at 96 h posttransfection of K562 cells (Figure 4b). A weaker knockdown by the modified miR-33a mimic is consistent with the general trend of miRNAs to repress expression of individual targets more moderately than siRNAs (Selbach *et al*., 2008). To evaluate if the miR-33a target site in the Pim-1 3′-UTR can also be accessed by an siRNA to possibly enhance the Pim-1 knockdown effect relative to miR-33a, we further tested siRNA 33a fully complementary to the miR-33a target site. Knockdown efficacy was similar to that caused by the modified miR-33a mimic, as inferred from western blot signal intensities (Figure 4c, cf. lanes 2 and 3). We also tested a modified miR-33b mimic but we were unable to detect any Pim-1 downregulation (data not shown).

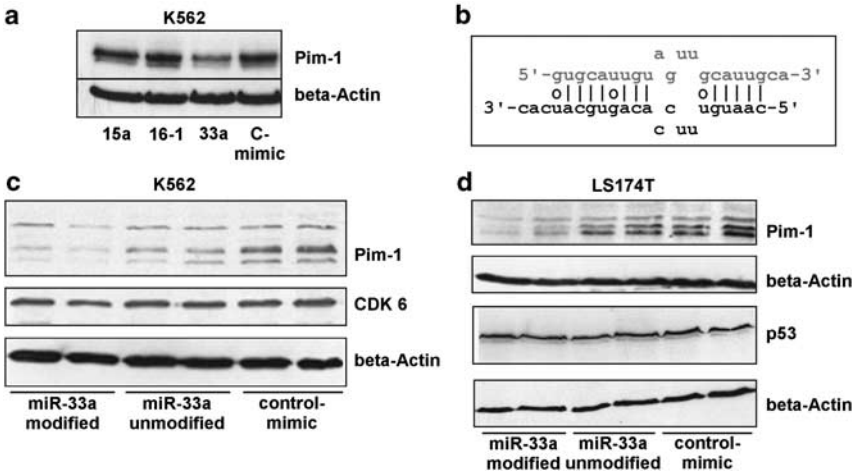

Figure 3 Human Pim-1 is a target for miR-33a. (**a**) Pim-1 is downregulated by a miR-33a mimic transfected into K562 cells, while miR-15a and miR-16-1 mimics as well as the control mimic have no measurable effects on Pim-1 expression levels. Total cellular protein preparations were separated on 15% sodium dodecyl sulfate-polyacrylamide gels and analyzed by western blotting with antibodies specific to Pim-1 or β-actin used as a loading control. (**b**) Structure of the unmodified miR-33a mimic tested in (**c**) next to a modified mimic obtained from Thermo Scientific Dharmacon; the unmodified miR-33a mimic corresponds to the natural Dicer processing product of pre-miR-33a, but lacking the 5′-phosphates; the miRNA strand is marked by gray letters; open circles indicate G-U wobble base pairs. (**c**) Pim-1 knockdown efficacy of the unmodified miR-33a mimic (miR-33a unmod.) was compared with that of a modified miR-33a mimic and the control mimic by western blotting using total protein extracts from K562 cells. After detection of β-actin, the membrane was again stripped to detect Cdk6 in the identical samples. The miR-33a mimics had no effect on Cdk6 expression levels although two miR-33a-binding sites are predicted in the Cdk6 3′-UTR by TargetScan 5.1 (Supplementary Figure S2). For further details, see (**a**). (**d**) Western blot analysis performed as in (**c**), but using LS174T cells. As another control of the miR-33a effect on Pim-1, the same protein samples were analyzed for the level of p53 recently reported to be a target of miR-33 in mice (Herrera-Merchan *et al*., 2010). However, we were unable to detect a significant repression of p53 by miR-33a in LS174T cells, as inferred from several independent experiments.

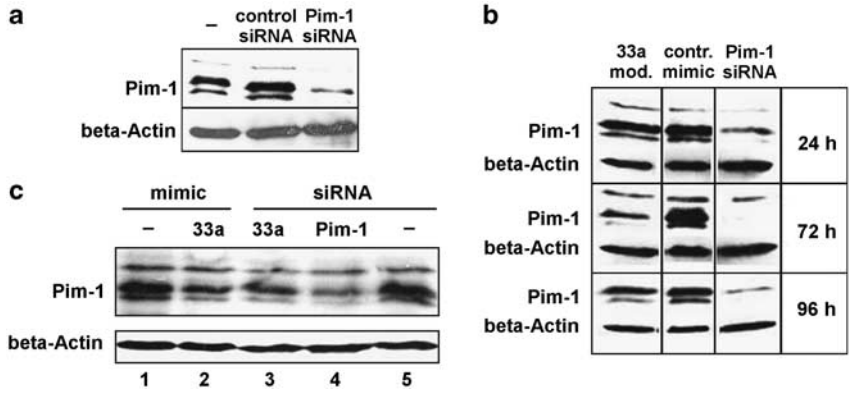

Figure 4 Comparison of Pim-1 knockdown by the miR-33a mimic versus a Pim-1-specific siRNA in K562 cells. (**a**) Knockdown efficacy of the Pim-1-specific siRNA1130 (Figure 1a) over mock-transfected (—) cells or negative control siRNA (VR1 siRNA), see Supplementary Information. (**b**) Comparison of the Pim-1 knockdown persistence for the modified miR-33a mimic versus the Pim-1 siRNA, measured 24, 72 and 96 h posttransfection. (**c**) Comparison of Pim-1 knockdown efficacy upon transfection with the modified miR-33a mimic (lane 2), the siRNA directed against the miR-33a target site (lane 3) or the Pim-1 siRNA1130 (lane 4). In all three panels, western blot experiments were conducted with an antibody specific to human Pim-1, and an antibody against β-actin was used as loading control.

Specificity of miR-33a binding to the Pim-1 3′-UTR

To further analyze the repression of Pim-1 expression by the miR-33a mimic (Figures 3 and 4), we cloned the 3′-UTR of Pim-1 into a luciferase reporter vector (pGL3 control). K562 cells were cotransfected with this construct and either the modified miR-33a mimic, siRNA 33a targeting the same Pim-1 mRNA sequence or the modified control mimic. A significant >50% reduction of luciferase activity was determined for the modified miR-33a mimic relative to the modified control mimic (Figure 5, open bars). Compared with the western blot analysis (Figure 4c), the siRNA 33a was more efficient than the modified miR-33a mimic in this reporter assay. This may suggest that either the luciferase reporter assay is more sensitive than western blot analysis, or the reporter assay system may somewhat differently respond to targeting by RNAi machineries than the Pim-1 3′-UTR in its natural context.

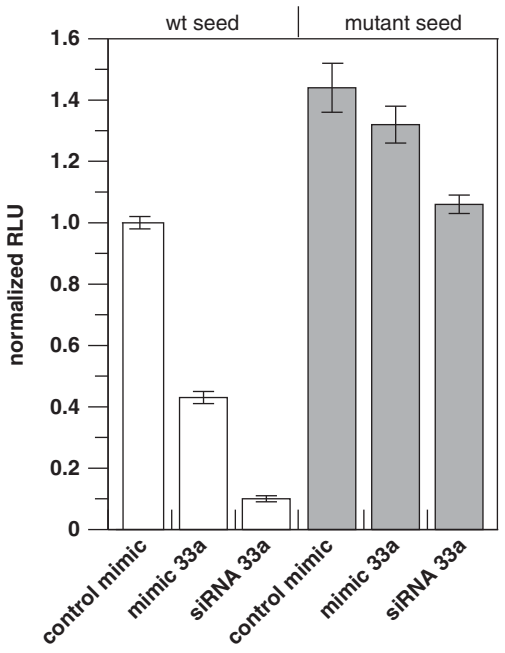

Figure 5 MiR-33a-specific regulation of Pim-1 expression. Reporter assay using a plasmid-based luciferase coding region fused to the 3′-UTR of Pim-1, either containing the wild-type miR-33a target sequence (wt seed 5′-ACAAUGCA, open bars) or a mutated miR-33a target site (mutant seed 5′-ACAGUGCG, gray bars). K562 cells were cotransfected with the control mimic, modified miR-33a mimic or siRNA 33a fully complementary to the mir-33a seed plus 11 nt upstream in the Pim-1 3′-UTR. Data represent mean values derived from at least three independent experiments; RLU, relative light units (±s.e.m.), normalized to those obtained with extracts from cells expressing the reporter mRNA with the wt seed and cotransfected with the control mimic (first bar on the left).

We further scrutinized the specificity of the observed miR-33a effect on Pim-1 expression by mutating the miR-33a seed region in the Pim-1-derived 3′-UTR of the luciferase reporter (from 5′-ACAATGCA to 5′-ACAGTGCG). Indeed, the repression effects observed for the modified miR-33a mimic or siRNA 33a were essentially abrogated in the presence of a mutated seed region (Figure 5, gray bars).

Ectopic expression of Pim-1 in Skov-3 cells

To further substantiate that miR-33a specifically and directly represses Pim-1 expression, we transfected the Pim-1-deficient ovarian cancer cell line Skov-3 with a human Pim-1 full-length cDNA. Pim-1 overexpression in Skov-3 cells resulted in Pim-1 western blot signals comparable to those observed in K562 cells (this also holds true for transfection of Hek293 cells with the same cDNA; data not shown). Cotransfection of the Pim-1-specific siRNA and the modified miR-33a mimic, but not the control mimic, resulted in Pim-1 downregulation (Figure 6a). However, a Pim-1 cDNA variant harboring a mutagenized miR-33a seed (see legend to Figure 5) remained responsive to the siRNA whose target site was not affected by the seed mutations, but lost its responsiveness to the miR-33a mimic (Figure 6b). Likewise, a deletion of the entire Pim-1 3′-UTR abolished the observed miR-33a-dependent Pim-1 downregulation (Figure 6c). Taken together, these findings further support our conclusion that miR-33a is able to specifically and directly suppress Pim-1 mRNA utilization via the identified miR-33a target site in the Pim-1 3′-UTR.

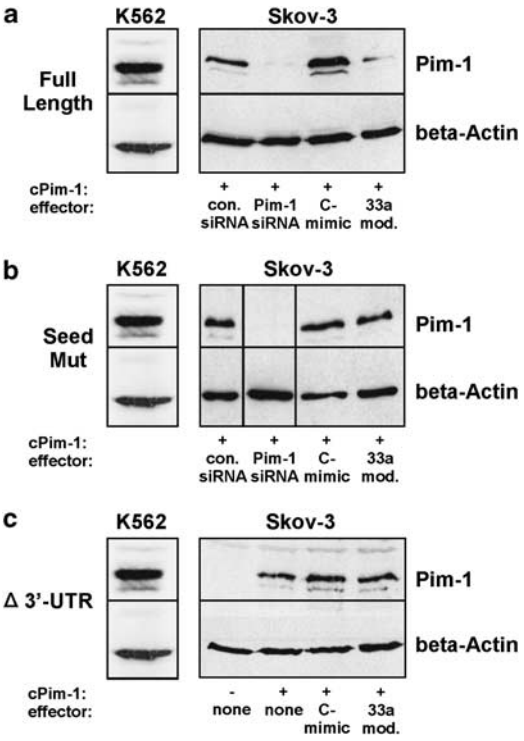

Figure 6 Effects of the miR-33a mimic and Pim-1 siRNA1491 on ectopic Pim-1 expression in Skov-3 cells. (**a**) A full-length Pim-1 cDNA (25–50 ng) was transfected into Pim-1-negative Skov-3 cells and overexpression of Pim-1 was detected by western blotting. Cotransfection of the modified miR-33a mimic or Pim-1 siRNA1491 (targeting exon 6 in the 3′-UTR of Pim-1; see Figure 1a) resulted in Pim-1 downregulation; con. siRNA, VR1 siRNA; C-mimic, modified control mimic. (**b**) Mutagenesis of the miR-33a target site (mutant seed 5′-ACAGUGCG) in the 3′-UTR of the full-length Pim-1 cDNA abrogated Pim-1 downregulation by the modified miR-33a mimic, but did not interfere with suppression by the Pim-1-specific siRNA1491; for further details, see (**a**); for uniformity, the control and Pim-1 siRNA lanes were interchanged in position relative to the original western blot, which is indicated by vertical lines. (**c**) Deletion of the 3′-UTR except for the 3′-terminal ~400 nt in the Pim-1 cDNA, which removes the binding site for miR-33a, resulted in a loss of Pim-1 downregulation by the modified miR-33a mimic; for further details, see (**a**); none, no effector siRNA or miRNA transfected. Western blot experiments in (**a**–**c**) were conducted with an antibody specific to human Pim-1, and an antibody against β-actin was used as loading control. The same western blot illustrating endogenous Pim-1 levels in K562 cells is shown in all panels for comparison on the left; minus sign (**c**), no transfection with Pim-1 cDNA plasmid; plus sign, transfected with the Pim-1 cDNA plasmid.

A miR-33a mimic decelerates tumor cell proliferation

To address the biological relevance of the observed miR-33a effects on Pim-1 expression, we hypothesized that

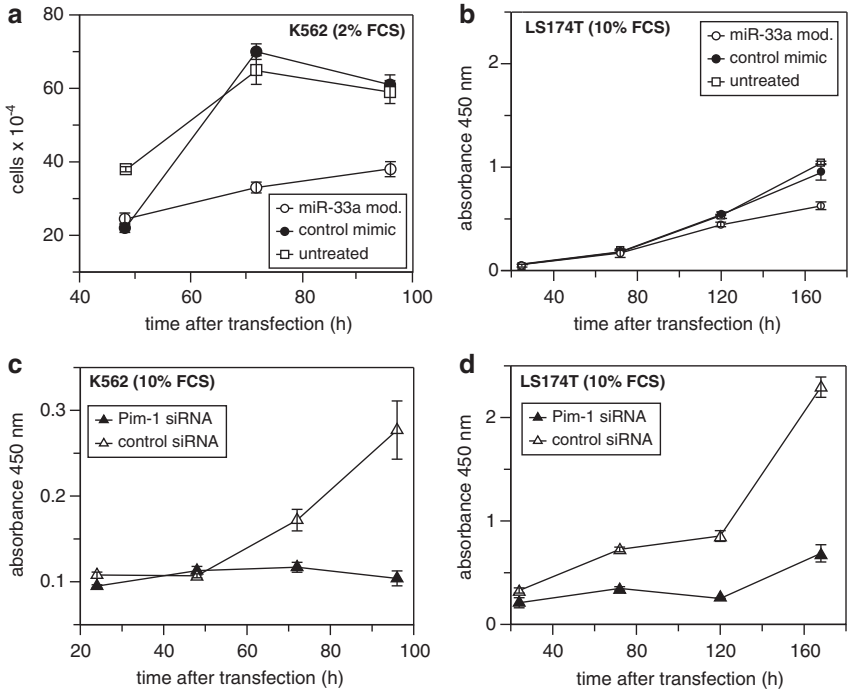

Figure 7 Anti-proliferative effects of a miR-33a- or siRNA-mediated Pim-1 knockdown. (**a**) Proliferation of untreated K562 cells compared with K562 cells transfected with the modified miR-33a mimic or the control mimic. Cells were cultivated in the presence of 2% FCS. Here, microscopic cell number counts are presented because in this case cell counting gave more reliable results than the WST-1 assay (Roche Applied Science, Mannheim, Germany). (**b**) Proliferation analysis of LS174T cells grown in the presence of 10% FCS. The amount of viable cells was determined by the WST-1 assay. (**c**) Proliferation of K562 cells in the presence of 10% FCS after transfection with the Pim-1-specific siRNA1130. Cell viability was determined by the WST-1 assay. (**d**) Proliferation of LS174T cells in the presence of 10% FCS after transfection with the Pim-1-specific siRNA1491. Data shown in (**a**–**d**) represent mean values (± s.e.m.) derived from at least three independent experiments.

miR-33a may negatively affect cell proliferation through reduction of Pim-1, since a previous study (Zhang *et al*., 2008) had suggested a direct role of Pim-1 in regulating K562 cell proliferation. Indeed, under reduced serum conditions (2% fetal calf serum (FCS)), but not in the presence of 10% FCS (Supplementary Figure S3a), an anti-proliferative effect of the miR-33a mimic was observed in K562 cells (Figure 7a). Consistently, Pim-1 levels in untreated K562 cells were reduced under these serum starvation conditions (2% FCS; Supplementary Figure S3b, left two lanes). This may suggest that Pim-1 levels need to fall below a threshold concentration, and/or that growth factors need to be lacking in the medium, to make the cells more sensitive towards miR-33a-mediated Pim-1 repression and thus to allow the detection of anti-proliferative effects in this cell line. In LS174T cells, reduced proliferation upon transfection with the modified miR-33a mimic was already seen in the presence of 10% FCS (Figure 7b). Again, this could be attributed to the already lower expression levels of Pim-1 in LS174T relative to K562 cells (Supplementary Figure S3b). In line with the more moderate miRNA effects observed above (see Figure 4b), analysis of K562 and LS174T cell proliferation upon transfection with Pim-1-specific siRNAs revealed more pronounced effects relative to those obtained with the modified miR-33a mimic. This was indicated by strong siRNA-mediated inhibition of cell proliferation in LS174T cells (Figures 7d versus b) and in K562 cells already under 10% FCS conditions (Figure 7c).

Cell-cycle analysis after miR-33a- or siRNA-mediated Pim-1 knockdown in K562 and LS174T cells provided evidence that a downregulation of Pim-1 results in a delay of cycle progression at the stage of the G2 to M phase transition (data not shown), which is in line with a previous study (Bachmann *et al*., 2004). This effect was more pronounced for K562 relative to LS174T cells, without any effects on apoptosis in both cell lines (Supplementary Figure S4).

Discussion

In this study, we newly establish miR-33a as a miRNA with potential tumor suppressor activity and demonstrate by western blot analysis and reporter assays (Figures 3–6) that the oncogenic kinase Pim-1 is an evolutionarily highly conserved, specific and direct target of miR-33a. Likewise, transfection of a miR-33a mimic decelerates proliferation in colon cancer and leukemia cells, and exerts similar effects as Pim-1-specific siRNAs.

Notably, miR-33a had not been implicated in tumor progression so far. In the human system, miR-33a and the second family member miR-33b are encoded in

introns of hSREBP-2 (chromosome 22) and hSREBP-1 (chromosome 17), respectively. Both are key transcription regulators of genes involved in cholesterol biosynthesis and uptake. Recently, it has been reported in two independent studies that miR-33a/b posttranscriptionally repress ABCA1, an important positive regulator of high-density lipoprotein synthesis and reverse cholesterol transport (Najafi-Shoushtari *et al*., 2010; Rayner *et al*., 2010). Tissue-specific miR-33a/b and hSREBP RNA levels were found to be tightly correlated, indicating that both intronic miRNAs are coordinatedly expressed with the pre-mRNA they reside in (Najafi-Shoushtari *et al*., 2010). In this context, antagonists of endogenous miR-33 were suggested as a potential therapeutic strategy to mitigate cardiometabolic diseases.

We have demonstrated that endogenous Pim-1 levels can be reduced in K562 and LS174T cells by a miR-33a mimic, siRNA 33a fully complementary to the miR-33a target site, and most efficiently, by two different siRNAs targeting other regions of the Pim-1 mRNA. The knockdown efficiency correlated with the strength of the inhibitory effect on cell proliferation ('gene dose effect,' see Figures 3, 4 and 7). Thus, these results confirm previous studies, which had shown that the reduction of endogenous Pim-1 levels by RNAi negatively affects the proliferation capacity of the human lung carcinoma cell line H1299, of the prostate cancer cell line PC-3 and of K562 cells (Zhang *et al*., 2007, 2008, 2010).

Pim kinases have partially overlapping functions with the survival kinase Akt (Amaravadi and Thompson, 2005) since (1) both kinases directly phosphorylate and inactivate the pro-apoptotic Bad protein (Datta *et al*., 1997; Aho *et al*., 2004), (2) both contribute to maintaining a high rate of protein translation through phosphorylation and inactivation of the translational repressor 4EBP1, either directly in the case of Pim-1 (Chen *et al*., 2005b; Xia *et al*., 2009), or indirectly via Tsc2 phosphorylation by Akt, which triggers 4EBP1 phosphorylation via the mTOR complex 1 (Huang and Manning, 2009); (3) Akt and Pim kinases can activate nuclear factor-κB-dependent transcription including that of an array of anti-apoptotic genes (reviewed in Amaravadi and Thompson, 2005). Thus, Pim kinases may act at some points as a cellular backup system for Akt, while supplementing Akt in other pathways to maintain cell proliferation and survival, such as during cardioprotection where Pim-1 acts downstream of Akt signaling (Muraski *et al*., 2007). We have demonstrated that the miR-33a target site in the Pim-1 3′-UTR is evolutionary strictly conserved, and Pim-1 suppression by miR-33a is direct and specific. This is a clear indication that Pim-1 is a genuine target of miR-33a, although we have not yet identified the biological constellation(s) under which endogenous miR-33a levels increase to an extent where they effectively repress Pim-1 expression. As discussed before, expression of miR-33a is rather low and uniform in the cancerous human cell lines tested here (Figure 2), as it is in various human normal and cancerous tissues (Najafi-Shoushtari *et al*., 2010; Willemijn Gommans, personal communication). This is also consistent with our finding that miR-33a levels in human colon samples (matching pairs of normal and tumor tissue) were very similar between normal and tumorous tissue (data not shown). This raises the question under which conditions miR-33a will be substantially upregulated. Since miR-33a expression is coupled to hSREBP-2 expression, a key transcription regulator of genes involved in cholesterol biosynthesis and uptake, it is not unlikely that cellular miR-33a upregulation may link cholesterol metabolism to cell proliferation via miR-33a-mediated repression of Pim-1. It is conceivable that miR-33a-mediated suppression of Pim-1 may be relevant in a specialized biological context such as cardioprotection or embryonic development.

Pim-1 is overexpressed to different extents in tumor cell lines, for example K562 or LS174T, where cell proliferation critically depends on the presence of Pim-1. Furthermore, Pim kinases are overexpressed in a series of human hematological malignancies and in several solid tumors. In the normal cellular context, Pim-1 is weakly or not at all expressed and appears to be largely dispensable, as inferred from the fact that knockout mice with a deletion of all three Pim isoforms (Pim-1, -2, -3) showed only moderate phenotypes (Mikkers *et al*., 2004). This qualifies Pim-1 as a promising target for anti-tumor strategies, for example through RNAi, since side effects on healthy tissues are expected to be moderate. In contrast, single knockouts of Akt isoforms (Akt-1, -2, -3) in mice resulted in severe phenotypes (Yang *et al*., 2004). This suggests that Pim-1 may be a more attractive target than Akt in tumor therapy.

Beyond the inhibition of Pim-1 on the protein level by small inhibitors or knockdown via siRNAs, we demonstrate in this paper that a therapeutic effect may also be achieved through miR-33a-mediated downregulation of Pim-1. MiRNAs are estimated to have, on average, up to 200 targets, which also opens the perspective to exploit synergistic effects on various targets to efficiently induce apoptosis and/or cell-cycle arrest in tumor cells. Indeed, the concept of miRNA replacement therapy has recently been successfully applied to the tumor suppressing miR-26a in a mouse model of hepatocellular carcinoma (Kota *et al*., 2009). This was the first proof-of-concept study demonstrating that miRNAs can be used as general anti-cancer compounds. Recently, the Slack group demonstrated the therapeutic potential of let-7 (Trang *et al*., 2009), a miRNA family whose members map to chromosomal regions frequently deleted in lung cancer (Calin *et al*., 2004), providing another example of miRNA replacement therapy in cancer treatment. Still, miRNA mimic or anti-miR strategies may also result in adverse effects, arising from the capacity of miRNAs to regulate multiple targets. This may also be true for miR-33a mimics which, beyond the anti-tumor effect via Pim-1 shown in this study, may well elicit aberrations of cholesterol metabolism (Najafi-Shoushtari *et al*., 2010; Rayner *et al*., 2010) or exert additional effects on so far unknown

targets. Thus, while we firmly establish the miR-33a/Pim-1 axis, the suitability of miR-33a mimics as therapeutic molecules remains to be shown and is currently under investigation in our laboratory. In fact, we already have experimental data obtained in a s.c. colon carcinoma xenograft model, showing a significant reduction in tumor growth upon nanoparticle-mediated delivery of miR-33a (Ibrahim *et al*., 2011).

Materials and methods

cDNA
The full-length human Pim-1 cDNA was purchased from OriGene (Rockville, MD, USA).

miRNA mimics
Modified miRNA mimics (exact structure and modification pattern not disclosed) were purchased from Thermo Scientific and were based on the sequence of the natural mature miRNA single strands:

miR-33a: 5′-GUG CAU UGU AGU UGC AUU GCA
miR-15a: 5′-UAG CAG CAC AUA AUG GUU UGU G
miR-16-1: 5′-UAG CAG CAC GUA AAU AUU GGC G
negative control mimic (C-mimic) sold by Thermo Scientific for this purpose: 5′-UCA CAA CCU CCU AGA AAG AGU AGA
miR-33b: 5′-GUG CAU UGC UGU UGC AUU GC

Unmodified miR-33a and miR-33b mimics were purchased from MWG (Eurofins MWG Operon, Ebersberg, Germany). Both represent the double-stranded Dicer processing product of pre-miR-33a and pre-miR-33b as published in miRBase/release14 (http://www.mirbase.org), but lacking the 5′-terminal phosphates.

siRNAs
siRNAs were purchased from Thermo Scientific:

Pim-1 siRNA1130: 5′-GAU AUG GUG UGU GGA GAU AdTdT (sense) and 5′-UAU CUC CAC ACA CCA UAU CdTdT (antisense);
Pim-1 siRNA1491: 5′-GGA ACA ACA UUU ACA ACU CdTdT (sense) and 5′-GAG UUG UAA AUG UUG UUC CdTdT (antisense);
VR1 siRNA (VsiRNA1; Grünweller *et al*., 2003) as negative control siRNA: 5′-GCG AUC UUC UAU UCA ACdT dT (sense) and 5′-GUU GAA GUA GAA GAU GCG CdTdT (antisense);
siRNA 33a (siRNA directed against the miR-33a target site in the Pim-1 3′-UTR): 5′-AAA AUG CAC AAA CAA UGC AdT dT (sense) and 5′-UGC AUU GUU UGU GCA UUU UdTdT (antisense).
Negative control siRNAs for transfection of LS174T cells: a) siRNA-luc (targets luciferase mRNA): 5′ -CUU ACG CUG AGU ACU UCG AdTdT (sense) and 5′-UCG AAG UAC UCA GCG UAA GdTdT (antisense).

Antibodies
Antibodies against Pim-1 (sc-13513), β-actin (sc-47778), Cdk6 (sc-177), p53 (sc-126), ABCA1 (ab-18180) as well as the secondary antibodies (sc-2004: goat anti-rabbit IgG HRP-conjugated; sc-2005: goat anti-mouse IgG HRP-conjugated) were from Santa Cruz Biotechnology (Heidelberg, Germany) except for the ABCA1 antibody purchased from Abcam (Cambridge, UK).

Plasmid construction, seed mutagenesis and luciferase reporter assay
The full-length Pim-1 cDNA clone was purchased from OriGene (Cat. No.: SC110975, Accession No.: NM_002648.2 hsa Pim-1 oncogene, vector pCMV6-XL4, vector size 4.7 kb plus 2.6 kb Pim-1 insert DNA). To construct the plasmid lacking two thirds of the 3′-UTR (including the miR-33a target site), 1 μg of full-length Pim-1 cDNA was digested with the *Hin*dIII fast digest enzyme (Fermentas, St Leon-Roth, Germany) to remove the ~0.9 kbp *Hin*dIII/*Hin*dIII fragment of the 3′-UTR, followed by vector religation. *Hin*dIII cleaves ~50 bp downstream of the Pim-1 stop codon (position 1424 in sequence NM_002648.3, see Figure 1a) and ~400 bp upstream of the poly(A) tail (position 2311). The Pim-1 cDNA clone containing the mutation in the miRNA-33a target site was derived from the existing 'pGL3 control Pim-1 3′-UTR mut 33a plasmid' (see below). For this purpose, the latter plasmid was also digested with *Hin*dIII, and the ~0.9 kbp *Hin*dIII/*Hin*dIII fragment containing the mutation in the miRNA-33a site was cloned into the Pim-1 cDNA clone (from OriGene, see above). The 3′-proximal 450 nt (including the miR-33a seed region) of all Pim-1 cDNA constructs (full-length wild-type, Pim-1 Δ 3′-UTR and full-length cDNA with mutated miR-33a seed) were verified by DNA sequencing.

The 3′-UTR of human Pim-1 was cloned into the pGL3 control luciferase reporter vector (Promega, Mannheim, Germany) via its *Xba*I site. The 3′-UTR was initially amplified from K562 genomic DNA with the forward primer 5′-GCT CTA GAG CTG TCA GAT GCC CGA GGG and reverse primer 5′-GCT CTA GAG CAA TAA GAT CTC TTT TAT TCC CCT GT (*Xba*I sites underlined). Two G-C base pairs were introduced beyond the *Xba*I sites for more efficient *Xba*I digestion of the PCR product. PCR mutagenesis of the miRNA-33a target site was carried out according to Brennecke *et al*. (2005) using the following primers (sites of mutation underlined): 5′-AAA AAA TGC ACA AAC AGT GCG ATC AAC AGA AAA GCT; 5′-AGC TTT TCT GTT GAT CGC ACT GTT TGT GCA TTT TTT. Mutations were verified by DNA sequencing.

A total of 5 μg of pGL3 derivatives were cotransfected with 1 μg of miRNA mimics per 1×10^6 K562 cells. After 48 h, luciferase assays were performed using the Promega Luciferase Assay System. Briefly, cells were lysed in 100 μl lysis buffer, and 10 μl of lysate was mixed with 25 μl substrate solution and immediately measured with a Safire2 microplate reader (Tecan, Crailsheim, Germany) in 96-well plates.

Conflict of interest

The authors declare no conflict of interest.

Acknowledgements

We thank Robert Prinz, Dorothee Hartmann, Dennis Streng, Meike Thomas and Heide Marika Genau for technical support. This study was supported by the Fritz Thyssen Stiftung (reference no. 10.06.1.186 to AG and RKH), the Deutsche Krebshilfe (reference no. 109260 to AG, RKH and AA, and reference no. 106992 to AA) and DFG Forschergruppe Nanohale (AI 24/6-1).

References

Aho TL, Sandholm J, Peltola KJ, Mankonen HP, Lilly M, Koskinen PJ. (2004). Pim-1 kinase promotes inactivation of the pro-apoptotic Bad protein by phosphorylating it on the Ser112 gatekeeper site. *FEBS Lett* **571**: 43–49.

Amaravadi R, Thompson CB. (2005). The survival kinases Akt and Pim as potential pharmacological targets. *J Clin Invest* **115**: 2618–2624.

Aqeilan RI, Calin GA, Croce CM. (2010). miR-15a and miR-16-1 in cancer: discovery, function and future perspectives. *Cell Death Differ* **17**: 215–220.

Bachmann M, Hennemann H, Xing PX, Hoffmann I, Möröy T. (2004). The oncogenic serine/threonine kinase Pim-1 phosphorylates and inhibits the activity of Cdc25C-associated kinase 1 (C-TAK1): a novel role for Pim-1 at the G2/M cell cycle checkpoint. *J Biol Chem* **279**: 48319–48328.

Bachmann M, Möröy T. (2005). The serine/threonine kinase Pim-1. *Int J Biochem Cell Biol* **37**: 726–730.

Bartel DP. (2004). MicroRNAs: genomics, biogenesis, mechanism, and function. *Cell* **116**: 281–297. Review.

Bartel DP. (2009). MicroRNAs: target recognition and regulatory functions. *Cell* **136**: 215–233. Review.

Bonci D, Coppola V, Musumeci M, Addario A, Giuffrida R, Memeo L *et al*. (2008). The miR-15a-miR-16-1 cluster controls prostate cancer by targeting multiple oncogenic activities. *Nat Med* **14**: 1271–1277.

Brault L, Gasser C, Bracher F, Huber K, Knapp S, Schwaller J. (2010). PIM serine/threonine kinases in the pathogenesis and therapy of hematologic malignancies and solid cancers. *Haematologica* **95**: 1004–1015. Review.

Brennecke J, Stark A, Russell RB, Cohen SM. (2005). Principles of microRNA-target recognition. *PLoS Biol* **3**: e85.

Calin GA, Dumitru CD, Shimizu M, Bichi R, Zupo S, Noch E *et al*. (2002). Frequent deletions and down-regulation of micro- RNA genes miR15 and miR16 at 13q14 in chronic lymphocytic leukemia. *Proc Natl Acad Sci USA* **99**: 15524–21559.

Calin GA, Sevignani C, Dumitru CD, Hyslop T, Noch E, Yendamuri S *et al*. (2004). Human microRNA genes are frequently located at fragile sites and genomic regions involved in cancers. *Proc Natl Acad Sci USA* **101**: 2999–3004.

Chen C, Ridzon DA, Broomer AJ, Zhou Z, Lee DH, Nguyen JT *et al*. (2005a). Real-time quantification of microRNAs by stem-loop RT-PCR. *Nucleic Acids Res* **33**: e179.

Chen WW, Chan DC, Donald C, Lilly MB, Kraft AS. (2005b). Pim family kinases enhance tumor growth of prostate cancer cells. *Mol Cancer Res* **3**: 443–451.

Cimmino A, Calin GA, Fabbri M, Iorio MV, Ferracin M, Shimizu M *et al*. (2005). miR-15 and miR-16 induce apoptosis by targeting BCL2. *Proc Natl Acad Sci USA* **102**: 13944–13949.

Croce CM. (2009). Causes and consequences of microRNA dysregulation in cancer. *Nat Rev Genet* **10**: 704–714. Review.

Crowell JA, Steele VE, Fay JR. (2007). Targeting the AKT protein kinase for cancer chemoprevention. *Mol Cancer Ther* **6**: 2139–2148.

Datta SR, Dudek H, Tao X, Masters S, Fu H, Gotoh Y *et al*. (1997). Akt phosphorylation of BAD couples survival signals to the cell-intrinsic death machinery. *Cell* **91**: 231–241.

Esquela-Kerscher A, Slack FJ. (2006). Oncomirs – microRNAs with a role in cancer. *Nat Rev Cancer* **6**: 259–269. Review.

Fox CJ, Hammerman PS, Cinalli RM, Master SR, Chodosh LA, Thompson CB. (2003). The serine/threonine kinase Pim-2 is a transcriptionally regulated apoptotic inhibitor. *Genes Dev* **17**: 1841–1854.

Gangaraju VK, Lin H. (2009). MicroRNAs: key regulators of stem cells. *Nat Rev Mol Cell Biol* **10**: 116–125.

Garzon R, Calin GA, Croce CM. (2009). MicroRNAs in cancer. *Annu Rev Med* **60**: 167–179.

Grimson A, Farh KK, Johnston WK, Garrett-Engele P, Lim LP, Bartel DP. (2007). MicroRNA targeting specificity in mammals: determinants beyond seed pairing. *Mol Cell* **27**: 91–105.

Grünweller A, Wyszko E, Bieber B, Jahnel R, Erdmann VA, Kurreck J. (2003). Comparison of different antisense strategies in mammalian cells using locked nucleic acids, 2′-O-methyl RNA, phosphorothioates and small interfering RNA. *Nucleic Acids Res* **31**: 3185–3193.

Herrera-Merchan A, Cerrato C, Luengo G, Dominguez O, Piris MA, Serrano M *et al*. (2010). miR-33-mediated downregulation of p53 controls hematopoietic stem cell self-renewal. *Cell Cycle* **15**: 3277–3285.

Huang J, Manning BD. (2009). A complex interplay between Akt, TSC2 and the two mTOR complexes. *Biochem Soc Trans* **37**: 217–222.

Ibrahim AF, Weirauch U, Thomas M, Grünweller A, Hartmann RK, Aigner A *et al*. (2011). MiRNA replacement therapy through PEI-mediated in vivo delivery of miR-145 or miR-33a in colon carcinoma. *Cancer Res* (doi:10.1158/0008-5472.CAN-10-4645).

Iorio MV, Ferracin M, Liu CG, Veronese A, Spizzo R, Sabbioni S *et al*. (2005). MicroRNA gene expression deregulation in human breast cancer. *Cancer Res* **65**: 7065–7070.

Johnson SM, Grosshans H, Shingara J, Byrom M, Jarvis R, Cheng A *et al*. (2005). RAS is regulated by the let-7 microRNA family. *Cell* **120**: 635–647.

Kota J, Chivukula RR, O'Donnell KA, Wentzel EA, Montgomery CL, Hwang HW *et al*. (2009). Therapeutic microRNA delivery suppresses tumorigenesis in a murine liver cancer model. *Cell* **137**: 1005–1017.

Lewis BP, Burge CB, Bartel DP. (2005). Conserved seed pairing, often flanked by adenosines, indicates that thousands of human genes are microRNA targets. *Cell* **120**: 15–20.

Liu J, Valencia-Sanchez MA, Hannon GJ, Parker R. (2005). MicroRNA-dependent localization of targeted mRNAs to mammalian P-bodies. *Nat Cell Biol* **7**: 719–723.

Martelli AM, Tazzari PL, Evangelisti C, Chiarini F, Blalock WL, Billi AM *et al*. (2007). Targeting the phosphatidylinositol 3-kinase/Akt/mammalian target of rapamycin module for acute myelogenous leukemia therapy: from bench to bedside. *Curr Med Chem* **14**: 2009–2023.

Meyerson M, Harlow E. (1994). Identification of G1 kinase activity for cdk6, a novel cyclin D partner. *Mol Cell Biol* **14**: 2077–2086.

Mikkers H, Nawijn M, Allen J, Brouwers C, Verhoeven E, Jonkers J *et al*. (2004). Mice deficient for all PIM kinases display reduced body size and impaired responses to hematopoietic growth factors. *Mol Cell Biol* **24**: 6104–6115.

Mochizuki T, Kitanaka C, Noguchi K, Muramatsu T, Asai A, Kuchino Y. (1999). Physical and functional interactions between Pim-1 kinase and Cdc25A phosphatase. Implications for the Pim-1-mediated activation of the c-Myc signaling pathway. *J Biol Chem* **274**: 18659–18666.

Muraski JA, Rota M, Misao Y, Fransioli J, Cottage C, Gude N *et al*. (2007). Pim-1 regulates cardiomyocyte survival downstream of Akt. *Nat Med* **13**: 1467–1475.

Najafi-Shoushtari SH, Kristo F, Li Y, Shioda T, Cohen DE, Gerszten RE *et al*. (2010). MicroRNA-33 and the SREBP host genes cooperate to control cholesterol homeostasis. *Science* **328**: 1566–1569.

Nawijn MC, Alendar A, Berns A. (2011). For better or for worse: the role of Pim oncogenes in tumorigenesis. *Nat Rev Cancer* **11**: 23–34. Review.

O'Donnell KA, Wentzel EA, Zeller KI, Dang CV, Mendell JT. (2005). c-Myc-regulated microRNAs modulate E2F1 expression. *Nature* **435**: 839–843.

Qian KC, Wang L, Hickey ER, Studts J, Barringer K, Peng C *et al*. (2005). Structural basis of constitutive activity and a unique nucleotide binding mode of human Pim-1 kinase. *J Biol Chem* **280**: 6130–6137.

Rayner KJ, Suárez Y, Dávalos A, Parathath S, Fitzgerald ML, Tamehiro N *et al*. (2010). miR-33 contributes to the regulation of cholesterol homeostasis. *Science* **328**: 1570–1573.

Rehwinkel J, Behm-Ansmant I, Gatfield D, Izaurralde E. (2005). A crucial role for GW182 and the DCP1:DCP2 decapping complex in miRNA-mediated gene silencing. *RNA* **11**: 1640–1647.

Selbach M, Schwanhäusser B, Thierfelder N, Fang Z, Khanin R, Rajewsky N. (2008). Widespread changes in protein synthesis induced by microRNAs. *Nature* **455**: 58–63.

Trang P, Medina PP, Wiggins JF, Ruffino L, Kelnar K, Omotola M *et al*. (2009). Regression of murine lung tumors by the let-7 microRNA. *Oncogene* **29**: 1580–1587.

van Lohuizen M, Verbeek S, Krimpenfort P, Domen J, Saris C, Radaszkiewicz T *et al*. (1989). Predisposition to lymphomagenesis in pim-1 transgenic mice: cooperation with c-myc and N-myc in murine leukemia virus-induced tumors. *Cell* **56**: 673–682.

Venturini L, Battmer K, Castoldi M, Schultheis B, Hochhaus A, Muckenthaler MU *et al*. (2007). Expression of the miR-17-92 polycistron in chronic myeloid leukemia (CML) CD34 + cells. *Blood* **109**: 4399–4405.

Verbeek S, van Lohuizen M, van der Valk M, Domen J, Kraal G, Berns A. (1991). Mice bearing the E mu-myc and E mu-pim-1 transgenes develop pre-B-cell leukemia prenatally. *Mol Cell Biol* **11**: 1176–1179.

Wang HW, Noland C, Siridechadilok B, Taylor DW, Ma E, Felderer K *et al*. (2009). Structural insights into RNA processing by the human RISC-loading complex. *Nat Struct Mol Biol* **16**: 1148–1153.

Wang Z, Bhattacharya N, Mixter PF, Wei W, Sedivy J, Magnuson NS. (2002). Phosphorylation of the cell cycle inhibitor p21Cip1/WAF1 by Pim-1 kinase. *Biochim Biophys Acta* **1593**: 45–55.

Xia Z, Knaak C, Ma J, Beharry ZM, McInnes C, Wang W *et al*. (2009). Synthesis and evaluation of novel inhibitors of Pim-1 and Pim-2 protein kinases. *J Med Chem* **52**: 74–86.

Xie Y, Xu K, Dai B, Guo Z, Jiang T, Chen H *et al*. (2006). The 44 kDa Pim-1 kinase directly interacts with tyrosine kinase Etk/BMX and protects human prostate cancer cells from apoptosis induced by chemotherapeutic drugs. *Oncogene* **25**: 70–78.

Yang ZZ, Tschopp O, Baudry A, Dümmler B, Hynx D, Hemmings BA. (2004). Physiological functions of protein kinase B/Akt. *Biochem Soc Trans* **32**: 350–354. Review.

Zhang T, Zhang X, Ding K, Yang K, Zhang Z, Xu Y. (2010). PIM-1 gene RNA interference induces growth inhibition and apoptosis of prostate cancer cells and suppresses tumor progression *in vivo*. *J Surg Oncol* **101**: 513–519.

Zhang W, Shay JW, Deisseroth A. (1993). Inactive p53 mutants may enhance the transcriptional activity of wild-type p53. *Cancer Res* **15**: 4772–4775.

Zhang Y, Wang Z, Li X, Magnuson NS. (2008). Pim kinase-dependent inhibition of c-Myc degradation. *Oncogene* **27**: 4809–4481.

Zhang Y, Wang Z, Magnuson NS. (2007). Pim-1 kinase-dependent phosphorylation of p21Cip1/WAF1 regulates its stability and cellular localization in H1299 cells. *Mol Cancer Res* **5**: 909–922.

Zippo A, De Robertis A, Serafini R, Oliviero S. (2007). PIM1-dependent phosphorylation of histone H3 at serine 10 is required for MYC-dependent transcriptional activation and oncogenic transformation. *Nat Cell Biol* **9**: 932–944.

Supplementary Information accompanies the paper on the Oncogene website (http://www.nature.com/onc)

SUPPLEMENTARY MATERIAL

1. Supplementary Materials and Methods

Cell culture and transfection

Cell lines (K562, LS174T and Skov-3) were cultivated under standard conditions (37°C, 5% CO_2 in a humidified atmosphere) in RPMI 1640 medium (K562) or IMDM medium (LS174T and Skov-3) containing 10 % FCS (PAA, Cölbe, Germany) unless stated otherwise. For transfection of K562 cells with miRNA mimics or siRNAs, cells were electroporated in 4 mm cuvettes with a single pulse at 330 V for 10 ms using a BioRad Gene Pulser XCell (Biorad, München, Germany). For 1 x 10^6 cells, 1 µg of the respective mimic or siRNA was used. LS174T cells were transfected with miRNA mimics using the INTERFERin siRNA transfection reagent (Peqlab, Erlangen, Germany) according to the manufacturer's protocol. Briefly, 1 x 10^3, 1.5 x 10^5 or 2.5 x 10^5 cells were seeded in 96-well, 24-well or 12-well plates, respectively, and cultivated under standard conditions. For complexation, 0.25 to 1 µl INTERFERin per pmol miRNA mimic was incubated with the RNA in serum-free medium for 10 min at room temperature. Complexes were added to the wells (5 µl INTERFERin complexed with 5 pmol miRNA for 24-well plates, 0.625 µl INTERFERin complexed with 2.5 pmol miRNA for 96-well plates), followed by incubation for 72 h (time point of the determination of knockdown efficacy) or for the time periods indicated in Fig. 7 of the main manuscript (proliferation assays). For the experiment in Fig. 3 of the main manuscript, LS174T cells were transfected with miRNA mimics using Lipofectamine™ 2000 (Life Technologies Invitrogen, Karlsruhe, Germany). The day before transfection 0.5 x 10^6 cells were seeded into 12-well plates. 40 pmol RNA and 2 µl Lipofectamine™ 2000 were mixed in Opti-MEM® 1 (Invitrogen, Karlsruhe, Germany) according to the instructions of the manufacturer and added to the cells. After 4 to 6 h, the transfection medium was aspirated and IMDM + 10% FCS was added. Cells were lysed 48 h after transfection.

For transfection of Skov-3 cells, 1 x 10^5 cells were seeded into 12-well plates. 2 µl Lipofectamine™ 2000, 25 ng of Pim-1 cDNA plasmid (full-length wild-type cDNA, full-length cDNA with mutagenized miR-33a seed, or a truncated cDNA with about two-thirds of the 3'-UTR deleted) and 20 pmol siRNA or miRNA mimic were mixed in Opti-MEM® 1 (Life Technologies Invitrogen, Karlsruhe, Germany) according to the instructions of the manufacturer and added to the cells. Cells were lysed 48 h after transfection and analyzed by Western blotting.

Quantitative RT-PCR for miRNA profiling

Small RNAs (< 200 nt) were isolated using the mirVana™ miRNA isolation kit from Ambion (Applied Biosystems, Darmstadt, Germany). For RT-PCR experiments, 100 ng of a mirVana RNA preparation was used. Reverse transcription was conducted using the Fermentas RevertAid™ H Minus First Strand cDNA Synthesis Kit (Fermentas, St. Leon-Roth, Germany) with 100 ng of a mirVana™ RNA preparation. Quantitative PCR (55 cycles) was performed in duplicate in a LightCycler®2.0 from Roche (Mannheim, Germany) with the Absolute™ QPCR SYBR® Green Capillary Mix (Thermo Scientific, Hamburg, Germany). All procedures and reactions were carried out according to the protocols provided by the manufacturers.

For the reverse transcription step, a miRNA-specific stem-loop primer (= looped primer) was used (5 pmol in 20 µl reaction volume) to generate the cDNA according to Chen et al. (2005). Stem-loop primers carried a 3'-overhang of 6 or 7 nucleotides complementarity to the 3'-portion of the respective mature miRNA sequence. In the quantitative PCR (qPCR) following reverse transcription (see above), 1/100 of the cDNA reaction was amplified in a LightCycler® 2.0 (Roche Applied Biosciences, Mannheim, Germany), using the Absolute™ QPCR SYBR® Green Capillary Mix (Thermo Scientific, Hamburg, Germany) and 10 pmol of each primer (10 µl reaction volume). Primers, including the stem-loop primers (see above), were obtained from Metabion (Metabion, Martinsried, Germany) and designed with Universal ProbeLibrary (Roche Applied Biosciences, Mannheim, Germany) according to Chen et al. (2005). The qPCR forward primer was a DNA mimic of the respective miRNA sequence (www.mirbase.org), but lacking the 3'-terminal 6 or 7 miRNA nucleotides to avoid hybridization with the stem-loop primer. The forward primer's 5'-end was extended by a variable number of G and C nucleotides to equalize the Tm values of PCR products to ~ 60°C. Quantitative PCR assays were conducted as follows: Thermo-Start™ DNA polymerase was activated for 15 min at 95°C followed by 40 amplification cycles with a denaturation step for 10 s, primer annealing for 20 s at 60°C and amplification at 72°C for 12 s. Subsequently, a melting curve was generated for the PCR products; samples were cooled from 95°C to 65°C (20°C per s), kept at 65°C for 15 s, followed by heating in steps of 0.1°C per second up to 98°C. Data were evaluated by determining the crossing point Cp value (= C_T value, cycle of threshold). This value is defined as the PCR cycle (specified with two decimals) at which the fluorescent signal of the reporter dye crosses an arbitrarily placed threshold. Data are presented as 2^{-Cp} according to Schmittgen and Livak (2008); to enable the reader to reconstruct the data shown in Fig. 2 of the main manuscript, we have added the raw data below (Table S1).

Primers used for miRNA profiling by the looped-primer technique

hsa-miR-15a
RT-qPCR stem-loop primer:
5'-GTCGTATCCAGTGCAGGGTCCGAGGTATTCGCACTGGATACGACCACAAAC
qPCR forward primer:
5'-CGCGCTAGCAGCACATAATG

hsa-miR-16-1
RT-qPCR stem-loop primer:
5'-GTCGTATCCAGTGCAGGGTCCGAGGTATTCGCACTGGATACGACCGCCAAT
qPCR forward primer:
5'-CGCGCTAGCAGCACGTAAAT

hsa-miR-17
RT-qPCR stem-loop primer:
5'-GTCGTATCCAGTGCAGGGTCCGAGGTATTCGCACTGGATACGACCTACCTG
qPCR forward primer:
5'-CGCGCCAAAGTGCTTACAGTG

hsa-miR-20a
RT-qPCR stem-loop primer:
5'-GTCGTATCCAGTGCAGGGTCCGAGGTATTCGCACTGGATACGACCTACCTG
qPCR forward primer:
5'-GCCGCGCTAAAGTGCTTATAGTG

hsa-miR-24
RT-qPCR stem-loop primer:
5'-GTCGTATCCAGTGCAGGGTCCGAGGTATTCGCACTGGATACGACCACCTGTTC
qPCR forward primer:
5'-CGCGCTGGCTCAGTTCAGCAG

hsa-miR-26a
RT-qPCR stem-loop primer:
5'-GTCGTATCCAGTGCAGGGTCCGAGGTATTCGCACTGGATACGACAGCCTAT
qPCR forward primer:
5'-CGCGCTTCAAGTAATCCAGG

hsa-miR-33a
RT-qPCR stem-loop primer:
5'-TGGATATCCACACCAGGGTCCGAGGTATTCGGTGTGGATATCCATGCAATG
(underlined positions: base exchanges relative to the other looped primers listed)
qPCR forward primer:
5'-CGCGCGTGCATTGTAGTTG
unique reverse primer qPCR:
5'-CACCAGGGTCCGAGGT
(underlined positions: base exchanges relative to the universal reverse primer specified at the end of this primer list)

hsa-miR-33b
RT-qPCR stem-loop primer:
5'-GTCGTATCCAGTGCAGGGTCCGAGGTATTCGCACTGGATACGACCGAATG
qPCR forward primer:
5'-CGCGCGTGCATTGTTCTTG

hsa-miR-144
RT-qPCR stem-loop primer:
5'-GTCGTATCCAGTGCAGGGTCCGAGGTATTCGCACTGGATACGACAGTACAT
qPCR forward primer:
5'-GCGCGCGCTACAGTATAGATG

hsa-miR-374a
RT-qPCR stem-loop primer:
5'-GTCGTATCCAGTGCAGGGTCCGAGGTATTCGCACTGGATACGACCACTTAT
qPCR forward primer:
5'-GCCGCGCTTATAATACAACCTG

universal reverse primer qPCR:
5'-GTGCAGGGTCCGAGGT

Western blotting

Cells were resuspended in lysis buffer (125 mM Tris-HCl pH 6.8, 4 % SDS, 1.4 M 2-mercaptoethanol, 0.05 % bromophenol blue) and heated at 95°C for 5 min. Lysed samples were directly loaded onto 15% SDS-polyacrylamide gels using the BioRad Mini-PROTEAN® 3 cell mini gel system (BioRad, München, Germany) and run for 1 h at 180 V. Proteins were transferred to an Immobilon™-P PVDF membrane (Millipore, MA, USA) for 90 min at 1 mA per cm^2 of membrane area using an EBU-4000 Semi-Dry Blotting System CE (C.B.S. Scientific, CA, USA). Primary and secondary antibodies were diluted in TBST (10 mM Tris-HCl, pH 7.6, 150 mM NaCl, 0.1% Tween 20) 1:500 (Pim-1), 1:2000 (Cdk6), 1:10000 or 1:1000 (ß-Actin), 1:1000 (p53), 1:1000 (ABCA1) and 1:5000 (secondary antibodies). After a final washing step, blots were incubated with Amersham ECL™ or ECLplus™ Western Blotting Detection Reagents according to the manufacturer's protocol. For detection of chemiluminescence, Kodak® BioMax™ light films, Kodak GBX Developer and Replenisher and GBX Fixer and Replenisher were used.

Proliferation assays

To determine the number of viable K562 cells as a measure of cell proliferation, 1 x 10^4 cells were seeded in 1.5 ml RPMI 1640 (plus 10% FCS) and cultivated under standard conditions. At the time points indicated, cells were pelleted and resuspended in 100 µl PBS, and 10 µl of the tetrazolium salt WST-1 were added to determine the activity of mitochondrial dehydrogenases. After incubation at 37°C for 2 h, absorbance was measured at 450 nm with 600 nm as reference wavelength using a Safire²™ microplate reader. Alternatively, K562 cells (0.1 –0.5 x 10^6 cells/ml) were counted at the indicated time points in a Neubauer chamber (Lauda-Königshofen, Germany).

For the assessment of LS174T cell proliferation, 1 x 10^3 cells per well were seeded in 96-well plates and transfected using INTERFERin as described above. At the time points indicated, the medium was aspirated and 50 µl WST-1, diluted 1:10 in serum-free medium,

was added to the cells. After incubation for 1 h at 37°C, absorbance at 450 nm was measured using a Dynex MRX microplate reader (Pegasus Scientific Inc., Rockville, MD, USA).

Apoptosis assays

For K562 cells, the Cell Death Detection ELISA (Roche Applied Biosciences, Mannheim, Germany) was utilized. Microtiter plates were pre-coated with an anti-histone antibody (clone H 11-4), incubated with lysed cells, followed by the addition of an anti-DNA antibody (clone MCA–33) and incubation for 90 min. For detection of mono- and oligonucleosomes, an 2,2'-Azinobis-3-ethylbenzthiazolin-6-sulfonic acid (ABTS) substrate solution was applied. Absorbance was measured with a Safire^{2TM} microplate reader at 405 nm.

To determine the apoptosis in LS174T cells, the Caspase-Glo® 3/7 Assay (Promega, Mannheim, Germany) was used acccording to the manufacturer's protocol. Briefly, 1 x 10^3 cells per well were seeded in 96-well plates and transfected as described above. After 120 h, the caspase Glo® 3/7 substrate was diluted 1+1 in serum-free medium and 100 µl were added to the cells prior to incubating for 1 h at room temperature. For the detection of caspase activity, luminescence was measured using a FLUOstar OPTIMA microplate reader (BMG Labtech, NYC, USA). Readings from caspase 3/7 measurements were normalized to cell densities.

2. Supplementary Results

Other potential miRNA binding sites in the Pim-1 3'-UTR

We excluded miR-124/506 as a serious candidate for regulation of Pim-1 mRNA translation in K562 and LS174T cells, because miR-124 is mainly expressed in the brain and involved in neurogenesis and neuronal differentiation (Cheng et al. 2009; Makeyev et al., 2007). Additionally, the miR-124 target site in Pim-1 is not well conserved upstream of the seed region between vertebrates (human to chicken) (see Fig. S1). Likewise, we disregarded miR-26a/b because the loop adjacent to the seed pairing as well as the second pairing region deviate from the Grimson rules (Fig. S1), although the target site is well conserved and the context score percentile was relative high (88 for miR-26a relative to 98 for miR-33a); however, Pim-1 was ranked (total context score -0.31) by TargetScan 5.1 below the most favorable 200 conserved targets of miR-26a. miR-24, reported to suppress translation of the tumor suppressor p16 (Lal et al., 2008), was not considered either as a primary candidate for Pim-1 suppression based on the relatively low context score percentile (77) and an overall weak conservation of its target site (Fig. S1). miR-144 (percentile 93) was not further

considered because target site conservation included mouse, rabbit and dog, but not chicken.

3. Supplementary Figure Legends

Figure S1: Phylogenetic conservation of predicted miRNA binding sites in the 3‘-UTR of Pim-1. The phylogenetic conservation based on alignment of sequences from human, mouse, rabbit, dog and chicken (except for miR-144, where the chicken sequence was excluded because of low conservation) is illustrated by weblogos. For comparison, weblogos for two established conserved miRNA target sites are shown at the bottom (let-7a in the Lin28 3’-UTR, and miR-15/16 in the Bcl2 3’-UTR). For miR-26a/b, although showing strong target site conservation based on the weblogo, the sequence alignment on the right revealed no clearly unpaired region adjacent to the seed.

Figure S2: miR-33a target sites in the Cdk6 3‘-UTR as predicted by TargetScan 5.1 with context score percentiles of 98 and 20 respectively. Both sites are only moderately conserved in the region immediately upstream of the seed. For details, see legend to Fig. 1 B, C of the main manuscript.

Figure S3: (**A**) Two independent experiments monitoring the growth of K562 cells in the presence of 10% FCS after transfection with the modified miR-33a mimic relative to the control mimic and untreated cells. No inhibitory effect of the miR-33a mimic was observed under these conditions. (**B**) Cultivation of K562 cells in the presence of 2% FCS leads to reduced expression levels of Pim-1 compared to cells grown under normal growth factor conditions (10% FCS). For comparison, Pim-1 levels in LS174T cells grown in the presence of 10% FCS are shown. ß-Actin was used as a loading control. For details on Western blot methodology, see Supplementary Materials and Methods above.

Figure S4: (**A**) Test for changes in apoptosis (inferred from quantitation of DNA fragmentation) upon Pim-1 knockdown (24 h posttransfection) in K562 cells. Cells were transfected with the Pim-1-specific siRNA1130 (Fig 1 A), a sequence-unrelated control siRNA (VR1 siRNA) or without any siRNA. No substantial changes in apoptosis were observed up to 96 h posttransfection (data not shown). (**B**) Test for changes in apoptosis (inferred from caspase activity) upon Pim-1 knockdown (120 h posttransfection) in LS174T cells. Caspase activity was normalized to values measured for cells transfected with the control siRNA. Values in panels A and B represent the mean (± SEM) of three (panel A) or nine (panel B) independent experiments.

Supplementary References

Chen C, Ridzon DA, Broomer AJ, Zhou Z, Lee DH, Nguyen JT et al. (2005a). Real-time quantification of microRNAs by stem-loop RT-PCR. *Nucleic Acids Res.* **33:** e179.

Cheng LC, Pastrana E, Tavazoie M, Doetsch F. (2009). miR-124 regulates adult neurogenesis in the subventricular zone stem cell niche. *Nat Neurosci.* **12:** 399-408.

Lal A, Kim HH, Abdelmohsen K, Kuwano Y, Pullmann R Jr, Srikantan S, Subrahmanyam R, Martindale JL, Yang X, Ahmed F, Navarro F, Dykxhoorn D, Lieberman J, Gorospe M. (2008). p16(INK4a) translation suppressed by miR-24. *PLoS One.* **3:** e1864.

Makeyev EV, Zhang J, Carrasco MA, Maniatis T. (2007). The MicroRNA miR-124 promotes neuronal differentiation by triggering brain-specific alternative pre-mRNA splicing. *Mol Cell.* **27:** 435-448.

Schmittgen TD, Livak KJ. (2008) Analyzing real-time PCR data by the comparative C(T) method. *Nat Protoc.* **3:** 1101-1108.

miRNA profilings (MV = mean value; NTC = non-template control = no RNA added; no RT = omission of Reverse Transcriptase)

K562

miRNA	MV 1 Cp	MV 2 Cp	MV 3 Cp	MV Cp	SEM Cp	no RT	NTC
hsa-miR-15a	20.25	19.59	19.55	19.80	0.227	-	>35
hsa-miR-16-1	18.07	17.54	17.81	17.81	0.153	>35	33.5
hsa-miR-17	15.03	15.00	15.13	15.05	0.039	24.32	28.58
hsa-miR-20a	16.11	15.14	14.44	15.23	0.484	-	-
hsa-miR-24-1	18.73	19.38	20.16	19.42	0.413	26.53	27.6

hsa-miR-26a	19.39	18.72	19.34	19.15	0.216	31.77	31.45
hsa-miR-33a	23.27	21.59	21.72	22.19	0.540	-	>35
hsa-miR-33b	-	-	-	-	-	-	-
hsa-miR-144	25.56	24.67	23.54	24.59	0.585	-	-
hsa-miR-374a	23.59	22.49	22.61	22.89	0.348	30.97	30.63

LS 174T

miRNA	MV 1 Cp	MV 2 Cp	MV 3 Cp	MV Cp	SEM Cp	no RT	NTC
hsa-miR-15a	20.77	19.35	21.56	20.56	0.647	-	-
hsa-miR-16-1	17.51	17.18	18.81	17.83	0.498	-	34.63
hsa-miR-17	17.69	17.12	18.37	17.73	0.361	27.97	27.58
hsa-miR-20a	18.68	17.96	19.63	18.76	0.484	>35	-
hsa-miR-24-1	18.04	18	19.54	18.53	0.507	28.35	27.84
hsa-miR-26a	19.91	19.1	20.73	19.91	0.471	25.69	26.33
hsa-miR-33a	23.18	21.41	22.62	22.40	0.522	-	-
hsa-miR-33b	-	-	-	-	-	-	-
hsa-miR-144	-	-	-	-	-	-	-

hsa-miR-374a	24.17	23.68	25.66	24.5	0.595	31.84	30.55

data miR-33a, different cell lines

cell line	**MV 1 Cp**	**MV 2 Cp**	**MV 3 Cp**	**MV Cp**	**SEM Cp**	**no RT**	**NTC**
HEK 293	24.30	22.84	23.60	23.58	0.419	-	-
Skov-3	22.55	21.43	21.61	21.86	0.347	-	-
HUH 7	21.77	22.91	21.22	21.97	0.498	-	-
HepG2	21.34	23.61	22.78	22.58	0.663	-	-

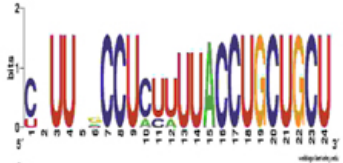

miR-15a/-16-1

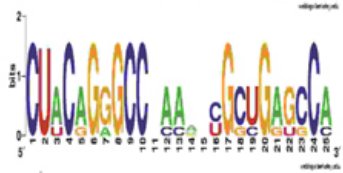

miR-24

miR-26a

target sites for miRNAs in the Pim-1 3'-UTR
(conserved to chicken except for miR-144)

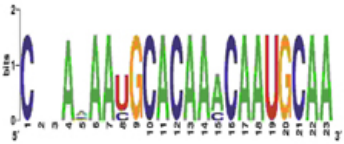

miR-33a

miR-124

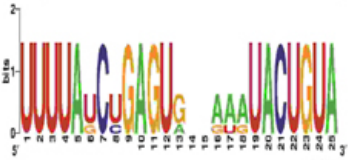

miR-144 (dog)

Seed Region

let-7a target site
in the Lin28 3´UTR

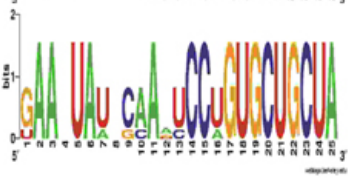

miR-15/16 in the
Bcl2 3'-UTR

```
 3'-UCGGAUAGGACCUAAUGAACUU  miR-26a1/2
    |o       | | ||||||||
5'-CUGUGCUGGGAGAAAUACUUGAA  human
    oo       ||| ||||||||
 3'-UGGAUAGGACUUAAUGAACUU  miR-26b

5'-CUGUGCUGGGAGAAAUACUUGAA  mouse
5'-CUGUGCUGGGAGAAAUACUUGAA  rabbit
5'-CUGUGCUGGAGGAAAUACUUGAA  dog
5'-CUGUGCUGGAGGAAAUACUUGAA  chicken
```

Fig. S1

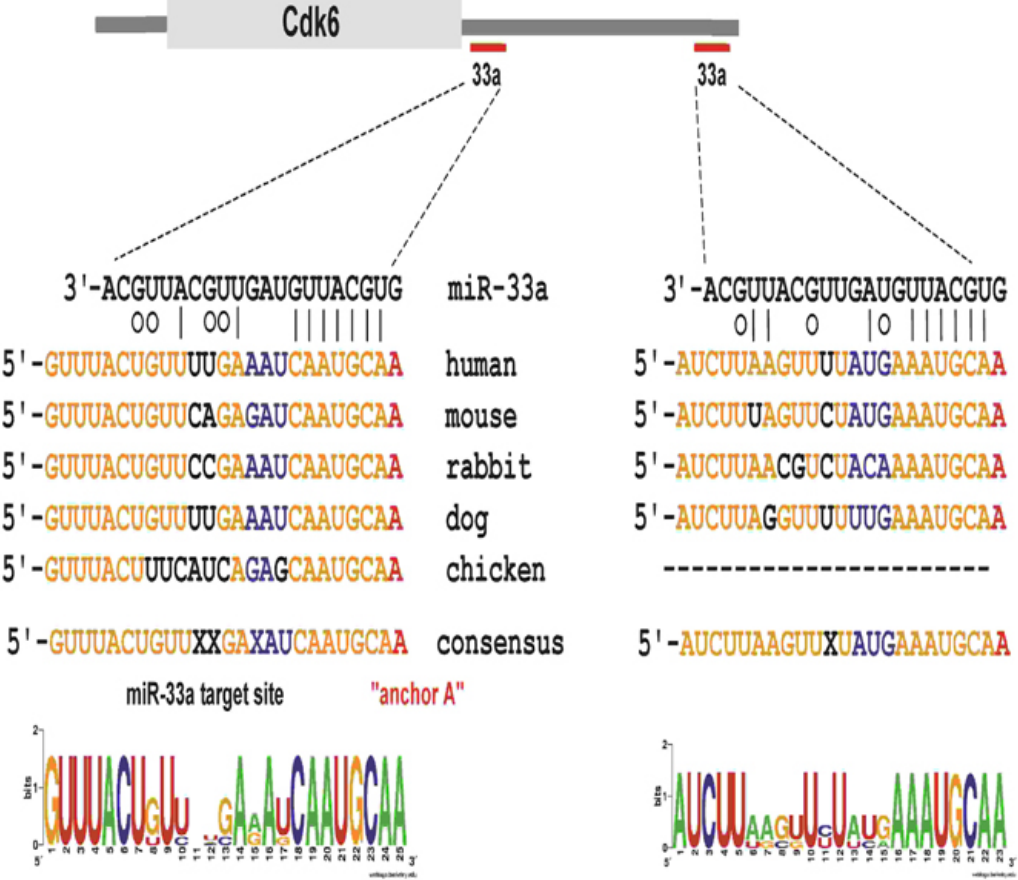
Cdk6
33a
33a
3'-ACGUUACGUUGAUGUUACGUG miR-33a
3'-ACGUUACGUUGAUGUUACGUG
5'-GUUUACUGUUUUGAAAUCAAUGCAA human
5'-AUCUUAAGUUUUAUGAAAUGCAA
5'-GUUUACUGUUCAGAGAUCAAUGCAA mouse
5'-AUCUUUAGUUCUAUGAAAUGCAA
5'-GUUUACUGUUCCGAAAUCAAUGCAA rabbit
5'-AUCUUAACGUCUACAAAAUGCAA
5'-GUUUACUGUUUUGAAAUCAAUGCAA dog
5'-AUCUUAGGUUUUUUGAAAUGCAA
5'-GUUUACUUUCAUCAGAGCAAUGCAA chicken
5'-GUUUACUGUUXXGAXAUCAAUGCAA consensus
5'-AUCUUAAGUUXUAUGAAAUGCAA
miR-33a target site
"anchor A"
bits

Fig. S2

A

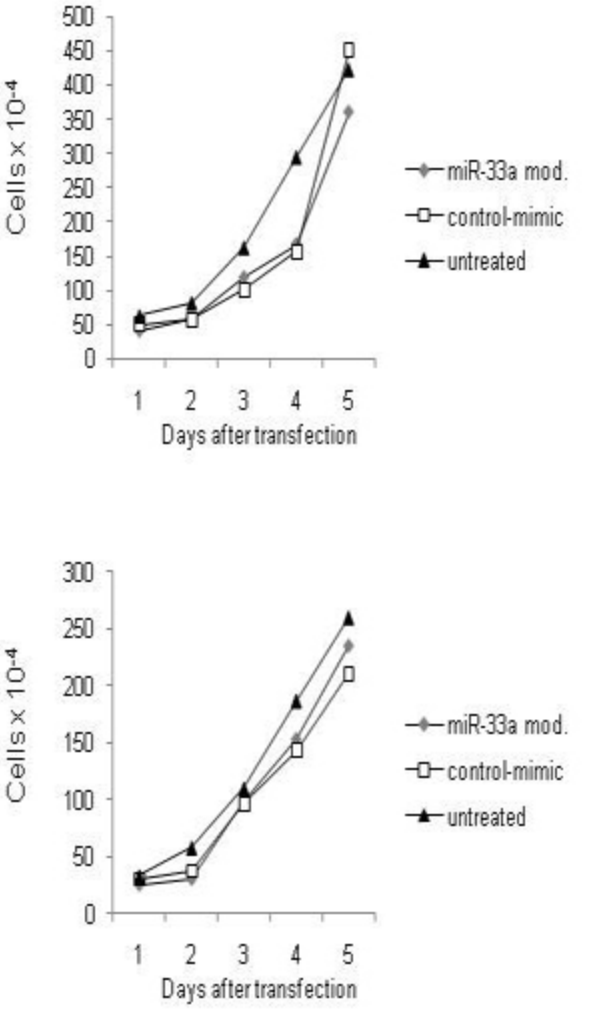
Cells x 10-4
500
450
400
350
300
250
200
150
100
50
0
1
2
3
4
5
Days after transfection
miR-33a mod.
control-mimic
untreated
Cells x 10-4
300
250
200
150
100
50
0
1
2
3
4
5
Days after transfection
miR-33a mod.
control-mimic
untreated

B

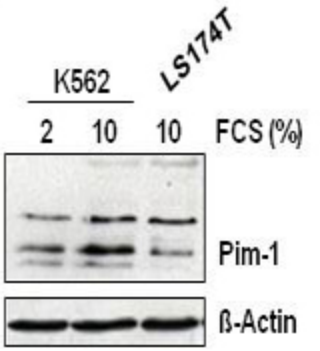
K562
LS174T
2
10
10
FCS (%)
Pim-1
ß-Actin

Fig. S3

A

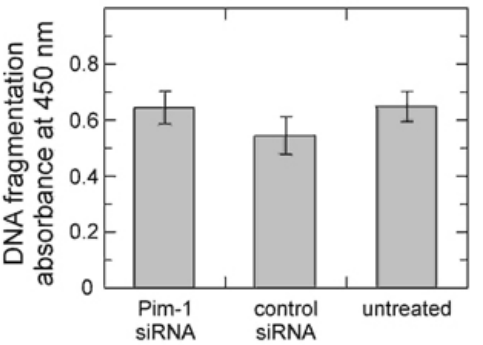
DNA fragmentation absorbance at 450 nm
0
0.2
0.4
0.6
0.8
Pim-1 siRNA
control siRNA
untreated

B

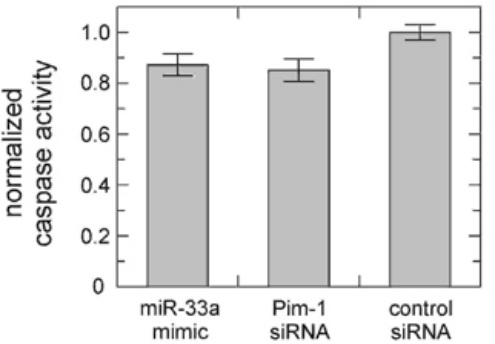
normalized caspase activity
0
0.2
0.4
0.6
0.8
1.0
miR-33a mimic
Pim-1 siRNA
control siRNA

Fig. S4

B. Publication II

MicroRNA Replacement Therapy for miR-145 and miR-33a Is Efficacious in a Model of Colon Carcinoma.

Cancer Res (2011), *71*, 5214-5224

Impact Factor: 7.86*

**2011 Journal Citation Reports* (Thomson Reuters, 2012)

Author contributions:

Research design: 5 %

Experimental work: 5 %

Data analysis and evaluation: 5 %

Manuscript writing: 5 %

Published OnlineFirst June 20, 2011; DOI:10.1158/0008-5472.CAN-10-4645

Therapeutics, Targets, and Chemical Biology

Cancer Research

MicroRNA Replacement Therapy for miR-145 and miR-33a Is Efficacious in a Model of Colon Carcinoma

Ahmed Fawzy Ibrahim[1], Ulrike Weirauch[1], Maren Thomas[2], Arnold Grünweller[2], Roland K. Hartmann[2], and Achim Aigner[1]

Abstract

MicroRNAs (miRNA) aberrantly expressed in tumors may offer novel therapeutic approaches to treatment. miR-145 is downregulated in various cancers including colon carcinoma in which *in vitro* studies have established proapoptotic and antiproliferative roles. miR-33a was connected recently to cancer through its capacity to downregulate the oncogenic kinase Pim-1. To date, miRNA replacement therapy has been hampered by the lack of robust nonviral delivery methods for *in vivo* administration. Here we report a method of miRNA delivery by using polyethylenimine (PEI)-mediated delivery of unmodified miRNAs, using miR-145 and miR-33a to preclinically validate the method in a mouse model of colon carcinoma. After systemic or local application of low molecular weight PEI/miRNA complexes, intact miRNA molecules were delivered into mouse xenograft tumors, where they caused profound antitumor effects. miR-145 delivery reduced tumor proliferation and increased apoptosis, with concomitant repression of c-Myc and ERK5 as novel regulatory target of miR-145. Similarly, systemic injection of PEI-complexed miR-33a was validated as a novel therapeutic targeting method for Pim-1, with antitumor effects comparable with PEI/siRNA-mediated direct *in vivo* knockdown of Pim-1 in the model. Our findings show that chemically unmodified miRNAs complexed with PEI can be used in an efficient and biocompatible strategy of miRNA replacement therapy, as illustrated by efficacious delivery of PEI/miR-145 and PEI/miR-33a complexes in colon carcinoma. *Cancer Res; 71(15); 5214–24. ©2011 AACR.*

Introduction

MicroRNAs (miRNA) are highly conserved, small 17 to 25 nucleotide (nt) noncoding RNA molecules which specifically interact with target mRNAs, thus inhibiting translation or leading to mRNA cleavage and degradation (1). It is estimated from *in silico* analyses that miRNAs can control the expression of approximately 30% of all proteins in humans (2), and it has become clear that miRNAs regulate various cellular processes. Many miRNAs are aberrantly expressed in pathologies such as cancer, leading to the identification of "miRNA signatures" characteristic of certain tumors (3). Tumor-specific miRNA expression profiles are also functionally relevant because many miRNAs act as tumor suppressors or, to the contrary, as oncogenes (oncomiRs). For many miRNAs, target genes have been identified which are relevant in tumorigenesis, tumor growth, tumor angiogenesis, and metastasis (see ref. 4 for review). Crucial for miRNA specificity is the "seed region" (nt 2–8); however, owing to this limited sequence, complementarity miRNAs are capable of simultaneously targeting different genes. In fact, it is estimated that some miRNAs may have more than 100 target genes. This translates into a complex pattern of control of gene expression and suggests potentially increased efficacies of miRNAs by acting through different genes and pathways.

The observation of pathologically decreased levels of certain miRNAs acting as tumor suppressors has led to the concept of miRNA replacement therapy. Indeed, the reintroduction of miR-26a in a liver cancer mouse model by using an adeno-associated viral vector resulted in the inhibition of cancer cell proliferation, induction of tumor-specific apoptosis, and protection from disease progression (5). In line with this, the adenovirus-mediated delivery of a plasmid coding for miRNA let-7 reduced lung tumor formation in an orthotopic lung cancer mouse model (6). Likewise, intranasal administration of a lentiviral let-7 miRNA construct led to reduced tumor burden in an autochthonous non–small cell lung carcinoma tumor mouse model (7). This study also explored synthetic, formulated let-7 oligonucleotides which, upon intratumoral (i.t.) injection, led to reduced tumor growth (7). Local and/or systemic delivery in non–small lung cancer xenografts showed antitumor effects upon application of miR-34 formulated with a lipid-based delivery reagent (8). The

Authors' Affiliations: [1]Institute of Pharmacology, Faculty of Medicine; and [2]Institute of Pharmaceutical Chemistry, Philipps-University, Marburg, Germany

Note: Supplementary data for this article are available at Cancer Research Online (http://cancerres.aacrjournals.org/).

A.F. Ibrahim and U. Weirauch contributed equally to the work.

Corresponding Author: Achim Aigner, Institute of Pharmacology, Faculty of Medicine, Philipps-University Marburg, Karl-von-Frisch-Strasse 1, D–35032 Marburg, Germany. Phone: 49-6421-286-2262; Fax: 49-6421-286-5600; E-mail: aigner@staff.uni-marburg.de

doi: 10.1158/0008-5472.CAN-10-4645

©2011 American Association for Cancer Research.

Downloaded from cancerres.aacrjournals.org on March 7, 2013
Copyright © 2011 American Association for Cancer Research

Published OnlineFirst June 20, 2011; DOI:10.1158/0008-5472.CAN-10-4645

same miRNA exhibited survivin downregulation and reduced metastatic tumor load in the lung when delivered in a liposomal nanoparticle formulation (9). In prostate tumors initiated in the bones of mice, intravenously (i.v.) injected atelocollagen-complexed miR-16 mimics led to reduced tumor growth (10). Finally, in colorectal carcinoma xenografts, i.t. or i.v. injection of miR-143 formulated in cationic liposomes resulted in antitumor effects in the case of modified (for increased nuclease resistance) miR-143, but not unmodified miR-145 (11). This so far limited number of studies that are not based on viruses indicates that applications aiming at miRNA replacement therapy critically depend on the development of miRNA delivery tools. Because viral delivery may raise several issues including potential safety problems because of the application of recombinant DNA, induction of toxic immune responses, and possible changes in gene expression upon random integration of DNA in the host genome, nonviral strategies would be preferable.

Colon carcinoma is the third most common form of cancer and the second leading cause of cancer-related death in the Western world. Despite a favorable prognosis when detected at early stages, it is associated with limited survival when metastatic disease is present, which indicates the need for novel treatment strategies. In colon carcinoma, decreased levels of miRNA-145 are observed (see ref. 12), and previous *in vitro* studies have established a proapoptotic and antiproliferative role of miR-145 (13). In contrast, the functional relevance of miR-33a in cancer has only recently been established. It was shown that miR-33a can repress the proto-oncogene Pim-1 to act as a tumor suppressor inhibiting cell-cycle progression (14). Thus, both miRNA-145 and miR-33a may represent attractive candidates for miRNA replacement therapy that have not been explored so far.

Polyethylenimines (PEI) are linear or branched polymers which are partially protonated under physiologic conditions, thus allowing the formation of complexes with nucleic acids (15). PEIs have been used previously for the delivery of DNA plasmids (15) and other DNA or RNA molecules including ribozymes (16) and siRNAs (17). PEI-based complexes (polyplexes) are able to enter the cells via caveolae- or clathrin-dependent routes and, once internalized, the high efficiency of PEI polyplexes is governed by their facilitated release from endosomes due to the so called "proton sponge effect" (18).

This is the first study to explore the therapeutic effects of PEI/miRNA complexes. We introduce the low molecular weight branched PEI F25-LMW (19, 20) as a delivery platform for nonmodified miRNAs in miRNA replacement therapy and show antitumor effects of PEI/miRNA complexes upon their local or systemic application.

Materials and Methods

miRNAs, siRNAs, tissue culture, and animals

Chemically synthesized miRNAs and siRNAs without modifications were purchased from MWG (Eurofins MWG Operon) or from Thermo Scientific. The used miRNAs represent the double-stranded Dicer processing product as published in miRBase/release14 (21), but lacking the 5′-terminal phosphates. Additional details and sequences can be found in the Supplementary Methods.

All cell lines were obtained from the American type culture collection and authenticated by the vendor. Cells were cultivated in a humidified incubator under standard conditions (37°C, 5% CO_2) in keratinocyte-SFM medium (Invitrogen GmbH) supplemented with 20 to 30 mg/mL bovine pituitary extract, 0.1 to 0.2 ng/mL rEGF, and 10% fetal calf serum (FCS; PAA; 1205LU cells) or IMDM/10% FCS (all other cell lines). Athymic nude mice (nu/nu) were purchased from Harlan Winkelmann and kept at 23°C in a humidified atmosphere with food and water *ad libitum*. Animal studies were done according to the national regulations and approved by the Regierungspräsidium Giessen, Germany.

PEI complexation of RNAs

PEI F25-LMW/miRNA complexes were prepared essentially as described previously for siRNAs (20, 22). Briefly, 10 μg miRNA was dissolved in 75 μL 10 mmol/L HEPES/150 mmol/L NaCl, pH 7.4, and incubated for 10 minutes. Ten microliters of PEI F25-LMW (5 μg/μL) (19) was dissolved in 75 μL of the same buffer, and after 10 minutes, pipetted to the miRNA solution. This resulted in an N/P ratio = 33 which had been determined as optimal for siRNAs (20). For *in vivo* experiments, the mixture was divided into aliquots and stored frozen (23). Prior to use, complexes were thawed and incubated for 1 hour at room temperature. jetPEI complexation was done in 1 mol/L HEPES/150 mmol/L NaCl, pH 7.4 at N/P = 5 as described previously (22).

miRNA tissue uptake *in vivo*

For the radioactive determination of miRNA tissue distribution, 0.6 μg (0.05 nmol) miRNA were [^{32}P] end–labeled at both strands by using T4 polynucleotide kinase (New England Biolabs) and γ-[^{32}P] ATP (GE Healthcare), prior to purification by microspin columns (Bio-Rad) to remove unbound radioactivity and complexation as described above. A total of 1.5×10^6 LS174T cells in 150 μL PBS were injected s.c. into both flanks of athymic nude mice (nu/nu) and grown until they reached a size of approximately 8 mm in diameter. The complexes, or noncomplexed labeled miRNAs as negative control, were dissolved in 200 μL or 100 μL PBS for intraperitoneal (i.p.) or i.v. injection, respectively. After 4 hours, mice were sacrificed, organs were removed, and subjected to RNA preparation as described above. The total RNA was dissolved in 200 μL DEPC-treated water, and 10-μL samples were mixed with loading buffer, heat denatured, and subjected to agarose gel electrophoresis before blotting and autoradiography (Biomax; Eastman-Kodak). Quantitation was done by phosphorimager analysis.

PEI F25-LMW/miRNA treatment in subcutaneous tumor models

Athymic nude mice (Hsd:Athymic Nude-Foxn1^{nu}, 6–8 weeks of age) were used and kept in tight cages with standard rodent chow and water available *ad libitum*, and a 12-hour light/dark cycle. A total of 1.5×10^6 LS174T or HCT116 cells in 150 μL PBS were injected s.c. into both flanks of the mice. When solid

Downloaded from cancerres.aacrjournals.org on March 7, 2013
Copyright © 2011 American Association for Cancer Research

Published OnlineFirst June 20, 2011; DOI:10.1158/0008-5472.CAN-10-4645

tumors were established, mice were randomized into specific treatment, negative control treatment, and nontreatment groups ($n = 12$ tumors per group). Treatment with PEI/miRNA or PEI/siRNA complexes was done by i.p. injection of 0.77 nmol (10 μg) or i.t. injection of 0.3 nmol (4 μg) PEI F25-LMW-complexed specific or nonspecific siRNA at the time points indicated in the figures. Tumor volumes were monitored every 2 to 3 days as indicated in the figures and, upon termination of the experiment, mice were sacrificed and tumors removed. Pieces of each s.c. tumor were immediately fixed in 10% paraformaldehyde for paraffin embedding or snap-frozen for RNA preparation or Western blot analysis.

Proliferation and soft agar assays

For the assessment of anchorage-dependent proliferation, cells were seeded 24 hours prior to transfection in 96-well plates at 1,000 (LS174T) or 300 (HCT-116) cells per well. Transfections were done by the addition of the specific or nonspecific PEI F25-LMW/miRNA or jetPEI/miRNA complexes corresponding to 10 pmol miRNA per well. At the time points indicated, the numbers of viable cells in 8 wells were determined by using a colorimetric assay according to the manufacturer's protocol (Cell Proliferation Reagent WST-1; Roche).

Anchorage-independent proliferation was studied in soft agar assays essentially as described previously (24). A total of 1×10^5 cells per well were transfected in 6-well plates with 100 nmol/L PEI-complexed miRNAs or nonspecific control siRNA and 24 hours after transfection, trypsinized and counted. A total of 20,000 cells in 0.35% agar (Bacto Agar; Becton Dickinson) were layered on top of 1 mL of a solidified 0.6% agar layer in a 35-mm dish. Growth media with 2% FCS were included in both layers. After 2 to 3 weeks of incubation, colonies more than 50 μm in diameter were counted by at least 2 independent blinded investigators.

Caspase assay and fluorescein isothiocyanate–Annexin assay

To test for apoptosis *in vitro*, a commercially available bioluminescent caspase-3/7 assay (Caspase-Glo 3/7 assay; Promega) was applied. The Caspase-Glo 3/7 assay was conducted in 96-wells with cells transfected as described above, and luminescence was measured after 1 hour incubation at 27°C in the dark by using a Fluostar Optima reader (BMG Labtec). To normalize for differences in cell densities, a WST-1 assay was carried out in parallel on the same plate, and the results of caspase activity were adjusted to cell numbers of the different cell lines.

To distinguish between early and late apoptosis, a fluorescein isothiocyanate (FITC)–Annexin assay was done (Becton Dickinson). LS174T cells were transfected with 100 nmol/L miRNAs in 6-well plates by using jetPEI as described above. After 120 hours, the cells were harvested by trypsinization, washed twice with cold PBS, and resuspended in 1× binding buffer (0.01 mol/L HEPES (pH 7.4), 140 mmol/L NaCl, and 2.5 mmol/L $CaCl_2$) at a concentration of 10^6 cells/mL. A total of 100 μL of the cell suspension were transferred to a new Eppendorf tube, 5 μL FITC–Annexin and then 5 μL propidium iodide were added, the mixture was gently vortexed and incubated for 15 minutes at room temperature in the dark. Directly before measurement, 400 μL 1× binding buffer was added to the mixture and samples were measured by FACS (FACSCalibur; Becton-Dickinson) within 1 hour.

RNA preparation and quantitative RT-PCR for mRNA and miRNA dectection

Total RNA from tumor cells was isolated by using the Trizol reagent (Sigma) according to the manufacturer's protocol. For tissue homogenization prior to RNA preparation, tissues were mixed with 200 μL Trizol reagent and homogenized. Reverse transcription (RT) by using the RevertAid H Minus First Strand cDNA Synthesis Kit from Fermentas and quantitative PCR in a LightCycler from Roche by using the QuantiTect SYBR Green PCR kit (Qiagen) were done according to the manufacturers' protocols and as described previously (20). To normalize for equal cDNA amounts, PCR reactions with ERK5-specific and with actin-specific primer sets were run in parallel for each sample, and ERK5 levels were determined by the formula $2^{CP_{(actin)}}/2^{CP_{(ERK5)}}$ with CP = cycle number at the crossing point (0.3).

To isolate miRNA, the mirVana miRNA isolation kit was used according to the manufacturer's protocol (Applied Biosystems). Adherent cells from a 6-well plate were trypsinized and washed in PBS, prior to adding 300 to 600 μL lysis binding buffer and vigorous vortexing. In case of tumor tissue, the lysis binding buffer was added as 10 volumes of the tumor weight. For miRNA RT, specific stem-looped RT primers were used as described previously (25). The RT product was diluted 1:10 in nuclease-free water and used as a template for quantitative real-time PCR (see Supplementary Methods for primer sequences) under the following conditions: 95°C for 15 minutes followed by 55 cycles comprising 95°C for 10 seconds, 55°C for 10 seconds, and 72°C for 10 seconds. Levels were determined as described above.

Western blots and immunohistochemistry

LS174T cells from 6-well plates were scraped at 96 hours posttransfection, lysed in 200 μL denaturating lysis buffer, and sonicated for 20 seconds, prior to incubation on ice for 30 minutes and centrifugation at 13,000 rpm for 25 minutes. Tumor tissue was homogenized in radioimmunoprecipitation assay buffer [25 mmol/L Tris-HCl (pH 7.6), 150 mmol/L NaCl, 1% NP-40, 1% sodium deoxycholate, 0.1% SDS] by using a Dounce homogenizer. After centrifugation and determination of the protein concentration in the supernatant, samples were analyzed by Western blotting (see Supplementary Methods for details).

Immunohistochemical staining of paraffin-embedded sections for proliferating cell nuclear antigen (PCNA) was done essentially as described previously (ref. 20; see Supplementary Methods for details). For the assessment of proliferation, the PCNA staining intensity after diaminobenzidine development was evaluated in at least 5 fields per section by rating as 0 (no staining), 1 (weak staining), 2 (intermediate staining), and 3 (strong staining), and expressed as PCNA score.

Downloaded from cancerres.aacrjournals.org on March 7, 2013
Copyright © 2011 American Association for Cancer Research

Published OnlineFirst June 20, 2011; DOI:10.1158/0008-5472.CAN-10-4645

ELISA

For the quantitation of Pim-1 by sandwich ELISA, the "Pim-1 Total Antibody Pair" and buffers (Invitrogen) were used. The procedure was done according to manufacturer's protocol (see Supplementary Methods), with 100 μL supernatant from a tumor sample (homogenized in PBS and centrifuged at 13,000 rpm) being analyzed per well.

Statistics

Statistical analyses were done by Student's *t* test, 1-way ANOVA/Tukey's multiple comparison posttests or 2-way ANOVA/Bonferroni posttests by using GraphPad Prism4, and significance levels were *, $P < 0.05$, **, $P < 0.01$, ***, $P < 0.001$, #, not significant.

Results

Analysis of miR-145 levels in tumor cells

Levels of miR-145 were assessed in various tumor cell lines and compared with the nontumor fibroblast cell line NIH/3T3 (Supplementary Fig. S1). Although our data confirm previous studies about the downregulation of miR-145 in tumors (12, 26, 27), we also show that miR-145 levels depend on the cell line. This is particularly true for prostate carcinoma cells with levels being very low in DU-145 cells, whereas in PC-3 cells, almost normal levels were observed. Likewise, 1205LU melanoma cells showed high miR-145 expression almost in the range of nontumor cells. Notably, all 7 colon carcinoma cell lines tested displayed low miR-145 levels, indicating that miR-145 downregulation is a general feature in colon carcinoma and relevant to the pathologic state of such tumors. For subsequent experiments, the tumorigenic colon carcinoma cell line LS174T and the particularly aggressive cell line HCT-116 were selected.

PEI-mediated miRNA delivery *in vitro*

To explore whether PEI is able to deliver miRNAs into cells, PEI complexes based on linear jetPEI or branched PEI F25-LMW were prepared. Transfection of LS174T cells with PEI/miRNA complexes led to more than 10-fold increase in intracellular miR-145 levels, indicating that the intact miRNA is efficiently delivered into the cells (Fig. 1A). JetPEI was used in these experiments, because *in vitro*, it displays higher transfection efficacy in this cell line than the branched PEI F25-LMW (data not shown). More importantly, PEI-mediated miRNA transfection led to markedly more than 60% reduced cell proliferation as compared with nontransfected or negative control transfected cells (Fig. 1B). As negative control, a small dsRNA molecule with length, structure, and GC content similar to that of the miRNAs studied here and directed against an irrelevant gene (luciferase) was employed, and complexed with PEI under identical conditions. The specific inhibition of cell proliferation confirms the biological relevance of miR-145 in colon carcinoma cells *in vitro* and shows that PEI-complexed miRNAs are functionally active. Results were confirmed in soft agar assays which monitor anchorage-independent cell growth. Again, a marked reduction in cell proliferation, as indicated by fewer and smaller colonies, was observed upon PEI-mediated miRNA delivery (Fig. 1C). The comparison between nontransfected and negative control transfected cells also shows the absence of nonspecific PEI effects on proliferation (Fig. 1B and C).

The tumor cell inhibition resulting from the PEI-mediated miR-145 delivery was studied in more detail on the cellular and molecular level. In a fluorescence-activated cell sorting (FACS)-based FITC–Annexin assay, a more than 2-fold increase in early-stage and late-stage apoptotic cells was observed upon PEI/miR-145 treatment as compared with negative controls (Fig. 1D). The parallel increase in caspase-3/-7 activation (Fig. 1E) indicated that this induction of apoptosis relied on a caspase-3/-7–dependent pathway. In addition, PEI/miR-145 treatment interfered with downstream signal transduction relevant to proliferation. More specifically, a decrease in ERK5 protein expression was observed; a parallel reduction in ERK5 mRNA levels was less pronounced and lacked statistical significance (Fig. 1F). Although miR-143 (see below) has been shown previously to directly target ERK5 (28), this establishes for the first time that ERK5 is modulated by miR-145 as well.

miR-143 belongs to the same miRNA family as miR-145 and has been shown to be downregulated along with miR-145 in tumors including colon carcinoma (29). Indeed, when monitoring anchorage-independent growth in soft agar assays, PEI-mediated delivery of miR-143 inhibited colony formation similar to miR-145 (Supplementary Fig. S2, right). Anchorage-dependent proliferation, however, was not impaired by miR-143 (Supplementary Fig. S2, left). Thus, whereas miR-143 exerts some tumor cell–inhibiting effects as well, our findings indicate differences between both miRNAs with regard to biological effects and targeted pathways as suggested previously (27). Because of its more universal antitumor effects, miR-145 was selected for subsequent *in vivo* experiments.

Antitumor effects upon systemic application of PEI/miR-145 complexes

LS174T colon carcinoma cells were s.c. injected into athymic nude mice, and upon establishment of tumor xenografts, mice were randomized into treatment and negative control groups. In untreated controls and in mice which were i.p. injected with PEI/nonspecific RNA complexes as negative controls, rapid tumor growth was detected, with an approximately 15-fold increase in tumor volume over 23 days. In contrast, i.p. injection of 10 μg PEI-complexed miR-145 three times per week resulted in a statistically significant, almost 50% decrease in tumor growth (Fig. 2A). Upon termination of the experiment, tumors (see representative examples in Fig. 2A, right panel) were analyzed for ERK5, which has been shown *in vitro* to be downregulated by miR-145 (see above). Indeed, a statistically significant, that is, approximately 50% decrease in ERK5 protein levels was detected in the tumors (Fig. 2B, left), whereas, again comparable with the *in vitro* situation, ERK5 mRNA levels remained largely unchanged (data not shown). This indicates that PEI-delivered miR-145 exerts antitumor effects through inhibition of ERK5 translation. Strikingly, the PEI/miR-145 effects on c-Myc, another

Downloaded from cancerres.aacrjournals.org on March 7, 2013
Copyright © 2011 American Association for Cancer Research

Published OnlineFirst June 20, 2011; DOI:10.1158/0008-5472.CAN-10-4645

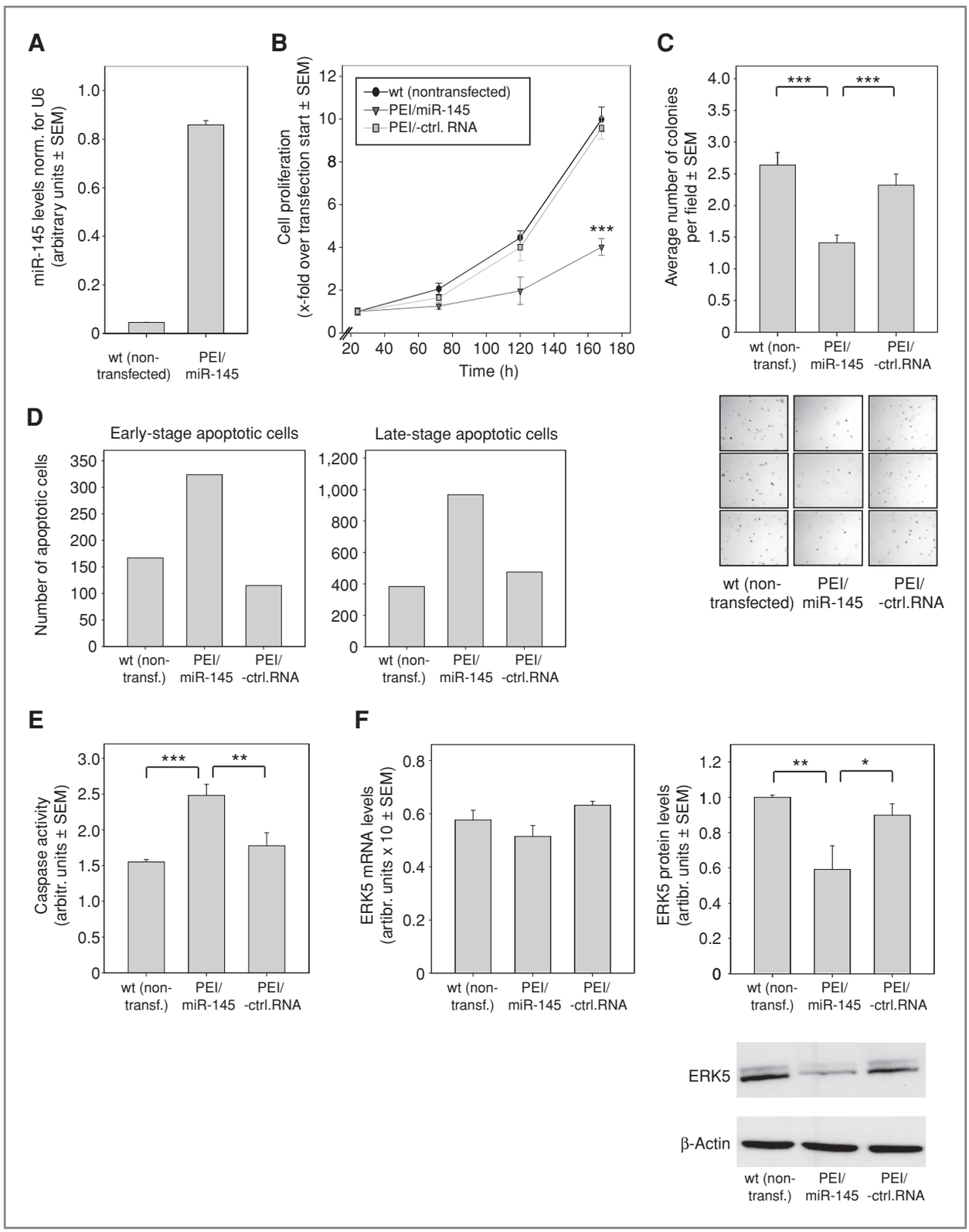

Figure 1. *In vitro* effects of PEI-mediated delivery of miR-145 in LS174T colon carcinoma cells. A, miR-145 levels are markedly upregulated upon PEI/miR-145 transfection as shown by qRT-PCR. PEI/miR-145 transfection reduces anchorage-dependent growth (B) and anchorage-independent soft agar colony formation (C). Increased apoptosis upon PEI-mediated miR-145 delivery is observed, as indicated by early-stage (D) and late-stage (E) apoptotic cells, and by caspase-3/-7 activation (E). ERK5 is established as novel target for miR-145, being downregulated on protein (F, right), but not on mRNA levels (F, left).

Downloaded from cancerres.aacrjournals.org on March 7, 2013
Copyright © 2011 American Association for Cancer Research

Published OnlineFirst June 20, 2011; DOI:10.1158/0008-5472.CAN-10-4645

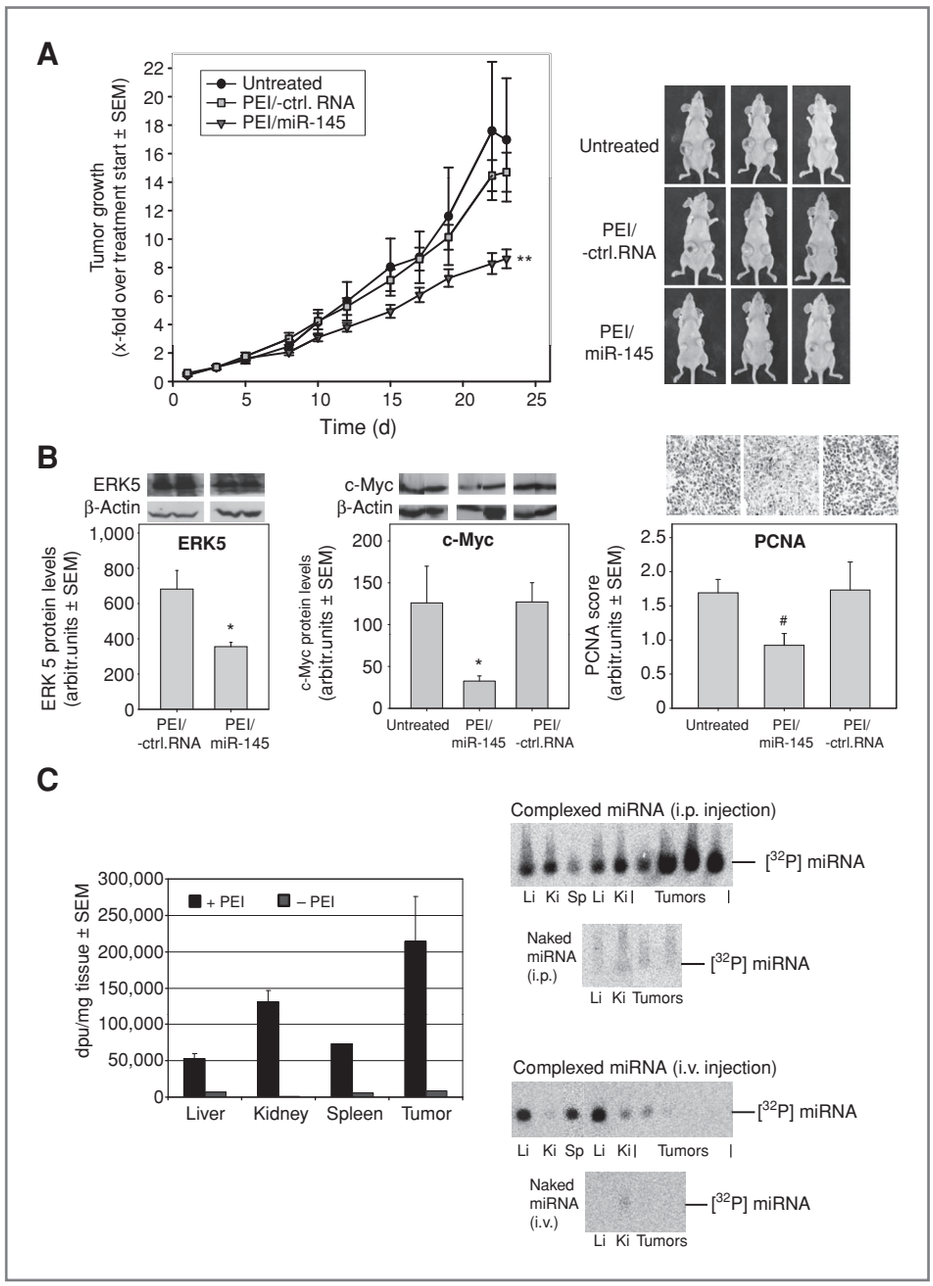

Figure 2. Antitumor effects of PEI/miR-145 treatment in s.c. LS174T colon carcinoma xenograft mouse models. A, systemic injection of PEI/miR-145 complexes results in reduced tumor growth as compared with untreated or PEI/RNA negative control–treated mice. Right: representative examples of mice after termination of the experiment. B, tumor-inhibitory effects of PEI/miR-145 complexes are mirrored by reduced protein levels of ERK5 (left) and c-Myc (middle), and by decreased cell proliferation in the tumor tissue as determined by immunohistochemical staining for PCNA (right). Representative examples of the Western blot data and of the immunohistochemical pictures are given. C, gel electrophoresis and autoradiography of [^{32}P] end–labeled miRNA reveals the delivery of intact full-length miRNA molecules to various tissues including liver (Li), kidney (Ki), spleen (Sp), and tumors (right). Differences in the biodistribution are observed between i.p. (top) and i.v. injection (bottom), with particularly efficient miRNA delivery into tumors upon i.p. administration. The delivery of intact miRNA is dependent on PEI complexation because no signals are observed upon injection of naked [^{32}P] end–labeled miRNAs. Left: quantitation of miRNA levels, on the basis of phosphoimaging, after i.p. injection.

established target for miR-145 (30), were even more profound with approximately 80% decreased c-Myc protein levels as compared with negative controls (Fig. 2B, middle). Concomitantly, an approximately 50% reduction in tumor cell proliferation was observed in the specific treatment group (Fig. 2B, right).

Radioactive biodistribution experiments confirmed that the observed effects were indeed based on the PEI-mediated delivery of intact miRNA molecules. Upon i.p. injection of PEI complexes containing [^{32}P]-labeled miRNA, total RNAs were prepared from tissues and analyzed by gel electrophoresis and autoradiography. This revealed substantial uptake of miRNA in liver and kidney, among others, and to a lesser extent in spleen (Fig. 2C, top right panel). Particularly high levels of intact, full-length miRNA were observed in the tumor xenografts (Fig. 2C, top right panel). In contrast, naked miRNA was detectable, though, at very low levels in the tested tissues, indicating the necessity for miRNA formulation with PEI (Fig. 2C, top right panel). The quantitation of miRNA bands and normalization for protein content confirmed the PEI-mediated miRNA delivery into the xenografts (Fig. 2C, left). To the contrary, i.v. injection resulted in strong signals in liver and spleen, but not in s.c. tumor xenografts, and was thus not employed in our experiments (Fig. 2C, bottom right

Downloaded from cancerres.aacrjournals.org on March 7, 2013
Copyright © 2011 American Association for Cancer Research

Published OnlineFirst June 20, 2011; DOI:10.1158/0008-5472.CAN-10-4645

panel). This also indicates that the mode of administration introduces at least some tissue preference of the complexes, even in the absence of an active ligand-mediated targeting. By comparing the data with naked miRNAs (Fig. 2C, bottom right panel), the i.v. injection also confirmed that the detection of intact miRNAs in a given tissue is dependent on PEI complexation.

Antitumor effects upon local application of PEI/miR-145 complexes

To further explore the therapeutic applicability of PEI/miR-145 complexes, a local treatment regimen was tested next. In these experiments, the particularly tumorigenic colon carcinoma cell line HCT-116 was selected. Pre-experiments *in vitro* confirmed that PEI-mediated delivery of miR-145 exerts antiproliferative effects also in this cell line, as seen by a less profound, although still statistically significant approximately 25% to 30% decrease in colony growth in soft agar assays (Supplementary Fig. S3). Again, the treatment 3 times per week was started after the establishment of tumor xenografts; however, because PEI complexes were applied locally, miRNA amounts were reduced to 4 μg. No unwanted side effects in terms of change in mouse body weight (Supplementary Fig. S4A, right), behavioral alterations or other signs of discomfort were observed. Untreated tumors showed a rapid growth with an approximately 8-fold increase over 2.5 weeks (Fig. 3A). Reduced tumor growth was observed in the PEI/negative control RNA group, indicating some nonspecific effects of the PEI complexes upon local injection (Fig. 3A). A control experiment confirmed the nonspecific reduction of tumor growth also upon injection of naked negative control RNA or PEI alone, indicating the possibility of some local effects of the components of the PEI complexes (Fig. 3B). Notably, however, the i.t. application of

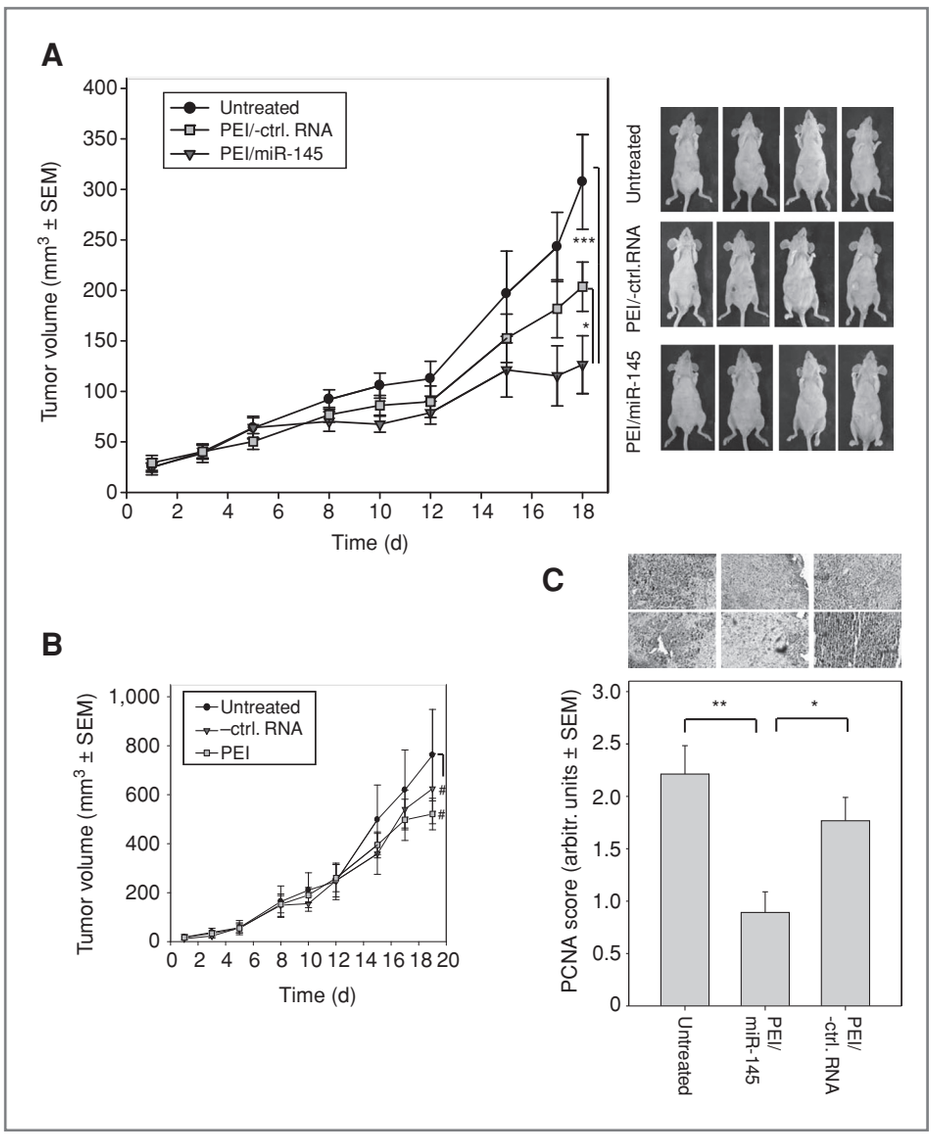

Figure 3. Tumor-inhibitory effects of PEI/miR-145 complexes in s.c. HCT-116 colon carcinoma xenografts upon i.t. injection. A, the local administration leads to some nonspecific effects of PEI/negative control RNA complexes as compared with untreated controls; more profound effects, however, are observed in the PEI/miR-145 treatment group. B, moderate nonspecific reduction of tumor growth upon injection of naked negative control RNA or PEI alone, indicating the possibility of some local effects of the components of the PEI complexes. C, specific antitumor effects are reflected by reduced tumor cell proliferation in the xenografts as determined by immunohistochemical staining for PCNA (right).

Downloaded from cancerres.aacrjournals.org on March 7, 2013
Copyright © 2011 American Association for Cancer Research

Published OnlineFirst June 20, 2011; DOI:10.1158/0008-5472.CAN-10-4645

PEI/miR-145 complexes resulted in a very profound tumor growth inhibition, with tumor volumes in the treatment group being reduced to approximately 40% or 60% of the untreated or negative control–treated tumors, respectively (Fig. 3A). After termination of the experiment, the immunohistochemical analysis of the tumors revealed a marked antiproliferative effect of the PEI/miR-145 treatment (Fig. 3C).

Antitumor effects by systemic administration of PEI/miR-33a complexes

To further substantiate the concept of PEI-mediated miRNA replacement therapy, we selected a second miRNA, miR-33a, which we showed more recently to be relevant in the context of the oncogenic kinase Pim-1 (14). Pim-1 is upregulated in various cancers including lymphoma and colon carcinoma, is a marker of poor prognosis in prostate carcinomas, and has been implicated in early transformation and tumor progression (31, 32). Importantly, Pim-1 is negatively regulated by miR-33a. Luciferase assays based on reporter constructs comprising the luciferase gene and the Pim-1 3′-UTR (untranslated region) revealed a direct effect of miR-33a on the Pim-1 3′-UTR, as indicated by a approximately 50% inhibition of luciferase activity (Supplementary Fig. S5A, left panel). This effect was abolished upon miR-33a seed mutagenesis in the reporter construct (Supplementary Fig. S5A, right panel), confirming the specificity of this effect. So far, miR-33a has only been implicated with posttranscriptional repression of the ATP-binding cassette transporter A1 (ABCA1) resulting in inhibition of cholesterol efflux from macrophages and maintenance of cholesterol homeostasis (33, 34). However, PEI-based *in vitro* transfection of miR-33a resulted in decreased cell proliferation in colon carcinoma cells, comparable with PEI/siRNA-mediated Pim-1 knockdown (Supplementary Fig. S5B). Thus, this establishes an antiproliferative role of miR-33a and makes it an attractive candidate miRNA for replacement therapy.

To assess the therapeutic antitumor activity of miR-33a *in vivo*, mice bearing s.c. LS174T tumor xenografts were treated by i.p. injection of PEI/miR-33a complexes. The systemic PEI/miR-33a treatment starting upon establishment of the tumors at day 7 after cell injection resulted in a statistically significant, that is, approximately 40% reduction of tumor growth as compared with negative control PEI/RNA-treated mice (Fig. 4A). Similar results were obtained upon PEI-mediated delivery of a Pim-1–specific siRNA (Fig. 4B; see Fig. 4C for representative mice). Concomitantly, the analysis of the tumors upon termination of the experiment revealed an approximately 40% downregulation of Pim-1 in both treatment groups (Fig. 4D). The analysis of the mouse body weights during the whole treatment period revealed no changes (Supplementary S4A, left), and no other unwanted side effects in terms of behavioral alterations or other signs of discomfort were observed. Upon termination of the experiment, the determination of TNFα serum levels showed no induction of TNFα, indicating the absence of an immune response upon PEI/miRNA treatment (Supplementary Fig. S4B). Likewise, no increase in the activity of the liver enzymes aspartate aminotransferase (AST; Supplementary Fig. S4C, left) or alanine aminotransferase (ALT; Supplementary Fig. S4C, right) were detected, thus confirming the absence of hepatotoxicity.

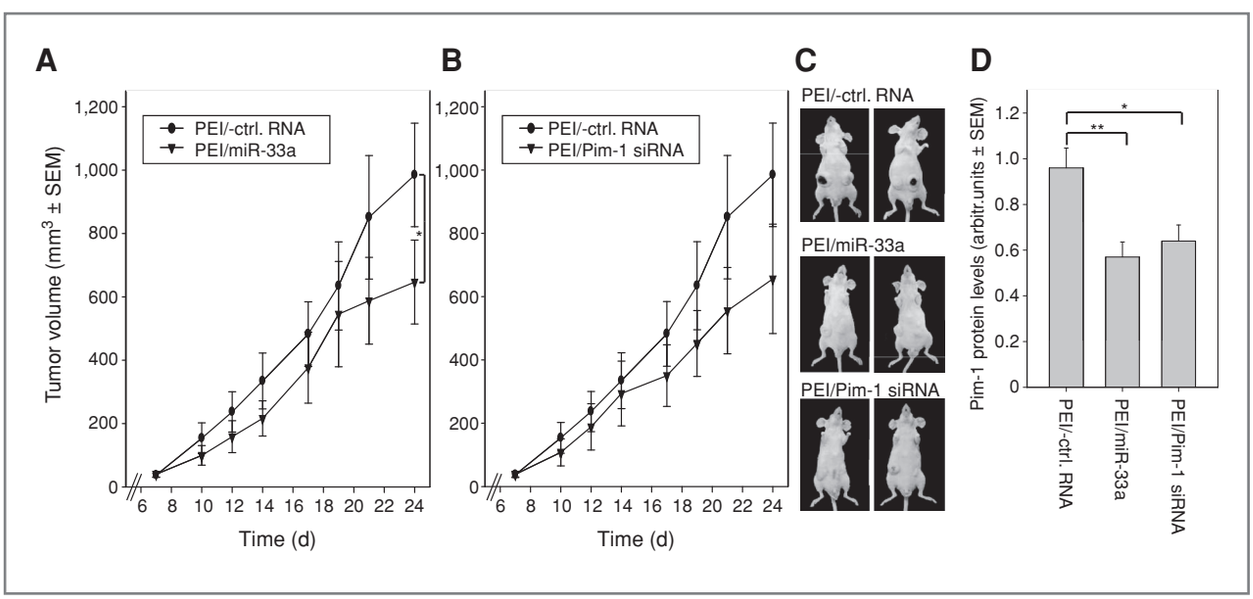

Figure 4. Antitumor effects of systemic PEI/miR-33a treatment in LS174T tumor xenografts as compared with PEI/siRNA-mediated knockdown of Pim-1. A, systemically injected PEI/miR-33a complexes result in inhibition of tumor growth as compared with negative control–treated mice. B, similar antitumor effects are observed upon PEI/siRNA treatment for Pim-1 knockdown. C, representative examples of mice. D, analysis of the tumor xenografts upon termination of the experiment reveals a comparable reduction of Pim-1 levels upon PEI/miR-33a or PEI/Pim-1 siRNA treatment as compared with negative control treatment.

Downloaded from cancerres.aacrjournals.org on March 7, 2013
Copyright © 2011 American Association for Cancer Research

Published OnlineFirst June 20, 2011; DOI:10.1158/0008-5472.CAN-10-4645

Discussion

With the discovery of RNA interference (RNAi), knockdown strategies have gained increasing interest for the specific inhibition of pathologically upregulated genes. More recently, particular miRNAs were found to be aberrantly expressed in several tumors, favoring tumor development (see ref. 3). The functional relevance of miRNA dysregulation is supported by the fact that the repression or reintroduction of a single miRNA is able to substantially contribute to tumorigenesis, tumor progression, and/or tumor metastasis, and can correlate with tumor differentiation, stage, and prognosis (for review, see refs. 4, 35). Thus, in the case of upregulation, miRNAs represent interesting target molecules for inhibition through miRNA antagonists such as antagomiRs or antimiRs (36, 37). However, miRNAs are more frequently downregulated in tumors (38). Although this indicates the usefulness of miRNA replacement therapy, only a very few studies have explored this strategy so far. Although the literature on miRNA functionality suggests that miRNA effects on a given gene may be less pronounced than siRNA-mediated knockdown through RNAi, the major advantage may lie in the fact that a given miRNA targets many, possibly hundreds of genes, and consequently induces more widespread changes in protein expression (39). In fact, it is the inherent mechanism of miRNAs to repress a large number of mRNAs, also in the case of less than 100% complementarity to the mRNA with high specificity. Thus, the therapeutic application of a tumor suppressor miRNA, which is downregulated in tumors, may indeed entail multiple antitumor effects by specifically interfering with several oncogenic pathways, thus making it more difficult for tumor cells to activate escape mechanisms. One feature of this interference is the rather modest effects on any given single gene, which may actually be an advantage because the subtle regulation of genes is the natural mechanism and therefore particularly attractive also from a therapeutic viewpoint.

Our results establish, for the first time, miR-33a as tumor-relevant miRNA suited for miRNA replacement therapy. Although miR-33a was previously shown to repress ABCA1, an important positive regulator of high-density lipoprotein synthesis and reverse cholesterol transport (33, 34), we have recently shown that it is able to repress the proto-oncogene Pim-1, thereby acting as a tumor suppressor (14). Here, we show antitumor effects of miR-33a delivery *in vivo*; however, it will have to be seen if a prolonged treatment may lead to unwanted other effects related to the other functions of miR-33a. Future studies with the goal to identify and verify other miR-33a target genes will help to further scrutinize the suitability of miR-33a for miRNA replacement therapy. To this end, *in silico* predictions are insufficient because we found that, for example Cdk6, although identified by TargetScan 5.1 as another high probability target, is not regulated by miR-33a (14). Consequently, experimental confirmation is always needed to firmly establish any regulatory mechanism of miRNAs. This is also true for miR-145, although several target genes have already been confirmed (see ref. 13), including c-Myc. Notably, we newly identify ERK5, which so far had only been reported as a target for the related miRNA miR-143 (40), as being directly or indirectly regulated by miR-145.

Still, major limitations of siRNA-mediated therapeutic knockdown strategies also apply to miRNAs: their protection upon systemic injection *in vivo*, efficient delivery to the target organ, cellular uptake, and intracellular release into the right compartment. Although certain PEIs have been used previously for the delivery of other nucleic acids including small RNA molecules *in vitro* and *in vivo* (see refs. 41, 42 for review), this article establishes for the first time a PEI-based miRNA replacement therapy. Notably, although several, if not all PEIs are able to complex and protect nucleic acids, efficient PEI/miRNA-mediated gene targeting *in vivo* relies on the sufficient stability of the complexes as well as favorable pharmacokinetic properties and high biocompatibility. Our biodistribution data show the PEI-dependent delivery of unmodified miRNAs into the tumors, where intact full-length miRNAs accumulate. No chemical modifications of the miRNAs are necessary and thus we avoid the term "miRNA mimics" to indicate that it is in fact the naturally occurring miRNA employed here.

The bioactivity and specificity of PEI/miRNA complexes is shown by their antitumor effects and their inhibition of specific targets (i.e., downregulation of c-Myc, ERK5, and Pim-1). The previously observed biocompatibility of PEI F25-LMW–based complexes (20), even upon repeated injection, was confirmed in this study also for PEI/miRNA complexes. Notably, they can be stored frozen for a prolonged time, thus allowing their standardized preparation and injection as efficient and stable ready-to-use formulations without the need of processing prior to administration.

The observed antitumor effects and the fact that no unwanted side effects were detected indicate that the clinically more relevant systemic delivery rather than an only local delivery (i.t. injection) can be pursued.

Interestingly, we observed that PEI-mediated miR-33a delivery versus PEI/siRNA-induced Pim-1 knockdown led to similar antitumor effects. This was true despite the fact that oncogenic lesions commonly result in the simultaneous repression of many miRNAs (ref. 43), suggesting that more than one miRNA might be needed for a successful therapeutic intervention. However, previous studies indicated as well that the delivery of just one miRNA already exerts tumor-inhibitory effects (5–8, 10, 11). Nevertheless, it should be noted that the nonviral delivery of miRNAs through PEI complexes easily allows the combination of several miRNAs, which may result in additive or synergistic effects. This may well lead to the development of more personalized treatment strategies by precisely analyzing miRNA expression profiles in a given tumor prior to selectively combining miRNAs identified as being downregulated.

Although miRNA replacement therapy seems to be rather mild and biocompatible, yet specific and efficient as a therapeutic strategy, it still requires the careful monitoring of unwanted specific or nonspecific effects. On the basis of the rather highly abundant delivery of miRNAs, any miRNA replacement therapy will have to be tested for RISC saturation, competition with other endogenous miRNAs, or

Downloaded from cancerres.aacrjournals.org on March 7, 2013
Copyright © 2011 American Association for Cancer Research

Published OnlineFirst June 20, 2011; DOI:10.1158/0008-5472.CAN-10-4645

overstimulation of a given pathway. Notably, however, the saturation of various cellular factors, which are required for the processing of small RNAs and whose saturation can result in lethal effects (44), is not an issue here because chemically synthesized mature miRNAs do not require cellular processing prior to RISC incorporation. Thus, miRNAs may provide better tools than DNA-based expression systems, as seen already in the case of small RNAs for gene knockdown (45). Still, any off-target effects of miRNA delivery will have to be monitored in preclinical studies. Although, in principal, nonspecific effects are rather unlikely because the applied miRNA is identical to the physiologically occurring one and is thus targeting the same mRNAs (as opposed to siRNAs which do not have natural counterparts), it has also been shown that off-target effects induced by certain sequence motifs of synthetic RNAs can be dose dependent (46). However, the literature on miRNA replacement approaches so far (5, 6, 8, 10), as well as our results even after prolonged treatment, do not support adverse effects. The fact that miRNAs exert only moderate effects on their target genes and are already present and functional under normal physiologic conditions may account for that. This may be particularly true for unmodified miRNAs, which are preferable because they preclude any potentially adverse effects resulting from chemical modification. Even more, however, this requires the development of powerful delivery techniques like PEI complexation which work for unmodified miRNAs.

Taken together, the PEI-based therapeutic application of unmodified miRNAs without any chemical modifications combines several favorable properties: (i) the miRNAs are identical to their naturally occurring counterparts (i.e., they are not just "biosimilars," but "bioidenticals") and, simultaneously, (ii) they are easy to produce via chemical synthesis. Previous studies (iii) have established the biocompatibility of low molecular weight PEIs, which in their linear form are already employed in clinical studies. The fact that (iv) no DNA-based expression constructs are employed, avoids safety issues, for example, related to insertional mutagenesis upon viral or nonviral delivery of DNAs or overloading of the cellular dsRNA processing system, and (v) the ability of miRNAs to target multiple oncogenic pathways predestines them for the therapy of cancer as a "pathway disease" (47).

Disclosure of Potential Conflicts of Interest

No potential conflicts of interest were disclosed.

Acknowledgments

We thank Andrea Wüstenhagen for expert technical assistance.

Grant Support

This work was supported by grants from the German Cancer Aid (Deutsche Krebshilfe, grants 106992 and 109260 to A. Grünweller, R.K. Hartmann, and A. Aigner) and the Deutsche Forschungsgemeinschaft (Forschergruppe 'Nanohale' AI 24/6-1 to A. Aigner), as well as by a Ph.D. fellowship grant from the Youssef Jameel Foundation to A.F. Ibrahim.

The costs of publication of this article were defrayed in part by the payment of page charges. This article must therefore be hereby marked *advertisement* in accordance with 18 U.S.C. Section 1734 solely to indicate this fact.

Received January 3, 2011; revised May 19, 2011; accepted June 1, 2011; published OnlineFirst June 20, 2011.

References

1. Bartel DP. MicroRNAs: genomics, biogenesis, mechanism, and function. Cell 2004;116:281–97.
2. Lewis BP, Burge CB, Bartel DP. Conserved seed pairing, often flanked by adenosines, indicates that thousands of human genes are microRNA targets. Cell 2005;120:15–20.
3. Calin GA, Croce CM. MicroRNA signatures in human cancers. Nat Rev Cancer 2006;6:857–66.
4. Aigner A. MicroRNAs (miRNAs) in cancer invasion and metastasis: therapeutic approaches based on metastasis-related miRNAs. J Mol Med 2011;89:445–57.
5. Kota J, Chivukula RR, O'Donnell KA, Wentzel EA, Montgomery CL, Hwang HW, et al. Therapeutic microRNA delivery suppresses tumorigenesis in a murine liver cancer model. Cell 2009;137:1005–17.
6. Esquela-Kerscher A, Trang P, Wiggins JF, Patrawala L, Cheng A, Ford L, et al. The let-7 microRNA reduces tumor growth in mouse models of lung cancer. Cell cycle 2008;7:759–64.
7. Trang P, Medina PP, Wiggins JF, Ruffino L, Kelnar K, Omotola M, et al. Regression of murine lung tumors by the let-7 microRNA. Oncogene 2010;29:1580–7.
8. Wiggins JF, Ruffino L, Kelnar K, Omotola M, Patrawala L, Brown D, et al. Development of a lung cancer therapeutic based on the tumor suppressor microRNA-34. Cancer Res 2010;70:5923–30.
9. Chen Y, Zhu X, Zhang X, Liu B, Huang L. Nanoparticles modified with tumor-targeting scFv deliver siRNA and miRNA for cancer therapy. Mol Ther 2010;18:1650–6.
10. Takeshita F, Patrawala L, Osaki M, Takahashi RU, Yamamoto Y, Kosaka N, et al. Systemic delivery of synthetic microRNA-16 inhibits the growth of metastatic prostate tumors via downregulation of multiple cell-cycle genes. Mol Ther 2010;18:181–7.
11. Akao Y, Nakagawa Y, Hirata I, Iio A, Itoh T, Kojima K, et al. Role of antioncomirs miR-143 and -145 in human colorectal tumors. Cancer Gene Ther 2010;17:398–408.
12. Slaby O, Svoboda M, Fabian P, Smerdova T, Knoflickova D, Bednarikova M, et al. Altered expression of miR-21, miR-31, miR-143 and miR-145 is related to clinicopathologic features of colorectal cancer. Oncology 2007;72:397–402.
13. Sachdeva M, Mo YY. miR-145-mediated suppression of cell growth, invasion and metastasis. Am J Transl Res 2010;2:170–80.
14. Thomas M, Lange-Grünweller K, Weirauch U, Gutsch D, Aigner A, Grünweller A, et al. The proto-oncogene Pim-1 is a target of miR-33a. Oncogene 2011 (in press).
15. Boussif O, Lezoualc'h F, Zanta MA, Mergny MD, Scherman D, Demeneix B, et al. A versatile vector for gene and oligonucleotide transfer into cells in culture and *in vivo*: polyethylenimine. Proc Natl Acad Sci U S A 1995;92:7297–301.
16. Aigner A, Fischer D, Merdan T, Brus C, Kissel T, Czubayko F. Delivery of unmodified bioactive ribozymes by an RNA-stabilizing polyethylenimine (LMW-PEI) efficiently down-regulates gene expression. Gene Ther 2002;9:1700–7.
17. Urban-Klein B, Werth S, Abuharbeid S, Czubayko F, Aigner A. RNAi-mediated gene-targeting through systemic application of polyethylenimine (PEI)-complexed siRNA *in vivo*. Gene Ther 2005;12:461–6.
18. Behr JP. The proton sponge: a trick to enter cells the viruses did not exploit. Chimia 1997;51:34–6.
19. Werth S, Urban-Klein B, Dai L, Hobel S, Grzelinski M, Bakowsky U, et al. A low molecular weight fraction of polyethylenimine (PEI) displays increased transfection efficiency of DNA and siRNA in fresh or lyophilized complexes. J Control Release 2006;112:257–70.

Downloaded from cancerres.aacrjournals.org on March 7, 2013
Copyright © 2011 American Association for Cancer Research

Published OnlineFirst June 20, 2011; DOI:10.1158/0008-5472.CAN-10-4645

20. Hobel S, Koburger I, John M, Czubayko F, Hadwiger P, Vornlocher HP, et al. Polyethylenimine/small interfering RNA-mediated knockdown of vascular endothelial growth factor *in vivo* exerts anti-tumor effects synergistically with Bevacizumab. J Gene Med 2010;12:287–300.
21. www.mirbase.org.
22. Grzelinski M, Urban-Klein B, Martens T, Lamszus K, Bakowsky U, Hobel S, et al. RNA interference-mediated gene silencing of pleiotrophin through polyethylenimine-complexed small interfering RNAs *in vivo* exerts antitumoral effects in glioblastoma xenografts. Hum Gene Ther 2006;17:751–66.
23. Hobel S, Prinz R, Malek A, Urban-Klein B, Sitterberg J, Bakowsky U, et al. Polyethylenimine PEI F25-LMW allows the long-term storage of frozen complexes as fully active reagents in siRNA-mediated gene targeting and DNA delivery. Eur J Pharm Biopharm 2008;70:29–41.
24. Wellstein A, Lupu R, Zugmaier G, Flamm SL, Cheville AL, Delli Bovi P, et al. Autocrine growth stimulation by secreted Kaposi's fibroblast growth factor but not by endogenous basic fibroblast growth factor. Cell Growth Differ 1990;1:63–71.
25. Chen C, Ridzon DA, Broomer AJ, Zhou Z, Lee DH, Nguyen JT, et al. Real-time quantification of microRNAs by stem-loop RT-PCR. Nucleic Acids Res 2005;33:e179.
26. Motoyama K, Inoue H, Takatsuno Y, Tanaka F, Mimori K, Uetake H, et al. Over- and under-expressed microRNAs in human colorectal cancer. IntJ Oncol 2009;34:1069–75.
27. Arndt GM, Dossey L, Cullen LM, Lai A, Druker R, Eisbacher M, et al. Characterization of global microRNA expression reveals oncogenic potential of miR-145 in metastatic colorectal cancer. BMC cancer 2009;9:374.
28. Clape C, Fritz V, Henriquet C, Apparailly F, Fernandez PL, Iborra F, et al. miR-143 interferes with ERK5 signaling, and abrogates prostate cancer progression in mice. PLoS One 2009;4:e7542.
29. Iio A, Nakagawa Y, Hirata I, Naoe T, Akao Y. Identification of non-coding RNAs embracing microRNA-143/145 cluster. Mol Cancer 2010;9:136.
30. Sachdeva M, Zhu S, Wu F, Wu H, Walia V, Kumar S, et al. p53 represses c-Myc through induction of the tumor suppressor miR-145. Proc Natl Acad Sci U S A 2009;106:3207–12.
31. Bachmann M, Moroy T. The serine/threonine kinase Pim-1. Int J Biochem Cell Biol 2005;37:726–30.
32. Shah N, Pang B, Yeoh KG, Thorn S, Chen CS, Lilly MB, et al. Potential roles for the PIM1 kinase in human cancer - a molecular and therapeutic appraisal. Eur J Cancer 2008;44:2144–51.
33. Najafi-Shoushtari SH, Kristo F, Li Y, Shioda T, Cohen DE, Gerszten RE, et al. MicroRNA-33 and the SREBP host genes cooperate to control cholesterol homeostasis. Science 2010;328:1566–9.
34. Rayner KJ, Suarez Y, Davalos A, Parathath S, Fitzgerald ML, Tamehiro N, et al. MiR-33 contributes to the regulation of cholesterol homeostasis. Science 2010;328:1570–3.
35. Lee YS, Dutta A. MicroRNAs in cancer. Annu Rev Pathol 2009;4:199–227.
36. Elmen J, Lindow M, Schutz S, Lawrence M, Petri A, Obad S, et al. LNA-mediated microRNA silencing in non-human primates. Nature 2008;452:896–9.
37. Krutzfeldt J, Rajewsky N, Braich R, Rajeev KG, Tuschl T, Manoharan M, et al. Silencing of microRNAs *in vivo* with 'antagomirs'. Nature 2005;438:685–9.
38. Lu J, Getz G, Miska EA, Alvarez-Saavedra E, Lamb J, Peck D, et al. MicroRNA expression profiles classify human cancers. Nature 2005;435:834–8.
39. Selbach M, Schwanhausser B, Thierfelder N, Fang Z, Khanin R, Rajewsky N. Widespread changes in protein synthesis induced by microRNAs. Nature 2008;455:58–63.
40. Akao Y, Nakagawa Y, Iio A, Naoe T. Role of microRNA-143 in Fas-mediated apoptosis in human T-cell leukemia Jurkat cells. Leuk Res 2009;33:1530–8.
41. Aigner A. Nonviral *in vivo* delivery of therapeutic small interfering RNAs. Curr Opin Mol Ther 2007;9:345–52.
42. Gunther M, Lipka J, Malek A, Gutsch D, Kreyling W, Aigner A. Polyethylenimines for RNAi-mediated gene targeting *in vivo* and siRNA delivery to the lung. Eur J Pharm Biopharm 2011;77:438–49.
43. Chang TC, Yu D, Lee YS, Wentzel EA, Arking DE, West KM, et al. Widespread microRNA repression by Myc contributes to tumorigenesis. Nat Genet 2008;40:43–50.
44. Grimm D, Streetz KL, Jopling CL, Storm TA, Pandey K, Davis CR, et al. Fatality in mice due to oversaturation of cellular microRNA/short hairpin RNA pathways. Nature 2006;441:537–41.
45. McBride JL, Boudreau RL, Harper SQ, Staber PD, Monteys AM, Martins I, et al. Artificial miRNAs mitigate shRNA-mediated toxicity in the brain: implications for the therapeutic development of RNAi. Proc Natl Acad Sci U S A 2008;105:5868–73.
46. Judge AD, Sood V, Shaw JR, Fang D, McClintock K, MacLachlan I. Sequence-dependent stimulation of the mammalian innate immune response by synthetic siRNA. Nat Biotechnol 2005;23:457–62.
47. Bader AG, Brown D, Winkler M. The promise of microRNA replacement therapy. Cancer Res 2010;70:7027–30.

Downloaded from cancerres.aacrjournals.org on March 7, 2013
Copyright © 2011 American Association for Cancer Research

Supplementary Materials and Methods

MiRNAs, siRNAs and primers for miRNA quantitation

Chemically synthesized miRNAs and siRNAs without modifications were purchased from MWG (Eurofins MWG Operon, Ebersberg, Germany) or from Thermo Scientific (Schwerte, Germany). The used miRNAs represent the double-stranded Dicer processing product as published in miRBase/ release14 (1), but lacking the 5'-terminal phosphates, and had the following sequences:

miR-33a sense strand: 5'-CAAUGUUUCCACAGUGCAUCAC-3´

antisense strand: 5'-GUGCAUUGUAGUUGCAUUGCA-3';

miR-143 sense strand: 5'-GGUGCAGUGCUGCAUCUCUGGU-3';

antisense strand: 5'-UGAGAUGAAGCACUGUAGCUC-3'

miR-145 sense strand: 5'-GUCCAGUUUUCCCAGGAAUCCCU-3';

antisense strand: 5'-GGAUUCCUGGAAAUACUGUUCU-3'

Pim-1 siRNA sense: 5'-GGAACAACAUUUACAACUCdTdT-3';

antisense strand 5'-GAGUUGUAAAUGUUGUUCCdTdT-3´.

An siRNA directed against an irrelevant gene (luciferase) was obtained from Thermo Scientific and used as negative control

sense strand: 5'-CUUACGCUGAGUACUUCGAdTdT-3';

antisense strand: 5'-UCGAAGUACUCAGCGUAAGdTdT-3'.

For miRNA reverse transcription, specific stem-looped RT primers were used as described previously (2). For quantitation, specific forward and universal primers were used:

miR-145 forward: 5'-CGCGCGTTCCAGTTTTCCCAGG-3';

miR-143 forward: CGCGCGTGAGATGAAGCACT-3';

universal reverse PCR primer: 5'-GTGCAGGGTCCGAGGT-3'.

Western blots and immunohistochemistry

Samples containing 100 µg protein were separated by SDS-PAGE (15% polyacrylamide gel) and transferred onto a nitrocellulose membrane (Protran Nitrocellulose Transfer Membrane 0.45 µm Schleicher&Schuell, Dassel, Germany). Membranes were blocked with 5% milk powder in Tris-buffered saline + Tween (TBST; 20 mM Tris, pH 7.5, 150 mM NaCl, and 0.1% Tween-20) and incubated with rabbit polyclonal primary antibodies (anti-c-Myc, 1:500 (Santa Cruz Biotechnology, CA, USA), anti-ERK5, 1:1000 (Cell Signalling), or, as loading control, anti-β-Actin, 1:5000 (Santa Cruz Biotechnology)). The blots were then washed in TBST and incubated for 1 h at RT with a horseradish peroxidase-coupled donkey anti-rabbit IgG secondary antibody (GE Healthcare Bio-Sciences, Uppsala, Sweden), diluted 1:2000 in TBST. After washing in TBST, bound antibodies were visualized by chemiluminescence (ECL SuperSignal West Pico Kit, Thermo Fisher Scientific,

Rockford, IL, USA). Bands were scanned and quantitated using ImageJ (National Institutes of Health, Maryland, USA).

Immunohistochemical staining of paraffin-embedded sections for PCNA was performed essentially as described previously (3). After deparaffinization with xylene and rehydration with graded alcohols, sections were boiled in 1% acetic acid in PBS for 10 min and endogenous peroxidases were inactivated with 0.3% hydrogen peroxide at 4°C for 30 min. After blocking with 10% normal horse serum in PBST/2% BSA for 1 h at RT, the slides were incubated overnight with mouse monoclonal anti-PCNA (proliferating cell nuclear antigen) antibodies (Dako, Hamburg, Germany), diluted 1:200 in PBST, at RT in a wet chamber. For detection, biotinylated goat anti-(mouse-IgG) antibody (Vector Laboratories, Burlingame, CA, 1:500) was applied for 1 h, and immunoreactivity on the sections was visualized using a streptavidin-biotin-peroxidase complex (ABC kit, Vector Laboratories) and the peroxidase substrate diaminobenzidine (brownish colour) according to the manufacturer's instructions.

ELISA

The "Pim-1 Total Antibody Pair" and buffers (Invitrogen) were used and the procedure was performed according to manufacturer's protocol. Round bottom Maxisorp 96-well microtiter plates (Nunc) where coated overnight at 4°C with 100 µl coating antibody, diluted 1:250 in Coating Buffer B. After washing with Washing Buffer and blocking for 1 h at RT with Assay Buffer, 100 µl supernatant from a tumor sample (homogenized in PBS and centrifuged at 13,000 rpm) was added per well, followed by incubation for 2 h at RT. Wells were then washed five times with Washing Buffer prior to addition of 100 µl Pim-1 detection antibody, diluted 1:250 in Assay Buffer, followed by incubation for 1 h at RT. After another five times washing as above, anti-rabbit-IgG-HRP (1:1000 in Assay Buffer) was added and samples were incubated for 30 min at RT. After five times washing, the signal was developed with TMB-substrate (R&D) and after 30 min the reaction was stopped with 2N H_2SO_4. Absorbance was measured in a microplate reader at 450 nm with the reference absorbance at 630 nm.

References

1. www.mirbase.org.

2. Chen C, Ridzon DA, Broomer AJ, Zhou Z, Lee DH, Nguyen JT, *et al.* Real-time quantification of microRNAs by stem-loop RT-PCR. Nucleic Acids Res 2005;33:e179.

3. Hobel S, Koburger I, John M, Czubayko F, Hadwiger P, Vornlocher HP, *et al.* Polyethylenimine/small interfering RNA-mediated knockdown of vascular endothelial growth factor in vivo exerts anti-tumor effects synergistically with Bevacizumab. J Gene Med 2010;12:287-300.

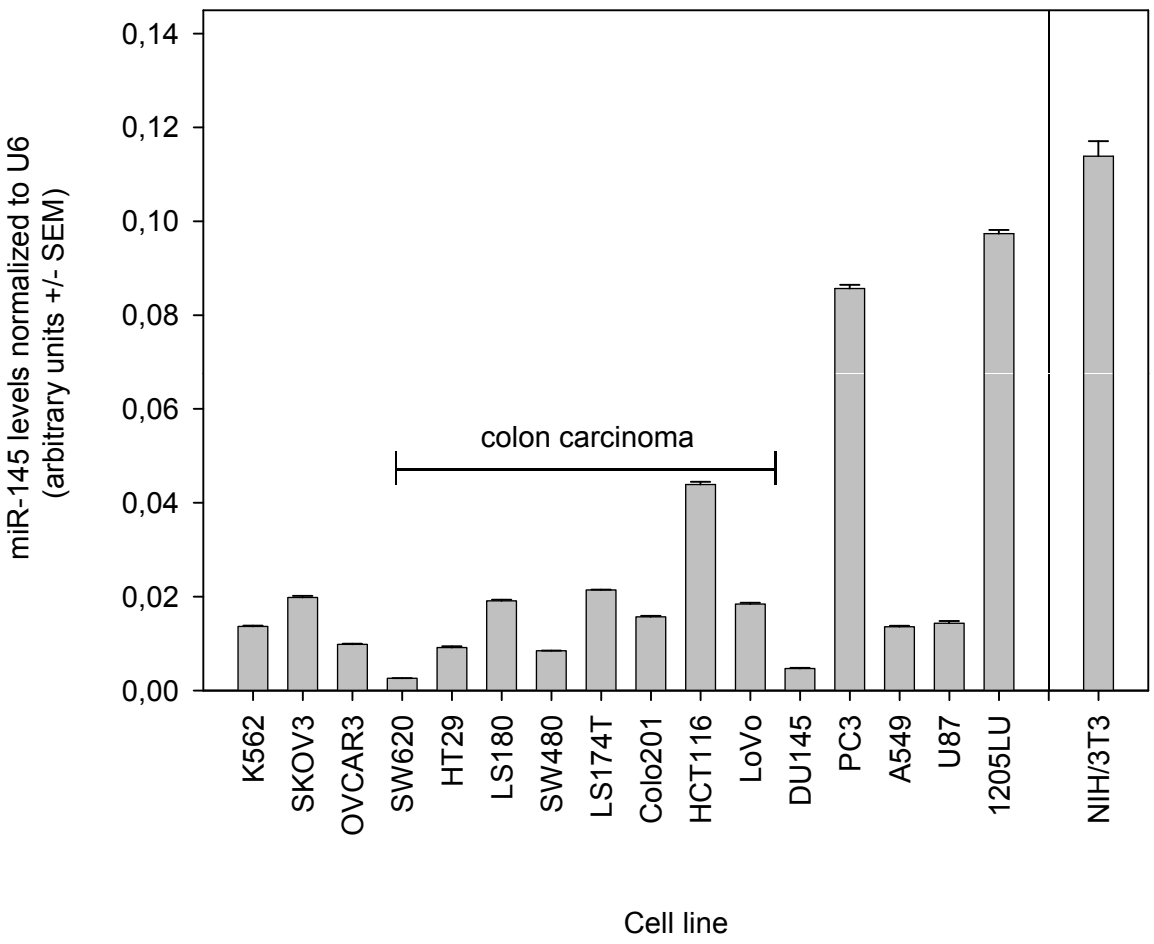

Ibrahim et al., Suppl. Fig. 1 - revised

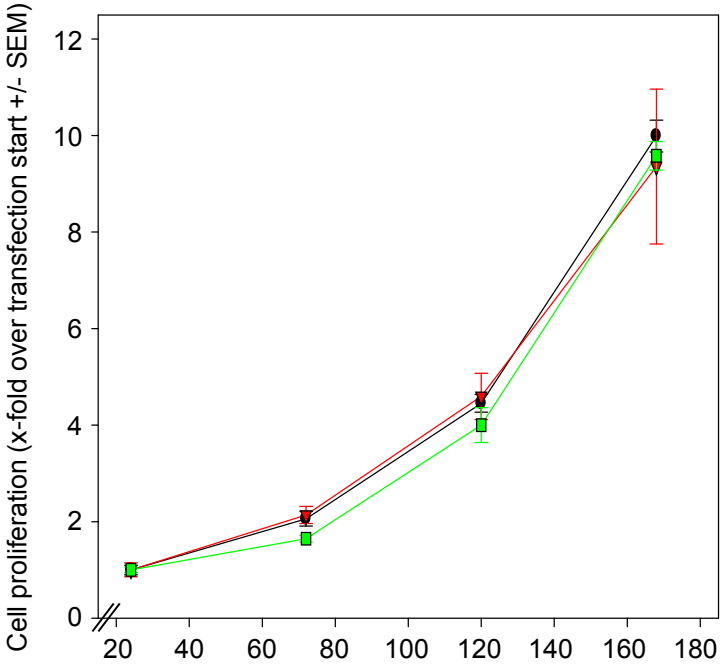

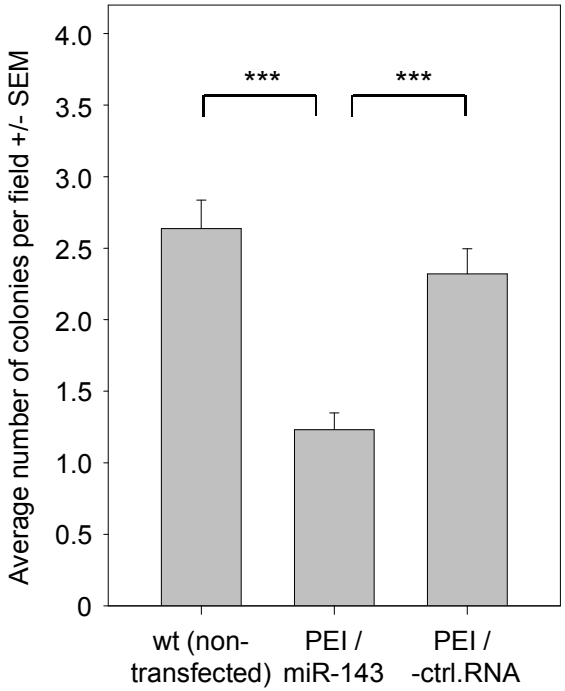

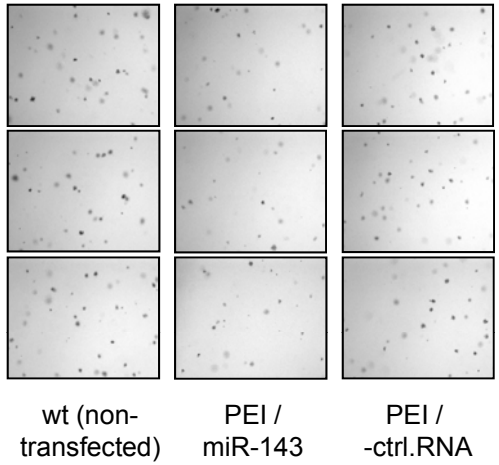

Ibrahim et al., Suppl. Fig. 2 - revised

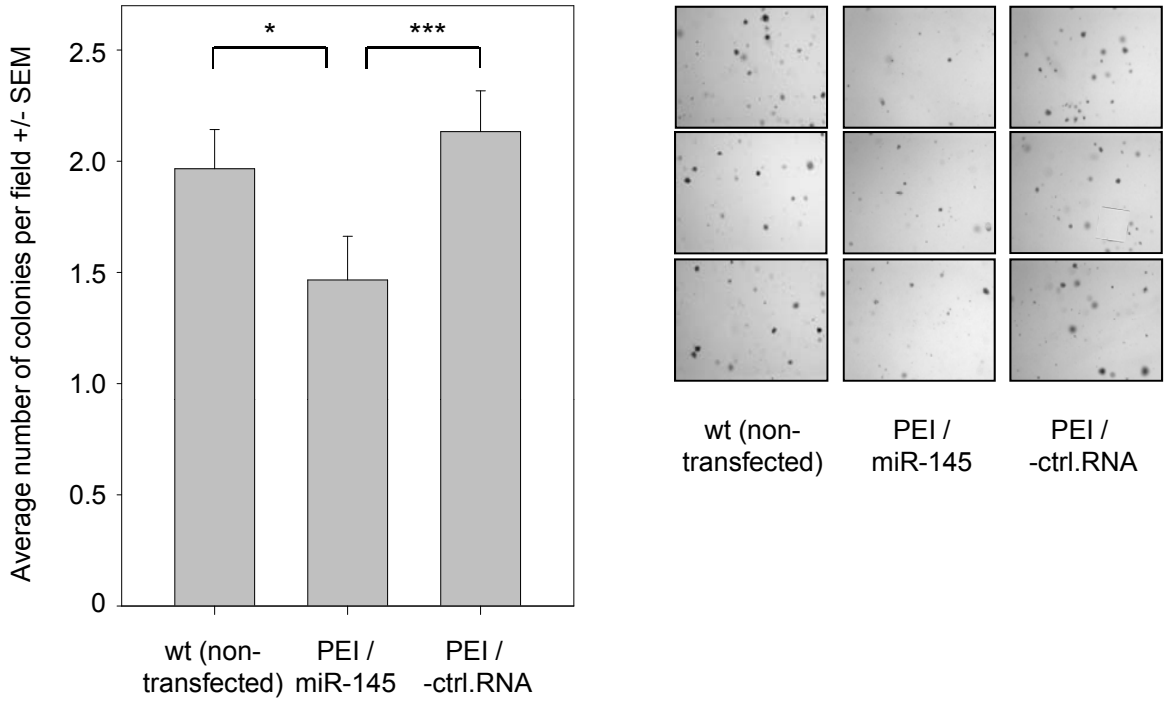

Ibrahim et al., Suppl. Fig. 3 - revised

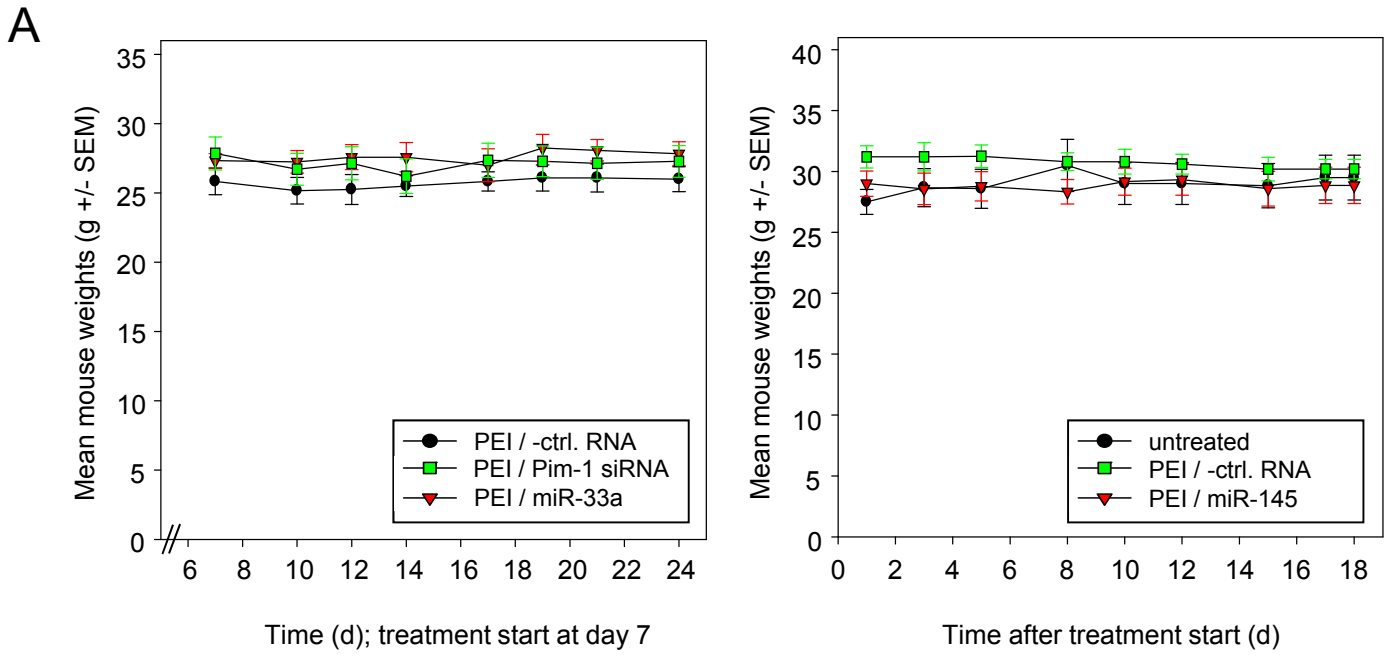

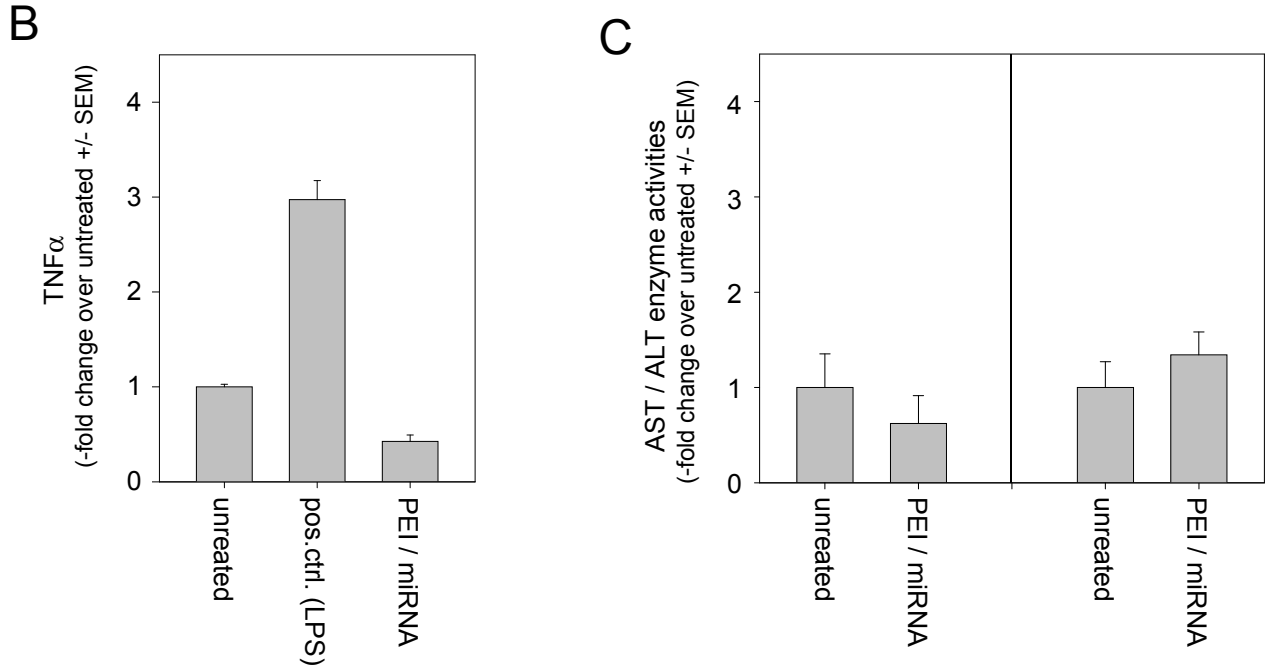

Ibrahim et al., Suppl. Fig. 4 - revised

A

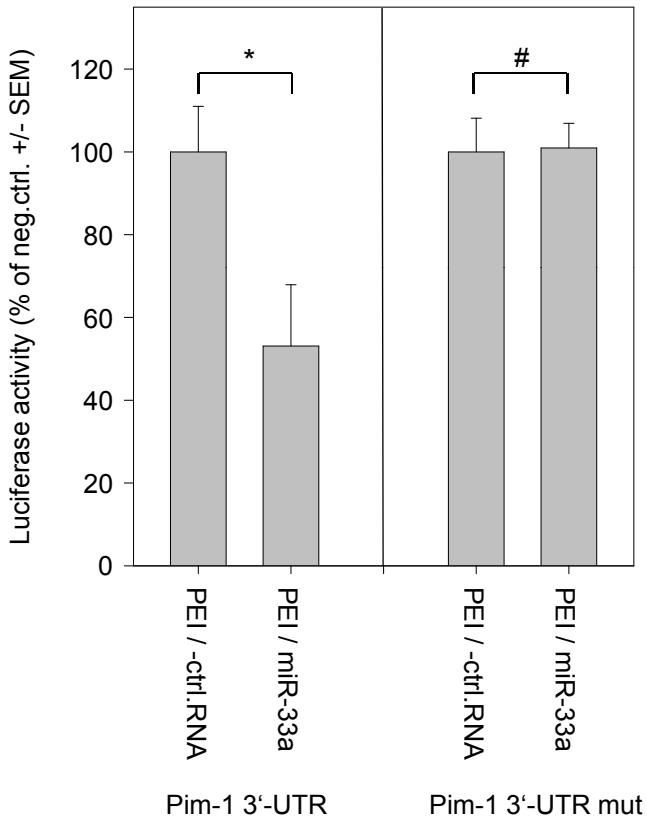

B

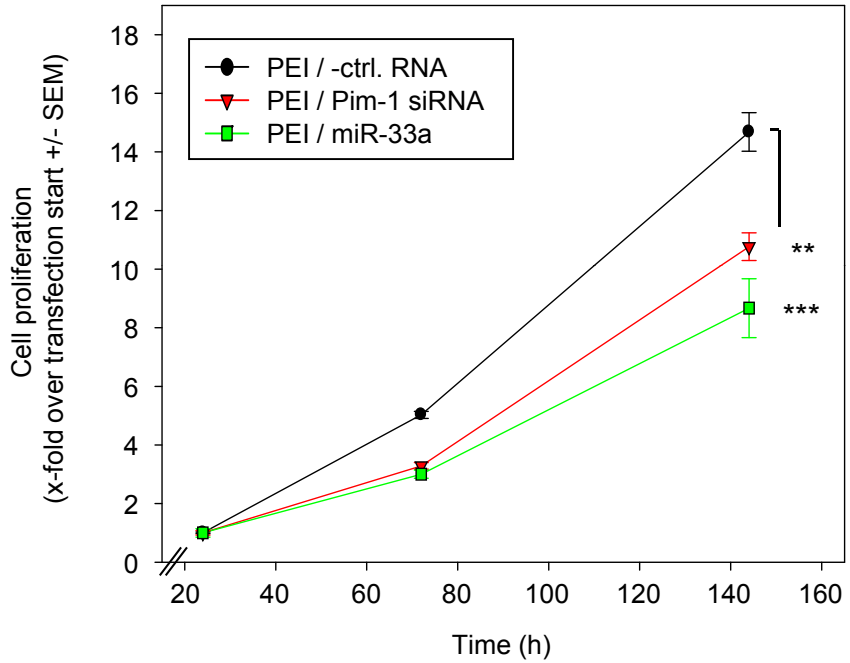

Ibrahim et al., Suppl. Fig. 5 - revised

Suppl. Figure 1. Expression of miR-145 in various tumor cell lines. All eight tested colon carcinoma cell lines display low miR-145 levels as compared to non-tumorous NIH3T3 or some other tumor cell lines.

Suppl. Figure 2. *In vitro* effects of PEI-mediated delivery of miR-143 in LS174T colon carcinoma cells. Upon PEI/miR-143 transfection no inhibition of anchorage-dependent proliferation is observed (A) while anchorage-independent colony formation in soft agar is reduced by ~ 50% (B).

Suppl. Figure 3. Inhibition of anchorage-independent growth of HCT-116 colon carcinoma cells upon PEI-mediated delivery of miR-145, as determined by colony formation in soft agar.

Suppl. Figure 4. Absence of non-specific effects upon PEI/miRNA treatment of mice. (A) Monitoring of tumor weights of mice upon repeated i.p. (left) or i.t. injection (right), referring to the experiments shown in Figs. 4 and 3, respectively, over the whole duration of the treatment. (B) Change in TNFα serum levels at 60 min after PEI/miRNA or lipopolysaccharide (LPS, positive control) treatment, as determined by ELISA according to the manufacturer's protocol (ELISA Development Kits from Preprotech, Rocky Hill, NJ). (C) Changes in the activity of liver enzymes aspartate aminotransferase (AST, SGOT; left) and alanine aminotransferase (ALT, SGPT; right) after four consecutive PEI/miRNA treatments (days 1, 3, 5, 8), as determined by enzyme assays (DiaSys Diagnostic Systems, Holzheim, Germany) 60 min after the last i.p. injections.

Suppl. Figure 5. Tumor cell-inhibitory effects of miR-33a mediated through Pim-1 inhibition. (A) Direct inhibititory effect of miR-33a on the Pim-1 3'-UTR. The transfection of the cells with PEI/miR-33a inhibits luciferase expression in the reporter construct containing the 3'-UTR of Pim-1 (left), but not upon miR-33a seed mutagenesis (right). Luciferase activities were determined 24 h after the co-transfection of 200 ng reporter plasmid and 1 pmol miRNA or negative control RNA into 100,000 LS174T cells in 24-well plates, using 1.5 µl jetPrime (Polyplus). (B) Anti-proliferative effects in anchorage-dependent growth of LS174T cells upon PEI/miR-33a or PEI/Pim-1 siRNA transfection.

C. Publication III

PEI-complexed LNA antiseeds as miRNA inhibitors.

RNA Biology (2012), *9(8)*, 1088-1098

Impact Factor: 5.56*

**RNA Biology (2011), 8(1)*

Author contributions:

Research design: 40 %

Experimental work: 60 %

Data analysis and evaluation: 70 %

Manuscript writing: 30 %

RNA Biology 9:8, 1088-1098; August 2012; © 2012 Landes Bioscience

PEI-complexed LNA antiseeds as miRNA inhibitors

Maren Thomas,[1] Kerstin Lange-Grünweller,[1] Eyas Dayyoub,[2] Udo Bakowsky,[2] Ulrike Weirauch,[3] Achim Aigner,[3] Roland K. Hartmann[1,*] and Arnold Grünweller[1,*]

[1]Institut für Pharmazeutische Chemie, Philipps-Universität Marburg; Marburg, Germany; [2]Institut für Pharmazeutische Technologie und Biopharmazie, Philipps-Universität Marburg; Marburg, Germany; [3]Rudolf-Boehm-Institut für Pharmakologie und Toxikologie, Universität Leipzig; Leipzig, Germany

Keywords: miRNA, miR-17-92, let-7a, antimiR, antiseed, LNA, PEI, p21, cancer

Abbreviations: PO, phosphodiester; 3'-UTR, 3'-untranslated region; LNA, locked nucleic acid; PEI, polyethylenimine; PS, phosphorothioate; PEI F25-LMW, polyethylenimine F25 low molecular weight; RLU, relative light units; FCS, fetal calf serum; WST-1, water soluble tetrazolium salt 1

Antisense inhibition of oncogenic or other disease-related miRNAs and miRNA families in vivo may provide novel therapeutic strategies. However, this approach relies on the development of potent miRNA inhibitors and their efficient delivery into cells. Here, we introduce short seed-directed LNA oligonucleotides (12- or 14-mer antiseeds) with a phosphodiester backbone (PO) for efficient miRNA inhibition. We have analyzed such LNA (PO) antiseeds using a *let-7a*-controlled luciferase reporter assay and identified them as active miRNA inhibitors in vitro. Moreover, LNA (PO) 14-mer antiseeds against ongogenic *miR-17–5p* and *miR-20a* derepress endogenous p21 expression more persistently than corresponding miRNA hairpin inhibitors, which are often used to inhibit miRNA function. Further analysis of the antiseed-mediated derepression of p21 in luciferase reporter constructs - containing the 3'-UTR of p21 and harboring two binding sites for miRNAs of the *miR-106b* family - provided evidence that the LNA antiseeds inhibit miRNA families while hairpin inhibitors act in a miRNA-specific manner. The derepression caused by LNA antiseeds is specific, as demonstrated via seed mutagenesis of the *miR-106b* target sites. Importantly, we show functional delivery of LNA (PO) 14-mer antiseeds into cells upon complexation with polyethylenimine (PEI F25-LMW), which leads to the formation of polymeric nanoparticles. In contrast, attempts to deliver a functional seed-directed tiny LNA 8-mer with a phosphorothioate backbone (PS) by formulation with PEI F25-LMW remained unsuccessful. In conclusion, LNA (PO) 14-mer antiseeds are attractive miRNA inhibitors, and their PEI-based delivery may represent a promising new strategy for therapeutic applications.

Introduction

Small non-coding RNAs (sRNA), such as miRNAs, are involved in the regulation of virtually all essential cellular processes, and their deregulation has important implications in pathogenesis. The impact of miRNAs on human diseases has been well established e.g., in the cancer field (for a review see ref. 1), where several miRNAs are either overexpressed in tumors (oncogenic miRNAs) or show reduced levels (miRNAs with tumor suppressor activity). This results in the downregulation of tumor suppressor genes or in the upregulation of cellular proto-oncogenes, respectively.[2] A well characterized and important cellular tumor suppressor is the cell cycle regulator p21, which is post-transcriptionally regulated by miRNAs of the oncogenic *miR-17–92* cluster.[3] Oncogenic miRNAs or miRNA clusters are often found in chromosomal regions that are amplified in tumor cells, which promotes their overexpression.[4,5] For example, the *miR-17–92* cluster is overexpressed in lymphoma as well as in a wide range of human solid tumors.[6] MiRNAs of this cluster (mainly *miR-17–5p*, *miR-19* and *miR-20a*) inhibit apoptosis, promote proliferation and induce tumor angiogenesis.[7,8]

Several strategies have been developed to block cellular miRNA function, including the use of miRNA sponges, masking of the mRNA target site or inhibition of miRNAs by antisense oligonucleotides (generally termed antimiRs; for a review see ref. 9). For therapeutic intervention the use of antisense strategies against miRNAs has been established in mice and non-human primates.[10,11] However, efficient delivery of antimiRs is still the main bottleneck for therapeutic applications. Several efforts have been made to deliver antimiRs into cells and tissues, e.g., the conjugation of modified antimiRs with cholesterol, which were termed antagomiRs.[12] Moreover, important improvements with regard to antimiR efficacy, stability and delivery have been achieved by the incorporation of modified nucleotides (for a review see ref. 13). In particular, 2'-fluor (2'-F), 2'-oxymethyl (2'-OMe), 2'-methoxyethyl (2'-MOE) and locked nucleic acid (LNA) modifications have been incorporated into antimiRs for in vivo applications. So far, the most efficient variants are 2'-F/2'-MOE mixmers directed against the complete miRNA guide strand,[11,14] 15- or 16-mer LNA/DNA mixmers with 2'-OMe cytosines and a phosphorothioate (PS)[10,15,16] or phosphodiester (PO) backbone,[17] and tiny LNA 8-mers with a PS backbone.[18,19] All these antimiRs

*Correspondence to: Roland K. Hartmann and Arnold Grünweller; Email: roland.hartmann@staff.uni-marburg.de and arnold.gruenweller@staff.uni-marburg.de
Submitted: 12/30/11; Revised: 04/24/12; Accepted: 06/19/12
http://dx.doi.org/10.4161/rna.21165

©2012 Landes Bioscience. Do not distribute

were applied by "gymnotic delivery,"[20] i.e., without any formulation. In contrast, the formulated delivery of unconjugated modified antimiRs into tissues has not been explored so far.

Here we introduce 14-mer LNA (PO) antiseeds as novel miRNA inhibitors that are particularly potent and can inhibit miRNAs for up to 7 d in cell culture. We have further established their complexation with a cationic polymer, the low molecular weight polyethylenimine PEI F25-LMW, to enable delivery into a broader spectrum of organs and tissues. Since we have shown recently that PEI-complexed siRNA or miRNA can be delivered into tumor xenografts leading to antitumor effects in mice,[21,22] it will be promising to explore the therapeutic potential of PEI-complexed LNA (PO) antiseeds.

Results

LNA antiseeds as miRNA inhibitors. The LNA/DNA mixmers used so far, as well as the tiny LNA 8-mers described recently,[19] are generally designed with a phosphorothioate (PS) backbone that is required for unformulated "gymnotic delivery" in vivo.[20] However, gymnotic delivery cannot be applied to all organs and tissues, which is a serious limitation for several therapeutic applications. Here, we explored short LNA antiseeds containing a phosphodiester (PO) backbone. These oligonucleotides are complementary to the 5'-terminal seed (nt 1–8) plus the 4–6 subsequent nucleotides of the mature miRNA strand.

As a first experimental approach, we cloned a *let-7a* target sequence in the functional forward orientation into the 3'-UTR of a luciferase reporter gene; a luciferase reporter gene with an inverted *let-7a* target sequence placed at the same position served as negative control (**Fig. 1A**). To determine the minimum antiseed length for blocking miRNA function, we analyzed the effects of 8-, 10-, 12- and 14-mer all-LNA (PO) antiseeds directed against *let-7a* (**Fig. 1B and C**). The luciferase reporter plasmid and LNA antiseeds at various concentrations (5, 20, 50 and 100 nM) were cotransfected into HeLa cells using lipofectamine and luciferase activity was measured as an indicator for derepression. Cells transfected with the luciferase reporter containing an inverted *let-7a* target site were used as the reference for maximum derepression. The 8- and 10-mer antiseeds showed no or only weak derepression activity, whereas the 12- and the 14-mer antiseeds efficiently derepressed the luciferase reporter (**Fig. 1C**). Next, we compared the derepression activity of the 12- and 14-mer antiseeds with a commercially available miRNA hairpin inhibitor[23] against *let-7a* (Thermo Scientific Dharmacon). Such hairpin inhibitors carry a central single-stranded sequence complementary to the entire mature miRNA strand and are capped on both ends by hairpins consisting of 8-bp stems and apical tetraloops.[23] As negative control, we employed an unrelated all-LNA 14-mer directed against the RNA subunit of RNase P from *E. coli*.[24] When using concentrations less than 10 nM, the 12- and 14-mer antiseeds showed derepression activities comparable to the hairpin inhibitor, with RLU values reaching approx. 60% of those measured for the inverted control (**Fig. 1D**). At 10 nM or 20 nM, however, the hairpin inhibitor partially or completely failed to derepress the luciferase mRNA, respectively, while the LNA antiseeds, and in particular the 14-mer, displayed constant activity between 5 and 20 nM (**Fig. 1D**). In the case of the hairpin inhibitor, concentrations > 20 nM even caused a further drop of luciferase activity to almost zero (0.026 +/- 0.011 or 0.042 +/- 0.018 at 50 or 100 nM, respectively; data not shown). Since cell viability did not seem to be affected by the hairpin inhibitor (data not shown), we speculate that the design of hairpin inhibitors[23] may favor nucleic acid aggregation at higher concentrations when using lipofectamine as the transfection reagent, leading to inefficient cotransfection.

We conclude from our results that 12- and 14-mer LNA antiseeds containing a PO backbone are active miRNA inhibitors with potencies comparable to commercial miRNA hairpin inhibitors (Thermo Scientific Dharmacon) which are often used for miRNA inhibition. In addition, transfection with lipofectamine seems to be more robust with LNA antiseeds than hairpin inhibitors.

Derepression of basal p21 levels in K562 cells. The erythroleukemia cell line K562 expresses the tumor suppressor protein p21 at levels that are barely detectable in western blot analyses, although substantial levels of p21 mRNA are present in these cells as inferred from RT-qPCR analyses (data not shown). This indicates that p21 expression is suppressed on the post-transcriptional level. Recently, it was shown that the p21 mRNA, whose 3'-UTR harbors two conserved binding sites for miRNAs of the *miR-106b* family, is indeed a target for these miRNAs.[3] Of note, the oncogenic *miR-17–92* cluster encoding three members of the *miR-106b* family, namely *miR-17–5p*, *miR-18a* and *miR-20a*, is overexpressed in K562 cells.[21,25] We therefore anticipated that the *miR-106b* family members *miR-17–5p* and *miR-20a* repress endogenous p21 mRNA in K562 cells and tested this by transfecting 14-mer LNA (PO) antiseeds directed against *miR-17–5p* and *miR-20a* into these cells by electroporation. Indeed, both antiseeds caused a substantial increase of p21 protein levels, whereas the all-LNA control 14-mer remained without effect (**Fig. 2**).

Since it was recently shown that LNA antisense effects are rather persistent,[26] we compared the duration of p21 derepression caused by the 14-mer LNA antiseeds 17–5p and 20a with that of the respective hairpin inhibitors. 48 h after transfection, all antisense molecules gave rise to substantial derepression of p21 in K562 cells (**Fig. 2**). However, after 72 h the hairpin inhibitors had substantially lost their capacity to derepress p21, while antiseed 17–5p derepressed p21 for up to 96 h and antiseed 20a for at least 120 h. Even after 168 h a weak derepression of p21 with antiseed 20a was still detectable (**Fig. 2**). Our results on antiseeds are consistent with the long-term effects of LNA antisense molecules described by others.[10,19]

Specificity of the antiseed effect. Next, we analyzed the specificity of derepression effects observed with the 14-mer antiseeds against *miR-17–5p* and *miR-20a* by using luciferase reporter assays. For this purpose, the 3'-UTR of p21 and a mutated version thereof with both seeds inactivated by two point mutations (**Fig. 3A**) were fused to the luciferase coding region. Cotransfection (with lipofectamine) of the luciferase reporter plasmid with one of the antiseeds, 17–5p or 20a, caused a more profound derepression

©2012 Landes Bioscience. Do not distribute

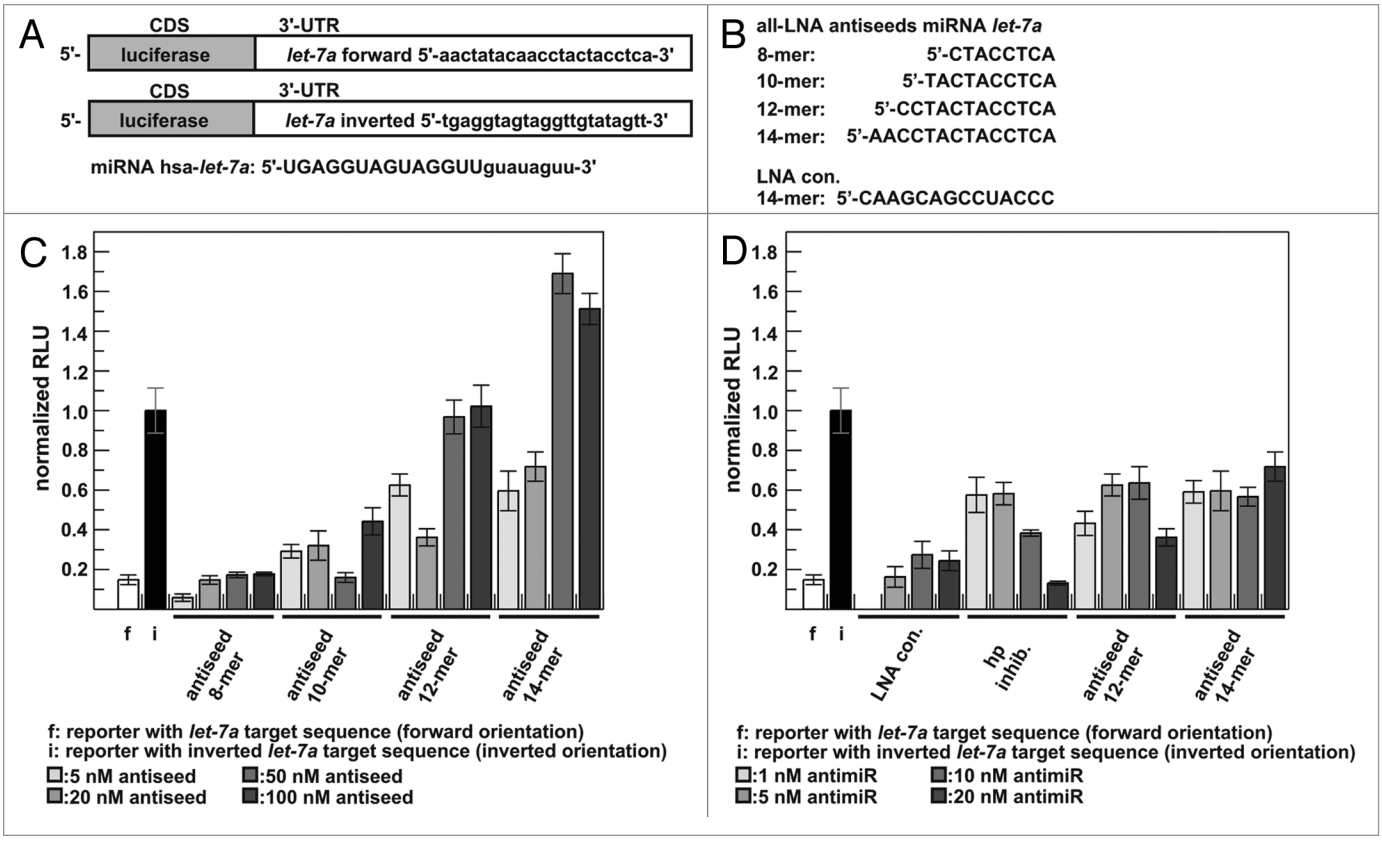

Figure 1. (A) Schematic view of the *let-7a* forward luciferase reporter and the inverted control construct; the target sequence fully complementary to mature miRNA hsa-*let-7a* and the inverted control sequence are depicted (in the sense of the RNA transcript). The sequence of mature miRNA hsa-*let-7a* is shown underneath, with upper case letters indicating the nucleotides targeted by the *let-7a* antiseeds. (B) Sequences of the used antiseeds directed against the 5'-region of miRNA *let-7a* and sequence of the LNA control oligonucleotide directed against bacterial RNase P RNA. (C) Derepression activity of *let-7a* antiseeds (8- to 14-mers) at the indicated concentrations (5–100 nM) in HeLa cells using lipofectamine as transfection agent. Luciferase activity of the control vector harboring the inverted *let-7a* target sequence was set to 1. Values are derived from at least three independent experiments (+/- S.D.). (D) Comparison of LNA 12- and 14-mer antiseeds containing a PO backbone with a hairpin inhibitor (hp inhib.) targeting *let-7a* at the indicated concentrations (1 to 20 nM) in HeLa cells. As control, the unrelated LNA 14-mer (LNA con.) was used. Values are derived from at least three independent experiments (+/- S.D.).

of the p21 reporter than cotransfection with hairpin inhibitor 17–5p or 20a at the same concentration (10 nM; **Fig. 3B**). This stronger derepression activity of the antiseeds as compared with the individual hairpin inhibitors was in line with the results from our western blot experiments (see **Fig. 2**). Next, we compared the derepression activity of an equimolar (each 5 nM) mixture of the two antiseeds with that of a mixture of both hairpin inhibitors. While the combination of the antiseeds did not further increase the derepression activity, the combined application of the two hairpin inhibitors resulted in an enhanced derepression activity that was now comparable to that of the single LNA antiseeds (**Fig. 3B**). This suggests that antiseeds are able to block miRNAs from the same family, while hairpin inhibitors are more specific for individual miRNAs.

As a further control we tested a tiny LNA 8-mer with a PS backbone targeting the seed region of miRNAs from the *miR-106b* family. Recently, it has been shown in cotransfection experiments with lipofectamine that only LNA (PS) 8-mers can derepress a luciferase reporter efficiently, whereas shorter or longer LNA (PS) oligonucleotides are inefficient.[19] Indeed, we found that the tiny LNA 8-mer (PS) was able to derepress the p21 reporter with high efficiency (**Fig. 3B**). When using the luciferase reporter with seed-mutagenized p21 3'-UTR, none of the antiseeds showed a substantial derepression effect (**Fig. 3C**). The miRNA hairpin inhibitors even somewhat reduced luciferase activity of the mutated reporter (**Fig. 3C**), suggesting unwanted side effects of such molecules in our experimental setup. Also, the LNA 8-mer (PS) slightly derepressed expression from the seed-mutagenized reporter (**Fig. 3C**), suggesting that the high derepression in **Figure 3B** includes contributions from this non-specific stimulation.

Taken together, our results establish 14-mer LNA antiseeds (PO) as interesting new miRNA or miRNA family inhibitors with favorable properties in terms of efficacy, duration and specificity of depression effects.

Functional delivery of LNA antiseeds with PEI F25-LMW. A major bottleneck for the therapeutic application of any nucleic acid, including LNA antiseeds, is its efficient and functional delivery in vivo. Previously, we have established nucleic acid complexation with low molecular weight polyethylenimine (PEI

©2012 Landes Bioscience. Do not distribute

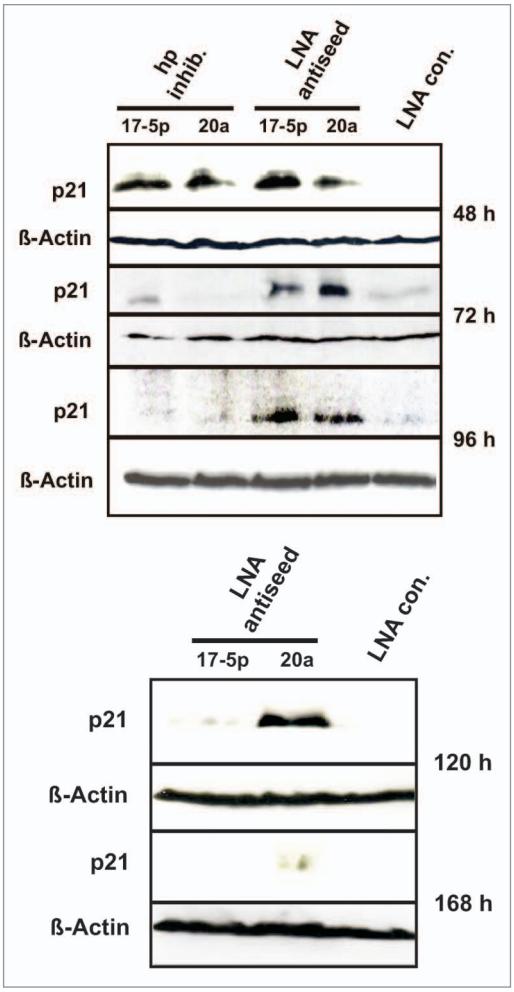

Figure 2. Duration of p21 derepression by LNA (PO) 14-mer antiseeds vs. hairpin inhibitors. Expression of p21 was analyzed by western blotting after transfection of LNA 14-mer antiseeds and miRNA hairpin inhibitors (hp inhib.) directed against *miR-17–5p* or *miR-20a* in K562 cells. As a control, the unrelated LNA 14-mer (LNA con., see Fig. 1B) was used. Beta-Actin served as a loading control.

F25-LMW) for the systemic administration of siRNA or miRNA in mice.[22,27-29] While PEI F25-LMW has cell type-dependent transfection efficacy in vitro, it is important to note that it can be used for efficient delivery of nucleic acids in vivo, which is not possible with other liposomal transfection reagents. More specifically, PEI F25-LMW is less toxic than other PEIs, and the formation of PEI-based nanoparticles protects nucleic acids from degradation in biological fluids, mediates their cellular uptake and triggers their release from the endosomal/lysosomal system due to the "proton-sponge effect."[27,29]

Here, we aimed at extending our PEI F25-LMW-based delivery platform toward LNA antimiRs for blocking the function of oncogenic or other disease-related miRNAs in vivo. We analyzed the derepression activity of PEI F25-LMW/antiseed complexes against *miR-17–5p* and *miR-20a* in HeLa cells and compared it with that of miRNA hairpin inhibitors and the tiny LNA 8-mer (PS) complexes in the same manner. Complexation was done at a PEI/nucleic acid mass ratio of 5:1, which had been determined as optimal in previous siRNA and miRNA experiments[22] with regard to complex stability and surface charge (zeta potential). In our experimental setup, HeLa cells were first transfected with the p21 reporter plasmid using lipofectamine, followed by transfection of PEI/nucleic acid complexes assembled at 10 nM of the respective nucleic acid. Similar derepression of the luciferase reporter carrying the p21 3'-UTR was observed with most antimiRs, while the hairpin inhibitor against *miR-20a* caused the highest derepression activity; no derepression at all was seen with the LNA (PS) 8-mer (**Fig. 4A**). Analysis of the same PEI/nucleic acid complexes in combination with the luciferase reporter encoding the seed-mutagenized p21 3'-UTR ruled out any non-specific effects (**Fig. 4B**). We further analyzed PEI/nucleic acid complexes for possible toxic side effects by using a WST-1 assay that senses cell viability via mitochondrial energy metabolism (see **Supplemental Materials**). We did not observe any significant negative effects on cell viability for up to 250 nM of PEI-complexed LNA antiseeds, hairpin inhibitors or the LNA 8-mer (PS) (**Fig. S1**).

The absence of LNA 8-mer (PS) activity (**Fig. 4A**), in contrast to antiseeds or hairpin inhibitors, prompted us to address the question if complexation by PEI F25-LMW might be inefficient for short single-stranded oligomers relative to siRNA duplexes. We thus compared PEI complexation of a double-stranded siRNA[30] with that of single-stranded RNA (14- or 8-mer) in an agarose gel assay (**Fig. 4C**). Different amounts of PEI F25-LMW were incubated with 500 ng of the respective RNA to obtain PEI/RNA mass ratios of 0.1 to 10. To visualize PEI/RNA complexes in agarose gels, trace amounts of the respective 5'-[^{32}P]-labeled RNA were added (~500- to 1000-fold excess of unlabeled RNA over labeled RNA). Notably, we observed no significant differences in complexation efficacies for the siRNA duplex or the single-stranded RNA oligomers of different length. In all cases, complex formation started at a PEI/RNA mass ratio of 0.25 (which corresponds to 125 ng PEI) and approximately 90% complexation at a PEI/RNA mass ratio of 1:1 (**Fig. 4C**). The quantitative analysis (**Fig. 4C**, bottom graph) revealed only minor differences in complexation efficacy of siRNA duplex and 8- or 14-meric RNA single strands. More importantly, at the PEI/oligonucleotide mass ratios of 2.5:1 or 5:1 used in our HeLa cell transfection experiments (see **Fig. 4A and 5**) all three types of RNA were fully complexed with PEI (**Fig. 4C**).

Visualization of PEI nanoparticles containing LNA antiseeds. Because 5′-[^{32}P]-labeling by T4 polynucleotide kinase using standard protocols was ineffective, we could not apply the same agarose gel-based complexation test to LNA oligomers. Also, staining of PEI/LNA complexes with SYBR® Gold or silver was unsuccessful (data not shown). Thus, we analyzed PEI/LNA complexes by atomic force microscopy (AFM). Indeed, upon mixing of PEI F25-LMW and LNA 14-mers (PO) at different mass ratios the formation of polymeric nanoparticles was observed (**Fig. 6**). At PEI/LNA mass ratios of 2.5:1 or 5:1 the resulting nanoparticles were quite homogeneous in size (diameters of ~ 80–150 nm). Polymeric PEI nanoparticles were also formed with the LNA 8-mer (PS) (**Fig. 6**). Thus, the inability to

©2012 Landes Bioscience. Do not distribute

raise derepressional effects with PEI/LNA 8-mer (PS) complexes (see **Fig. 4A**) has very likely reasons other than inefficient PEI nanoparticle formation.

After demonstrating the efficient formation of homogeneous PEI/LNA complexes at mass ratios of 2.5:1 and 5:1, we analyzed our PEI-based delivery strategy in the *let-7a*-specific luciferase reporter system (see **Fig. 1A**). The efficient repression of the *let-7a* reporter in HeLa cells (**Fig. 1C**, cf. bars for "f" and "antiseed 14-mer" at 50–100 nM) qualified this reporter system as optimal for further validating the relatively weak derepression effects of PEI-complexed LNA antiseeds on the p21 3'-UTR reporter system (see **Fig. 4A**). We now used a PEI/nucleic acid mass ratio of 2.5:1 and varied the 14-meric *let-7a* LNA antiseed concentrations between 10 and 250 nM. In this setup, the 14-mer LNA antiseed caused a specific approx. 3-fold derepression of the *let-7a* reporter at 100 nM or 250 nM (**Fig. 5**), which is a more robust effect than that observed in **Figure 4A**. We conclude that PEI F25-LMW efficiently complexes LNA antiseeds and allows for their delivery in vitro, thus providing the basis for future in vivo experiments.

Discussion

The inhibition of miRNAs is an important strategy to analyze their cellular functions and to reduce miRNA overexpression levels in several disease states. This may well lead to novel therapeutic treatments based on reversion of the consequences of aberrantly high miRNA expression levels. One promising approach to block miRNAs is the use of LNA-based antisense strategies. LNA has several advantages over other nucleic acids, including the increase in T_m values of usually 2–4°C per LNA modification compared with DNA, its resistance against intracellular nucleases and nucleases in biological fluids, improved mismatch discrimination (for reviews see refs. 13,31 and 32) and low toxicity profiles in preclinical in vivo studies.[10] The rate constant k_{off} of LNA/RNA hybrids is dramatically reduced[24,33] and therefore steric blockage of target nucleic acids is anticipated to be very efficient and persistent. Recently, the successful use of LNA-modified antisense oligonucleotides against miRNAs has been described, for example tiny LNA 8-mers with a PS backbone or various LNA/DNA mixmers (see Introduction). However, the identification of short-sized (~14 nt) LNA oligonucleotides that have the capacity to target miRNA families with common seeds, in combination with the development of efficient strategies for their delivery, is an important exercise toward in vivo applications.

In this study we have introduced 14-mer LNA antiseeds with a PO backbone, which displayed several context-dependent advantages over other miRNA inhibitors. By using a miRNA (*let-7a*)-regulated reporter gene assay in HeLa cells and lipofectamine as transfection agent we found 12- or 14-meric LNA antiseeds to be more potent than shorter variants (8- or 10-mer; **Fig. 1C**). Also, in this assay system, a commonly used miRNA hairpin inhibitor[23] lost its otherwise similar inhibition capacity at higher inhibitor concentrations (≥ 20 nM), possibly due to aggregation effects (**Fig. 1D**). In our second test system, where we transfected K562 cells by electroporation, derepression of endogenous p21 expression was much more persistent with LNA (PO) 14-mer

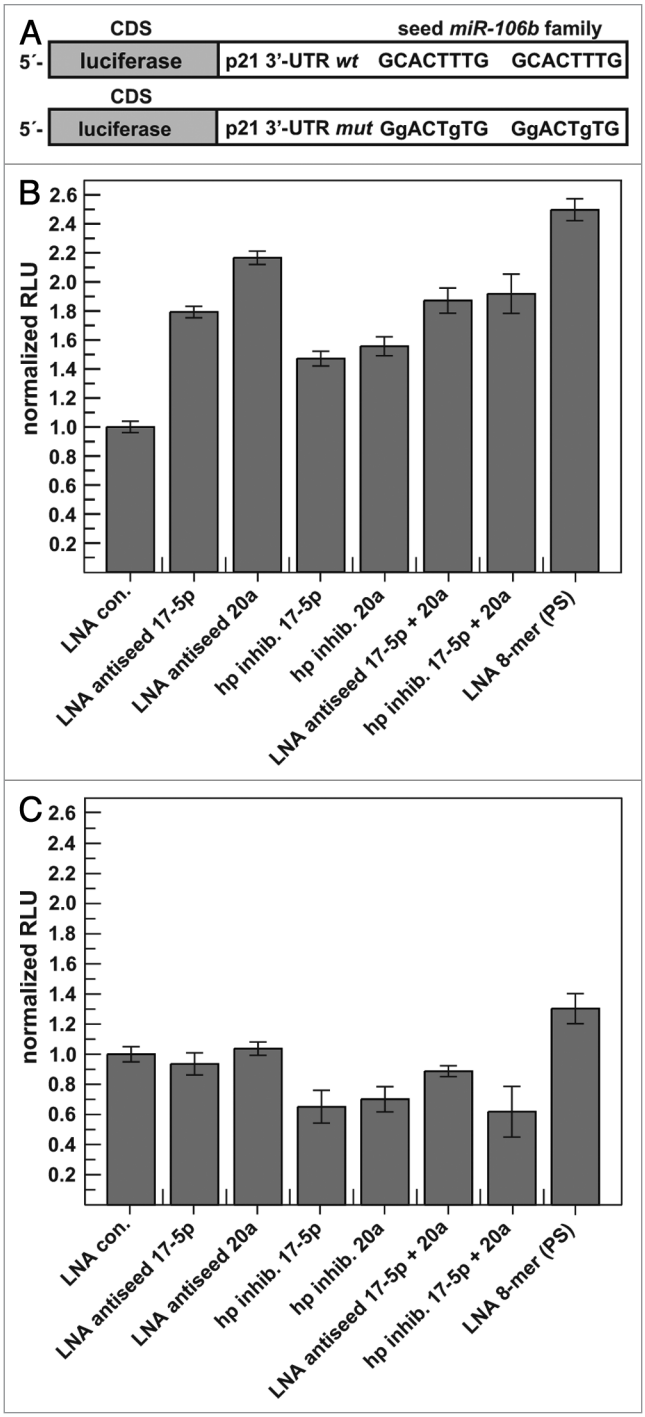

Figure 3. (A) Schematic presentation of the reporter carrying the luciferase coding sequence (CDS) followed by the p21 3'-UTR that harbours two *miR-106b* family seed regions (top). The seed regions are mutated in the variant reporter construct underneath, with lower case letters indicating the mutated nucleotides. (B) Derepression activity of the indicated miRNA inhibitors (hp inhib. or 14-meric LNA antiseeds) directed against *miR-17–5p* and *miR-20a* after lipofectamine-mediated cotransfection with the luciferase/p21 3'-UTR reporter plasmid into HeLa cells. Luciferase activity values obtained after cotransfection with the LNA con. 14-mer were set to 1. Values are derived from at least three independent experiments (+/- S.E.M.). (C) Effects of the indicated miRNA inhibitors on luciferase expression using the seed-mutated version of the reporter (see panel A). Values are derived from at least three independent experiments (+/- S.E.M.).

©2012 Landes Bioscience. Do not distribute

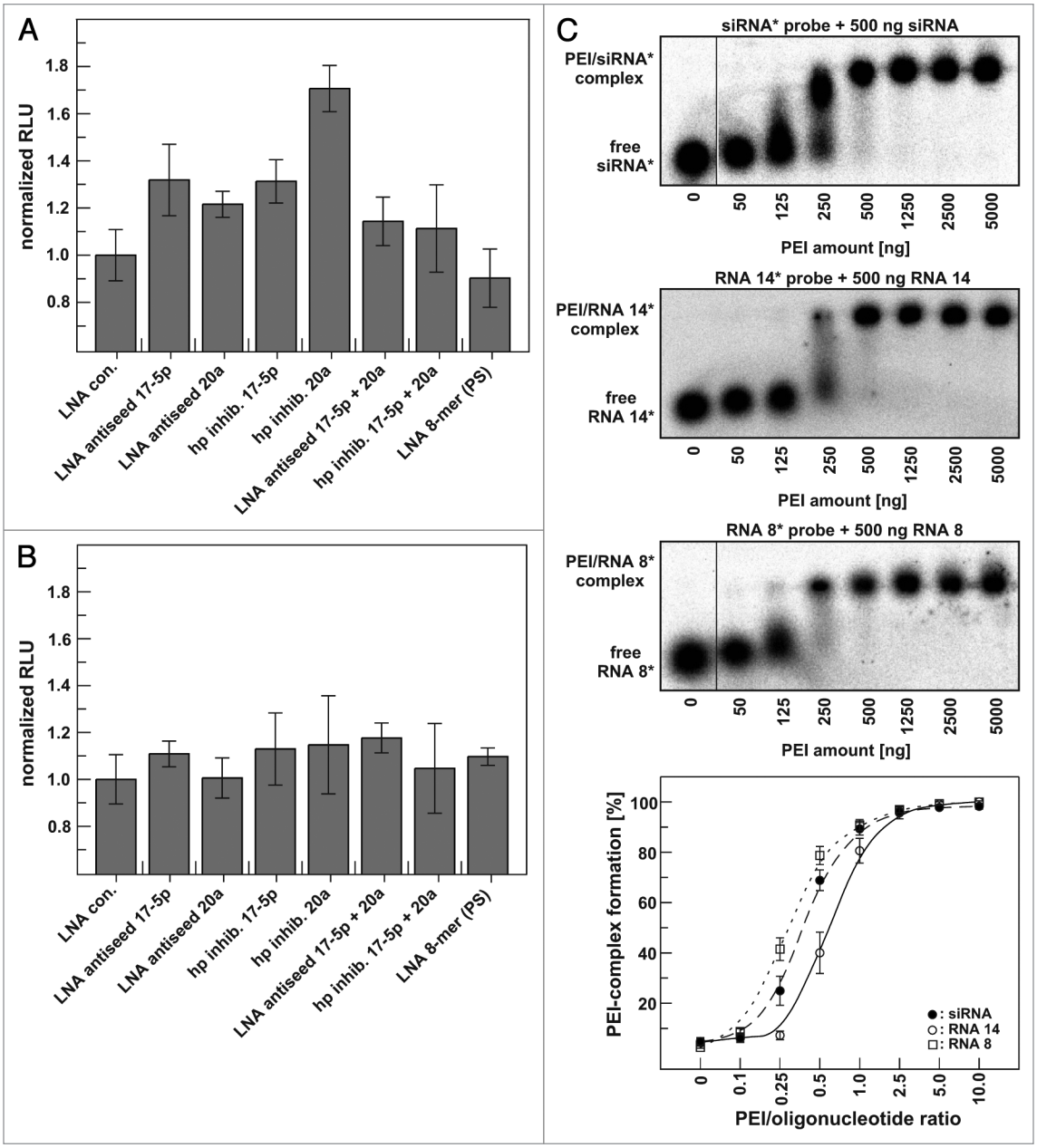

Figure 4. (A) Derepression of the luciferase/p21 3'-UTR reporter by PEI F25-LMW-complexed LNA (PO) 14-mer antiseeds, miRNA hairpin inhibitors (hp inhib.) and an LNA (PS) 8-mer directed against *miR-17–5p* and *miR-20a* in HeLa cells. The LNA con. 14-mer was used as a reference and the luminescence measured for cell lysates harboring LNA con. was set to 1. Values are derived from four independent experiments (+/- S.E.M.). (B) Effects of the indicated PEI-complexed miRNA inhibitors on luciferase expression using the seed-mutated version of the reporter (see Fig. 3A). Values are derived from four independent experiments (+/- S.E.M.). (C) PEI-complexation experiments using 5'-[^{32}P]-endlabeled double-stranded siRNA or single-stranded 8- or 14-meric RNA (10^4 Cerenkov cpm per lane) as probes; PEI/RNA complexes are indicated by retarded mobility of the RNA probe. To obtain PEI/RNA mass ratios of 0.1 to 10, 500 ng of either unlabeled siRNA duplex, 14-meric RNA or 8-meric RNA were combined with the corresponding labeled probes and incubated with different amounts of PEI F25-LMW as indicated. Representative agarose gels are shown. A quantitative analysis based on at least three independent experiments is shown at the bottom (+/- S.E.M.).

antiseeds than with corresponding hairpin inhibitors (**Fig. 2**). In our third analysis, which was comparable to the first assay system except for the reporter carrying the p21 3'-UTR with two *miR-106b* target sites, we found that LNA (PO) 14-mer antiseeds were again active (**Fig. 3B**). These experiments provided evidence that the LNA (PO) 14-mer antiseeds tend to target an entire miRNA family, while the hairpin inhibitors are more specific for individual miRNAs. This was inferred from the observation that hairpin inhibitors, but not antiseeds, against *miR-17–5p* and *miR-20a* showed synergistic effects (**Fig. 3B**). A seed-targeting tiny LNA 8-mer (PS), which has the capacity to block miRNA families,[19] appeared to even perform best in this assay, although control experiments with the reporter gene that contain mutations in the *miR-17–5p* and *miR-20a* target sites pointed to some

©2012 Landes Bioscience. Do not distribute

unspecific stimulatory effect of this type of inhibitor on reporter expression (**Fig. 3C**). From our results we conclude that hairpin inhibitors are suited to dissect the functions of single miRNAs of a miRNA family, while the broader effect of our 14-mer LNA (PO) antiseeds on more than one miRNA family member may well enhance possible therapeutic effects.

In our fourth approach (**Fig. 4**) we employed PEI F25-LMW as transfection agent instead of lipofectamine, keeping in mind that efficient and functional delivery in vivo remains the critical issue for nucleic acid-based therapeutic applications and common transfection reagents cannot be used here (for review, see e.g., ref. 34).

As shown previously, PEI complexation of nucleic acids leads to polymeric nanoscale particles that (1) allow the complete protection of the nucleic acid against degradation, (2) mediate the cellular uptake of the cargo, (3) trigger the release from the endosomal/lysosomal system due to the proton-sponge effect and (4) release the nucleic acid into the cytoplasm (for a review see ref. 35). Notably, at the amounts used for therapeutic intervention, the low molecular weight PEI F25-LMW[28] has been shown to exert no toxicity and no immunostimulatory or otherwise non-specific effects in vitro and in vivo.[29,36] In line with these previous findings, we have not observed any toxic effects of PEI F25-LMW-complexed LNA antiseeds in the study presented here (**Fig. S1**).

Here we demonstrate that single-stranded 14-mer LNA (PO) antiseeds can be functionally delivered by PEI F25-LMW (**Fig. 4A and 5**) with efficacies comparable to hairpin inhibitors (**Fig. 4A**). In contrast, the tiny LNA 8-mer (PS) failed to show an inhibitory effect when using PEI F25-LMW as the delivery agent (**Fig. 4A**). This has other reasons than incomplete PEI complexation of the LNA 8-mer (PS) because neither (1) its short length, (2) its PS backbone, (3) its single-stranded character nor (4) its LNA modifications had any significant negative effect on particle formation with PEI F25-LMW (**Fig. 4C and 6**). One possibility among several is that very short oligonucleotides such as 8-mers are inefficiently released from the nanoparticle within cells.

Taken together, our results establish the efficiency of LNA (PO) 14-mer antiseeds as new miRNA inhibitors, and demonstrate the capability of such LNA antiseeds to build functional complexes with PEI that can be delivered into cancer cells in order to derepress tumor suppressor genes such as p21. Thus, our results open up an avenue toward therapeutic application of LNA antiseeds for miRNA inhibition.

Materials and Methods

Oligonucleotides and antibodies. Locked nucleic acids (LNA) antisense oligonucleotides (antiseeds) were purchased from RiboTask (Odense, Denmark). Antiseed sequences were as follows:

Antiseed against *miR-17–5p* (PO): 5'-CTG TAA GCA CT[mU]TG;

Antiseed against *miR-20a* (PO): 5'-CTA TAA GCA [mC] T[mU]TA;

Antiseed against *miR-17–5-p/20a* (PS): 5'-GCA CT[mU]TG.

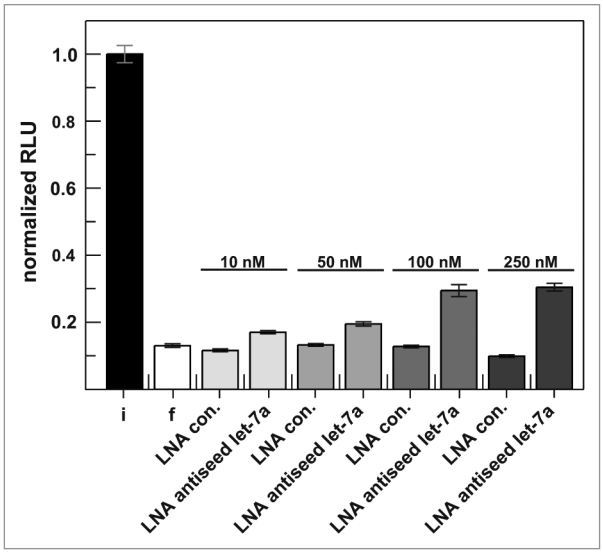

Figure 5. Derepression of the *let-7a*-responsive luciferase reporter by the PEI F25-LMW-complexed LNA (PO) 14-mer antiseed against *let-7a* in HeLa cells. For the control LNA 14-mer (LNA con.), see Fig. 1B. Luciferase activity of lysates derived from cells harboring the control vector with an inverted *let-7a* target sequence (Fig. 1A) was set to 1. Values are derived from at least three independent experiments (+/- S.E.M.).

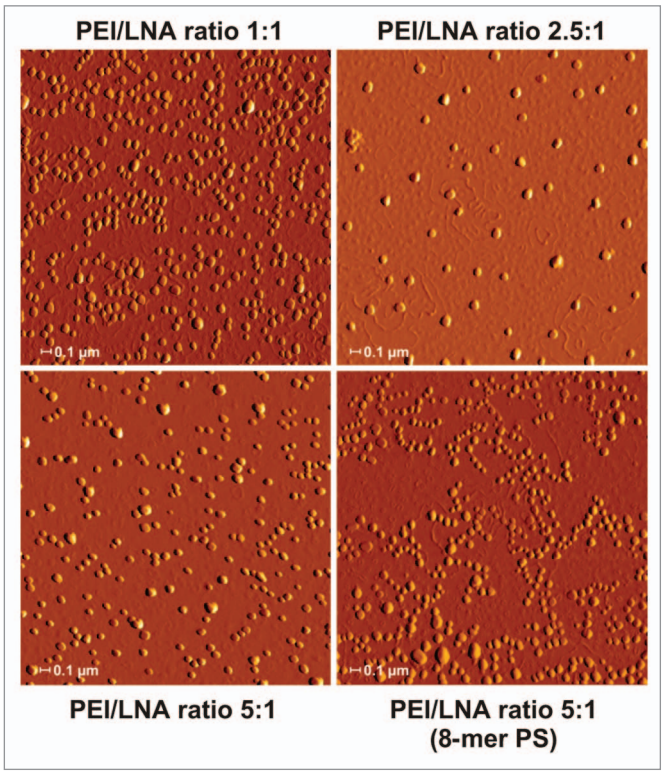

Figure 6. Detection of PEI F25-LMW/LNA nanoparticles using atomic force microscopy. Shown are four representative images of PEI/LNA complexes at the indicated mass ratios, containing either the LNA (PS) 8-mer (lower panel on the right) or an LNA (PO) 14-mer (all other panels). For details, see Materials and Methods.

©2012 Landes Bioscience. Do not distribute

All residues were LNA, except for isolated 2'-oxymethyl pyrimidines marked as [mU] and [mC]. These changes are expected to reduce self-pairing without disturbing target binding.

LNA antiseeds directed against hsa-*let-7a* were of different lengths (14- to 8-mers):

Antiseed *let7a*-14-mer: 5'-AAC CTA CTA CCT CA;

Antiseed *let7a*-12-mer: 5'-CCT ACT ACC TCA;

Antiseed *let7a*-10-mer: 5'-TAC TAC CTC A;

Antiseed *let7a*-8-mer: 5'-CTA CCT CA.

Escherichia coli RNase P RNA 5'-CAA GCA GCC UAC CC[24] was used as negative control.

The sequence of the RNA 14-mer, which was used for PEI-complexation studies, is: 5'-GUU CGG UCA AAA CU

The sequence of the RNA 8-mer, which was used for PEI-complexation studies, is:

5'-GUU CGG UC

The sequence of the VR1 siRNA, which was used for PEI-complexation studies, is:

5'-GCG AUC UUC UAU UCA ACdTdT (sense)

and 5'-GUU GAA GUA GAA GAU GCG CdTdT (antisense)[30]

MiRIDIAN hairpin inhibitors against hsa-*let-7a*, hsa-*miR-17–5-p* and hsa-*miR-20a* were purchased from Dharmacon (Thermo Scientific, Langenselbold, Germany).

Antibodies against p21 (sc-6246) and β-Actin (sc-47778) as well as the secondary antibody (sc-2005) were purchased from Santa Cruz Biotechnology (Heidelberg, Germany).

Cell culture. Cells (K562 and HeLa) were cultured under standard conditions (37°C, 5% CO_2 in a humidified atmosphere) in RPMI 1640 (K562) or IMDM (HeLa), supplemented with 10% FCS (PAA, Cölbe, Germany).

Transfection procedures. *Reporter assays using let-7a antimiRs in HeLa cells.* HeLa cells were transfected with the LNA antiseeds, controls or the hairpin inhibitors using Lipofectamine™ 2000 (Life Technologies Invitrogen, Darmstadt, Germany) according to the manufacturer's protocol. One day before transfection, 8 × 10^4 cells were seeded into 24-well plates and cultivated under standard conditions. Twenty-four hours after seeding, cells were cotransfected with 0.5 μg of vector DNA (plasmid "pGL3 control" with a *let-7a* or an inverted *let-7a* target sequence) and with 0, 10, 20, 50 or 100 nM of the LNA antiseed, LNA control or hairpin inhibitor, respectively, according to the manufacturer's protocol. Co-complexation was performed in Opti-MEM® 1 medium (Life Technologies Invitrogen). After 4 to 6 h, the transfection medium without serum was aspirated and replaced by Iscove's modified Dulbecco's medium (IMDM) containing 10% FCS. Forty-eight hours after transfection, cells were lysed and prepared for reporter assay measurements.

p21 derepression in K562 cells. For transfection experiments, 1 × 10^6 K562 cells were electroporated in 4 mm cuvettes with a single pulse at 330 V for 10 ms using a BioRad GenePulser XCell (Biorad, München, Germany). Cells were transfected with 1 μg LNA antiseeds, LNA controls or hairpin inhibitors. Forty-eight hours after transfection, cells were lysed and lysates were analyzed in western blot experiments.

Specificity of p21 derepression in HeLa cells. The transfection of HeLa cells was performed using Lipofectamine™ 2000 (Life Technologies Invitrogen). One day prior to transfection, 4 × 10^4 cells were seeded into 24-well plates; for co-complexation, 1 μl Lipofectamine™ 2000 was combined with 10 nM LNA antiseed, LNA control or hairpin inhibitor and 0.5 μg of vector DNA (plasmid "pGL3 control" containing the p21 3'-UTR or the mutated p21 3'-UTR) in Opti-MEM® 1 medium according to the instructions of the manufacturer; the mixture was added to the cells, proceeding as described above (see Reporter assays using *let-7a* antimiRs in HeLa cells).

PEI complexation and delivery. *Using the p21 reporter system.* For complexation of miRNA inhibitors with PEI F25-LMW, cells were pre-transfected with vector DNA ("pGL3 control" plasmid containing the p21 3'-UTR or the mutated p21 3'-UTR) using Lipofectamine™ 2000 as described above (see Specificity of p21 derepression in HeLa cells). After 6 h, the medium was replaced with IMDM/10% FCS, and PEI complexes were added. For PEI F25-LMW complexation, LNA antiseeds, LNA control oligonucleotide, tiny LNA 8-mer with PS backbone or hairpin inhibitors were diluted in complexation buffer (150 mM NaCl, 10 mM HEPES pH 7.4). To gain a final concentration of 10 nM, 18 ng of LNA 8-mer (PS), 28.5 ng of LNA 14-mers (control, antiseed 17–5p or antiseed 20a) and 80 ng of hairpin inhibitors 17–5p or 20a were diluted in 50 μl complexation buffer and equilibrated 5 min at room temperature. To obtain a PEI / oligonucleotide mass ratio of 5:1, 90 ng PEI was used for complexation of the LNA 8-mer (PS), 142.5 ng PEI for complexation of the LNA antiseeds and LNA 14-mer control, and 390 ng PEI was required for the hairpin inhibitor complexes. After equilibration of PEI to room temperature in complexation buffer, the oligonucleotide and the PEI solution were mixed, briefly vortexed and incubated for 30–60 min at room temperature to allow complex formation. PEI F25-LMW complexes were then added to the cells (see above), and 48 h later cells were lysed and prepared for reporter assay measurements.

Using the let-7a reporter system. Cells were pre-transfected with vector DNA ("pGL3 control" plasmid containing the *let-7a* forward or inverted target sequence) using Lipofectamine™ 2000 as described above (see Reporter assays using *let-7a* antimiRs in HeLa cells). After 6 h, the medium was replaced with IMDM/2% FCS, and PEI complexes were added. For PEI F25-LMW complexation, the *let-7a* LNA 14-mer and the LNA control 14-mer were diluted in complexation buffer (150 mM NaCl, 10 mM HEPES pH 7.4). To gain a final oligonucleotide concentration of 10, 50, 100 or 250 nM, 115, 575, 1,150 or 2,875 ng of the LNA 14-mers were diluted in 50 μl complexation buffer and equilibrated to room temperature. PEI F25-LMW was used at a final PEI / oligonucleotide mass ratio of 2.5:1; therefore 288, 1,440, 2,880 or 7,200 ng of PEI was diluted in 50 μl complexation buffer and also equilibrated 5 min at room temperature. Complexation was initiated by mixing PEI and oligonucleotide solutions, followed by incubation at room temperature for 30 - 60 min. PEI / LNA complexes were finally added to the cells and luciferase reporter measurements were performed 48 h posttransfection.

©2012 Landes Bioscience. Do not distribute

Determination of PEI complexation efficacy. To determine the complexation efficacy of PEI F25-LMW, a radioactive assay was employed as described previously.[37] For this purpose, 500 ng of single-stranded 14- or 8-meric RNA or double-stranded siRNA were used, mixed with trace amounts (10^4 Cerenkov cpm) of 5'-[^{32}P]-endlabeled RNA 14-mer, RNA 8-mer or siRNA, respectively. Complexation was performed with the indicated amounts of PEI (see "PEI complexation and delivery" above and **Fig. 4C**). Samples were mixed with DNA loading buffer (10 mM Tris/HCl (pH 7.6), 80% glycerol, 0.03% bromophenol blue, 0.03% xylene cyanol blue) and analyzed by 1% agarose gel electrophoresis, run at 50 mA for 2 h (PEQLAB Biotechnologie). Complex formation was analyzed by autoradiography of the agarose gel for 3 h using a Fuji FLA-3000 R Phosphorimager (Fujifilm); the ratio of free to partially and fully complexed RNA was calculated using the software AIDA (Version 3.45).

Atomic force microscopy. PEI/LNA complexes were analyzed by atomic force microscopy (AFM). Complexes were prepared as described above with 500 ng of LNA 14-mer 17–5p (PO) or LNA 8-mer (PS) and the indicated amounts of PEI F25-LMW (see **Fig. 6**). Complexes were directly transferred onto a silicon chip by dipping the chip into the complex solution. AFM was performed on a vibration-damped NanoWizard (JPK instruments, Berlin, Germany) as described in detail elsewhere.[38,39] Commercially available pyramidal Si_3N_4 tips (NSC16 AIBS, Micromasch, Estonia) mounted to a cantilever with a length of 230 μm, a resonance frequency of about 170 kHz and a nominal force constant of about 40 N/m were used. To avoid damage of the sample surface, measurements were performed in intermitted contact. The scan speed was proportional to the scan size, and the scan frequency was between 0.5 and 1.5 Hz. Images were obtained by displaying the amplitude signal of the cantilever in the trace direction, and the height signal in the retrace direction, both signals being simultaneously recorded. The complexes were visualized either in height or in amplitude mode (512 × 512 pixel).

Plasmid construction and seed mutagenesis. To introduce a hsa-*let-7a* site, two complementary DNA oligonucleotides encoding the *let-7a* target sequence (MIMAT0000062) were annealed, cleaved with *XbaI*, and cloned into the unique *XbaI* site of the reporter plasmid pGL3-Control (Promega, Mannheim, Germany); the *XbaI* cleavage site is located immediately downstream of the luciferase coding sequence. Insertion of the fragment was identified through linearizing of recombinant plasmids via the unique *BlpI* site introduced with the insert (see below). Cloning of the insert resulted in two opposite orientations, which were identified by DNA sequencing. Clones giving rise to RNA transcripts with a *let-7a* target site were classified as "forward orientation"; clones with the opposite insert orientation were classified as "inverted orientation" and were used as controls for the absence of a *let-7a* target site in the RNA transcript. The two annealed DNA oligonucleotides had the following sequences:

let-7a sense *XbaI*:

5'-GCT CTA GAG C*TG AGG TAG TAG GTT GTA TAG TT*G CTC AGC GCT CTA GAG C-3'

let-7a antisense *XbaI*:

5'-GCT CTA GAG CGC TGA GCA ACT ATA CAA CCT ACT ACC TCA GCT CTA GAG C-3'

(*XbaI* and *BlpI* sites underlined and the hsa-*let-7a* sense sequence in italics).

To determine the effects of LNA antiseeds that are directed against mature *miR-106* family members on the expression of the p21 protein, the 3'-untranslated region (3'-UTR) of p21 was cloned into the pGL3 control luciferase reporter vector (Promega, Mannheim, Germany) via its *Xba*I site. The 3'-UTR was initially amplified from K562 genomic DNA with the forward primer 5'-TCT AGA CCT CAA AGG CCC GCT CTA-3' and the reverse primer 5'-TCT AGA GGA GGA GCT GTG AAA GAC ACA-3'; the amplicon was subcloned into a pCR 2.1-TOPO vector (TOPO TA Cloning® kit, Invitrogen, Karlsruhe, Germany) prior to insertion into the pGL3 vector. PCR mutagenesis of the two miRNA seed target sites was done according to Brennecke et al.[40] The following primers were used for mutagenesis (sites of mutation underlined):

5'-target site forward: 5'-GAA GTA AAC AGA TGG GAC TGT GAA GGG GCC TCA CC-3',

5'- target site reverse: 5'-GGT GAG GCC CCT TCA CAG TCC CAT CTG TTT ACT TC-3',

3'-target site forward: 5'-CTC CCC AGT TCA TTG GAC TGT GAT TAG CAG CGG AA-3',

3'-target site reverse: 5'-TTC CGC TGC TAA TCA CAG TCC AAT GAA CTG GGG AG-3'. Mutations were verified by DNA sequencing.

Luciferase reporter assays. Luciferase reporter assays were performed using the Promega Luciferase Assay System (Promega, Mannheim, Germany). After aspirating the media, cells were washed with PBS and lysed in 100 μl reporter lysis buffer. In a 96-well plate, 10 μl lysate were mixed with 10 μl substrate, and the luminescence was measured immediately in a Safire^{2} ™ microplate reader (Tecan, Crailsheim, Germany). In the case of the *let-7a*-responsive reporter assay, the measured luminescence was normalized to that of lysates from cells harboring the inverted target vector (which was set to 1), yielding the normalized "relative light units" (RLU). In the case of the reporter with p21 3'-UTR, RLU were normalized to the luminescence of the reporter in the presence of the control LNA 14-mer (set to 1) to illustrate the relative weak derepression effects of PEI-complexed oligonucleotides.

Western blotting. Cells were lysed in lysis buffer (125 mM Tris/HCl pH 6.8, 4% SDS, 1.4 M 2-mercaptoethanol, 0.05% bromophenol blue) and heated at 95°C for 5 min. Samples were loaded onto 15% SDS-polyacrylamide gels (Mini-PROTEAN® 3 cell mini gel system, BioRad) and run for 1 h at 180 V. Proteins were transferred onto an Immobilon™-P PVDF membrane for 30 min at 10 V using a Trans-Blot® SD Semi-Dry Transfer Cell (BioRad), followed by blocking of the membrane with 5% milk powder dissolved in TBST [10 mM Tris/HCL (pH 7.6), 150 mM NaCl, 0,1% Tween 20]. Primary and secondary antibodies were diluted in TBST 1:200 (p21), 1:5000 (β-Actin) and 1:5000 (goat anti-mouse IgG-HRP, secondary antibody). After a final washing step, blots were incubated with Amersham ECL™ or ECLplus™ Western Blotting Detection Reagents according

©2012 Landes Bioscience. Do not distribute

to the manufacturer's protocol. For detection of chemiluminescence, Kodak® BioMax™ light films, Kodak GBX Developer and Replenisher and GBX Fixer and Replenisher were used.

Disclosure of Potential Conflicts of Interest

No potential conflicts of interest were disclosed.

Acknowledgements

We are grateful to Andrea Wüstenhagen and Dominik Helmecke for technical assistance and Markus Gössringer for fruitful discussions. This work was supported by grants from the German Cancer Aid (Deutsche Krebshilfe, grants 106992 and 109260 to A.G., R.K.H. and A.A.) and the Deutsche Forschungsgemeinschaft (Forschergruppe 'Nanohale' AI 24/6–1 to A.A.)

Supplemental Materials

Supplemental materials may be found here: www.landesbioscience.com/journals/rnabiology/article/21165

References

1. Garzon R, Marcucci G, Croce CM. Targeting microRNAs in cancer: rationale, strategies and challenges. [Review]. Nat Rev Drug Discov 2010; 9:775-89; PMID:20885409; http://dx.doi.org/10.1038/nrd3179.
2. Kasinski AL, Slack FJ. Epigenetics and genetics. MicroRNAs en route to the clinic: progress in validating and targeting microRNAs for cancer therapy. Nat Rev Cancer 2011; 11:849-64; PMID:22113163; http://dx.doi.org/10.1038/nrc3166.
3. Ivanovska I, Ball AS, Diaz RL, Magnus JF, Kibukawa M, Schelter JM, et al. MicroRNAs in the miR-106b family regulate p21/CDKN1A and promote cell cycle progression. Mol Cell Biol 2008; 28:2167-74; PMID:18212054; http://dx.doi.org/10.1128/MCB.01977-07.
4. O'Donnell KA, Wentzel EA, Zeller KI, Dang CV, Mendell JT. c-Myc-regulated microRNAs modulate E2F1 expression. Nature 2005; 435:839-43; PMID:15944709; http://dx.doi.org/10.1038/nature03677.
5. Ambs S, Prueitt RL, Yi M, Hudson RS, Howe TM, Petrocca F, et al. Genomic profiling of microRNA and messenger RNA reveals deregulated microRNA expression in prostate cancer. Cancer Res 2008; 68:6162-70; PMID:18676839; http://dx.doi.org/10.1158/0008-5472.CAN-08-0144.
6. Volinia S, Calin GA, Liu CG, Ambs S, Cimmino A, Petrocca F, et al. A microRNA expression signature of human solid tumors defines cancer gene targets. Proc Natl Acad Sci U S A 2006; 103:2257-61; PMID:16461460; http://dx.doi.org/10.1073/pnas.0510565103.
7. He L, Thomson JM, Hemann MT, Hernando-Monge E, Mu D, Goodson S, et al. A microRNA polycistron as a potential human oncogene. Nature 2005; 435:828-33; PMID:15944707; http://dx.doi.org/10.1038/nature03552.
8. Olive V, Bennett MJ, Walker JC, Ma C, Jiang I, Cordon-Cardo C, et al. miR-19 is a key oncogenic component of mir-17-92. Genes Dev 2009; 23:2839-49; PMID:20008935; http://dx.doi.org/10.1101/gad.1861409.
9. Small EM, Olson EN. Pervasive roles of microRNAs in cardiovascular biology. [Review]. Nature 2011; 469:336-42; PMID:21248840; http://dx.doi.org/10.1038/nature09783.
10. Elmén J, Lindow M, Schütz S, Lawrence M, Petri A, Obad S, et al. LNA-mediated microRNA silencing in non-human primates. Nature 2008; 452:896-9; PMID:18368051; http://dx.doi.org/10.1038/nature06783.
11. Rayner KJ, Esau CC, Hussain FN, McDaniel AL, Marshall SM, van Gils JM, et al. Inhibition of miR-33a/b in non-human primates raises plasma HDL and lowers VLDL triglycerides. Nature 2011; 478:404-7; PMID:22012398; http://dx.doi.org/10.1038/nature10486.
12. Krützfeldt J, Rajewsky N, Braich R, Rajeev KG, Tuschl T, Manoharan M, et al. Silencing of microRNAs in vivo with 'antagomirs'. Nature 2005; 438:685-9; PMID:16258535; http://dx.doi.org/10.1038/nature04303.
13. Kurreck J. Antisense technologies. Improvement through novel chemical modifications. [Review]. Eur J Biochem 2003; 270:1628-44; PMID:12694176; http://dx.doi.org/10.1046/j.1432-1033.2003.03555.x.
14. Davis S, Propp S, Freier SM, Jones LE, Serra MJ, Kinberger G, et al. Potent inhibition of microRNA in vivo without degradation. Nucleic Acids Res 2009; 37:70-7; PMID:19015151; http://dx.doi.org/10.1093/nar/gkn904.
15. Corsten MF, Miranda R, Kasmieh R, Krichevsky AM, Weissleder R, Shah K. MicroRNA-21 knockdown disrupts glioma growth in vivo and displays synergistic cytotoxicity with neural precursor cell delivered S-TRAIL in human gliomas. Cancer Res 2007; 67:8994-9000; PMID:17908999; http://dx.doi.org/10.1158/0008-5472.CAN-07-1045.
16. Worm J, Stenvang J, Petri A, Frederiksen KS, Obad S, Elmén J, et al. Silencing of microRNA-155 in mice during acute inflammatory response leads to derepression of c/ebp Beta and down-regulation of G-CSF. Nucleic Acids Res 2009; 37:5784-92; PMID:19596814; http://dx.doi.org/10.1093/nar/gkp577.
17. Kocerha J, Faghihi MA, Lopez-Toledano MA, Huang J, Ramsey AJ, Caron MG, et al. MicroRNA-219 modulates NMDA receptor-mediated neurobehavioral dysfunction. Proc Natl Acad Sci U S A 2009; 106:3507-12; PMID:19196972; http://dx.doi.org/10.1073/pnas.0805854106.
18. Patrick DM, Montgomery RL, Qi X, Obad S, Kauppinen S, Hill JA, et al. Stress-dependent cardiac remodeling occurs in the absence of microRNA-21 in mice. J Clin Invest 2010; 120:3912-6; PMID:20978354; http://dx.doi.org/10.1172/JCI43604.
19. Obad S, dos Santos CO, Petri A, Heidenblad M, Broom O, Ruse C, et al. Silencing of microRNA families by seed-targeting tiny LNAs. Nat Genet 2011; 43:371-8; PMID:21423181; http://dx.doi.org/10.1038/ng.786.
20. Stein CA, Hansen JB, Lai J, Wu S, Voskresenskiy A, Høg A, et al. Efficient gene silencing by delivery of locked nucleic acid antisense oligonucleotides, unassisted by transfection reagents. Nucleic Acids Res 2010; 38:e3; PMID:19854938; http://dx.doi.org/10.1093/nar/gkp841.
21. Thomas M, Lange-Grünweller K, Weirauch U, Gutsch D, Aigner A, Grünweller A, et al. The proto-oncogene Pim-1 is a target of miR-33a. Oncogene 2012; 31:918-28; PMID:21743487; http://dx.doi.org/10.1038/onc.2011.278.
22. Ibrahim AF, Weirauch U, Thomas M, Grünweller A, Hartmann RK, Aigner A. MicroRNA replacement therapy for miR-145 and miR-33a is efficacious in a model of colon carcinoma. Cancer Res 2011; 71:5214-24; PMID:21690566; http://dx.doi.org/10.1158/0008-5472.CAN-10-4645.
23. Vermeulen A, Robertson B, Dalby AB, Marshall WS, Karpilow J, Leake D, et al. Double-stranded regions are essential design components of potent inhibitors of RISC function. RNA 2007; 13:723-30; PMID:17400817; http://dx.doi.org/10.1261/rna.448107.
24. Gruegelsiepe H, Brandt O, Hartmann RK. Antisense inhibition of RNase P: mechanistic aspects and application to live bacteria. J Biol Chem 2006; 281:30613-20; PMID:16901906; http://dx.doi.org/10.1074/jbc.M603346200.
25. Venturini L, Battmer K, Castoldi M, Schultheis B, Hochhaus A, Muckenthaler MU, et al. Expression of the miR-17-92 polycistron in chronic myeloid leukemia (CML) CD34+ cells. Blood 2007; 109:4399-405; PMID:17284533; http://dx.doi.org/10.1182/blood-2006-09-045104.
26. Soifer HS, Koch T, Lai J, Hansen B, Hoeg A, Oerum H, et al. Silencing of gene expression by gymnotic delivery of antisense oligonucleotides. Methods Mol Biol 2012; 815:333-46; PMID:22131003; http://dx.doi.org/10.1007/978-1-61779-424-7_25.
27. Urban-Klein B, Werth S, Abuharbeid S, Czubayko F, Aigner A. RNAi-mediated gene-targeting through systemic application of polyethylenimine (PEI)-complexed siRNA in vivo. Gene Ther 2005; 12:461-6; PMID:15616603; http://dx.doi.org/10.1038/sj.gt.3302425.
28. Werth S, Urban-Klein B, Dai L, Höbel S, Grzelinski M, Bakowsky U, et al. A low molecular weight fraction of polyethylenimine (PEI) displays increased transfection efficiency of DNA and siRNA in fresh or lyophilized complexes. J Control Release 2006; 112:257-70; PMID:16574264; http://dx.doi.org/10.1016/j.jconrel.2006.02.009.
29. Höbel S, Koburger I, John M, Czubayko F, Hadwiger P, Vornlocher HP, et al. Polyethylenimine/small interfering RNA-mediated knockdown of vascular endothelial growth factor in vivo exerts anti-tumor effects synergistically with Bevacizumab. J Gene Med 2010; 12:287-300; PMID:20052738.
30. Grünweller A, Wyszko E, Bieber B, Jahnel R, Erdmann VA, Kurreck J. Comparison of different antisense strategies in mammalian cells using locked nucleic acids, 2'-O-methyl RNA, phosphorothioates and small interfering RNA. Nucleic Acids Res 2003; 31:3185-93; PMID:12799446; http://dx.doi.org/10.1093/nar/gkg409.
31. Grünweller A, Hartmann RK. Locked nucleic acid oligonucleotides: the next generation of antisense agents? [Review]. BioDrugs 2007; 21:235-43; PMID:17628121.
32. Veedu RN, Wengel J. Locked nucleic acid as a novel class of therapeutic agents. [Review]. RNA Biol 2009; 6:321-3; PMID:19458498; http://dx.doi.org/10.4161/rna.6.3.8807.
33. Christensen U, Jacobsen N, Rajwanshi VK, Wengel J, Koch T. Stopped-flow kinetics of locked nucleic acid (LNA)-oligonucleotide duplex formation: studies of LNA-DNA and DNA-DNA interactions. Biochem J 2001; 354:481-4; PMID:11237851; http://dx.doi.org/10.1042/0264-6021:3540481.

©2012 Landes Bioscience. Do not distribute

34. Aigner A. Cellular delivery in vivo of siRNA-based therapeutics. [Review]. Curr Pharm Des 2008; 14:3603-19; PMID:19075737; http://dx.doi.org/10.2174/138161208786898815.
35. Aigner A. Nonviral in vivo delivery of therapeutic small interfering RNAs. [Review]. Curr Opin Mol Ther 2007; 9:345-52; PMID:17694447.
36. Beyerle A, Höbel S, Czubayko F, Schulz H, Kissel T, Aigner A, et al. In vitro cytotoxic and immunomodulatory profiling of low molecular weight polyethylenimines for pulmonary application. Toxicol In Vitro 2009; 23:500-8; PMID:19444927; http://dx.doi.org/10.1016/j.tiv.2009.01.001.
37. Malek A, Czubayko F, Aigner A. PEG grafting of polyethylenimine (PEI) exerts different effects on DNA transfection and siRNA-induced gene targeting efficacy. J Drug Target 2008; 16:124-39; PMID:18274933; http://dx.doi.org/10.1080/10611860701849058.
38. Sitterberg J, Ozcetin A, Ehrhardt C, Bakowsky U. Utilising atomic force microscopy for the characterisation of nanoscale drug delivery systems. Eur J Pharm Biopharm 2010; 74:2-13; PMID:19755155; http://dx.doi.org/10.1016/j.ejpb.2009.09.005.
39. Oberle V, Bakowsky U, Zuhorn IS, Hoekstra D. Lipoplex formation under equilibrium conditions reveals a three-step mechanism. Biophys J 2000; 79:1447-54; PMID:10969006; http://dx.doi.org/10.1016/S0006-3495(00)76396-X.
40. Brennecke J, Stark A, Russell RB, Cohen SM. Principles of microRNA-target recognition. PLoS Biol 2005; 3:e85; PMID:15723116; http://dx.doi.org/10.1371/journal.pbio.0030085.

©2012 Landes Bioscience. Do not distribute

Supplemental Material to: Maren Thomas, Kerstin Lange-Grünweller, Eyas Dayyoub, Udo Bakowsky, Ulrike Weirauch, Achim Aigner, et al. PEI-complexed LNA antiseeds as miRNA inhibitors. RNA Biology 2012; 8(9); DOI: 10.4161/rna.21165;
http://www.landesbioscience.com/journals/rnabiology/article/21165/

Supplementary Material

Toxicity studies using the WST-1 assay

WST-1 assays were performed to analyze for toxicity of the PEI/LNA complexes (Roche, Mannheim, Germany). HeLa cells (0.5×10^4) were seeded into a 96-well plate and cultivated under standard conditions. 24 h after seeding, PEI F25-LMW complexes (PEI/nucleic acid mass ratio of 5:1 at the indicated nucleic acid concentrations, see Fig. S1) were added to the cells. 48 h after cultivating in medium containing 2 % FCS, WST-1 assays were performed as described by manufacturer. Absorbance was measured in a Tecan Safire^2 plate reader at a fixed wavelength of 450 nm and at 600 nm as background control. Measurements were done at 0.5, 1, 2 and 4 h to determine cell viability.

Supplementary Figure

Figure Legend

Figure S1: WST-1 cell viability assay of HeLa cells transfected with the 14-mer LNA antiseed 17-5p, the hairpin inhibitor 20a and the 8-mer LNA (PS). Oligonucleotides were complexed with PEI F25-LMW at the indicated concentrations using a PEI/oligonucleotide mass ratio of 5:1. After 48 h, WST-1 activity was measured at 450 nm with an incubation period of 2 h. Untransfected HeLa cells grown in 2% FCS were used as a control and their activity was set to 1 for normalization. Values are derived from three independent experiments (+/- S.E.M.).

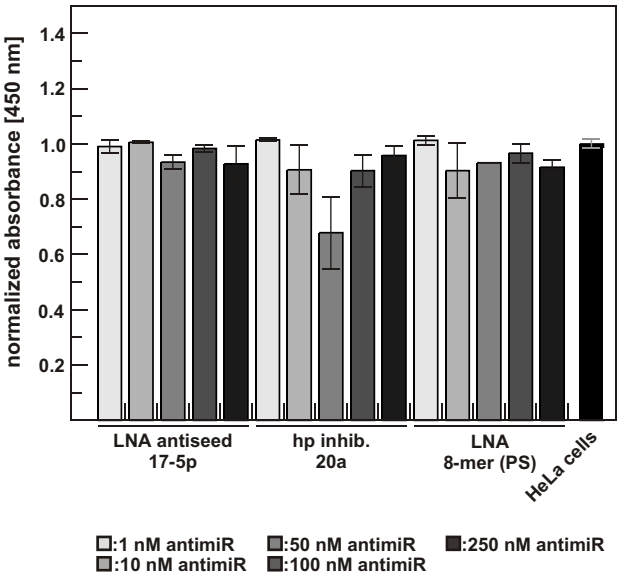
normalized absorbance [450 nm]
1.4
1.2
1.0
0.8
0.6
0.4
0.2
LNA antiseed 17-5p
hp inhib. 20a
LNA 8-mer (PS)
HeLa cells
:1 nM antimiR
:10 nM antimiR
:50 nM antimiR
:100 nM antimiR
:250 nM antimiR

Fig. S1

D. Publication IV

Pim-1 Dependent Transcriptional Regulation of the Human miR-17-92 Cluster.

Manuscript in preparation

Author contributions:

Research design: 35 %

Experimental work: 60 %

Data analysis and evaluation: 65 %

Manuscript writing: 50 %

Pim-1 Dependent Transcriptional Regulation of the Human miR-17-92 Cluster*

Maren Thomas[1,+], Kerstin Lange-Grünweller[1,+], Dorothee Hartmann[1], Lara Golde[1], Julia Schlereth[1], Achim Aigner[2], Arnold Grünweller[1,#] and Roland K. Hartmann[1,#]

[1]Institut für Pharmazeutische Chemie, Philipps-Universität Marburg; Marburg, Germany

[2]Medizinische Fakultät, Rudolf-Boehm-Institut für Pharmakologie und Toxikologie, Universität Leipzig; Leipzig, Germany
[+]The authors contribute equally to this work.

*****Running title: *Transcriptional regulation of human miR-17-92*

[#]To whom correspondence should be addressed: Roland K. Hartmann and Arnold Grünweller, Philipps-Universität Marburg, Institut für Pharmazeutische Chemie, Marbacher Weg 6, 35037 Marburg, Tel.: +49-6421-28-25553; Fax: +49-6421-28-25854; E-mail: roland.hartmann@staff.uni-marburg.de and arnold.gruenweller@staff.uni-marburg.de

Keywords: miRNA, miR-17-92 cluster, Pim-1, miRNA promoter, c-Myc, HP1γ, RNAi

Background: Expression of the human miR-17-92 cluster is driven from a host gene promoter located within a CpG island and from an intronic A/T-rich region located directly upstream of the first miRNA 17-5p.
Results: Substantial transcriptional activity from the A/T-rich region relies on c-Myc binding to a functional E-box element (E3 site) and involves a synergism between c-Myc and the protooncogene Pim-1.
Conclusion: Pim-1 is part of the transcriptional network that regulates expression of the human miR-17-92 cluster.
Significance: Little is known about promoters of oncogenic miRNAs or miRNA clusters. Understanding the regulation of oncogenic miRNA expression opens up new perspectives for the prevention of cancer.

SUMMARY

The human polycistronic miRNA cluster miR-17-92 is frequently overexpressed in hematopoietic malignancies and cancers. Its transcription is in part controlled by an E2F-regulated host gene promoter. An intronic A/T-rich region directly upstream of the miRNA coding region also contributes to cluster expression. Deletion analysis of the A/T-rich region revealed a strong dependence on c-Myc binding to the functional E3 site. Yet, constructs lacking the 5'-proximal ~1.3 kb or 3'-distal ~0.1 kb of the 1.5 kb A/T-rich region still retained residual specific promoter activity, suggesting multiple transcription start sites (TSS) in this region. Furthermore, the protooncogenic kinase Pim-1, its phosphorylation target HP1γ and c-Myc colocalize to the E3 region, as inferred from chromatin immunoprecipitation. Analysis of pri-mir-17-92 expression levels in K562 and HeLa cells revealed that silencing of E2F3, c-Myc or Pim-1 negatively affects cluster expression, with a synergistic effect caused by c-Myc/Pim-1 double knockdowns in HeLa cells. Thus, we show for the first time, that Pim-1 is part of the transcriptional network that regulates the human miR-17-92 cluster.

MicroRNAs (miRNAs) are important post-transcriptional riboregulators of gene expression with high relevance to cancer formation and metastasis (1). In general, miRNAs are derived from RNA polymerase II (RNAPII) primary transcripts (pri-miRNA) that are further processed to ~70 nt precursors (pre-miRNA) and after nuclear export to mature miRNAs by the activity of the two endonucleases DROSHA/DGCR8 and DICER (2-5). MiRNAs are incorporated into the miRNA-induced silencing complex (miRISC) and act as repressors of translation by imperfect base-pairing to their target sites in mRNAs (3). The majority of miRNAs is encoded in intronic regions, either individually or as "polycistronic" miRNA clusters that are cotranscribed (3,6).

Several deregulated miRNAs or miRNA clusters are involved in tumorigenesis,

accounting for their designation as oncogenic miRNAs (7). Such miRNAs can downregulate targets involved in the regulation of apoptosis or cell cycle progression (1). One well-characterized polycistronic cluster is the miR-17-92 cluster, also known as OncomiR-1 or C13*orf*25. This cluster encodes six miRNAs belonging to four different seed families: (i) the miR-17 family with miR-17 and miR-20a, (ii) the miR-18 family with miR-18a, (iii) the miR-19 family with miR-19a and miR-19b-1, and (iv) the miR-92 family (8-11). The human miR-17-92 cluster is encoded in the chromosomal region 13q31.3 and is amplified in several solid tumors as well as in some hematopoietic malignancies (8,12). Because of numerous known targets of its individual miRNAs, the miR-17-92 locus exerts pleiotropic functions during development, proliferation, apoptosis and angiogenesis in different cell systems (13-15). In mice, deletion of the cluster prevents normal B-cell development as a consequence of premature cell death (14). In a mouse B-cell lymphoma model, simultaneous overexpression of c-Myc and the miR-17-92 cluster accelerated lymphomagenesis (9). This oncogenic effect could later be assigned primarily to miR-19a/b which dampens expression of the tumor suppressor PTEN, thereby repressing apoptosis (13,15).

Analyses of transcriptional regulation of oncogenic miRNAs and miRNA clusters are of great importance for strategies aiming at cancer prevention. Unfortunately, most miRNA promoters have not been characterized or identified yet (16). In case of the miR-17-92 cluster, expression is thought to be promoted from a host gene promoter region upstream of exon 1, with transcription starting at a consensus initiator sequence downstream of a non-consensus TATA box (17,18). Additionally, this core promoter region contains functional E2F transcription factor binding sites. E2F1-3 were shown to activate C13*orf*25 expression from this promoter and chromatin immunoprecipitation assays (ChIP) identified E2F3 to be the main E2F variant associated with the host gene promoter (17, 18). No E2F binding was detected in the region between the host gene promoter and the miR-17-92 cluster (18). Furthermore, nucleosome mapping combined with chromatin signatures for transcriptionally active promoters (19-21) indicated that transcriptional activity of the miR-17-92 cluster also originates from the intronic A/T-rich region directly upstream of the miRNA coding sequences (16). This is in line with the finding that cluster expression is activated by c-Myc binding to a conserved E-box element (E3) ~1.5 kb upstream of the miRNA coding sequence (9,10,20). Indeed, luciferase reporter assays confirmed that both, the host gene promoter and the intronic region, confer transcriptional activity (16,21).

Here, we subjected the intronic A/T-rich region to deletion analysis using luciferase reporter constructs. Transcription was found to strongly depend on c-Myc, but even shorter fragments (< 0.3 kb) of sequences directly preceding the miR-17-92 coding sequence still promoted residual, but substantial and specific transcriptional activity. Furthermore, we identified the protooncogene Pim-1 and one of its phosphorylation targets HP1γ (22) to be associated with the chromatin region containing the E3 site, suggesting that the human C13*orf*25 locus belongs to the set of genes that are synergistically regulated by c-Myc and Pim-1 (23,24). SiRNA-mediated Pim-1 knockdown indeed resulted in reduced pri-mir-17-92 levels, as did a knockdown of c-Myc or E2F3. In Hela cells, a double knockdown of c-Myc/Pim-1 decreased the pri-mir-17-92 levels more than single knockdowns, providing further evidence for a synergism of c-Myc and Pim-1 at the intronic C13*orf*25 promoter.

EXPERIMENTAL PROCEDURE

Oligonucleotides - Small interfering RNAs (siRNAs) were purchased from Dharmacon (Boulder, USA):

VR1 siRNA (25) was used as an unrelated negative control, with the following sequences of sense and antisense strand:.

VR1 siRNA sense 5'-GCG CAU CUU CUA CUU CAA CdTdT and antisense 5'-GUU GAA GUA GAA GAU GCG CdTdT.

The sequences of all other siRNAs used in this study are:

Pim-1 siRNA sense 5'-GAU AUG GUG UGU GGA GAU AdTdT and antisense 5'-UAU CUC CAC ACA CCA UAU CdTdT; Pim-1 siRNA 2 sense 5'-GGA ACA ACA UUU ACA ACU CdTdT and antisense 5'-GAG UUG UAA AUG UUG UUC CdTdT; c-Myc siRNA sense 5'-CAG GAA CUA UGA CCU CGA CUA dTdT and antisense 5'-UAG UCG AGG UCA UAG UUC CUG dTdT; E2F3 siRNA sense 5'- ACA GCA AUC UUC CUU

AAU AdTdT and antisense 5'- UAU UAA GGA AGA UUG CUG UdTdT.

Antibodies - Antibodies against c-Myc (sc-40) and Pim-1 (sc-13513) as well as the secondary antibody (sc-2005: goat anti-mouse IgG HRP conjugated) were purchased from Santa Cruz Biotechnology (Heidelberg, Germany) except for the Phospho HP1γ (Ser83) antibody (2600S), which was obtained from Cell Signaling Technology (Danvers, MA, USA).

Plasmid construction and seed mutagenesis For the construction of promoter-luciferase fusions, the SV40 promoter of plasmid "pGL3 control" (Promega, Mannheim, Germany) was removed via digestion with *Bgl*II and *Hind*III (Thermo Fisher Scientific, Schwerte, Germany) and replaced with fragments derived from the intronic A/T-rich region of C13*orf*25 (reference nucleotide sequence NG_032702.1). Promoter fragments were amplified from genomic DNA of the human cell line K562 using primers specified in Supplementary Material. PCR products were purified using the Wizard® SV Gel and PCR Clean-Up System (Promega, Mannheim, Germany) and digested with *Bgl*II and *Hind*III for insertion into pGL3. All constructs were cloned in *E. coli* DH5α cells and verified via DNA sequencing. The pGL3 vector lacking the SV40 promoter as well as the pGL3 construct carrying the C13*orf*25-derived 339 bp fragment in inverse orientation (pGL3 339 bp inv) were used as negative controls.

Transfection procedures and Luciferase reporter assays - Assays are described in detail in Supplementary Material.

Chromatin immunoprecipitation - Chromatin immunoprecipitation (ChIP) was performed according to a protocol from the Or Gozani lab at Stanford University (http://www.stanford.edu/group/gozani), with some modifications. For details, see Supplementary Material.

RESULTS

C-Myc-dependent intronic transcriptional activity within the human miR-17-92 locus – The 3.4 kb upstream genomic region of the miR-17-92 coding sequence can be subdivided into a G/C-rich and an A/T-rich part. The former is a CpG island (~1.9 kb, 78 % GC content; see http://genome.ucsc.edu, GRCh37/hg19 assembly) that has its 5'-boundary ~0.4 kb upstream of the TSS of the host gene promoter (20) and its 3'-boundary ~1.4 kb upstream of the miR-17-5p coding sequence, representing the 5'-terminal miRNA of the cluster. The A/T-rich region (~64 % A/T content) following the CpG island begins immediately downstream of a functional and highly conserved c-Myc binding site (5'-CATGTG, E-box E3) which is localized ~1.5 kb upstream of the miR-17-5p coding sequence (10) (Fig. 1A, S1).

We have analyzed the intronic region of C13*orf*25, including the preceding functional c-Myc box E3 (20) and truncated segments of the A/T-rich region (Fig. 1B), for independent transcriptional activity and c-Myc dependence. For this purpose, luciferase reporter constructs were transfected into K562 and HeLa cells. We selected these two cell lines because they express the miR-17-92 cluster at very high (K562) and high (HeLa) levels (26, Fig. S2).

The ~1.5 kb reporter construct, comprising c-Myc box E3 (Fig. 1A, S1) and the A/T-rich region except for the 113 bp preceding the mature miR-17-5p coding sequence, showed substantial transcriptional activity, amounting to 30-35 % in both cell lines relative to the pGL3 control plasmid harboring an SV40 promoter (Fig. 1C). This is in line with results of a similar study of the mouse miR-17-92 locus (21). Furthermore, Ozsolak et al. (16) predicted an intronic TSS to be localized ~0.2 kb downstream of the E3 site. Indeed, truncating the 1.5 kb fragment to 625 bp, which deletes the E3 site, strongly reduced reporter activity, ~4.5-fold in K562 and almost 20-fold in HeLa cells compared to the activity of the ~1.5 kb construct (Fig. 1C). To substantiate this finding, we tested the ~1.5 kb construct in K562 cells under conditions of an siRNA-mediated knockdown of c-Myc. This reduced reporter expression to a similar extent as the truncation to 625 bp, supporting the notion that c-Myc binding to the E3 site plays a key role in activating transcription from this intronic region (Fig. 1C). As the 625 bp fragment still conferred basal promoter activity, we further shortened this region to ~340 bp, ~280 bp and ~200 bp. Additionally, we included short fragments with their 3'-boundary ~290 bp upstream of the mature miR-17-5p coding sequence (250, 190 and 108 bp in Fig. 1B). We also inversed the orientation of the ~340 bp fragment in front of the luciferase gene (Fig. 1C, 339 bp inv) to include a control fragment with comparable A/T content. This inversed fragment conferred reporter activity 5.3-fold (K562) or 2.4-fold

(HeLa) higher than that of the pGL3 control vector lacking the SV40 promoter (ΔSV40, Fig. 1C).

All the fragments ≤ 340 bp conferred residual promoter activity, some clearly to a higher extent than the inverted 339 bp fragment in both cell lines (see the 279 and 197 bp fragments, Fig. 1 C). This indicates that parts of the intronic A/T-rich region promote specific transcriptional activity, the extent partly differing between the two cell lines (Fig. 1 C). Unfortunately, we were unable to identify any convincing correlation between fragment activity and promoter elements predicted in this region using a variety of web-based promoter prediction tools (see Suppl. Material). In K562 cells, the smaller fragments, including the 625 bp fragment, showed an overall trend towards stronger expression relative to HeLa cells.

Pim-1 and HP1γ are associated with the intronic c-Myc binding site - We next asked if other factors beyond c-Myc may be involved in human miR-17-92 cluster expression from the A/T-rich region. Transcriptional regulation by c-Myc is associated with Pim-1-dependent H3S10 phosphorylation in about 20 % of all genes regulated by c-Myc (24). Moreover, Pim-1 and c-Myc act synergistically in severe forms of B-cell lymphomas, and Pim-1 as well as the miR-17-92 cluster are overexpressed in the myeloid leukemia suspension cell line K562 (27). We performed ChIP assays to test whether c-Myc and Pim-1 localize to the internal promoter region of the miR-17-92 cluster. For this analysis, we amplified a ~90 bp DNA fragment (segment A1 in Fig. 2A) 0.1 kb downstream of the functional c-Myc E3 site. The same DNA segment was analyzed in a previous study (10). Our ChIP analysis revealed that not only c-Myc, as expected, but also Pim-1 localizes to this genomic region (Fig. 2B, upper and middle panels). Indeed, this is consistent with the finding that Pim-1-catalyzed H3S10 phosphorylation is required for c-Myc-dependent transcriptional activation (24). We further analyzed another known phosphorylation target of Pim-1, the heterochromatin protein-1 gamma (HP1γ) (22), for its association with the E3 region. HP1γ localized to this genomic area as well (Fig. 2B, lower panel). Moreover, we were able to identify an association of HP1γ along the miRNA coding region which is indicative of active transcription (see Fig. S3 and Discussion section).

Transcriptional activity of the human miR-17-92 cluster depends on c-Myc and Pim-1 - To further substantiate the role of Pim-1 in miR-17-92 cluster expression we quantified the cellular pri-mir-17-92 levels by qRT-PCR after siRNA-mediated Pim-1 knockdown relative to a c-Myc knockdown in K562 and HeLa cells. Since combined ChIP and reporter gene assays suggested that transcription factor E2F3 is a major activator of transcription initiated at the host gene promoter (17,18), we included E2F3 in our knockdown experiments as a possible measure for the contribution of the host gene promoter to miR-17-92 expression. We also quantified the levels of c-Myc, E2F3 and Pim-1 mRNAs after knockdown by qRT-PCR to evaluate knockdown efficiencies (Table S1). For Pim-1, we have shown good correlation between mRNA and protein levels (27). In the study presented here, only experiments with a knockdown efficiency > 50 % were considered (Table S1). Single knockdowns of either c-Myc, E2F3 or Pim-1 decreased the pri-mir-17-92 levels in HeLa cells to ~35, 60 and 60 %, respectively, relative to the control siRNA (Fig. 3B), and to ~30, 30 and 45 %, respectively, in K562 cells (Fig. 3C). Double knockdowns had additive suppression effects on pri-mir-17-92 levels in the case of c-Myc/E2F3 (HeLa and K562), c-Myc/Pim-1 (Hela) and E2F3/Pim-1 (HeLa).

DISCUSSION

Transcription of the oncogenic miR-17-92 cluster is thought to originate from two different TSSs: one is localized in close proximity to the host gene promoter element (17) (Fig. S1), and the other TSS was predicted to map to the region ~200 bp downstream of the functional c-Myc site E3 (Fig. 1A, S1). The latter prediction was based on nucleosome mapping and chromatin signatures for active promoters. The derived algorithm identified 175 human promoters proximal to miRNA coding sequences, and was reported to correctly predict transcription initiation regions to a resolution of 150 bp with high sensitivity and specificity. The majority of predictions were also consistent with known “expressed sequence tag” (EST) TSSs or cDNA 5’-ends (16).

Here, we investigated the intronic A/T-rich region preceding the human miR-17-92 cluster

in more detail than previously done by similar reporter gene assays (16,20,21). In addition, we analyzed the impact of an siRNA-mediated c-Myc knockdown (efficieny ~80 %) on reporter expression in K562 cells. The observed effect was similar to the one obtained by reducing the 1.5 kb fragment to 625 bp (Fig. 1), which deleted the c-Myc E3 site. Our findings substantiate the notion that this site plays a crucial role in activating transcription from the intronic promoter region (16,20,21). Noteworthy, the 625 bp and even some of the further truncated fragments (~280 and ~200 bp) of the A/T-rich region conferred residual specific promoter activity in both cell types (Fig. 1), indicating that parts of the A/T-rich region, downstream and independent of the c-Myc E3 site, contribute to cluster expression. This c-Myc E3 box-independent activation was more pronounced for K562 relative to HeLa cells, which correlates with the particularly high cluster expression in K562 cells (Fig. S2).

ChIP assays revealed that c-Myc, the protooncogene Pim-1 and its phosphorylation target HP1γ associate with the chromatin region harboring the c-Myc E3 site (Fig. 2B). Importantly, Pim-1-catalyzed phosphorylation of H3S10 at c-Myc target genes is necessary to regulate key genes required for c-Myc-dependent oncogenic transformation (26).

In mammals, three paralogs of HP1 (α, β and γ) regulate heterochromatin formation, gene silencing or gene activation (28,29). HP1α and β proteins are mainly recruited to heterochromatin regions harboring H3K9me2,3 modifications, whereas HP1γ is found in association with euchromatin (30) and active genes (29). Furthermore, HP1c, the *Drosophila* homolog of HP1γ, associates with trancriptionally active chromatin containing H3K4me3 and H3K36me3 histone marks (28). HP1γ can further be recruited to inducible promoters where it replaces HP1β, thereby inducing a switch from the repressive to the active transcriptional state. This replacement with HP1γ requires H3 phospho-acetylation (31). In this context, a transient phosphorylation of H3S10 (via Aurora B kinase) was shown to be necessary for the dissociation of HP1 proteins from chromatin during M phase of the cell cycle (32). In the induced state, HP1γ can also be localized within coding regions of protein genes together with elongating RNA polymerase II (31).

Our data, showing that HP1γ colocalizes with Pim-1 and c-Myc (Fig. 2), is in line with the aforementioned activating role of HP1γ during transcription. We extended our ChIP assays to the miRNA coding region of C13*orf*25 to analyze HP1γ association with this part of the cluster. Indeed, ChIP analysis along the miRNA coding sequence identified HP1γ at all four analyzed subregions (A2-A5, Fig. S3). This is to our knowledge the first indication that HP1γ is involved in the activation of miRNA gene transcription.

Association of Pim-1 with the intronic chromosomal region near the c-Myc E3 site gave rise to the assumption that Pim-1 plays an important role in the transcriptional activation of the miR-17-92 cluster. This was tested by RNAi also including E2F3 as an assumed indicator of host gene promoter activity. The strong negative effects of individual knockdowns of c-Myc, Pim-1 and E2F3 on pri-mir-17-92 levels indicate that all three proteins are important for cluster expression and suggests their direct involvement in C13*orf*25 expression, either affecting transcription from the host gene promoter (E2F3) or the intronic promoter region (c-Myc, Pim-1). Of course, we cannot exclude that indirect effects have contributed as well, e.g. due to effects originating from inhibition of cell proliferation (Pim-1), changes in the kinetics of pri-mir-17-92 processing, global changes in transcriptional networks (E2F3, c-Myc) or mutual transactivation (E2F3 and c-Myc) (33-35). Further complication may arise from the fact that miR-17-5p and miR-20a of the cluster are negative regulators of E2F1-3 mRNAs (10, 18).

The siRNA-mediated c-Myc knockdown, decreasing c-Myc mRNA levels on average by 65 % (HeLa) or 81 % (K562; see Table S1), resulted in a 60-70 % reduction in pri-mir-17-92 levels in HeLa and K562 cells (Fig. 3). This effect may report a rough estimate of the proportion of cluster transcripts normally initiated in the intronic promoter region in these two cell lines, for the following reasons. The C13*orf*25 region contains four c-Myc binding sites (boxes E1-4) and two additional ones with lower c-Myc occupancy (relative to E1) upstream of the host gene promoter (20). Box E1, immediately downstream of host gene promoter's TSS, was shown by deletion analysis to be inhibitory, which correlates with c-Myc forming heterodimers with MXI or

MNT at this site to repress transcription (20). Thus, host gene promoter activity may even somewhat increase under conditions of a c-Myc knockdown, although such an effect could in turn be neutralized by reduced c-Myc-mediated transactivation of E2F (35). ChIP-Seq data for K562 and HeLa-S3 cells revealed the by far highest c-Myc occupancy at site E3 (little at E2 and E4), where c-Myc forms heterodimers with MAX to activate transcription (20). A straightforward interpretation of the additive effect of a c-Myc/E2F3 double knockdown in Hela and K562 cells is that this combination negatively affected transcription from the host gene and intronic promoter regions.

A major finding of our study is the involvement of the oncogenic kinase Pim-1 in miR-17-92 expression, as inferred from its recruitment to the intronic c-Myc E3 site (Fig. 2) and the strong negative effect of a Pim-1 knockdown on cluster expression (Fig. 3B and C). Moreover, double knockdown experiments in HeLa cells revealed a synergistic effect relative to individual c-Myc and Pim-1 knockdowns (Fig. 3B). This was not seen for K562 cells, attributable to the extremely high expression of Pim-1 in this cell line (27) which makes it more difficult to deplete Pim-1 in K562 cells below a crititcal threshold. Furthermore, the siRNA-mediated reduction of c-Myc and Pim-1 mRNAs were on average 86 % and 77 % in HeLa and 86 % and 52 %, respectively, in K562 cells (Table S1). The somewhat weaker suppression of Pim-1 in the c-Myc/Pim-1 double knockdown context (cf. with single knockdowns, Table S1) in K562 versus HeLa cells may have contributed to the absence of a clear additive effect upon c-Myc/Pim-1 double knockdown in K562 cells.

In conclusion, we report here that miR-17-92 cluster expression from the intronic A/T-rich promoter region, although critically depending on c-Myc binding, includes a c-Myc-independent specific contribution of sequences within ~0.7 kb upstream of the mature miR-17-5p coding sequence. Our reporter expression data suggest multiple TSSs within this A/T-rich region, although the transcription initiation region predicted by Ozsolak et al. (16), ~0.2 kb downstream of the c-Myc E3 box, may well be the major one. C-Myc-independent transcription initiation within ~0.7 kb upstream of the mature miR-17-5p coding sequence was more pronounced in K562 versus HeLa cells (Fig. 1), indicating cell type-specific differences in cluster expression from the intronic promoter region. Our RNAi results are consistent with E2F3 activating the C13*orf*25 host gene promoter and Pim-1 acting in concert with c-Myc at the E3 site to activate transcription from the intronic promoter region.

REFERENCES

1. Iorio, M. V, and Croce, C. M. (2009) MicroRNAs in cancer: small molecules with a huge impact. *Journal of Clinical Oncology* **27**, 5848–56
2. Krol, J., Loedige, I., and Filipowicz, W. (2010) The widespread regulation of microRNA biogenesis, function and decay. *Nature Reviews. Genetics* **11**, 597–610
3. Bartel, D. P. (2004) MicroRNAs: Genomics, Biogenesis, Mechanism, and Function. *Cell* **116**, 281–297
4. Denli, A. M., Tops, B. B. J., Plasterk, R. H. a, Ketting, R. F., and Hannon, G. J. (2004) Processing of primary microRNAs by the Microprocessor complex. *Nature* **432**, 231–5
5. Yi, R., Qin, Y., Macara, I. G., and Cullen, B. R. (2003) Exportin-5 mediates the nuclear export of pre-microRNAs and short hairpin RNAs. *Genes & Development* **17**, 3011–6
6. Lee, Y., Jeon, K., Lee, J.-T., Kim, S., and Kim, V. N. (2002) MicroRNA maturation: stepwise processing and subcellular localization. *The EMBO Journal* **21**, 4663–70
7. Esquela-Kerscher, A., and Slack, F. J. (2006) Oncomirs - microRNAs with a role in cancer. *Nature Reviews. Cancer* **6**, 259–69
8. Ota, A., Tagawa, H., Karnan, S., Tsuzuki, S., Karpas, A., Kira, S., Yoshida, Y., and Seto, M. (2004) Identification and Characterization of a Novel Gene, C13orf25, as a Target for 13q31-q32 Amplification in Malignant Lymphoma. *Cancer Research* **64**, 3087–3095
9. He, L., Thomson, J. M., Hemann, M. T., Hernando-Monge, E., Mu, D., Goodson, S., Powers, S., Cordon-Cardo, C., Lowe, S. W., Hannon, G. J., and Hammond, S. M. (2005) A microRNA polycistron as a potential human oncogene. *Nature* **435**, 828–33

10. O'Donnell, K. A., Wentzel, E. A., Zeller, K. I., Dang, C. V, and Mendell, J. T. (2005) c-Myc-regulated microRNAs modulate E2F1 expression. *Nature* **435**, 839–43
11. Tanzer, A., and Stadler, P. F. (2004) Molecular evolution of a microRNA cluster. *Journal of Molecular Biology* **339**, 327–35
12. Lu, J., Getz, G., Miska, E. A., Alvarez-Saavedra, E., Lamb, J., Peck, D., Sweet-Cordero, A., Ebert, B. L., Mak, R. H., Ferrando, A. A., Downing, J. R., Jacks, T., Horvitz, H. R., and Golub, T. R. (2005) MicroRNA expression profiles classify human cancers. *Nature* **435**, 834–8
13. Olive, V., Bennett, M. J., Walker, J. C., Ma, C., Jiang, I., Cordon-Cardo, C., Li, Q.-J., Lowe, S. W., Hannon, G. J., and He, L. (2009) miR-19 is a key oncogenic component of mir-17-92. *Genes & Development* **23**, 2839–49
14. Ventura, A., Young, A. G., Winslow, M. M., Lintault, L., Meissner, A., Erkeland, S. J., Newman, J., Bronson, R. T., Crowley, D., Stone, J. R., Jaenisch, R., Sharp, P. A., and Jacks, T. (2008) Targeted deletion reveals essential and overlapping functions of the miR-17 through 92 family of miRNA clusters. *Cell* **132**, 875–86
15. Mu, P., Han, Y.-C., Betel, D., Yao, E., Squatrito, M., Ogrodowski, P., De Stanchina, E., D'Andrea, A., Sander, C., and Ventura, A. (2009) Genetic dissection of the miR-17~92 cluster of microRNAs in Myc-induced B-cell lymphomas. *Genes & Development* **23**, 2806–11
16. Ozsolak, F., Poling, L. L., Wang, Z., Liu, H., Liu, X. S., Roeder, R. G., Zhang, X., Song, J. S., and Fisher, D. E. (2008) Chromatin structure analyses identify miRNA promoters. *Genes & Development* **22**, 3172–83
17. Woods, K., Thomson, J. M., and Hammond, S. M. (2007) Direct regulation of an oncogenic micro-RNA cluster by E2F transcription factors. *The Journal of Biological Chemistry* **282**, 2130–4
18. Sylvestre, Y., De Guire, V., Querido, E., Mukhopadhyay, U. K., Bourdeau, V., Major, F., Ferbeyre, G., and Chartrand, P. (2007) An E2F/miR-20a autoregulatory feedback loop. *The Journal of Biological Chemistry* **282**, 2135–43
19. Guenther, M. G., Levine, S. S., Boyer, L. A., Jaenisch, R., and Young, R. A. (2007) A Chromatin Landmark and Transcription Initiation at Most Promoters in Human Cells. *Cell* **130**, 77–88
20. Ji, M., Rao, E., Ramachandrareddy, H., Shen, Y., Jiang, C., Chen, J., Hu, Y., Rizzino, A., Chan, W. C., Fu, K., and McKeithan, T. W. (2011) The miR-17-92 microRNA cluster is regulated by multiple mechanisms in B-cell malignancies. *The American Journal of Pathology* **179**, 1645–56
21. Pospisil, V., Vargova, K., Kokavec, J., Rybarova, J., Savvulidi, F., Jonasova, A., Necas, E., Zavadil, J., Laslo, P., and Stopka, T. (2011) Epigenetic silencing of the oncogenic miR-17-92 cluster during PU.1-directed macrophage differentiation. *The EMBO Journal* **30**, 4450–64
22. Koike, N., Maita, H., Taira, T., Ariga, H., and Iguchi-Ariga, S. M. M. (2000) Identification of heterochromatin protein 1 (HP1) as a phosphorylation target by Pim-1 kinase and the effect of phosphorylation on the transcriptional repression function of HP1. *FEBS Letters* **467**, 17–21
23. Nawijn, M. C., Alendar, A., and Berns, A. (2011) For better or for worse: the role of Pim oncogenes in tumorigenesis. *Nature Reviews. Cancer* **11**, 23–34
24. Zippo, A., De Robertis, A., Serafini, R., and Oliviero, S. (2007) PIM1-dependent phosphorylation of histone H3 at serine 10 is required for MYC-dependent transcriptional activation and oncogenic transformation. *Nature Cell Biology* **9**, 932–44
25. Grünweller, A., Gillen, C., Erdmann, V. A., and Kurreck, J. (2003) Cellular uptake and localization of a Cy3-labeled siRNA specific for the serine/threonine kinase Pim-1. *Oligonucleotides* **13**, 345–52
26. Venturini, L., Battmer, K., Castoldi, M., Schultheis, B., Hochhaus, A., Muckenthaler, M. U., Ganser, A., Eder, M., and Scherr, M. (2007) Expression of the miR-17-92 polycistron in chronic myeloid leukemia (CML) CD34+ cells. *Blood* **109**, 4399–405
27. Thomas, M., Lange-Grünweller, K., Weirauch, U., Gutsch, D., Aigner, A., Grünweller, A., and Hartmann, R. K. (2012) The proto-oncogene Pim-1 is a target of miR-33a. *Oncogene* **31**, 918–28
28. Kwon, S.H., and Workman, J.L. (2011) HP1c casts light on dark matter. *Cell Cycle* **15**, 625-30

29. Vakoc, C. R., Mandat, S. A., Olenchock, B. A., and Blobel, G. A. (2005) Histone H3 lysine 9 methylation and HP1gamma are associated with transcription elongation through mammalian chromatin. *Molecular Cell* **19**, 381–91
30. Minc, E., Allory, Y., Worman, H. J., Courvalin, J., and Buendia, B. (1999) Localization and phosphorylation of HP1 proteins during the cell cycle in mammalian cells. *Chromosoma* **108**, 220–234
31. Mateescu, B., Bourachot, B., Rachez, C., Ogryzko, V., and Muchardt, C. (2008) Regulation of an inducible promoter by an HP1beta-HP1gamma switch. *EMBO Reports* **9**, 267–72
32. Fischle, W., Tseng, B. S., Dormann, H. L., Ueberheide, B. M., Garcia, B. A., Shabanowitz, J., Hunt, D. F., Funabiki, H., and Allis, C. D. (2005) Regulation of HP1-chromatin binding by histone H3 methylation and phosphorylation. *Nature* **438**, 1116–22
33. Adams, M.R., Sears, R., Nuckolls, F., Leone, G., and Nevins, J.R. (2000) Complex transcriptional regulatory mechanisms control expression of the E2F3 locus. *Mol Cell Biol.* **20**, 3633-9
34. Thalmeier, K., Synovzik, H., Mertz, R., Winnacker, E.L., and Lipp, M. (1989) Nuclear factor E2F mediates basic transcription and trans-activation by E1a of the human MYC promoter. *Genes Dev.* **3**, 527-36
35. Wong, J.V., Dong, P., Nevins, J.R., Mathey-Prevot, B., and You, L. (2011) Network calisthenics: control of E2F dynamics in cell cycle entry. *Cell Cycle.* **15**, 3086-94

Conflict of Interest - The authors declare no conflict of interest.

Acknowledgments - We are grateful to Lisa Schemberger, Nicole Bürger and Moana Klein for technical assistance, Marcus Lechner for statistical analyses, and Dr. Markus Gößringer for fruitful discussions. The work was supported by grants of the German Cancer Aid (Deutsche Krebshilfe, grants 106992 and 109260 to A.G., R.K.H. and A.A.).

FOOTNOTES

*This work was supported by grants of the German Cancer Aid (Deutsche Krebshilfe, grants 106992 and 109260 to A.G., R.K.H. and A.A.).

[1]To whom correspondence should be addressed: Roland K. Hartmann and Arnold Grünweller, Philipps-Universität Marburg, Institut für Pharmazeutische Chemie, Marburg, Germany, Tel.: +49-6421-28-25553; Fax: +49-6421-28-25854; E-mail: roland.hartmann@staff.uni-marburg.de and arnold.gruenweller@staff.uni-marburg.de

[2]Medizinische Fakultät, Rudolf-Boehm-Institut für Pharmakologie und Toxikologie, Universität Leipzig; Leipzig, Germany

[3]The abbreviations used are: AB (antibody), bp (base pair), C13*orf*25 (chromosome 13 *open reading frame* 25), ChIP (chromatin immunoprecipitation), FCS (fetal calf serum), kb (= kbp; kilo base pair), miRISC (miRNA-induced silencing complex), miRNA (microRNA), mRNA (messenger RNA), nt (nucleotide), pre-miRNA (precursor miRNA), pri-miRNA (primary miRNA), qRT-PCR (quantitative real-time polymerase chain reaction), RLU (relative light units), RNAi (RNA interference), siRNA (small interfering RNA), TSS (transcription start site)

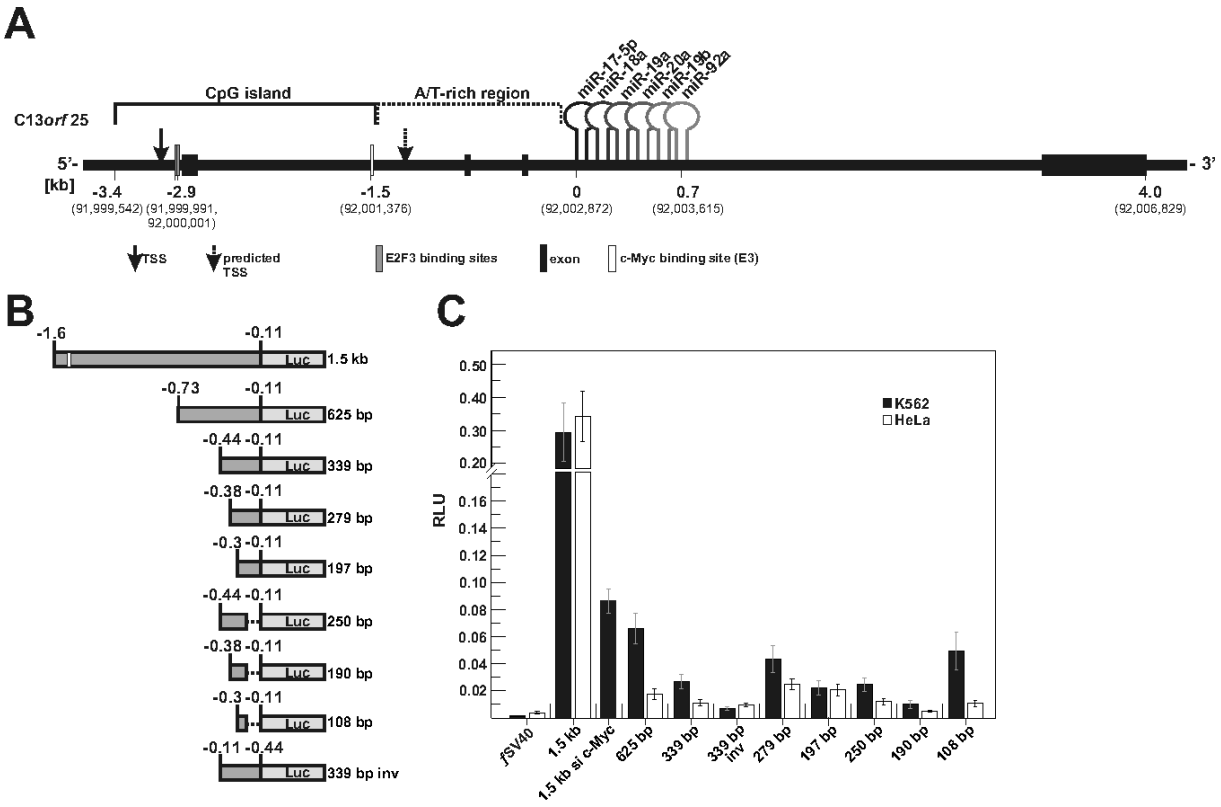
A
CpG island
A/T-rich region
miR-17-5p
miR-18a
miR-19a
miR-20a
miR-19b
miR-92a
C13orf 25
5'-
- 3'
[kb]
-3.4
-2.9
-1.5
0
0.7
4.0
(91,999,542)
(91,999,991, 92,000,001)
(92,001,376)
(92,002,872)
(92,003,615)
(92,006,829)
TSS
predicted TSS
E2F3 binding sites
exon
c-Myc binding site (E3)
B
-1.6
-0.11
Luc
1.5 kb
-0.73
625 bp
-0.44
339 bp
-0.38
279 bp
-0.3
197 bp
250 bp
190 bp
108 bp
339 bp inv
C
RLU
K562
HeLa
0.50
0.40
0.30
0.20
0.16
0.14
0.12
0.10
0.08
0.06
0.04
0.02
pSV40
1.5 kb
1,5 kb si c-Myc
625 bp
339 bp
339 bp inv
279 bp
197 bp
250 bp
190 bp
108 bp

Fig. 1

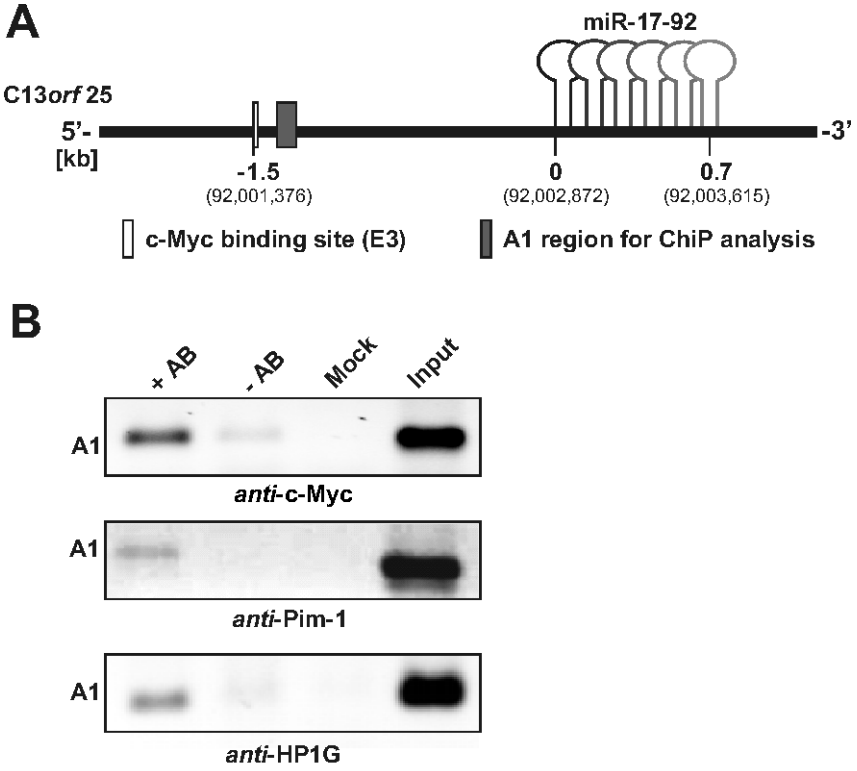
A
miR-17-92
C13orf 25
5'-
[kb]
-3'
-1.5
(92,001,376)
0
(92,002,872)
0.7
(92,003,615)
c-Myc binding site (E3)
A1 region for ChiP analysis
B
+ AB
- AB
Mock
Input
A1
anti-c-Myc
A1
anti-Pim-1
A1
anti-HP1G

Fig. 2

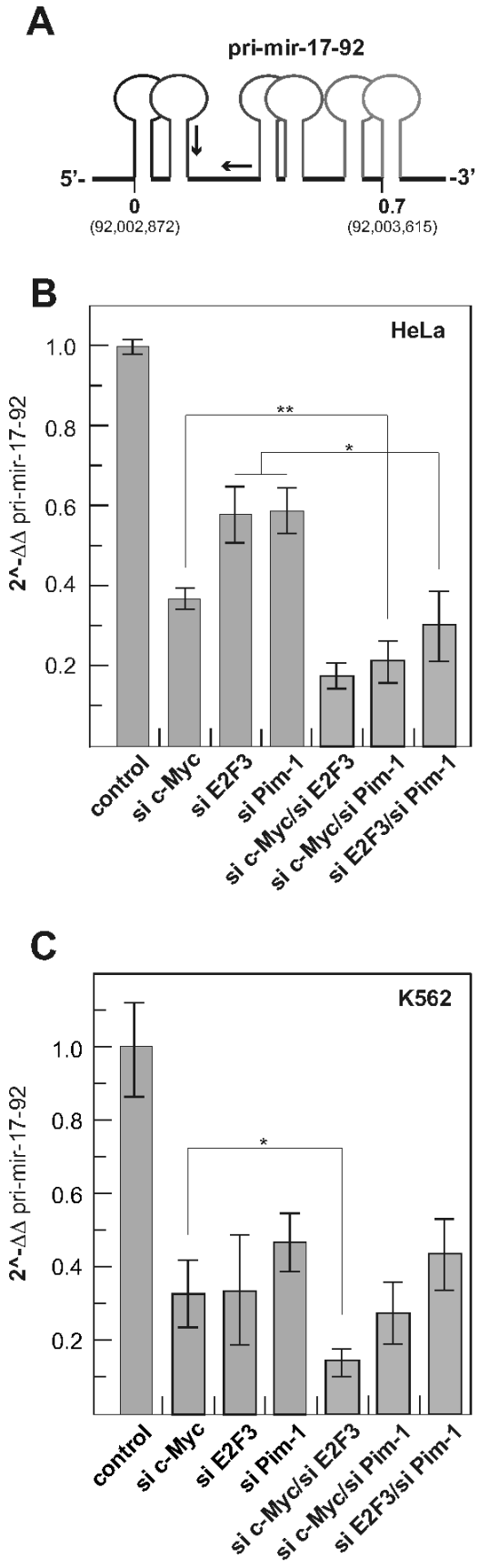
A
pri-mir-17-92
5'-
-3'
0
(92,002,872)
0.7
(92,003,615)
B
HeLa
2^-ΔΔ pri-mir-17-92
1.0
0.8
0.6
0.4
0.2
**
*
control
si c-Myc
si E2F3
si Pim-1
si c-Myc/si E2F3
si c-Myc/si Pim-1
si E2F3/si Pim-1
C
K562
2^-ΔΔ pri-mir-17-92
1.0
0.8
0.6
0.4
0.2
*
control
si c-Myc
si E2F3
si Pim-1
si c-Myc/si E2F3
si c-Myc/si Pim-1
si E2F3/si Pim-1

Fig. 3

FIGURE LEGENDS

FIGURE 1. (**A**) Genomic organization of C13*orf*25. The locus consists of four exons and three introns; the six miRNAs of the miR-17-92 cluster are encoded in intron 3. Sequences upstream of the cluster can be subdivided into a G/C-rich CpG island and an A/T-rich downstream part. The host gene promoter thought to be activated by E2F3 is located in the CpG island about 3.4 kb upstream of the miR-17-5p coding sequence. The functional c-Myc site (E3) is located ~1.5 kb upstream of miR-17-5p. Sequence numbering is based on the NCBI reference sequence NG_032702.1 and the GRCh37/hg19 assembly (http://genome.ucsc.edu). Note that previous related studies referred to the numbering system of the previous hg18 assembly (16,17,20,21). The numbering of the hg18 and hg19 assemblies is correlated as follows: nt 92,002,872 (0 kb in Fig. 1A) of hg19 is nt 90,800,873 of hg18. (**B**) Schematic representation of the different C13*orf*25 portions fused to the luciferase structural gene. The functional E3 box for c-Myc binding is indicated in the 1.5 kb construct (white vertical line). (**C**) Promoter activities of the different luciferase reporter constructs in K562 and HeLa cells. Obtained luciferase activities were normalized to the pGL3 control plasmid carrying the SV40 promoter (Promega). A reporter construct lacking the SV40 promoter as well as a construct harboring the 339 bp fragment of the A/T-rich intronic region in inverted orientation were used as controls. RLU values of the individual constructs were derived from 5 to 16 experiments (+/- S.E.M.).

FIGURE 2. (**A**) Schematic representation of the intronic A/T-rich region preceding the miR-17-92 coding sequence. The region A1 defines the genomic sequence 0.1 kb downstream of the functional c-Myc binding site (E3 box) that was amplified in ChIP analyses. (**B**) ChIP analysis of the intronic region A1 in K562 cells, using antibodies specific for c-Myc, Pim-1 and HP1γ. + AB: with antibody; - AB: without antibody; Mock: buffer only without cell lysate; Input: supernatant of the - AB-sample after immunoprecipitation and centrifugation (for details, see Supplementary Material).

FIGURE 3. (**A**) Illustration of the primers (arrows) used for the qRT-PCR quantification of pri-mir-17-92 transcript levels. (**B**) Quantitative RT-PCR of pri-mir-17-92 transcript levels in HeLa cells after siRNA-mediated knockdown of c-Myc, E2F3 or Pim-1and after combined knockdown of c-Myc/E2F3, c-Myc/Pim-1 or E2F3/Pim-1. 2^-ΔΔpri-17-92 values were normalized against 5S rRNA and an internal control siRNA (si VR1), representing mean values from at least three independent experiments (+/- S.E.M.). Statistical analyses were done using the software R. (**C**) Same as in panel B, but using K562 instead of HeLa cells.

SUPPLEMENTARY MATERIAL

Supplementary methods

Cell culture - Cells (K562 and HeLa) were cultivated under standard conditions in a humidified atmosphere (37 °C, 5 % CO_2) supplemented with RPMI 1640 (K562) or IMDM (HeLa) containing 10 % FCS (PAA, Cölbe, Germany).

Chromatin immunoprecipitation (ChIP) - 2 • 10^7 K562 cells in 13 mL RPMI medium were crosslinked with 1 % formaldehyde for 10 min at 37 °C. Reactions were stopped by adjusting to 0.125 M glycine, and cells were collected by centrifugation at 400 *g* for 5 min at room temperature. For cell lysis, cells were resuspended in 750 µL RIPA-buffer (10 mM Tris-HCl pH 7.4, 150 mM NaCl, 1 % deoxycholate, 1 % NP40, 0.1 % SDS, 0.2 mM PMSF) supplemented with the cOmplete Mini Protease Inhibitor Mix from Roche (Mannheim, Germany) according to the manufacturer's instructions. Lysed cells were sonicated in a Branson Sonifier 250 (duty cycle 50 %, output control 2, for 3.5 min, on ice water) (Heinemann, Schwäbisch Gmünd, Germany) and centrifuged at 16.000 *g* for 10 min at 4 °C. The supernatant was pre-cleared with 10 µL of blocked *Staphylococcus aureus* cells (Pansorbin® Cells, Calbiochem/Merck, Darmstadt, Germany) for 15 min at 4 °C on a rotor wheel. After a second centrifugation step (16.000 *g*, 5 min, room temperature), the supernatant was split into two samples (each ~350 µL, representing + and – specific antibody (AB)), which were adjusted to buffer D (16.7 mM Tris-HCl pH 8.1, 167 mM NaCl, 1.2 mM EDTA, 1.1 % Triton-X 100, 0.01 % SDS) and a total volume of 500 µL. 1 µg (1 to 5 µL) of the respective antibody was added to "+ AB" samples, whereas the same volume buffer D was added to "- AB" samples. At this point, also the "Mock" control was prepared, consisting of 500 µL buffer D. "+ AB", "- AB" and "Mock" samples were then incubated for at least 3 h at 4 °C. The following antibodies were used: monoclonal anti-c-Myc (sc-40) and anti-Pim-1 (sc-13513) (Santa Cruz Biotechnology (Heidelberg, Germany), anti-Phospho HP1γ (Ser83) polyclonal antibody (2600S) (Cell Signaling Technology, Danvers, MA, USA). In the case of mouse monoclonal antibodies (c-Myc and Pim-1), samples were additionally incubated for 1 h with a second monoclonal goat anti-mouse IgG antibody (sc-2005, Santa Cruz Biotechnology, Heidelberg, Germany). Immunoprecipitation was initiated by adding 10 µL of Pansorbin® cells (see above) to the "+ AB", "- AB" and "Mock" samples, followed by incubation for 15 min at room temperature. Samples were centrifuged (16.000 *g*, 3 min, room temperature); the supernatant of the "- AB" sample was saved, later serving as the input

control. Pellets were washed twice with dialysis buffer (50 mM Tris-HCl pH 8.0, 2 mM EDTA) and four times with IP-wash buffer (100 mM Tris-HCl pH 9.0, 500 mM LiCl, 1 % NP40, 1 % deoxycholate). Antibody-bound material was eluted from Pansorbin® cells by adding 150 µL elution buffer (50 mM $NaHCO_3$, 1 % SDS), vortexing for 3 s, and centrifugation (16.000 *g*, 3 min, room temperature). The supernatant was collected and the procedure was repeated. Reverse crosslinking and RNA digestion was performed in 280 µL buffer (0.3 M NaCl, and 1 µL RNase A (10 mg/mL)) for 5 h at 67 °C. Chromatin was precipitated with ethanol, followed by a Proteinase K digest (Thermo Fisher Scientific). DNA was purified by phenol/chloroform extraction and ethanol precipitation in the presence of 0.3 M NaOAc, pH 5.2. PCR amplification using Taq DNA polymerase and the co-immunoprecipitated DNA as template was done under the following conditions: 2 min at 95 °C in the absence of enzyme, followed by 35 amplification cycles of 45 s at 95 °C / 45 s at 60 °C / 45 s at 72 °C using the following primers:

A1 forward 5'-AAA GGC AGG CTC GTC GTT G
A1 reverse 5'-CGG GAT AAA GAG TTG TTT CTC CAA
A2 forward 5'-ACA TGG ACT AAA TTG CCT TTA AAT G
A2 reverse 5'-AAT CTT CAG TTT TAC AAG GTG ATG
A3 forward 5'-ACT GCA GTG AAG GCA CTT GT
A3 reverse 5'-TGC CAG AAG GAG CAC TTA GG
A4 forward 5'-CCA ATA ATT CAA GCC AAG CAA
A4 reverse 5'-AAA TAG CAG GCC ACC ATC AG
A5-forward 5'-GCC CAA TCA AAC TGT CCT GT
A5-reverse 5'-CGG GAC AAG TGC AAT ACC AT

Transfection of reporter constructs - For transfection of the suspension cell line K562, cells were washed in medium without serum, followed by electroporation in a BioRad Gene Pulser XCell (München, Germany) with a single pulse in a 4 mm cuvette, using 5 µg of the respective pGL3 derivative plasmid per million cells. 48 h after transfection, cells were washed in PBS, lysed and prepared for luciferase reporter assay measurements.

Transfection of siRNAs - Transfection of the suspension cell line K562 was performed by electroporation. After a washing step in medium without serum, 10^6 cells were mixed with 1 µg of siRNA (VR1 siRNA, Pim-1 siRNA, c-Myc siRNA or E2F3 siRNA). For the double knockdown experiments, 1 µg of each siRNA, respectively, was used. Cells were electroporated at 330 V with a single pulse in a BioRad Gene Pulser XCell (München, Germany) using a 4 mm cuvette. After electroporation, K562 cells were resuspended in

medium containing 10 % FCS and cultivated in a humidified atmosphere at 37 °C for 24 h. Cells were washed with PBS and prepared for total RNA extraction.

Transfection of HeLa cells was done using the transfection agent Lipofectamine™ 2000 (Life Technologies Invitrogen, Darmstadt, Germany). One day before transfection, $8 \bullet 10^4$ cells were seeded into 24-well plates and cultivated under standard conditions. SiRNA complexes (VR1 siRNA, Pim-1 siRNA, c-Myc siRNA or E2F3 siRNA) were prepared according to the manufacturer's protocol. To perform single knockdown experiments, 40 pmol of the respective siRNA were used. In case of the double knockdown experiments, 20 pmol of each siRNA were mixed in Opti-MEM® 1 (Life Technologies Invitrogen, Darmstadt, Germany). 4 to 6 h after transfection, the medium was replaced with IMDM containing 10 % FCS. Cells were cultivated 48 h under standard conditions until preparation for total RNA extraction.

RNA preparation and quantitative real-time PCR – For total RNA isolation, transfected cells (K562 or HeLa) were lysed (vortexing or mixing by pipetting up and down) in 750 µL lysis solution (0.8 M guanidinium-thiocyanate, 0.4 M ammonium-thiocyanate, 0.1 M sodium acetate pH 5.0, 5 % glycerin, 38 % phenol pH 4.5-5.0 [Roth®-Aqua-Phenol, Roth, Karlsruhe, Germany], 1 pellet 8-hydroxychinolin). Then, 200 µL of chloroform was added and phases were separated by centrifugation. The aqueous phase was mixed with 2 volumes of isopropanol, followed by incubation for 15 min at room temperature and centrifugation. The air-dried RNA pellet was dissolved in RNase-free water and incubated for 30 min at 37 °C with 1 U DNase I per µg RNA in 100 µL 1 x DNase I buffer (DNase I, Thermo Fisher Scientific, Schwerte, Germany) according to the manufacturer's instructions. Then, another identical aliquot of DNase I was added, followed by incubation at 37 °C for another 30 min. Samples were extracted with an equal volume of Roth®-Aqua-Phenol (see above), followed by extraction of the aqueous phase with chloroform and isopropanol precipitation as above. RNA pellets were finally washed with 75 % ethanol, air-dried and redissolved in 10 µL RNase-free water. 0.5 to 1 µg of total RNA were reverse-transcribed with RevertAid H Minus RT Polymerase (Thermo Fisher Scientific) according to the manufacturer's protocol. For determination of KD efficiencies a random hexamer primer was used to generate cDNA samples. In case of calculating pri-mir-17-92 levels the gene-specific reverse primer specified below was used for cDNA synthesis. Quantitative RT-PCR was performed in duplicate in a BioRad iQ™5 (BioRad, München, Germany) with the Absolute qPCR SYBR Green Capillary Mix (Thermo Scientific AbGene, Hamburg, Germany); cDNAs were diluted 1:5 or 1:10 and 4 µL of the reaction mixture used for determining RNA transcription levels.

Quantitative PCR assays for miRNA detection were conducted as follows: Thermo-Start™ DNA polymerase was activated for 15 min at 95 °C followed by 55 amplification cycles of 10 s at 95 °C / 20 s at 60 °C / 12 s at 72 °C. Subsequently, melting curves of the PCR products were generated: samples were cooled from 95 °C to 65 °C (20 °C per s), kept at 65 °C for 20 s, followed by heating steps of 1 °C per cycle up to 95 °C and kept for 10 s at 95 °C.

Quantitative RT-PCR assays for mRNA detection were changed as follows: Thermo-Start™ DNA polymerase was activated for 15 min at 95 °C followed by 55 amplification cycles with a denaturation step for 10 s, primer annealing for 10 s at 55 °C and amplification at 72 °C for 10 s. Subsequently, a melting curve was generated for the PCR products; samples cooled from 95 °C to 65 °C (20 °C per s), kept at 65 °C for 20 s, followed by heating steps of 1 °C per cycle up to 95 °C and kept for 10 s at 95 °C.

The mRNA and pri-mir-17-92 levels were calculated from the crossing points by the 2^-$\Delta\Delta C_T$ method (Schmittgen and Livak, 2008) using β-Actin mRNA or 5S rRNA as internal controls. Knockdown efficiency was quantitated by qRT-PCR and only those experiments showing more than 65 % reduction in protein levels were used for quantification of pri-mir-17-92 levels. All primers for qPCR measurements were purchased from Metabion (Martinsried, Germany) and designed using the software tool Universal ProbeLibrary (Roche Applied Biosystems, Mannheim, Germany). A list of all primer sequences according to the human sequences is shown underneath:

Pri-mir-17-92: forward primer 5'-CAT CTA CTG CCC TAA GTG CTC CTT and reverse primer 5'-GCT TGG CTT GAA TTA TTG GAT GA;

5S rRNA: 5'- TCT CGT CTG ATC TCG GAA GC and 5'- AGC CTA CAG CAC CCG GTA TT;

c-Myc mRNA: forward primer 5'-CCT TGC AGC TGC TTA GAC and reverse primer 5'-GAG TCG TAG TCG AGG TCA T;

E2F3 mRNA: forward primer 5'-GAG ACT GAA ACA CAC AGT CC and reverse primer 5'-CCT GAG TTG GTT GAA GCC;

Pim-1 mRNA: forward primer 5'-ATC AGG GGC CAG GTT TTC T and reverse primer 5'-GGG CCA AGC ACC ATC TAA T;

Actin mRNA: forward primer 5'-CCA ACC GCG AGA AGA TGA and reverse primer 5'-CCA GAG GCG TAC AGG GAT AG.

Luciferase reporter assays - Luciferase reporter assays were performed using the Promega Luciferase Assay System (Promega, Mannheim, Germany). After aspirating the medium, cells were washed with PBS and lysed in 100 µL 1.2 x reporter lysis buffer. In a 96-well plate, 10

µL of the respective cell lysate were mixed with 10 µL of luciferase substrate. Chemiluminescence was measured immediately in a Safire^{2} ^{TM} micro-plate reader (Tecan, Crailshaim, Germany).

Plasmid construction and seed mutagenesis - All primers, which were used for plasmid construction and seed mutagenesis, are listed below (restriction sites in italics):

pGL3 1.5 kb: 5'-ATA T*AG ATC T*TG CCG CCG GGA AAC GGG TT and reverse primer R1 5'-ATA T*AA GCT T*CC ATA CAA ATT CAG CAT AAT CCC TAA TGG;

pGL3 625 bp: 5'-ATA TAG ATC TCT TTA GAC AAT GTA CCT TTT CTG and reverse primer R1 (see above);

pGL3 339 bp: 5'-ATA T*AG ATC T*GT GGA AGC CAG AAG AGG AGG A and reverse primer R1 (see above);

pGL3 279 bp: 5'-ATA TAG ATC TGG TAC ACA TGG ACT AAA TTG CC and reverse primer R1 (see above);

pGL3 197 bp: 5'-ATA T*AG ATC T*CT CTA TGT GTC AAT CCA TTT GGG AG and reverse primer R1 (see above);

pGL3 250 bp: 5'-ATA T*AG ATC T*GT GGA AGC CAG AAG AGG AGG A and reverse primer R3 5'- ATA T*AA GCT T*GC CTT AAG AAT TCT TTA CAG AAG GC;

pGL3 190 bp: 5'-ATA T*AG ATC T*GG TAC ACA TGG ACT AAA TTG CC and reverse primer R3 (see above);

pGL3 108 bp: 5'-ATA T*AG ATC T*CT CTA TGT GTC AAT CCA TTT GGG AG and reverse primer R3 (see above);

pGL3 339 inv: 5'-ATA T*AA GCT T*GT GGA AGC CAG AAG AGG AGG A and 5'-ATA T*AG ATC T*CC ATA CAA ATT CAG CAT AAT CCC TAA TGG.

Bioinformatical promoter analysis - For promoter analyses of the intronic A/T-rich region, a sequence of 1490 bp (human), beginning at the functional c-Myc site (E3) and ending at the 5'-end of the first mature miRNA sequence, miR-17-5p (for details, see Fig. S1), was analyzed with several web-based promoter prediction tools. The following tools were used to predict promoter elements or putative TSSs:

Neural Network promoter prediction: (Reese, 2001)
(http://www.fruitfly.org/seq_tools/promoter.html);

McPromoter006: (Ohler, 2006)
(http://tools.genome.duke.edu/generegulation/McPromoter/);

Promoter 2.0 Prediction Server: (Knudsen, 1999) (http://www.cbs.dtu.dk/services/Promoter/);

PromPredict: (Rangannan and Bansal, 2009)

(http://nucleix.mbu.iisc.ernet.in/prompredict/prompredict.html).

Putative TSSs were predicted and calculated using the software available at http://rulai.cshl.org/tools/genefinder/CPROMOTER/human.htm (Zhang, 1998).

All promoter prediction tools predicted several different promoter elements in the 1.5 kb region upstream of miR-17-5p and only the web-based tool Promoter 2.0 failed. The calculated promoter predictions of the indicated tools did not match in any sequence region, giving the assumption that the A/T-rich 1.5 kb intronic region in front of the miR-17-92 coding sequence has only weak promoter activity itself. Due to the fact that this intronic region has an overall high A/T-content, nearly all software programs were able to detect putative promoter regions.

Statistical analysis - Statistical analyses were done using the software R (R Core Team, 2012). P-values were calculated with the Welch Two Sample Test.

References

Knudsen, S. (1999) Promoter2.0: for the recognition of PolII promoter sequences. *Bioinformatics* **15**, 356–361.

Ohler, U. (2006) Identification of core promoter modules in *Drosophila* and their application in accurate transcription start site prediction. *Nucleic Acids Research* **34**, 5943–5950.

Rangannan, V., and Bansal, M. (2009) Relative stability of DNA as a generic criterion for promoter prediction: whole genome annotation of microbial genomes with varying nucleotide base composition. *Molecular BioSystem* **5**, 1758–1769.

R Core Team (2012) R: A Language and Environment for Statistical Computing. *R Foundation for Statistical Computing*

Reese, M. G. (2001) Application of a time-delay neural network to promoter annotation in the *Drosophila melanogaster* genome. *Computers & Chemistry* **26**, 51–6.

Schmittgen, T. D., and Livak, K. J. (2008) Analyzing real-time PCR data by the comparative CT method. *Nature Protocols* **3**, 1101–1108.

Zhang, M. Q. (1998) Identification of human gene core promoters *in silico*. *Genome Res.* **8**, 319–326.

Supplementary figure legends

Fig. S1: Relevant sequence region of C13*orf*25, including the CpG island harboring the host gene promoter, the A/T-rich region, and the miR-17-92 cluster; sequence and position of the last exon 4 of C13*orf*25 is indicated at the end. Shown sequences are based on the NCBI reference sequence NG_032702.1 and the GRCh37/hg19 assembly (http://genome.ucsc.edu). The boundaries of the CpG island, important previously identified regulatory elements, mature miRNA coding sequences and relevant primer sequences are highlighted in the sequence and annotated at the margins.

Fig S2. Quantitative RT-PCR of the pri-mir-17-92 transcription levels in the human cell lines K562, HeLa and HUH7. 2^-ΔΔpri-mir-17-92 values are normalized against 5S rRNA and obtained from at least 3 independent experiments (+/- S.E.M.). The amount of pri-mir-17-92 transcript in K562 cells was set to 1.

Fig. S3. (**A**) Schematic representation of the intronic A/T-rich region preceding the miR-17-92 coding sequence. The region A1 defines the genomic sequence 0.1 kb downstream of the functional c-Myc binding site (E3 box) that was amplified in ChIP analyses. A2 covers a segment immediately upstream of the miRNA-coding region; A3-A5 are located along the coding sequence of the human miR-17-92 cluster. The length (bp) of each amplicon is indicated at the top. (**B**) ChIP analysis of the regions A1 to A5 in K562 cells, using an antibody specific for HP1γ or RNA polymerase II (only A2 analyzed); +AB: with antibody; -AB: without antibody; Mock: buffer only without cell lysate; Input: supernatant of the "- AB" sample after immunoprecipitation and centrifugation (for details, see Supplementary Material). (**C**) ChIP analysis of the A2 region in HeLa cells using the antibody specific for HP1γ.

Table S1:

K562	c-Myc KD		E2F3 KD		Pim-1 KD	
	$2^{-\Delta\Delta C_T}$ pri-mir-17-92	KD efficiency	$2^{-\Delta\Delta C_T}$ pri-mir-17-92	KD efficiency	$2^{-\Delta\Delta C_T}$ pri-mir-17-92	KD efficiency
	0.13	77	0.21	95	1.23	72
	0.02	87	0.16	98	0.16	69
	0.56	59	0.60	19	1.39	55
	0.75	74			0.76	59
	0.33	75			0.22	49
	0.14	99			2.38	78
	0.20	97			1.84	87
	0.55	80			0.80	88
					0.27	85
					0.40	89
					0.52	67
					0.69	65
					0.37	87
Mean	**0.33**	**81**	**0.34**	**89**	**0.47**	**73**
SEM	0.09	5.0	0.15	8.0	0.08	5.0

K562	c-Myc / E2F3 KD		c-Myc / Pim-1 KD		Pim-1 / E2F3 KD	
	$2^{-\Delta\Delta C_T}$ pri-mir-17-92	KD efficiency	$2^{-\Delta\Delta C_T}$ pri-mir-17-92	KD efficiency	$2^{-\Delta\Delta C_T}$ pri-mir-17-92	KD efficiency
	0.22	82 / 75	0.45	72 / 55	0.69	88 / 86
	0.23	86 / 72	0.19	90 / 54	0.56	68 / 73
	0.15	81 / 48	0.19	95 / 48	0.19	95 / 99
	0.08	99 / 99			0.52	87 / 81
	0.04	99 / 99			0.23	91 / 93
Mean	**0.15**	**89 / 79**	**0.28**	**86 / 52**	**0.44**	**86 / 86**
SEM	0.04	4.0 / 9.6	0.08	7.0 / 2.2	0.09	4.7 / 4.5

HeLa	c-Myc KD		E2F3 KD		Pim-1 KD	
	$2^{-\Delta\Delta C_T}$ pri-mir-17-92	KD efficiency	$2^{-\Delta\Delta C_T}$ pri-mir-17-92	KD efficiency	$2^{-\Delta\Delta C_T}$ pri-mir-17-92	KD efficiency
	0.37	70	0.72	51	0.50	47
	0.29	82	0.66	78	0.34	72
	0.32	61	0.40	76	0.71	63
	0.41	99	0.53	73	0.58	80
	0.48	55	0.64	73	0.54	87
	0.37	64			0.78	72
					0.70	76
Mean	**0.37**	**65**	**0.59**	**70**	**0.59**	**71**
SEM	0.03	6.7	0.07	6.3	0.06	4.9

HeLa	c-Myc / E2F3 KD		c-Myc / Pim-1 KD		Pim-1 / E2F3 KD	
	$2^{-\Delta\Delta C_T}$ pri-mir-17-92	KD efficiency	$2^{-\Delta\Delta C_T}$ pri-mir-17-92	KD efficiency	$2^{-\Delta\Delta C_T}$ pri-mir-17-92	KD efficiency
	0.24	79 / 64	0.24	79 / 84	0.49	81 / 96
	0.13	91 / 81	0.25	77 / 61	0.33	91 / 85
	0.11	93 / 86	0.15	86 / 58	0.10	97 / 94
	0.12	90 / 91	0.12	95 / 91	0.26	92 / 94
	0.23	87 / 74	0.41	84 / 73		
	0.26	83 / 66	0.10	97 / 95		
Mean	**0.18**	**87 / 77**	**0.21**	**86 /77**	**0.30**	**90 / 92**
SEM	0.03	2.2 / 4.4	0.053	3.3 / 6.0	0.08	3.3 / 2.5

NCBI Reference Sequence: NG_032702.1

Homo sapiens mir-17-92 microRNA cluster containing MIR17HG, MIR17, MIR18A, MIR19A, MIR19B1, MIR20A, and MIR92A1 (MIR17-MIR92); and microRNA 17 (MIR17); and miR-17-92 cluster host gene (non-protein coding) (MIR17HG); and microRNA 18a (MIR18A); and microRNA 19a ...

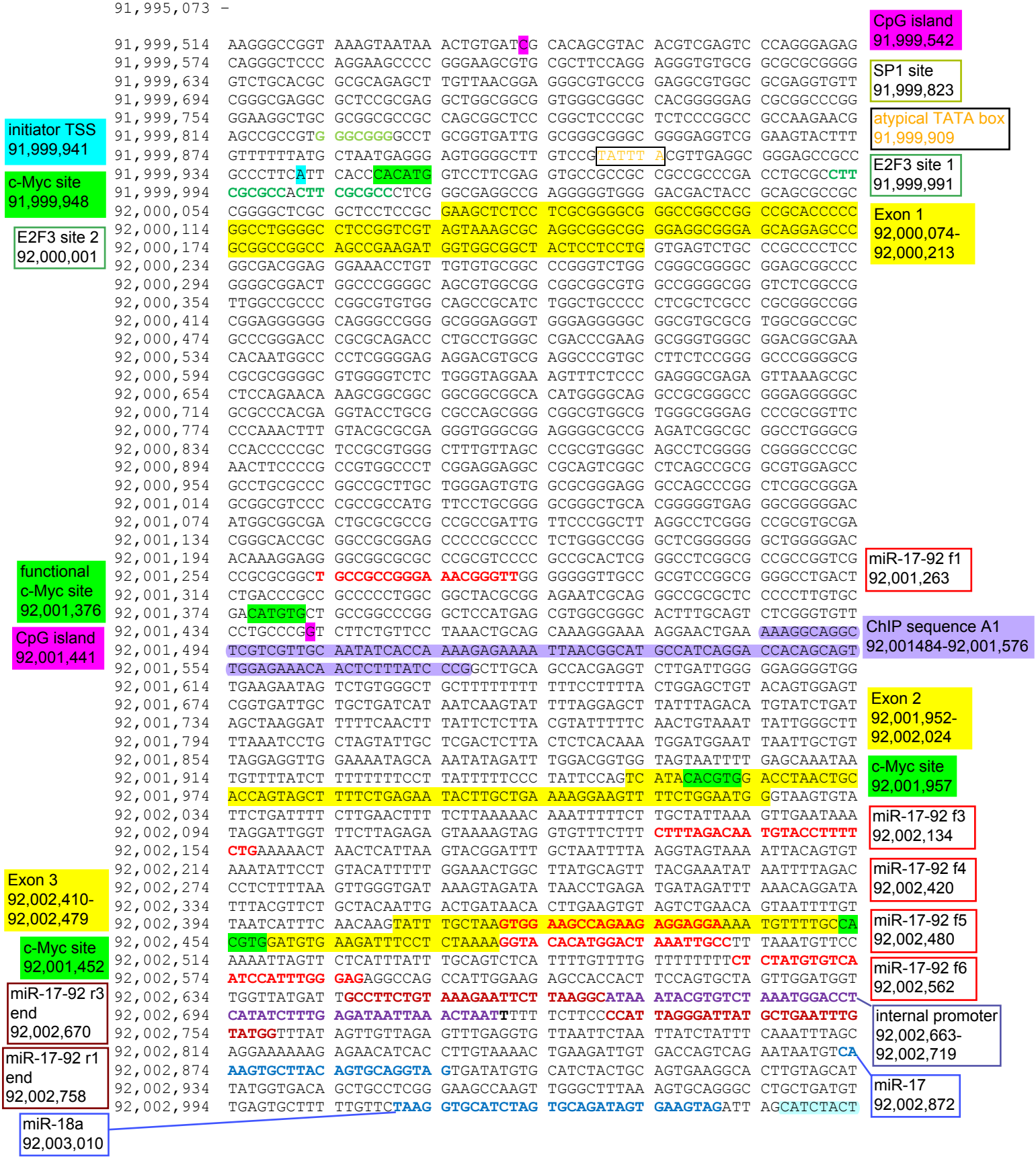

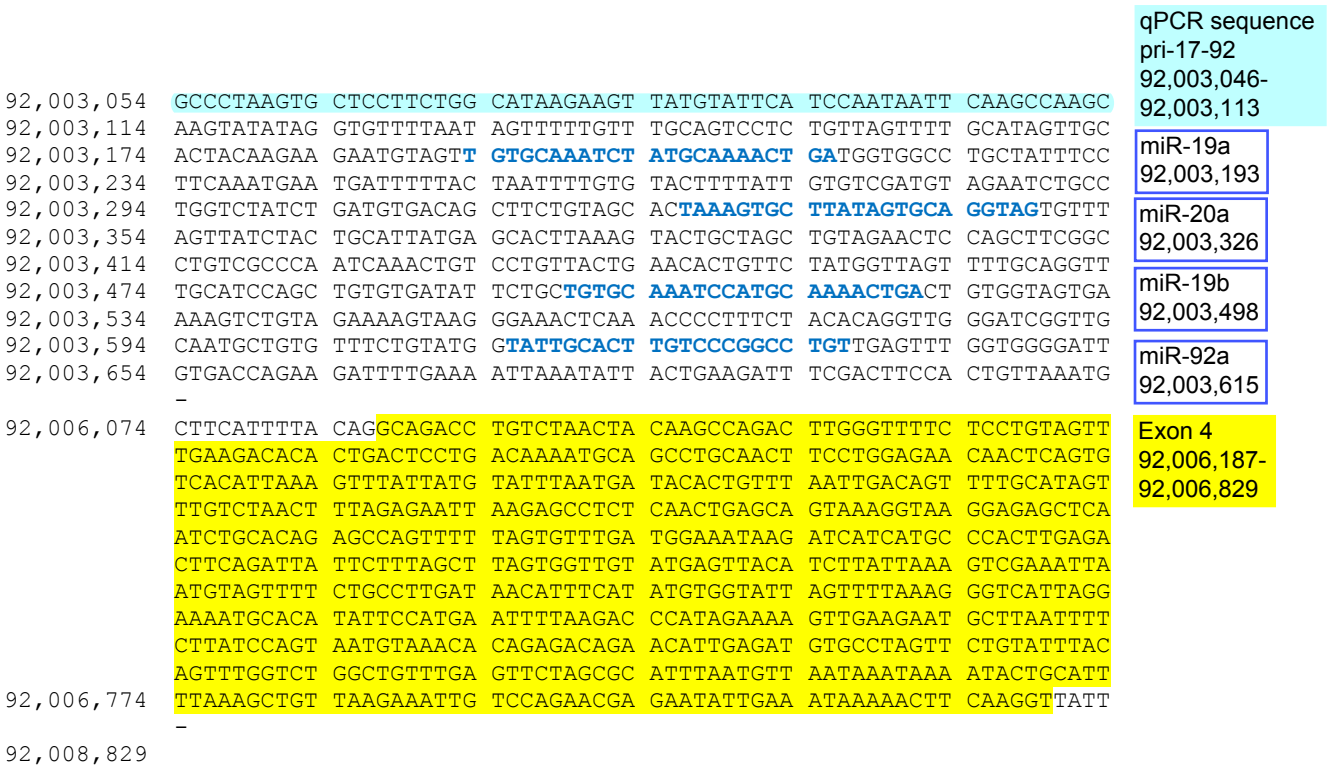
qPCR sequence
pri-17-92
92,003,046-
92,003,113
miR-19a
92,003,193
miR-20a
92,003,326
miR-19b
92,003,498
miR-92a
92,003,615
Exon 4
92,006,187-
92,006,829
92,003,054 GCCCTAAGTG CTCCTTCTGG CATAAGAAGT TATGTATTCA TCCAATAATT CAAGCCAAGC
92,003,114 AAGTATATAG GTGTTTTAAT AGTTTTTGTT TGCAGTCCTC TGTTAGTTTT GCATAGTTGC
92,003,174 ACTACAAGAA GAATGTAGTT GTGCAAATCT ATGCAAAACT GATGGTGGCC TGCTATTTCC
92,003,234 TTCAAATGAA TGATTTTTAC TAATTTTGTG TACTTTTATT GTGTCGATGT AGAATCTGCC
92,003,294 TGGTCTATCT GATGTGACAG CTTCTGTAGC ACTAAAGTGC TTATAGTGCA GGTAGTGTTT
92,003,354 AGTTATCTAC TGCATTATGA GCACTTAAAG TACTGCTAGC TGTAGAACTC CAGCTTCGGC
92,003,414 CTGTCGCCCA ATCAAACTGT CCTGTTACTG AACACTGTTC TATGGTTAGT TTTGCAGGTT
92,003,474 TGCATCCAGC TGTGTGATAT TCTGCTGTGC AAATCCATGC AAAACTGACT GTGGTAGTGA
92,003,534 AAAGTCTGTA GAAAAGTAAG GGAAACTCAA ACCCCTTTCT ACACAGGTTG GGATCGGTTG
92,003,594 CAATGCTGTG TTTCTGTATG GTATTGCACT TGTCCCGGCC TGTTGAGTTT GGTGGGGATT
92,003,654 GTGACCAGAA GATTTTGAAA ATTAAATATT ACTGAAGATT TCGACTTCCA CTGTTAAATG
92,006,074 CTTCATTTTA CAGGCAGACC TGTCTAACTA CAAGCCAGAC TTGGGTTTTC TCCTGTAGTT
TGAAGACACA CTGACTCCTG ACAAAATGCA GCCTGCAACT TCCTGGAGAA CAACTCAGTG
TCACATTAAA GTTTATTATG TATTTAATGA TACACTGTTT AATTGACAGT TTTGCATAGT
TTGTCTAACT TTAGAGAATT AAGAGCCTCT CAACTGAGCA GTAAAGGTAA GGAGAGCTCA
ATCTGCACAG AGCCAGTTTT TAGTGTTTGA TGGAAATAAG ATCATCATGC CCACTTGAGA
CTTCAGATTA TTCTTTAGCT TAGTGGTTGT ATGAGTTACA TCTTATTAAA GTCGAAATTA
ATGTAGTTTT CTGCCTTGAT AACATTTCAT ATGTGGTATT AGTTTTAAAG GGTCATTAGG
AAAATGCACA TATTCCATGA ATTTTAAGAC CCATAGAAAA GTTGAAGAAT GCTTAATTTT
CTTATCCAGT AATGTAAACA CAGAGACAGA ACATTGAGAT GTGCCTAGTT CTGTATTTAC
AGTTTGGTCT GGCTGTTTGA GTTCTAGCGC ATTTAATGTT AATAAATAAA ATACTGCATT
92,006,774 TTAAAGCTGT TAAGAAATTG TCCAGAACGA GAATATTGAA ATAAAAACTT CAAGGTTATT
92,008,829

Fig. S1

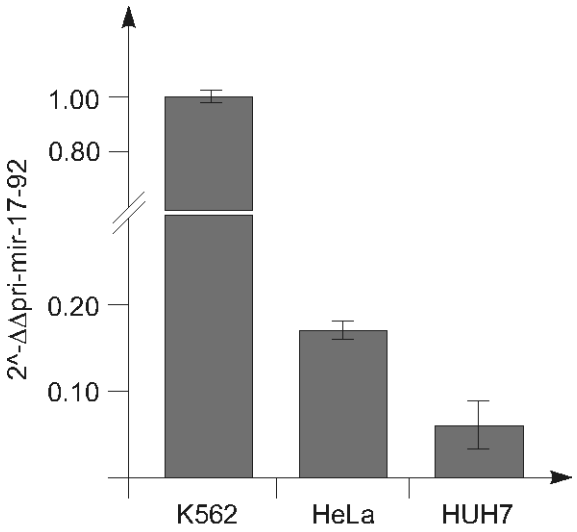

Fig. S2

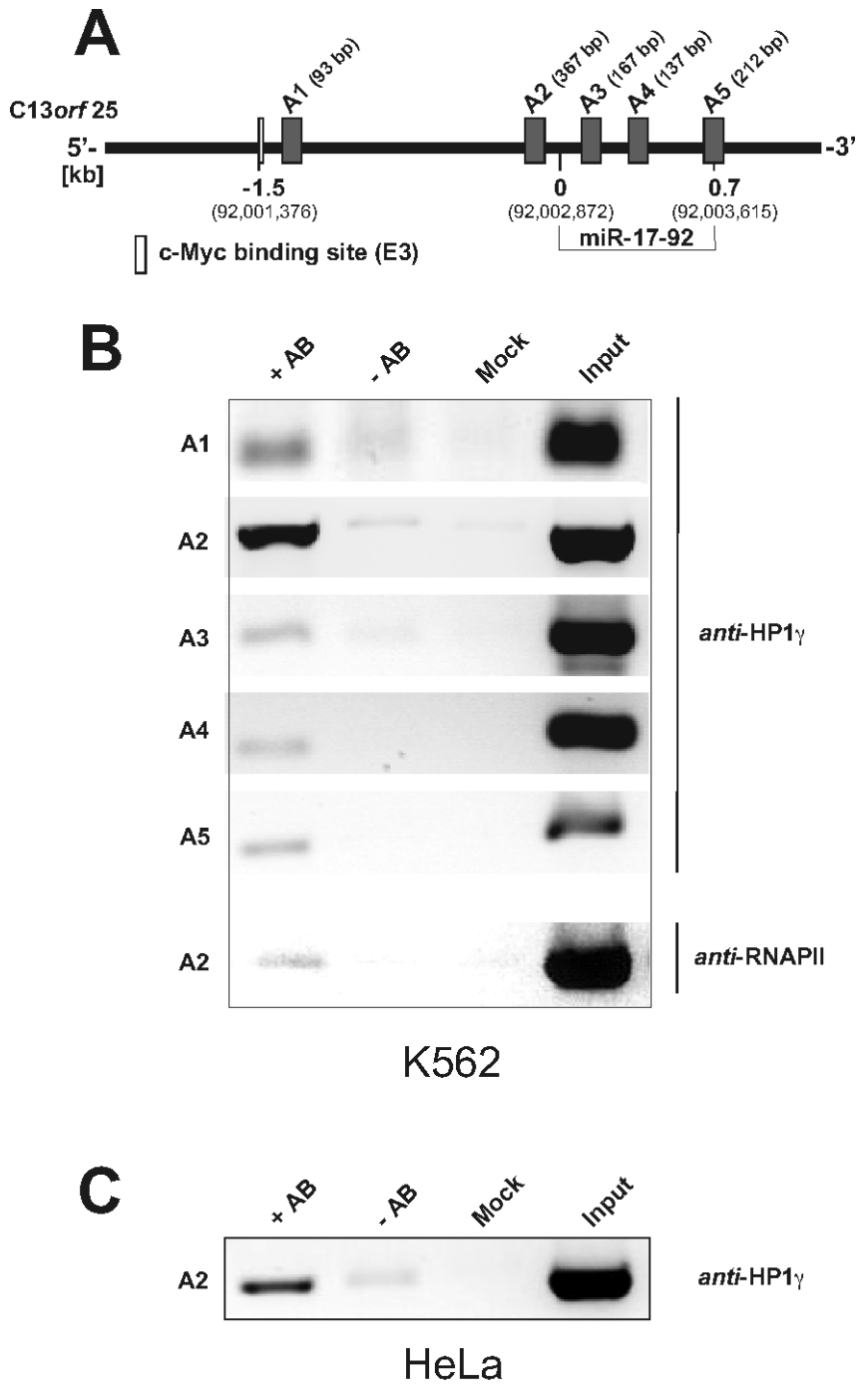
A
C13orf 25
5'-
[kb]
-3'
A1 (93 bp)
A2 (367 bp)
A3 (167 bp)
A4 (137 bp)
A5 (212 bp)
-1.5
(92,001,376)
0
(92,002,872)
0.7
(92,003,615)
miR-17-92
c-Myc binding site (E3)
B
+ AB
- AB
Mock
Input
A1
A2
A3
A4
A5
anti-HP1γ
A2
anti-RNAPII
K562
C
+ AB
- AB
Mock
Input
A2
anti-HP1γ
HeLa

Fig. S3

E. Acronyms and units

Acronyms and units	
%	percentage
[γ^{32}P]-ATP	gamma ^{32}P-adenosine triphosphate
°C	degree Celsius
ε	molar absorptivity/ extinction coefficient
µg	microgram
µL	microliter
µM	micromolar
µm	micrometer
2'-F	2'-fluoro
2'-O-Me	2'-O-methyl
2'-O-MOE	2'-O-methoxyethyl
^{32}P	^{32}phosphor isotope
5S rRNA	5S ribosomal RNA
A	adenine
A_{260}	absorption at 260 nm
A_{280}	absorption at 280 nm
AAV	adenovirus-associated vector
ABCA1	ATP-binding cassette transporter A1
AFM	atomic force microscopy
AGO	argonaute RISC catalytic component
ALT	alanine transaminase
APS	ammonium persulfate
AST	aspartate transaminase
ATP	adenosine triphosphate
AURKB	aurora kinase B
BAD	BCL-2 associated agonist of cell death
BCL2	B-cell lymphoma 2
BCL2L11	BCL2-like apoptosis facilitator
B-CLL	B-cell chronic lymphocytic leukemia
BLAST	Basic Local Alignment Search Tool
bp	base pair
BPB	bromophenol blue
C	cytosine
c	concentration
C. elegans	Caenorhabditis elegans
C13orf25	chromosome 13 open reading frame 25

Acronyms and units	
Ca^{2+}	calcium ion
CBX3	chromobox homolog 3
CDC25A	cell division cycle 25A
CDC25C	cell division cycle 25C
cDNA	complementary DNA
Cel	Caenorhabditis elegans
ChIP	chromatin immunoprecipitation
ChIPX	cross-linked chromatin immunoprecipitation
cm	centimeter
CMV	cytomegalovirus
cpm	counts per minute
CTGF	connective tissue growth factor
ddH_2O	double-distilled water
DGCR8	DiGeorge syndrome critical region 8
DICER1	Dcr-1 homolog (Drosohphila)
DNA	deoxyribonucleic acid
DNaseI	deoxyribonuclease I
dNTP	deoxynucleotide triphosphate
dsDNA	double-stranded DNA
dT	deoxythymidines
DTT	dithiothreitol
E	extinction
E. coli	Escherichia coli
e.g.	exempli gratia, for example
E2F	E2F transcription factor
E-box	enhancer box
EDTA	ethylenediamine tetraacedic acid
EIF4E	eukaryotic translation initiation factor 4E
ELISA	enzyme linked immunosorbent assay
FACS	fluorescence-activated cell sorting
FastAP	fast alkaline phosphatase
FCS	fetal calf serum
FD	fast digest
FDU	fast digest unit
fwd	forward
G	guanine
g	gravitational force
g	gram
gDNA	genomic DNA
GM-CSF	granulocyte macrophage colony-stimulating factor

Acronyms and units	
G-phase	gap phase
GTP	guanosine triphosphate
h	hour
H3	histone 3
H3S10	histone 3 serine 10
HCV	hepatitis C virus
HeLa	Henrietta Lacks
HEPES	4-(2-hydroxyethyl)-1-piperazineethanesulfonic acid
HP1G	heterochromatin protein 1 gamma
HRP	horse-radish peroxidase
hsa	homo sapiens
HSP90	heat shock protein 90
Hz	hertz
i.p.	intraperitoneal
i.t.	intratumoral
i.v.	intravenous
IgG	immunoglobulin G
IL	interleukin
IMDM	Iscove's Modified Dulbecco Medium
kb	(=kbp) kilo base pair
kDa	kilo Dalton
kHz	kilo hertz
KRAS	Kirsten rat sarcoma viral oncogene homolog
l	length
L	liter
LAV	lentivirus-associated vector
LB	lysogeny broth
let-7a	lethal-7a
LNA	locked nucleic acid
LPS	lipopolysaccharide
luc	luciferase
M	molar
m	meter
mA	milliampere
mAB	monoclonal antibody
MAX	MYC-associated factor X
mC	2'-oxymethyl cytosine
Mg^{2+}	magnesium ion
min	minute
miRISC	miRNA-induced silencing complex

Acronyms and units	
miRNA	microRNA
mL	milliliter
mM	millimolar
mm	millimeter
M-MuLV RT	moloney murine leukemia virus reverse transcriptase
MOPS	3-(N-morpholino)propanesulfonic acid
M-phase	mitosis phase
mRNA	messenger RNA
msec	millisecond
mU	2'-oxymethyl uracil
MuLV	murine leukemia virus
MYC	v-myc myelocytomatosis viral oncogene homolog
N	Newton
N/P ratio	nitrogen per nucleic acid phosphate ratio
NCBI	National Center for Biotechnology Information
ncRNA	non-coding RNA
ng	nanogram
nm	nanometer
NP-40	nonyl phenoxypolyethoxylethanol
nt	nucleotide
OD	optical density
OD_{576}	optical density at 576 nm
OH	hydroxyl
P21	cyclin-dependent kinase inhibitor 1A (CDKN1A, P21)
P27	cyclin-dependent kinase inhibitor 1B (CDKN1B, P27)
PAGE	polyacrylamide gel electrophoresis
PBS	phosphate buffered saline
PCR	polymerase chain reaction
PEI	polyethylenimine
PEI F25 LMW	polyethylenimine F25 low molecular weight
PIM	proviral integration site of murine leukemia virus
pmol	picomol
PMSF	phenylmethylsulfonyl fluoride
PO	phosphodiester
POLR2	RNA polymerase II
PP2A	protein phosphatase 2A
pre-B-cell	progenitor B-cell
pre-miRNA	precursor miRNA
pri-miRNA	primary miRNA
pRNA	product RNA

Acronyms and units	
PS	phosphorothioate
PTEN	phosphatase and tensin homolog
PVDF	polyvinylidine fluoride
qPCR	quantitative real time PCR
QT	quantitative
RAN	Ras-related nuclear protein
rev	reverse
RISC	RNA-induced silencing complex
RNA	ribonucleic acid
RNAi	RNA interference
RNase	ribonuclease
RNaseP	ribonuclease P
rpm	rounds per minute
RPMI	Roswell Park Memorial Institute
RT	reverse transcriptase
RT	room temperature
S	serin
s.c.	subcutaneous
SDS	sodiumdodecylsulfate
SDS PAGE	sodiumdodecylsulfate polyacrylamide gel electrophoresis
sec	second
SGOT	serum glutamic oxaloacetic transaminase
SGPT	serum glutamic pyruvate transaminase
Si_3N_4	trisilicon tetranitride
siRNA	small interfering RNA
SNP	single nucleotide polymorphism
SOCS	suppressor of cytokine signaling
S-phase	synthesis phase
ssDNA	single-stranded DNA
STAT	signal transducer and activator of transcription
SV40	simian vacuolating virus 40
T	thymine
T4 PNK	T4 polynucleotide kinase
TBE	Tris-HCl, borate, EDTA
TBST	Tris-HCl-buffered-saline-Tween 20
TEMED	tetramethylethylenediamine
TGFB	tissue growth factor beta
TNFα	tumor necrosis factor alpha
TP53	tumor protein 53

Acronyms and units	
TSP1	thrombospondin-1
TU	transcription unit
U	uracil
U	unit
UTR	untranslated region
UV	ultraviolet
V	voltage
v/v	volume per volume %
VR1	vanilloid receptor 1
w/v	mass per volume %
WST-1	water soluble tetrazolium salt-1
XCB	xylene cyanol blue
XPO5	Exportin-5

F. Gene nomenclature

Gene nomenclature was applied according to the guidelines provided by the HUGO Gene Nomenclature Committee (HGNC) at http://www.genenames.org/guidelines.html (259). Gene symbols are italicized and all letters are in upper case. CDNA and mRNA use the gene symbol and formatting conventions. Protein designations are the same as the gene symbol, but using only upper case letters.

Abbreviation gene symbol, cDNA, mRNA, protein	
ABCA1	ATP-binding cassette transporter A1
AGO1-4	argonaute RISC catalytic component 1-4
AURKB	aurora kinase B
BAD	BCL-2 associated agonist of cell death
BCL2	B-cell lymphoma 2
BCL2L11	BCL2-like apoptosis facilitator
C13orf25	chromosome 13 open reading frame 25
CBX3	chromobox homolog 3
CDC25A	cell division cycle 25A
CDC25C	cell division cycle 25C
CTGF	connective tissue growth factor
DGCR8	DiGeorge syndrome critical region 8
DICER1	Dcr1-homolog (Drosophila)
E2F 1-3	E3F transcription facto 1-3r
EIF4E	eukaryotic translation initiation factor 4E
GM-CSF	granulocyte macrophage colony-stimulating factor
HP1G	heterochromatin protein 1 gamma
HSP90	heat shock protein 90
KRAS	Kirsten rat sarcoma viral oncogene homolog
MAX	MYC-associated factor X
MYC	v-myc myelocytomatosis viral oncogene homolog
P21	cyclin-dependent kinase inhibitor (CDKN1A, P21)
P27	cyclin-dependent kinase inhibitor (CDKN1B, P27)
PIM1-3	proviral integration site of murine leukemia virus 1-3
POLR2	RNA polymerase II
PP2A	protein phosphatase 2A
PTEN	phosphatase and tensin homolog
RAN	Ras-related nuclear protein
SOCS	suppressor of cytokine signaling

Abbreviation gene symbol, cDNA, mRNA, protein	
STAT 3/5	signal transducer and activator of transcription 3/5
TGFB	tissue growth factor beta
TP53	tumor protein 53
TSP1	thrombospondin-1
XPO5	Exportin-5

G. List of figures

H. List of tables

I. List of equations

J. Primers for cloning

Plasmid	Name of DNA primer	Sequence 5' → 3'	Construct length [bp]
pGL3 Pim-1 3'-UTR (*)	Inv. hPim-1 3'-UTR F CCE	GCT CTA GAG CTG TCA GAT GCC CGA GGG	1264
	Inv. hPim-1 3'-UTR R CCE	GCT CTA GAG CAA TAA GAT CTC TTT TAT TCC CCT GT	
pGL3 Pim-1 3'-UTR miR-33a mut (*)	Pim-1 miR-33a mut f1	AAA AAA TGC ACA AAC AGT GCG ATC AAC AGA AAA GCT	1264
	Pim-1 miR-33a mut r1	AGC TTT TCT GTT GAT CGC ACT GTT TGT GCA TTT TTT	
pGL3 let-7a construct forward (*)	let-7a sense XbaI	GCT CTA GAG CTG AGG TAG TAG GTT GTA TAG TTG CTC AGC GCT CTA GAG C	33
	let-7a as XbaI	GCT CTA GAG CGC TGA GCA ACT ATA CAA CCT ACT ACC TCA GCT CTA GAG C	
pGL3 let-7a construct inverted (*)	let-7a as XbaI	GCT CTA GAG CGC TGA GCA ACT ATA CAA CCT ACT ACC TCA GCT CTA GAG C	33
	let-7a sense XbaI	GCT CTA GAG CTG AGG TAG TAG GTT GTA TAG TTG CTC AGC GCT CTA GAG C	
pGL3 P21 3'-UTR (*)	Invitrogen P21 3'-UTR F (CCE)	GCT CTA GAG CCC TCA AAG GCC CGC TCT A	1445
	Invitrogen P21 3'-UTR R (CCE)	GCT CTA GAG CGG AGG AGC TGT GAA AGA CAC A	
pGL3 P21 3'-UTR miR-17/20a mut (*)	mir17/20a mut F1	GAA GTA AAC AGA TGG GAC TGT GAA GGG GCC TCA CC	1445
	mir17/20a mut R1	GGT GAG GCC CCT TCA CAG TCC CAT CTG TTT ACT TC	
	miR-17/20a mut F2	CTC CCC AGT TCA TTG GAC TGT GAT TAG CAG CGG AA	
	miR-17/20a mut R2	TTC CGC TGC TAA TCA CAG TCC AAT GAA CTG GGG AG	
pGL3 1,5 kb (*)	miR-17-92 f1	ATA TAG ATC TTG CCG CCG GGA AAC GGG TT	1496
	miR-17-92 r1	ATA TAA GCT TCC ATA CAA ATT CAG CAT AAT CCC TAA TGG	
pGL3 625 bp (*)	miR-17-92 f3	ATA TAG ATC TCT TTA GAC AAT GTA CCT TTT CTG	625
	miR-17-92 r1	ATA TAA GCT TCC ATA CAA ATT CAG CAT AAT CCC TAA TGG	
pGL3 339 bp (*)	miR-17-92 f4	ATA TAG ATC TGT GGA AGC CAG AAG AGG AGG A	339
	miR-17-92 r1	ATA TAA GCT TCC ATA CAA ATT CAG CAT AAT CCC TAA TGG	
pGL3 279 bp (+)	miR-17-92 f5	ATA TAG ATC TGG TAC ACA TGG ACT AAA TTG CC	279
	miR-17-92 r1	ATA TAA GCT TCC ATA CAA ATT CAG CAT AAT CCC TAA TGG	
pGL3 197 bp (+)	miR-17-92 f6	ATA TAG ATC TCT CTA TGT GTC AAT CCA TTT GGG AG	197
	miR-17-92 r1	ATA TAA GCT TCC ATA CAA ATT CAG CAT AAT CCC TAA TGG	
pGL3 250 bp	miR-17-92 f4	ATA TAG ATC TGT GGA AGC CAG AAG AGG AGG A	250
	miR-17-92 r3	ATA TAA GCT TGC CTT AAG AAT TCT TTA CAG AAG GC	

Plasmid	Name of DNA primer	Sequence 5' → 3'	Construct length [bp]
pGL3 190 bp	miR-17-92 f5	ATA TAG ATC TGG TAC ACA TGG ACT AAA TTG CC	190
	miR-17-92 r3	ATA TAA GCT TGC CTT AAG AAT TCT TTA CAG AAG GC	
pGL3 108 bp	miR-17-92 f6	ATA TAG ATC TCT CTA TGT GTC AAT CCA TTT GGG AG	108
	miR-17-92 r3	ATA TAA GCT TGC CTT AAG AAT TCT TTA CAG AAG GC	
pGL3 339 inv (+)	miR-17-92 f4 invers	ATA TAA GCT TGT GGA AGC CAG AAG AGG AGG A	339
	miR-17-92 r1 invers	ATA TAG ATC TCC ATA CAA ATT CAG CAT AAT CCC TAA TGG	

(*): (194); (+): (196)

K. Primers for sequencing

Plasmid	Name of DNA primer	Sequence 5' → 3'
cDNA clone variants OriGene	VP 1,5 seq	GGA CTT TCC AAA ATG TCG
	XL 39 seq	ATT AGG ACA AGG CTG GTG GG
	Pim-1 3rd	TCT CCA AAA ATC TGC CTG GGT T
pGL3 Pim-1 3'-UTR variants	Pim-1 3rd	TCT CCA AAA ATC TGC CTG GGT T
	Inv. hPim-1 3'-UTR R CCE	GCT CTA GAG CAA TAA GAT CTC TTT TAT TCC CCT GT
pGL3 let-7a variants	pGL3 ctr let7 01	TCG CCA GTC AAG TAA CAA CC
pGL3 P21 3'-UTR variants	P21 3'-UTR 3rd	TCC TCT AAG GTT GGG CAG G
	Invitrogen P21 3'-UTR R (CCE)	GCT CTA GAG CGG AGG AGC TGT GAA AGA CAC A
pGL3 1,5 kb variants	miR-17-92 f1	ATA TAG ATC TTG CCG CCG GGA AAC GGG TT
	miR-17-92 r1	ATA TAA GCT TCC ATA CAA ATT CAG CAT AAT CCC TAA TGG
	RVprimer3	CTA GCA AAA TAG GCT GTC CC
	seq miR-Promo 2F	TGG TGA AGA ATA GTC TGT GGG C
pGL3 625 bp	RVprimer3	CTA GCA AAA TAG GCT GTC CC
	miR-17-92 r1	ATA TAA GCT TCC ATA CAA ATT CAG CAT AAT CCC TAA TGG
pGL3 339 bp	RVprimer3	CTA GCA AAA TAG GCT GTC CC
	miR-17-92 r1	ATA TAA GCT TCC ATA CAA ATT CAG CAT AAT CCC TAA TGG
pGL3 279 bp	RVprimer3	CTA GCA AAA TAG GCT GTC CC
pGL3 339 inv	RVprimer3	CTA GCA AAA TAG GCT GTC CC
	miR-17-92 r1	ATA T*AA GCT T*CC ATA CAA ATT CAG CAT AAT CCC TAA TGG

L. MiRNA sequences

miRNA name	miRBase Release 19.0 accession number	sequence 5' → 3'
hsa-miR-15a-5p	MIMAT0000068	UAG CAG CAC AUA AUG GUU UGU G
hsa-miR-16-5p	MIMAT0000069	UAG CAG CAC GUA AAU AUU GGC G
hsa-miR-17-5p	MIMAT0000070	CAA AGU GCU UAC AGU GCA GGU AG
hsa-miR-20a-5p	MIMAT0000075	UAA AGU GCU UAU AGU GCA GGU AG
hsa-miR-24-3p	MIMAT0000080	UGG CUC AGU UCA GCA GGA ACA G
hsa-miR-26a-5p	MIMAT0000082	UUC AAG UAA UCC AGG AUA GGC U
hsa-miR-33a-5p	MIMAT0000091	GUG CAU UGU AGU UGC AUU GCA
hsa-miR-33b-5p	MIMAT0003301	GUG CAU UGC UGU UGC AUU GC
hsa-miR-144-3p	MIMAT0000436	UAC AGU AUA GAU GAU GUA CU
hsa-miR-374a-5p	MIMAT0000727	UUA UAA UAC AAC CUG AUA AGU G
hsa-miR-423-5p	MIMAT0004748	UGA GGG GCA GAG AGC GAG ACU UU

M. Equipment

Device	Manufacturer
Agarose gel chamber	PerfectBlue Gel System Mini S/M, *PEQLAB* Biotechnology GMBH
Autoclave	V 95, *Systec*
Automatic weighing machine	*Sartorius* *DENVER Instruments*
Blotting equipment	Trans-Blot® SD Semi-Dry Transfer cell, *Bio-Rad*
Cell culture dishes	*SARSTEDT*
Cell culture plates	Cellstar®, *greiner-bio-one*
Centrifuges	Biofuge pico, Fresco 17, *HERAUS* 5810R, *Eppendorf*
Cryo pure tubes	*SARSTEDT*
Cuvettes	Gene Pulser Cuvette, 4mm, *Bio-Rad*
Detection films	*Kodak*
Electroporation system	Gene Pulser Xcell, *Bio-Rad*
Gel documentation	Gerix 1000, *Biostep* GS-800 Calibrated Densitometer, *Bio-Rad*
Hand monitor	LB 1210 B, *Berthold*
Heating block	TB1, *Biometra*
Hemocytometer	Neubauer bright-line, *MarienFeld*
Hybridization oven	OV3, *Biometra*
Imager cassettes	Bas cassette 4043, *Fuji Film*
Incubator	BE 400, *Memmert* NuAire, *Memmert*
Luminescence detector	Safire²™ micro plate reader, *Tecan*
Magnetic stirrer	*Heidolph Instruments GmbH and Co*
Micro plate reader	Safire²™ micro plate reader, *Tecan*
Microscope	AE20, *Motic*
Microwave oven	8020 E, *Privileg*
Pasteur pipette	*SARSTEDT*
Petri dishes	*SARSTEDT*
pH-meter	inoLab, *SENTON*
Phosphorimager	Fuji FLA-3000 R; *Fuji Film*
Pipet boy	Pipetboy acu, *IBS*
Pipettes	*ABiMED* (0.1 – 2 µL; 2 – 20 µL; 20 – 200 µL; 100 – 1000 µL)
Polyacrylamide gel chamber	custom-made, *University of Lübeck*
Power supply	Power N Pac 3000, *Bio-Rad*
PVDF membrane	Immobilon™-P, *Millipore*
Quartz cuvette	104-QS, 10 mm; *Hellma*

Device	Manufacturer
Real time PCR system	LightCycler®2.0, *Roche* MyiQ™5 Real-Time PCR Detection System, *Bio-Rad*
Rotor wheel	LMOM1203, *Kobe*
Safety cabinet	HERAsafe KS, *Thermo Scientific*
Scintillation analyzer	1900 CA TRI-CARB® Liquid Scintillation Analyzer, *Perkin Elmer*
SDS-PAGE equipment	Mini Protean® 3 Cell, *Bio-Rad*
Serological pipettes	*SARSTEDT*
Shaking incubator	3033, *GFL*
Sonifier	Branson 250, *Heinemann*
Spectral photometer	Biomate 3, *Thermo Scientific*
Spin columns	illustra Micro-Spin G-25, *GE Healthcare Life Sciences*
Thermocycler	TGradient, *Biometra*
Thermomixer	5436, *Eppendorf*
Tips	*SARSTEDT*
Tubes	*SARSTEDT*
Vortexer	7-2020, *NeoLab*
Water bath	water bath with polycarbonate basin, *NeoLab*
Whatman filter	Thick Blot Paper, *Bio-Rad*

N. Chemicals

Chemical	Manufacturer
2-mercaptoethanol	*Merck*
Acetic acid	*Roth*
Acrylamide/bisacrylamide (48:2) for PAA gels	*Roth*
Acrylamide/bisacrylamide 30 % for SDS gels	*Gerbu*
Agar agar	*Serva*
Agarose GTQ	*Roth*
Ammonium acetate	*Roth*
APS	*Roth*
Ammonium thiocyanate	*Roth*
Ampicillin	*Roth*
Aqua-phenol	*Roth*
Boric acid	*Roth*
Bromophenol blue	*Merck*
Calcium chloride	*Roth*
Chloroform	*Merck*
Crystal violet	*Merck*
Deoxycholate	*Roth*
Deoxynucleosidtriphosphates	*Thermo Fisher Scientific*
DTT	*Gerbu*
Ethanol	*Roth*
EDTA	*Gerbu*
FCS	*PAA*
Formaldehyde	*Roth*
Formamide	*Gerbu*
Glycerol (99,5 %)	*Gerbu*
Glycine	*Roth*
Guanidinium thiocyanate	*Roth*
HEPES	*Gerbu*
Hydrochloric acid	*Roth*
IMDM cell culture medium	*PAA*
Isopropanol	*Roth*
Lithium chloride	*Roth*
Magnesium chloride	*Roth,* *Thermo Fisher Scientific*
Magnesium sulfate	*Roth,* *Thermo Fisher Scientific*

Chemical	Manufacturer
Methanol	*Roth*
Milk powder, blotting grade	*Roth*
MOPS	*Gerbu*
Nocodazole	*Sigma-Aldrich*
NP-40	*Sigma-Aldrich*
PBS solution for cell culture	*PAA*
Peptone	*Roth*
Phenol	*Roth*
PMSF	*Sigma-Aldrich*
Potassium chloride	*Roth*
Potassium hydroxide	*Roth*
Propidium iodide	*Sigma-Aldrich*
RPMI cell culture medium	*PAA*
Rubidium chloride	*Roth*
SDS ultra-pure	*Roth*
Silver nitrate	*Roth*
Sodium acetate	*Fluka*
Sodium carbonate	*Roth*
Sodium chloride	*Roth*
Sodium hydrogen carbonate	*Roth*
Sodium thiosulfate	*Gerbu*
TEMED	*Roth*
Tris B	*Gerbu*
Tris X	*Roth*
Triton-X	*Sigma-Aldrich*
Trypsine/EDTA solution for cell culture	*PAA*
Tween 20	*Sigma-Aldrich*
Urea	*Gerbu*
Water, demineralized	*self-made*
Water, double-distilled	*self-made*
XCB	*Merck*
Yeast extract	*Gerbu*

O. Enzymes, Kits and Reagents

Enzyme, kit, reagent	Purpose	Manufacturer
Absolute qPCR SYBR Green Mix	quantitative PCR	Thermo Fisher Scientific
Amersham ECL™/ECL plus™ Western Blotting Detection Reagent	Western Blot	GE Healthcare Life Sciences
Cell Death Detection ELISA	apoptosis assay	Roche Applied Biosciences
Cell proliferation reagent WST-1	proliferation assay	Roche
cOmplete Mini Protease Inhibitor Cocktail	protease inhibition	Roche
DNaseI, RNase-free	DNA digestion	Thermo Fisher Scientific
DNeasy® Blood & Tissue Kit	genomic DNA purification	Quiagen
Ethidiumbromide for agarose gels (0.025 %)	nucleic acid staining	Roth
Ethidiumbromide for PAA gels (0.5 %)	nucleic acid staining	Roth
FastAP Thermosensitive Alkaline Phosphatase	dephosphorylation reaction	Thermo Fisher Scientific
FastDigest enzyme *Bgl*II	restriction digest	Thermo Fisher Scientific
FastDigest enzyme *Blp*I	restriction digest	Thermo Fisher Scientific
FastDigest enzyme *Hind*III	restriction digest	Thermo Fisher Scientific
FastDigest enzyme *Xba*I	restriction digest	Thermo Fisher Scientific
GBX Developer and Replenisher	Western Blot detection	Kodak®
GBX Fixer and Replenisher	Western Blot detection	Kodak®
GeneJet™ Plasmid Miniprep Kit	plasmid Miniprep	Thermo Fisher Scientific
Lipofectamine™ 2000	transfection of mammalian cells	Invitrogen™ Life Technologies
Luciferase Assay System	luciferase assay	Promega
*mir*Vana™ miRNA Isolation Kit	miRNA isolation	Ambion Life Technologies
NucleoBond® PC 500 purification kit	plasmid Maxiprep	Macherey-Nagel
Optimem I	transfection of mammalian cells	Invitrogen™ Life Technologies
PANSORBIN® Staph A cells	anti-IgG reagent for ChIP assay	Calbiochem/Merck
PEI F25 LMW	transfection of mammalian cells	custom-made, Sigma-Aldrich
Pfu DNA polymerase	amplification of DNA	Thermo Fisher Scientific
Proteinase K	protein digestion	Thermo Fisher Scientific
RevertAid H Minus First Strand cDNA Synthesis Kit	cDNA generation	Thermo Fisher Scientific
RNase A	RNA digestion	Thermo Fisher Scientific
SYBR® gold	nucleic acid staining	Invitrogen™ Life Technologies
T4 DNA ligase	ligation reaction	Thermo Fisher Scientific
T4 polynucleotide kinase	phosphorylation reaction	Thermo Fisher Scientific
Taq DNA polymerase	amplification of DNA	Thermo Fisher Scientific
Wizard®SV Gel and PCR Clean-Up System	agarose gel extraction, PCR purification	Promega

P. Vector sequence pCMV-XL4 (OriGene)

Nucleotide Sequence of pCMV6-XL4

GenBank Accession Number: AF067196

```
AACAAAATAT TAACGCTTAC AATTTCCATT CGCCATTCAG GCTGCGCAAC
TGTTGGGAAG GGCGATCGGT GCGGGCCTCT TCGCTATTAC GCCAGCTGGC
GAAAGGGGGA TGTGCTGCAA GGCGATTAAG TTGGGTAACG CCAGGGTTTT
CCCAGTCACG ACGTTGTAAA ACGACGGCCA GTGCCAAGCT GATCTATACA
TTGAATCAAT ATTGGCAATT AGCCATATTA GTCATTGGTT ATATAGCATA
AATCAATATT GGCTATTGGC CATTGCATAC GTTGTATCTA TATCATAATA
TGTACATTTA TATTGGCTCA TGTCCAATAT GACCGCCATG TTGACATTGA
TTATTGACTA GTTATTAATA GTAATCAATT ACGGGGTCAT TAGTTCATAG
CCCATATATG GAGTTCCGCG TTACATAACT TACGGTAAAT GGCCCGCCTG
GCTGACCGCC CAACGACCCC CGCCCATTGA CGTCAATAAT GACGTATGTT
CCCATAGTAA CGCCAATAGG GACTTTCCAT TGACGTCAAT GGGTGGAGTA
TTTACGGTAA ACTGCCCACT TGGCAGTACA TCAAGTGTAT CATATGCCAA
GTCCGCCCCC TATTGACGTC AATGACGGTA AATGGCCCGC CTGGCATTAT
GCCCAGTACA TGACCTTACG GGACTTTCCT ACTTGGCAGT ACATCTACGT
ATTAGTCATC GCTATTACCA TGGTGATGCG GTTTTGGCAG TACACCAATG
GGCGTGGATA GCGGTTTGAC TCACGGGGAT TTCCAAGTCT CCACCCCATT
GACGTCAATG GGAGTTTGTT TTGGCACCAA AATCAACGGG ACTTTCCAAA
ATGTCGTAAT AACCCCGCCC CGTTGACGCA AATGGGCGGT AGGCGTGTAC
GGTGGGAGGT CTATATAAGC AGAGCTCGTT TAGTGAACCG TCAGAATTTT
GTAATACGAC TCACTATAGG GCGGCCGCGA ATTCAGATCT GGTACCGATA
TCAAGCTTGT CGACTCTAGA TTGCGGCCGC GGTCATAGCT GTTTCCTGAA
CAGATCC CGGGTGGCAT CCCTGTGACC CCTCCCCAGT GCCTCTCCTG
GCCCTGGAAG TTGCCACTCC AGTGCCCACC AGCCTTGTCC TAATAAAATT
AAGTTGCATC ATTTTGTCTG ACTAGGTGTC CTTCTATAAT ATTATGGGGT
GGAGGGGGGT GGTATGGAGC AAGGGGCAAG TTGGGAAGAC AACCTGTAGG
GCCTGCGGGG TCTATTGGGA ACCAAGCTGG AGTGCAGTGG CACAATCTTG
GCTCACTGCA ATCTCCGCCT CCTGGGTTCA AGCGATTCTC CTGCCTCAGC
CTCCCGAGTT GTTGGGATTC CAGGCATGCA TGACCAGGCT CAGCTAATTT
TTGTTTTTTT GGTAGAGACG GGGTTTCACC ATATTGGCCA GGCTGGTCTC
CAACTCCTAA TCTCAGGTGA TCTACCCACC TTGGCCTCCC AAATTGCTGG
GATTACAGGC GTGAACCACT GCTCCCTTCC CTGTCCTTCT GATTTTAAAA
TAACTATACC AGCAGGAGGA CGTCCAGACA CAGCATAGGC TACCTGGCCA
TGCCCAACCG GTGGGACATT TGAGTTGCTT GCTTGGCACT GTCCTCTCAT
GCGTTGGGTC CACTCAGTAG ATGCCTGTTG AATTGGGTAC GCGGCCAGCT
TGGCTGTGGA ATGTGTGTCA GTTAGGGTGT GGAAAGTCCC CAGGCTCCCC
AGCAGGCAGA AGTATGCAAA GCATGCATCT CAATTAGTCA GCAACCAGGT
GTGGAAAGTC CCCAGGCTCC CCAGCAGGCA GAAGTATGCA AAGCATGCAT
CTCAATTAGT CAGCAACCAT AGTCCCGCCC CTAACTCCGC CCATCCCGCC
CCTAACTCCG CCCAGTTCCG CCCATTCTCC GCCCCATGGC TGACTAATTT
TTTTTATTTA TGCAGAGGCC GAGGCCGCCT CGGCCTCTGA GCTATTCCAG
AAGTAGTGAG GAGGCTTTTT TGGAGGCCTA GGCTTTTGCA AAAAGCTCCT
CGAGGAACTG AAAAACCAGA AAGTTAATTC CCTATAGTGA GTCGTATTAA
ATTCGTAATC ATGTCATAGC TGTTTCCTGT GTGAAATTGT TATCCGCTCA
CAATTCCACA CAACATACGA GCCGGAAGCA TAAAGTGTAA AGCCTGGGGT
GCCTAATGAG TGAGCTAACT CACATTAATT GCGTTGCGCT CACTGCCCGC
TTTCCAGTCG GGAAACCTGT CGTGCCAGCT GCATTAATGA ATCGGCCAAC
GCGCGGGGAG AGGCGGTTTG CGTATTGGGC GCTCTTCCGC TTCCTCGCTC
ACTGACTCGC TGCGCTCGGT CGTTCGGCTG CGGCGAGCGG TATCAGCTCA
CTCAAAGGCG GTAATACGGT TATCCACAGA ATCAGGGGAT AACGCAGGAA
AGAACATGTG AGCAAAAGGC CAGCAAAAGG CCAGGAACCG TAAAAAGGCC
GCGTTGCTGG CGTTTTTCCA TAGGCTCCGC CCCCCTGACG AGCATCACAA
```

AAATCGACGC TCAAGTCAGA GGTGGCGAAA CCCGACAGGA CTATAAAGAT
ACCAGGCGTT TCCCCCTGGA AGCTCCCTCG TGCGCTCTCC TGTTCCGACC
CTGCCGCTTA CCGGATACCT GTCCGCCTTT CTCCCTTCGG GAAGCGTGGC
GCTTTCTCAT AGCTCACGCT GTAGGTATCT CAGTTCGGTG TAGGTCGTTC
GCTCCAAGCT GGGCTGTGTG CACGAACCCC CCGTTCAGCC CGACCGCTGC
GCCTTATCCG GTAACTATCG TCTTGAGTCC AACCCGGTAA GACACGACTT
ATCGCCACTG GCAGCAGCCA CTGGTAACAG GATTAGCAGA GCGAGGTATG
TAGGCGGTGC TACAGAGTTC TTGAAGTGGT GGCCTAACTA CGGCTACACT
AGAAGAACAG TATTTGGTAT CTGCGCTCTG CTGAAGCCAG TTACCTTCGG
AAAAAGAGTT GGTAGCTCTT GATCCGGCAA ACAAACCACC GCTGGTAGCG
GTGGTTTTTT TGTTTGCAAG CAGCAGATTA CGCGCAGAAA AAAAGGATCT
CAAGAAGATC CTTTGATCTT TTCTACGGGG TCTGACGCTC AGTGGAACGA
AAACTCACGT TAAGGGATTT TGGTCATGAG ATTATCAAAA AGGATCTTCA
CCTAGATCCT TTTAAATTAA AAATGAAGTT TTAAATCAAT CTAAAGTATA
TATGAGTAAA CTTGGTCTGA CAGTTACCAA TGCTTAATCA GTGAGGCACC
TATCTCAGCG ATCTGTCTAT TTCGTTCATC CATAGTTGCC TGACTCCCCG
TCGTGTAGAT AACTACGATA CGGGAGGGCT TACCATCTGG CCCCAGTGCT
GCAATGATAC CGCGAGACCC ACGCTCACCG GCTCCAGATT TATCAGCAAT
AAACCAGCCA GCCGGAAGGG CCGAGCGCAG AAGTGGTCCT GCAACTTTAT
CCGCCTCCAT CCAGTCTATT AATTGTTGCC GGGAAGCTAG AGTAAGTAGT
TCGCCAGTTA ATAGTTTGCG CAACGTTGTT GCCATTGCTA CAGGCATCGT
GGTGTCACGC TCGTCGTTTG GTATGGCTTC ATTCAGCTCC GGTTCCCAAC
GATCAAGGCG AGTTACATGA TCCCCCATGT TGTGCAAAAA AGCGGTTAGC
TCCTTCGGTC CTCCGATCGT TGTCAGAAGT AAGTTGGCCG CAGTGTTATC
ACTCATGGTT ATGGCAGCAC TGCATAATTC TCTTACTGTC ATGCCATCCG
TAAGATGCTT TTCTGTGACT GGTGAGTACT CAACCAAGTC ATTCTGAGAA
TAGTGTATGC GGCGACCGAG TTGCTCTTGC CCGGCGTCAA TACGGGATAA
TACCGCGCCA CATAGCAGAA CTTTAAAAGT GCTCATCATT GGAAAACGTT
CTTCGGGGCG AAAACTCTCA AGGATCTTAC CGCTGTTGAG ATCCAGTTCG
ATGTAACCCA CTCGTGCACC CAACTGATCT TCAGCATCTT TTACTTTCAC
CAGCGTTTCT GGGTGAGCAA AAACAGGAAG GCAAAATGCC GCAAAAAAGG
GAATAAGGGC GACACGGAAA TGTTGAATAC TCATACTCTT CCTTTTTCAA
TATTATTGAA GCATTTATCA GGGTTATTGT CTCATGAGCG GATACATATT
TGAATGTATT TAGAAAAATA AACAAATAGG GGTTCCGCGC ACATTTCCCC
GAAAAGTGCC ACCTGACGCG CCCTGTAGCG GCGCATTAAG CGCGGCGGGT
GTGGTGGTTA CGCGCAGCGT GACCGCTACA CTTGCCAGCG CCCTAGCGCC
CGCTCCTTTC GCTTTCTTCC CTTCCTTTCT CGCCACGTTC GCCGGCTTTC
CCCGTCAAGC TCTAAATCGG GGGCTCCCTT TAGGGTTCCG ATTTAGTGCT
TTACGGCACC TCGACCCCAA AAAACTTGAT TAGGGTGATG GTTCACGTAG
TGGGCCATCG CCCTGATAGA CGGTTTTTCG CCCTTTGACG TTGGAGTCCA
CGTTCTTTAA TAGTGGACTC TTGTTCCAAA CTGGAACAAC ACTCAACCCT
ATCTCGGTCT ATTCTTTTGA TTTATAAGGG ATTTTGCCGA TTTCGGCCTA
TTGGTTAAAA AATGAGCTGA TTTAACAAAA ATTTAACGCG AATTTTAACA
AAATATT

Q. Vector sequence pGL3 control (Promega)

pGL3-Control Vector

This vector can be obtained from Promega Corporation, Madison, WI. Call one of the following numbers for order or technical information.

Order or Technical 1-800-356-9526
Outside U.S. 608-274-4330

pGL3-Control Vector sequence reference points:

Base pairs	5256
Multiple cloning region	1-41
Promoter	48-250
Luciferase gene (luc+)	280-1932
GLprimer2 binding site	281-303
SV40 late poly (A) signal	1964-2185
Enhancer	2205-2441
RVprimer4 binding site	2518-2499
ColE1-derived plasmid replication origin	2756
Beta-lactamase gene (Ampr)	3518-4378
F1 origin	4510-4965
Synthetic (upstream) poly (A) signal	5096-5249
RVprimer3 binding site	5198-5217

..

```
    1  GGTACCGAGC TCTTACGCGT GCTAGCCCGG GCTCGAGATC TGCGATCTGC

   51  ATCTCAATTA GTCAGCAACC ATAGTCCCGC CCCTAACTCC GCCCATCCCG

  101  CCCCTAACTC CGCCCAGTTC CGCCCATTCT CCGCCCCATC GCTGACTAAT

  151  TTTTTTTATT TATGCAGAGG CCGAGGCCGC CTCGGCCTCT GAGCTATTCC

  201  AGAAGTAGTG AGGAGGCTTT TTTGGAGGCC TAGGCTTTTG CAAAAAGCTT

  251  GGCATTCCGG TACTGTTGGT AAAGCCACCA TGGAAGACGC CAAAAACATA

  301  AAGAAAGGCC CGGCGCCATT CTATCCGCTG GAAGATGGAA CCGCTGGAGA

  351  GCAACTGCAT AAGGCTATGA AGAGATACGC CCTGGTTCCT GGAACAATTG

  401  CTTTTACAGA TGCACATATC GAGGTGGACA TCACTTACGC TGAGTACTTC

  451  GAAATGTCCG TTCGGTTGGC AGAAGCTATG AAACGATATG GGCTGAATAC

  501  AAATCACAGA ATCGTCGTAT GCAGTGAAAA CTCTCTTCAA TTCTTTATGC

  551  CGGTGTTGGG CGCGTTATTT ATCGGAGTTG CAGTTGCGCC CGCGAACGAC

  601  ATTTATAATG AACGTGAATT GCTCAACAGT ATGGGCATTT CGCAGCCTAC

  651  CGTGGTGTTC GTTTCCAAAA AGGGGTTGCA AAAAATTTTG AACGTGCAAA

  701  AAAAGCTCCC AATCATCCAA AAAATTATTA TCATGGATTC TAAAACGGAT

  751  TACCAGGGAT TTCAGTCGAT GTACACGTTC GTCACATCTC ATCTACCTCC

  801  CGGTTTTAAT GAATACGATT TTGTGCCAGA GTCCTTCGAT AGGGACAAGA

  851  CAATTGCACT GATCATGAAC TCCTCTGGAT CTACTGGTCT GCCTAAAGGT

  901  GTCGCTCTGC CTCATAGAAC TGCCTGCGTG AGATTCTCGC ATGCCAGAGA

  951  TCCTATTTTT GGCAATCAAA TCATTCCGGA TACTGCGATT TTAAGTGTTG

 1001  TTCCATTCCA TCACGGTTTT GGAATGTTTA CTACACTCGG ATATTTGATA
```

```
1051  TGTGGATTTC GAGTCGTCTT AATGTATAGA TTTGAAGAAG AGCTGTTTCT
1101  GAGGAGCCTT CAGGATTACA AGATTCAAAG TGCGCTGCTG GTGCCAACCC
1151  TATTCTCCTT CTTCGCCAAA AGCACTCTGA TTGACAAATA CGATTTATCT
1201  AATTTACACG AAATTGCTTC TGGTGGCGCT CCCCTCTCTA AGGAAGTCGG
1251  GGAAGCGGTT GCCAAGAGGT TCCATCTGCC AGGTATCAGG CAAGGATATG
1301  GGCTCACTGA GACTACATCA GCTATTCTGA TTACACCCGA GGGGGATGAT
1351  AAACCGGGCG CGGTCGGTAA AGTTGTTCCA TTTTTTGAAG CGAAGGTTGT
1401  GGATCTGGAT ACCGGGAAAA CGCTGGGCGT TAATCAAAGA GGCGAACTGT
1451  GTGTGAGAGG TCCTATGATT ATGTCCGGTT ATGTAAACAA TCCGGAAGCG
1501  ACCAACGCCT TGATTGACAA GGATGGATGG CTACATTCTG GAGACATAGC
1551  TTACTGGGAC GAAGACGAAC ACTTCTTCAT CGTTGACCGC CTGAAGTCTC
1601  TGATTAAGTA CAAAGGCTAT CAGGTGGCTC CCGCTGAATT GGAATCCATC
1651  TTGCTCCAAC ACCCCAACAT CTTCGACGCA GGTGTCGCAG GTCTTCCCGA
1701  CGATGACGCC GGTGAACTTC CCGCCGCCGT TGTTGTTTTG GAGCACGGAA
1751  AGACGATGAC GGAAAAAGAG ATCGTGGATT ACGTCGCCAG TCAAGTAACA
1801  ACCGCGAAAA AGTTGCGCGG AGGAGTTGTG TTTGTGGACG AAGTACCGAA
1851  AGGTCTTACC GGAAAACTCG ACGCAAGAAA AATCAGAGAG ATCCTCATAA
1901  AGGCCAAGAA GGGCGGAAAG ATCGCCGTGT AATTCTAGAG TCGGGGCGGC
1951  CGGCCGCTTC GAGCAGACAT GATAAGATAC ATTGATGAGT TTGGACAAAC
2001  CACAACTAGA ATGCAGTGAA AAAAATGCTT TATTTGTGAA ATTTGTGATG
2051  CTATTGCTTT ATTTGTAACC ATTATAAGCT GCAATAAACA AGTTAACAAC
2101  AACAATTGCA TTCATTTTAT GTTTCAGGTT CAGGGGGAGG TGTGGGAGGT
2151  TTTTTAAAGC AAGTAAAACC TCTACAAATG TGGTAAAATC GATAAGGATC
2201  TGAACGATGG AGCGGAGAAT GGGCGGAACT GGGCGGAGTT AGGGGCGGGA
2251  TGGGCGGAGT TAGGGGCGGG ACTATGGTTG CTGACTAATT GAGATGCATG
2301  CTTTGCATAC TTCTGCCTGC TGGGGAGCCT GGGGACTTTC CACACCTGGT
2351  TGCTGACTAA TTGAGATGCA TGCTTTGCAT ACTTCTGCCT GCTGGGGAGC
2401  CTGGGGACTT TCCACACCCT AACTGACACA CATTCCACAG CGGATCCGTC
2451  GACCGATGCC CTTGAGAGCC TTCAACCCAG TCAGCTCCTT CCGGTGGGCG
2501  CGGGGCATGA CTATCGTCGC CGCACTTATG ACTGTCTTCT TTATCATGCA
2551  ACTCGTAGGA CAGGTGCCGG CAGCGCTCTT CCGCTTCCTC GCTCACTGAC
2601  TCGCTGCGCT CGGTCGTTCG GCTGCGGCGA GCGGTATCAG CTCACTCAAA
2651  GGCGGTAATA CGGTTATCCA CAGAATCAGG GGATAACGCA GGAAAGAACA
2701  TGTGAGCAAA AGGCCAGCAA AAGGCCAGGA ACCGTAAAAA GGCCGCGTTG
```

```
2751  CTGGCGTTTT TCCATAGGCT CCGCCCCCCT GACGAGCATC ACAAAAATCG
2801  ACGCTCAAGT CAGAGGTGGC GAAACCCGAC AGGACTATAA AGATACCAGG
2851  CGTTTCCCCC TGGAAGCTCC CTCGTGCGCT CTCCTGTTCC GACCCTGCCG
2901  CTTACCGGAT ACCTGTCCGC CTTTCTCCCT TCGGGAAGCG TGGCGCTTTC
2951  TCATAGCTCA CGCTGTAGGT ATCTCAGTTC GGTGTAGGTC GTTCGCTCCA
3001  AGCTGGGCTG TGTGCACGAA CCCCCCGTTC AGCCCGACCG CTGCGCCTTA
3051  TCCGGTAACT ATCGTCTTGA GTCCAACCCG GTAAGACACG ACTTATCGCC
3101  ACTGGCAGCA GCCACTGGTA ACAGGATTAG CAGAGCGAGG TATGTAGGCG
3151  GTGCTACAGA GTTCTTGAAG TGGTGGCCTA ACTACGGCTA CACTAGAAGA
3201  ACAGTATTTG GTATCTGCGC TCTGCTGAAG CCAGTTACCT TCGGAAAAAG
3251  AGTTGGTAGC TCTTGATCCG GCAAACAAAC CACCGCTGGT AGCGGTGGTT
3301  TTTTTGTTTG CAAGCAGCAG ATTACGCGCA GAAAAAAAGG ATCTCAAGAA
3351  GATCCTTTGA TCTTTTCTAC GGGGTCTGAC GCTCAGTGGA ACGAAAACTC
3401  ACGTTAAGGG ATTTTGGTCA TGAGATTATC AAAAAGGATC TTCACCTAGA
3451  TCCTTTTAAA TTAAAAATGA AGTTTTAAAT CAATCTAAAG TATATATGAG
3501  TAAACTTGGT CTGACAGTTA CCAATGCTTA ATCAGTGAGG CACCTATCTC
3551  AGCGATCTGT CTATTTCGTT CATCCATAGT TGCCTGACTC CCCGTCGTGT
3601  AGATAACTAC GATACGGGAG GGCTTACCAT CTGGCCCCAG TGCTGCAATG
3651  ATACCGCGAG ACCCACGCTC ACCGGCTCCA GATTTATCAG CAATAAACCA
3701  GCCAGCCGGA AGGGCCGAGC GCAGAAGTGG TCCTGCAACT TTATCCGCCT
3751  CCATCCAGTC TATTAATTGT TGCCGGGAAG CTAGAGTAAG TAGTTCGCCA
3801  GTTAATAGTT TGCGCAACGT TGTTGCCATT GCTACAGGCA TCGTGGTGTC
3851  ACGCTCGTCG TTTGGTATGG CTTCATTCAG CTCCGGTTCC CAACGATCAA
3901  GGCGAGTTAC ATGATCCCCC ATGTTGTGCA AAAAAGCGGT TAGCTCCTTC
3951  GGTCCTCCGA TCGTTGTCAG AAGTAAGTTG GCCGCAGTGT TATCACTCAT
4001  GGTTATGGCA GCACTGCATA ATTCTCTTAC TGTCATGCCA TCCGTAAGAT
4051  GCTTTTCTGT GACTGGTGAG TACTCAACCA AGTCATTCTG AGAATAGTGT
4101  ATGCGGCGAC CGAGTTGCTC TTGCCCGGCG TCAATACGGG ATAATACCGC
4151  GCCACATAGC AGAACTTTAA AAGTGCTCAT CATTGGAAAA CGTTCTTCGG
4201  GGCGAAAACT CTCAAGGATC TTACCGCTGT TGAGATCCAG TTCGATGTAA
4251  CCCACTCGTG CACCCAACTG ATCTTCAGCA TCTTTTACTT TCACCAGCGT
4301  TTCTGGGTGA GCAAAAACAG GAAGGCAAAA TGCCGCAAAA AAGGGAATAA
4351  GGGCGACACG GAAATGTTGA ATACTCATAC TCTTCCTTTT TCAATATTAT
4401  TGAAGCATTT ATCAGGGTTA TTGTCTCATG AGCGGATACA TATTTGAATG
4451  TATTTAGAAA AATAAACAAA TAGGGGTTCC GCGCACATTT CCCCGAAAAG
```

```
 4501  TGCCACCTGA CGCGCCCTGT AGCGGCGCAT TAAGCGCGGC GGGTGTGGTG
 4551  GTTACGCGCA GCGTGACCGC TACACTTGCC AGCGCCCTAG CGCCCGCTCC
 4601  TTTCGCTTTC TTCCCTTCCT TTCTCGCCAC GTTCGCCGGC TTTCCCCGTC
 4651  AAGCTCTAAA TCGGGGGCTC CCTTTAGGGT TCCGATTTAG TGCTTTACGG
 4701  CACCTCGACC CCAAAAAACT TGATTAGGGT GATGGTTCAC GTAGTGGGCC
 4751  ATCGCCCTGA TAGACGGTTT TTCGCCCTTT GACGTTGGAG TCCACGTTCT
 4801  TTAATAGTGG ACTCTTGTTC CAAACTGGAA CAACACTCAA CCCTATCTCG
 4851  GTCTATTCTT TTGATTTATA AGGGATTTTG CCGATTTCGG CCTATTGGTT
 4901  AAAAAATGAG CTGATTTAAC AAAAATTTAA CGCGAATTTT AACAAAATAT
 4951  TAACGCTTAC AATTTGCCAT TCGCCATTCA GGCTGCGCAA CTGTTGGGAA
 5001  GGGCGATCGG TGCGGGCCTC TTCGCTATTA CGCCAGCCCA AGCTACCATG
 5051  ATAAGTAAGT AATATTAAGG TACGGGAGGT ACTTGGAGCG GCCGCAATAA
 5101  AATATCTTTA TTTTCATTAC ATCTGTGTGT TGGTTTTTTG TGTGAATCGA
 5151  TAGTACTAAC ATACGCTCTC CATCAAAACA AAACGAAACA AAACAAACTA
 5201  GCAAAATAGG CTGTCCCCAG TGCAAGTGCA GGTGCCAGAA CATTTCTCTA
 5251  TCGATA
```

Sequence revised 16-Apr-02.

Acknowledgments

All good things must come to an end.

On that note, I would like to thank…

…above all…

… Prof. Dr. Roland K. Hartmann for affording me the opportunity to start my PhD, for being addressable at all times to discuss any problems and for his excellent supervision during the progress of my work,

… Prof. Dr. Jens Kurreck for his readiness to act as the second reviewer of my PhD thesis and for great conversations at poster sessions,

… Prof. Dr. Carsten Culmsee for participating as chairperson in my examination committee,

… Prof. Dr. Maike Petersen for attending my examination committee,

…more grand persons…

… Dr. Arnold Grünweller for writing protocol during my exam, for one of the most interesting research topics ever, for brilliant scientific discussions, for excellent co-supervision and for great barbeques at his home,

… all colleagues of the 'KMaren office' - I shall treasure this memory and wish you all the very best,

… Katja, Markus, Dominik, Arnold, Kerstin, Astrid, Karen, Philipp, Marcus, Katrin, Julia, Dennis, Dennis and Tanja for supporting me in complicated affairs, for many fun and a friendly atmosphere in the lab and for one or two beers after work,

… all former colleagues particularly Steffi for spending a glorious time,

… Prof. Dr. Achim Aigner and Ulrike for excellent discussions about science and for a very fruitful cooperation,

…last but not least…

… Meike and Kari for critically reading my PhD thesis, for helpful comments and for enduring friendship,

… Rina and Matt for sincere friendship and for correcting a lot of mistakes including bad grammar,

… Gilla for always having a sympathetic ear and for believing in me,

… my families - I couldn't have done it without you,

… Flo for encouraging me for all these years, for sympathizing with me even in the hard times and for his infinite love.

Academic achievement

Publications

Thomas M, Lange-Grünweller K, Weirauch U, Gutsch D, Aigner A, Grünweller A and Hartmann RK: **The proto-oncogene Pim-1 is a target of miR-33a.** *Oncogene (2012)*, *31*, 918-928

Ibrahim AF, Weirauch U, Thomas M, Grünweller A, Hartmann RK and Aigner A: **MicroRNA Replacement Therapy for miR-145 and miR-33a Is Efficacious in a Model of Colon Carcinoma.** *Cancer Res (2011)*, *71*, 5214-5224

Thomas M, Lange-Grünweller K, Dayyoub E, Bakowsky U, Weirauch U, Aigner A, Hartmann RK and Grünweller A: **PEI-complexed LNA antiseeds as miRNA inhibitors.** *RNA Biology (2012)*, *9(8)*, 1088-1098

Weirauch U, Beckmann N, Thomas M, Grünweller A, Huber K, Bracher F, Hartmann RK and Aigner A: **Functional role and therapeutic potential of the Pim-1 kinase in colon carcinoma.** *Neoplasia*, status: accepted

Thomas M, Lange-Grünweller K, Hartmann D, Golde L, Schlereth J, Aigner A, Grünweller A and Hartmann RK: **Pim-1 Dependent Transcriptional Regulation of the Human miR-17-92 Cluster.** *Manuscript in preparation*

Oral presentations

10th NordForsk Meeting, 2011, Stockholm, Sweden: **The proto-oncogene Pim-1 is a target of miR-33a.**

EMBO Workshop 'The reciprocal interactions of signaling pathways and non-coding RNA', 2012, Ascona, Schweiz: **PEI-complexed LNA antiseeds as miRNA inhibitors.**

Poster presentations

6th Meeting of the GBM study section 'RNA-Biochemistry' in cooperation with the GEN AG2 ‘Regulatory RNA’ of the German Genetics Society, 2010, Hohenwart, Germany: **Repression of the proto-oncogene Pim-1 by miR-33a**

7th Meeting of the GBM study section ‘RNA-Biochemistry’ in cooperation with the GEN AG2 ‘Regulatory RNA’ of the German Genetics Society, 2012, Bonn, Germany: **PEI-complexed LNA antiseeds as miRNA inhibitors**, poster award of the RNA society

Curriculum Vitae

Personal Details

Name	Thomas
First name	Maren
Date of Birth	April 04th, 1984
Place of Birth	Freudenberg/Westfalen
Nationality	German
Email address	maren_thomas@gmx.de

Education

Since September 2009	Ph.D. studies, Institute of Pharmaceutical Chemistry, Philipps-Universität Marburg
06/2009	medical license as pharmacist; *Approbation*
2004-2009	Studies in pharmacy (Staatsexamen), Philipps-Universität Marburg

Ph.D thesis

Title	RNAi-based anti-cancer strategies – targeting the proto-oncogene PIM1 and oncogenic miRNAs
Supervisor	Prof. Dr. Roland K. Hartmann (Philipps-Universität Marburg)

Experience

Field of interest	Molecular biology, RNA biochemistry, immunology, pharmacology, toxicology
Teaching	Supervision of undergraduate lab courses; supervision of undergraduates in scientific work (master thesis)
Working	as a side job (2009-2012): pharmacist (Schloss Apotheke Siegen)

Scientific skills and methods

Molecular biology	Work with genetically modified organisms (bacteria and eukaryotic cell lines); isolation, cultivation and differentiation of primary cells; transient transfection methods; standard DNA techniques (preparation/modification); cloning; PCR; RT-PCR; quantitative real-time PCR

RNA methods	RNA isolation; *in vitro* transcription; RNAi-mediated protein knockdown
Protein methods	Recombinant/native protein expression and purification using affinity, gel filtration or FPLC based chromatography, Western blotting; ELISA; immunoprecipitation

Scientific achievements

Poster presentations

7th Meeting of the GBM study section 'RNA-Biochemistry' in cooperation with the GEN AG2 'Regulatory RNA' of the German Genetics Society, 2012, Bonn, Germany: **PEI-complexed LNA antiseeds as miRNA inhibitors**, poster award of the RNA society

6th Meeting of the GBM study section 'RNA-Biochemistry' in cooperation with the GEN AG2 'Regulatory RNA' of the German Genetics Society, 2010, Hohenwart, Germany: **Repression of the proto-oncogene Pim-1 by miR-33a**

Oral presentations

EMBO Workshop 'The reciprocal interactions of signaling pathways and non-coding RNA', 2012, Ascona, Schweiz: **PEI-complexed LNA antiseeds as miRNA inhibitors**

10th NordForsk Meeting, 2011, Stockholm, Sweden: **The proto-oncogene Pim-1 is a target of miR-33a**

Publications

Thomas M, Lange-Grünweller K, Weirauch U, Gutsch D, Aigner A, Grünweller A and Hartmann RK: The proto-oncogene Pim-1 is a target of miR-33a. *Oncogene (2012)*, *31*, 918-928

Ibrahim AF, Weirauch U, **Thomas M**, Grünweller A, Hartmann RK and Aigner A: MicroRNA Replacement Therapy for miR-145 and miR-33a Is Efficacious in a Model of Colon Carcinoma. *Cancer Res (2011)*, *71*, 5214-5224

Thomas M, Lange-Grünweller K, Dayyoub E, Bakowsky U, Weirauch U, Aigner A, Hartmann RK and Grünweller A: PEI-complexed LNA antiseeds as miRNA inhibitors. *RNA Biology (2012)*, *9(8)*, 1088-1098

Weirauch U, Beckmann N, **Thomas M**, Grünweller A, Huber K, Bracher F, Hartmann RK and Aigner A: Functional role and therapeutic potential of the Pim-1 kinase in colon carcinoma. *Neoplasia*, status: accepted

Languages

German	Native
English	Very good; ongoing experience in reading English literature, giving talks and writing proposals
French	School education for three years

Declaration/Erklärung

Hiermit versichere ich, dass die vorgelegte Dissertation

“RNAi-based anti-cancer strategies -

targeting the proto-oncogene PIM1 and oncogenic miRNAs”

von mir selbstständig und ohne unerlaubte Hilfe angefertigt wurde und ich mich keiner anderen als der von mir ausdrücklich bezeichneten Quellen und Hilfen bedient habe.

Die Dissertation wurde in der jetzigen oder in ähnlicher Form noch an keiner anderen Hochschule eingereicht und hat noch keinen sonstigen Prüfungszwecken gedient.

Marburg, 12. März 2013

Maren Thomas